Nitwit! Blubber! Oddment! Tweak!

Albus Dumbledore

Seasonal variability in leaf and whole-tree responses of *Populus tremula* L. to elevated CO$_2$ and drought

Fran Lauriks

Promoters

Prof. Dr. ir. Kathy Steppe
Laboratory of Plant Ecology
Department of Plants and Crops
Faculty of Bioscience Engineering
Ghent University, Belgium

Dr. ir. Roberto Luis Salomón
Grupo de Investigación
Sistemas Naturales e Historia Forestal
Universidad Politécnica de Madrid
Spain

Members of the examination board

Prof. Dr. ir. Kris Verheyen (chairman)
Department of Environment, Ghent University, Belgium

Prof. Dr. ir. Pieter De Frenne (secretary)
Department of Environment, Ghent University, Belgium

Dr. ir. Maarten Ameye
Department of Plants and Crops, Ghent University, Belgium

Prof. Dr. Matteo Campioli
Plants and Ecosystems, Faculty of Science, University of Antwerp, Belgium

Prof. Dr. John Drake
Department of Sustainable Resources Management,
College of Environmental Science and Forestry, United States

Dean

Prof. Dr. ir. Marc Van Meirvenne

Rector

Prof. Dr. ir. Rik Van de Walle

Dutch translation of the title: Seizoensgebonden variabiliteit in blad- en boomrespons van *Populus tremula* L. op verhoogde CO$_2$ en droogte

Preface

Een doctoraat schrijven. Wat een zot idee. Na vier jaar lang experimenten uitvoeren, data analyseren, figuren maken, teksten schrijven en aanpassingen doorvoeren, is het moment eindelijk aangebroken voor wat echt belangrijk is: het dankwoord. Want een doctoraat schrijven, dat doe je niet alleen, gelukkig maar.

Merci aan alle vrienden en familie. Wat een bizar en onvoorspelbaar jaar hebben we met z'n allen achter de rug. Om zo veel redenen is het dit jaar duidelijk geworden hoe hard ik op jullie kan rekenen en dat in een jaar waarin we elkaar noodgedwongen op afstand moesten houden. Dus daarom merci. Merci om mee te gaan op de zotste reizen, alles te relativeren, te begrijpen waarom ik pas maanden te laat een baby-bezoekje kwam brengen, me te verrassen met een mysterieuze puzzel-post of een luidkeels raam-bezoek langs de faculteit, mijn knorrig gedrag wijselijk te negeren, zorgeloos thuis mee in de zetel te ploffen, professionele Whatsapp *peptalks* te voorzien, Tunke voor haar *free of charge* Adobe Illustrator kunsten en Melle fotoreportages, … Maar misschien vooral om me af en toe te verplichten die laptop ook gewoon eens toe te klappen. Ik maak het hierbij graag officieel: jullie zijn helden.

Bedankt Kathy. Vandaag kan ik het eerlijk toegeven, ik had nooit gedacht een doctoraat te schrijven. Dat leek me enkel iets voor echte wetenschappers en totaal niet aan bij besteed. Maar dat was voor ik had kennisgemaakt met jouw enthousiasme en overtuigingskracht. De motivatie waarmee jij je iedere dag opnieuw smijt voor het onderzoek is terecht alom geprezen en goed op weg wereldberoemd te worden. Dus bedankt om mij vijf jaar geleden over de streep te trekken en die wetenschapper in mij te zien.

Thank you to the members of the examination board, for your time and the effort you put in reading and critically assessing this dissertation. Thanks to your valuable comments and suggestions the quality of the work has substantially improved. My gratitude also goes to all co-authors, who often took care of tasks for which I did not even know where to begin. Willem and Olivier, thanks for your incredible wood anatomy skills and beautiful pictures. Juan, thank you for spending all that time in the lab for the NSC analysis.

Dankjewel aan iedereen van het Labo Plant Ecologie. Wat een voorrecht is het geweest om deel uit te maken van deze geweldige groep. Het is onvoorstelbaar dat in een team waar collega's zo snel toekomen en opnieuw vertrekken, toch zo een gezellige sfeer en collegialiteit kan heersen. Chaotische drukke koffiepauzes, ietwat verplichte traktaties, spontane pintjes in de Koepuur of op het dak, emmervolle-Sangria namiddagen, bowlingavonden met officiële prijsuitreikingen, samen professioneel de Gentse Feesten inzetten of een online kerstfeest inclusief receptie-box, verkleedpartijtjes en kerst-elf-awards. We hebben ons goed weten te amuseren. Maar ook als het met wetenshap te maken had, stonden we steeds voor elkaar klaar. R codes werden zonder probleem uitgewisseld, ogenschijnlijk onoplosbare problemen werden toch in groep opgelost en er was steeds wel iemand beschikbaar die een dagje de handen uit de mouwen wou steken als je hulp nodig had bij een experiment. Als we sukkelden deden we dat samen en dan valt alles best wel mee.

Petje af voor Ann, Pui Yi, Erik, Geert, en Philip. Want het zijn deze vijf vaste rotsen in de branding die een labo, overspoeld met overenthousiaste schoolverlaters, draaiende weten te houden. Merci voor jullie geduld, onvoorstelbaar collectief geheugen en warm hart voor iedereen in het labo. Ann en Pui Yi, jullie zorgden vanaf dag één voor een warm welkom. Voor de kleinste (administratieve) vraag, nieuwtjes heet van de naald of beste sappige verhalen, wist ik steeds waar ik moest zijn. Bedankt voor de meest oprechte *"hoe is het?"*, voor de beste get-togethers en labo-uitstappen, voor lunch-interventies en zelfs vers bereide avondmalen in de afgelopen maanden. Erik, hoewel je zelf hebt gezegd dat ik u niet hoef te bedanken, doe ik het toch… Want ik ben zo blij dat ik me 4 jaar niet ongerust moest maken over 3d-printers of *zigbee*'s en ik ook vandaag de schouders kan ophalen als het over *putty* gaat. Ik kreeg Melle-data te zien op mijn computer en dat is gewoon helemaal jouw verdienste. Geert en Philip, het is wonderbaarlijk dat ik ondanks mijn twee linkerhanden (jullie weten ondertussen dat ik niet kan zagen), ogenschijnlijk niets kon misdoen. Niet alleen zijn jullie de *masterminds* achter de Melle serretjes, jullie fiksten steeds opnieuw het kleinste en grootste technische probleem en sprongen in de auto als de *plomb* in Melle weer eens afsprong (hoe belangrijk kan de aankomst van de Ronde zijn?). Merci!

Hans, bedankt! Zonder jou was ik simpelweg nooit gestart aan het labo. Ons jaartje *Frans* gaf mij de kans sensoren te installeren zonder dat ik me al te veel zorgen hoefde te maken over of die resultaten wel bruikbaar zouden zijn voor een doctoraat. Maar vooral dikke merci voor de laatste maanden. Als recente doctor navigeerde jij zonder al te veel problemen door Plato en kon je je als geen ander inleven in mijn gemoedstoestand. Hoe

jij en Simon de laatste maanden met mij als bureaugenoot hebben weten door te komen, is een klein mirakel.

But most importantly: thank you to Team Melle. This PhD really has been a team effort and would probably not have succeeded if it wasn't for each and every one of you. You helped making the Melle site the most wanted experimental site of the lab, including a dragon swimming pool, hammock and the most creative naming of our measuring days. Founding father Michiel, Osmocote and sliding dolphin master Jens and compassionate and caring Aida, it was wonderful to have you around joining for experiments or providing crucial information.

Al is het zo goed als onmogelijk Linus te bedanken in vijf zinnen, ik doe graag mijn best. Merci om als *Frinus*-teamgenoot drie jaar iedere zomer met mij in een serre te kruipen, om steeds ons VC-tijdrecord te willen verbeteren, om altijd chauffeur te zijn, en om me, na al die jaren, te verplichten met R te werken. Maar vooral merci om me te doen relativeren. Soms lopen dingen fout in een proef, maar dat betekent niet dat een pintje niet kan smaken.

Finally, a big thanks to Roberto. I think it's fair to say that this PhD would not be half as good as it is today, if it wasn't for you. As mastermind behind the set-up, world-famous-cuvettes-constructor, professional-data cleaner and thought-through-outsourcer, you poses the gift of doing the best research while keeping your calm no matter what. It has been a blast having you being a part of the Melle team and as a co-promotor. Thank you for your inexhaustible effort in writing and correcting the dissertation during the last months. I hope we can celebrate soon with some Belgian beer. ¡Salud!

Table of contents

ii

List of abbreviations and symbols

[CO$_2$]	Concentration of carbon dioxide
[NSC]	Non-structural carbohydrate concentration
[SS]	Soluble sugars concentration
[Starch]	Starch concentration
A	Carbon assimilation
A$_{v\_all}$	Total vessel conducting area
A$_{xylem}$	Xylem area
aD	Treatment group with drought stress trees exposed to ambient CO$_2$
aCO$_2$	Ambient atmospheric CO$_2$ concentration
AE	Acoustic emission
AE$_{12}$	Xylem water potential at 12 % of the related AE signals
AE$_{50}$	Xylem water potential at 50 % of the related AE signals
AE$_{88}$	Xylem water potential at 88 % of the related AE signals
A$_n$	Net carbon assimilation
aW	Treatment group with well-watered trees exposed to ambient CO$_2$
BA	Basal stem area
C	Carbon
CAM	Crassulacean Acid Metabolism
CH$_4$	Methane
CO$_2$	Carbon dioxide
DC	Desorption curve
DG	Daily radial stem growth
d$_h$	Hydraulic weighted vessel diameter
d$_{h\_all}$	Hydraulic weighted vessel diameter for the total xylem area
d$_{h\_class}$	Hydraulic weighted vessel diameter for each vessel diameter size class
d$_v$	Vessel diameter
DOY	Day of the year
DW	Dry weight

DS	Daily radial stem shrinkage
E_A	Stem CO_2 efflux to the atmosphere
eCO_2	Elevated atmospheric CO_2 concentration
eCO_{2_effect}	Effect of elevated atmospheric CO_2
eD	Treatment group with drought stress trees exposed to elevated CO_2
ESE	Early season experiment
eD	Treatment group with well-watered trees exposed to elevated CO_2
ET	Evapotranspiration
FACE	Free-air CO_2 enrichment
F_{nv}	Vessel non-lumen fraction
GPP	Gross primary production
g_c	Canopy conductance
g_{c_daily}	Daily canopy conductance
g_s	Stomatal conductance
g_{s_12}	Xylem water potential at 12 % stomatal closure
g_{s_88}	Xylem water potential at 50 % stomatal closure
g_{s_88}	Xylem water potential at 88 % stomatal closure
GHG	Greenhouse gas
H_2O	Water
IRGA	Infrared gas analyser
k_{h_all}	Theoretical hydraulic conductivity of the total xylem area
k_{h_class}	Theoretical hydraulic conductivity for each vessel diameter size class
LA	Leaf area
LAI	Leaf area index
LGR	Leaf growth rate
LSE	Late season experiment
LVDT	Linear variable displacement transducers
M_i	Initial stem mass before bench top dehydration
M_f	Stem mass after bench top dehydration
M_{fresh}	Sampled stem mass
M_{dry}	Oven dried stem mass
N	Nitrogen
N_2O	Nitrous oxide
ND	Non-dynamic tree responses to elevated CO_2
NEE	Net ecosystem carbon exchange

NPP	Net primary production
NSC	Non-structural carbohydrate
N_{v_all}	Total number of vessels
N_{v_class}	Number of vessels per vessel size class
P	Phosphorous
P_{50}	Water potential corresponding with 50 % loss of hydraulic conductivity
PAR	Photosynthetically active radiation
PLA	Projected leaf area
Q_{10}	Temperature sensitivity of E_A
RH	Relative humidity
R_L	Leaf respiration
RuBisCo	Ribulose-1,5-bifosfaat carboxylase oxygenase
SE	Standard error
SF	Sap flow
Sfd	Sap flux density
SS	Soluble sugars
SSP	Socioeconomic pathway
SWC	Soil water content
T	Temperature
Tr	Transpiration
TWD	Tree water deficit
TWD_{12}	Xylem water potential at 12 % of the TWD
TWD_{50}	Xylem water potential at 50 % of the TWD
TWD_{88}	Xylem water potential at 88 % of the TWD
V	Volume
VC	Vulnerability curve
VC_{AE}	Acoustic emission vulnerability curve
v_g	Vessel grouping index
VGr	Volumetric growth rate
VOC	Volatile organic compounds
VPD	Vapor pressure deficit
ΔCO_2	Difference in [CO_2] between input and output air of cuvette
ΔD	Stem diameter variation
ΔD_{irrev}	Irreversible growth-driven stem diameter variation
ΔD_{rev}	Reversible water-driven stem diameter variation

ΔD	Total stem diameter variation
ΔD_{xylem}	Xylem diameter variation
ρ_{stem}	Stem wood density
ΔΨ	Water potential gradient
Ψ	Water potential
Ψ_{xylem}	Xylem water potential
Ψ_{pd}	predawn water potential

1

Introduction and thesis outline

Introduction

2020: turning point for global CO_2 emissions?

416.75 ppm. That was the average atmospheric carbon dioxide concentration ($[CO_2]$) at time of publication in February 2021 (NOAA 2021). Over the past 800,000 years, $[CO_2]$ has been largely fluctuating within the 172 and 300 ppm range (Lüthi et al. 2008). However, continuous monitoring of recent $[CO_2]$ variations indicate a clear increase since 1960 (Figure 1.1a, NOAA 2020). Likewise, also the atmospheric concentration of methane (CH_4) and nitrous oxide (N_2O) have rapidly increased (NOAA 2020), resulting in an unprecedented alteration of the atmospheric greenhouse gas (GHG) composition and in a consequent increase of global temperature (IPCC 2018). Despite public quarrel, a large scale survey indicated striking agreement among scientists, as 97-98 % of the climate researchers attributed current climate changes to anthropogenic factors (Anderegg et al. 2010). This concern was also translated in the 2014 IPCC report, where there was no room left for doubt, and anthropogenic GHG emissions were appointed the main cause of the ongoing global climate change. The importance of these statements can hardly be underestimated, as it does not only hold humans responsible for the observed climate changes, but it also underlines societal responsibility to turn current trends.
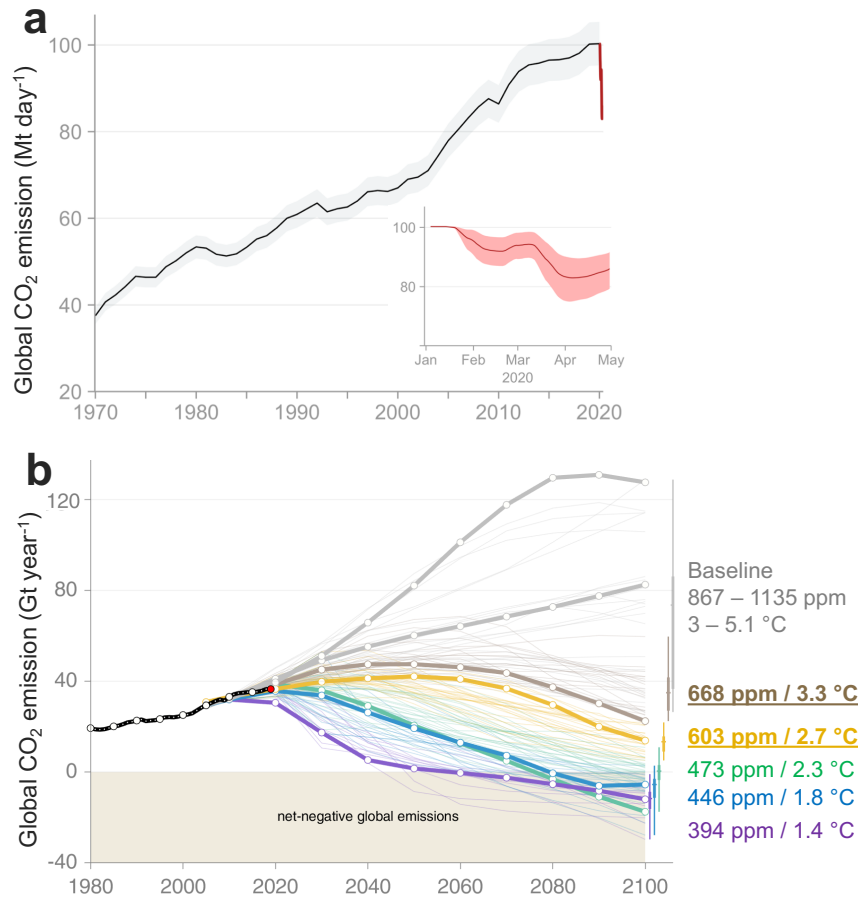
Figure 1.1 Global carbon dioxide (CO_2) emission (a) evolution measured (in $MtCO_2$ day^{-1}) over the last five decades and (inset) during the global confinement period as a result of the COVID-19 pandemic (early 2020) (modified from Le Quéré et al. 2020) and (b) projected (in $GtCO_2$ year^{-1}) for the next eight decades under different shared socio-economic pathways (SSP). Projected CO_2 concentration and temperature in 2100 is indicated for each possible SSP. Most likely SSP following current policies are underlined and bolded (i.e. grey SSP4 and yellow SSP2, modified from Riahi et al. 2017, Rogelj et al. 2018, Hausfather and Peters 2020, Meinshausen et al. 2020).

To this end, policymakers worldwide pledged in the Paris Agreement (2015) to limit effects of climate change and keep global average temperature below 2 °C above pre-industrial levels (UN 2015). In 2019, the European commission raised their goals by introducing the European Green Deal, aiming to reduce CO_2 emissions by 2030 down to 50 – 55 % of those during the 90´s, and being the first climate neutral continent in 2050 (EU 2019). To meet these goals, there has been a rapid expansion in the use of renewable energy resources (IRENA 2020, Ripple et al. 2020) while the use of coal for energy production has stabilized (Ritchie and Roser 2020). This lowered the annual increase of CO_2 emissions from 3 % (average from 2000 to 2009) to 0.9 % (average from 2010 to 2018) and even 0.6 % for 2019 (Friedlingstein

et al. 2019, Peters et al. 2020a). Although the relative annual variation in CO_2 emissions has never been negative since the 1960's (Peters et al. 2020a), the year 2020 might have been the first to break this trend (Figure 1.1a inset; Le Quéré et al. 2020). The confinement period during the COVID-19 pandemic reduced April daily CO_2 emission by 17 % overall, with remarkable reductions in industry (19 %), public buildings and commerce (21 %), surface transport (36 %) and aviation (60 %) (Le Quéré et al. 2020). The question now poses how policy makers will respond to this unexpected global sanitary crisis. Initially, the European council indicated the Green Deal would serve as a compass, guiding the EU recovery after the COVID-19 crisis (Colli 2020, Gornall 2020). Nonetheless, after calls from European industry (Vestager et al. 2020), some initiatives of the European Green Deal now face delay due to the coronavirus (Frédéric 2020a, 2020b). Also, it is expected that economic recovery will be prioritized over climate goals, hindering countries' CO_2 targets (Le Quéré et al. 2020). The way countries worldwide will draw up their economic recovery plans, and the extent to which sustainable development is integrated, will largely determine the pathway of CO_2 emission for the decades to come (Le Quéré et al. 2020).

Despite the uncertainty of near future political actions, it remains highly likely the Earth's atmosphere will become even more CO_2 enriched. To predict future climate conditions, different plausible global development pathways (known as the shared socioeconomic pathways, SSPs) have been described (O'Neill et al. 2017), and corresponding climate scenarios have been predicted (Figure 1.1b; Riahi et al. 2017, Rogelj et al. 2018, Meinshausen et al. 2020). Depending on the SSP, atmospheric $[CO_2]$ predictions in 2100 can vary from 394 ppm assuming Paris goals are met, to 1135 ppm in case no action is taken (Meinshausen et al. 2020). Given current policies, it is most likely $[CO_2]$ in 2100 will reach approximately 650 ppm (Meinshausen et al. 2020) causing a global temperature increase of 3°C above pre-industrial levels (Hausfather and Peters 2020) (Figure 1.1b). The consequences for the global climate when temperature would increase 3 °C are expected to be severe. Arctic sea ice will continue to melt aggravating the sea level rise, pressure on ecosystems and biodiversity will further grow and extreme weather events including tropical storms, heat waves and prolonged droughts will become even more frequent and intense (IPCC 2018).

Forests face the climate

Climate change is, however, no longer a future projection. Over the last decades, drought events, often in combination with high temperatures, have increased in frequency, duration

and severity (Spinoni et al. 2017, Hao et al. 2018a) putting ecosystems worldwide, including forests, at risk (Allen et al. 2010, 2015, Jump et al. 2017, Hartmann et al. 2018, McDowell et al. 2020). Trees' ability to adapt and acclimate to new growing conditions remains insufficient to mitigate adverse effects of changing climate (Franks et al. 2014) that occurs at a faster rate. For instance, drought tolerance has been observed to vary in different tree species as a result of adaptive mechanisms and genomic plasticity (Viger et al. 2016, Esperon-Rodriguez et al. 2020, Zas et al. 2020). Nonetheless, limited drought safety margins (Choat et al. 2012) and widespread drought-induced tree mortality raises the concern that induced stress is exceeding tree tolerances to cope with climate change (Anderegg et al. 2019). During the heatwave of the summer of 2018 in northern and central Europe, the importance of the interaction between plant productivity and drought vulnerability was highlighted. Although Europe has been struck by several summer droughts over the last decades, the 2018 heat wave differed from previous ones as it was preceded by a warm and moderately wet spring. This induced an excessive vegetative growth during spring which contributed to a faster depletion of the soil water pools, aggravating negative effects of the summer drought in plants (Bastos et al. 2020).

Forests are dependent on their surrounding climate, but they are also capable to affect their living conditions for two main reasons. First, forests lower local temperature as a direct effect of trees' transpiration (Moss et al. 2019). Tree water release to the atmosphere also induces cooling through cloud formation and local or far-off precipitation (Bonan 2008). Therefore, role of forests' evapotranspiration in the global water cycling cannot be underestimated. On average 40 % of the precipitation over land is dependent on forests' evapotranspiration (Ellison et al. 2017); this value rises up to 70 % in regions surrounding the Amazon forest (Van Der Ent et al. 2010). Second, forests play an important role in the mitigation of climate change, as forested biomes are responsible for the uptake of approximately 30 % of the anthropogenic CO_2 emissions (Friedlingstein et al. 2019, Pugh et al. 2019). Afforestation is therefore considered a cost-efficient and readily available strategy to offset CO_2 emissions (Doelman et al. 2020), and eventually achieve climate goals (IPCC 2018). Understanding how forests and trees will respond to increasing CO_2 and more intense and severe droughts remains therefore crucial to predict forests' ability to sequester carbon (C) and survive under future climate conditions (Cernusak et al. 2019, Anderegg et al. 2020). Within this context, this PhD dissertation assesses the effects of elevated atmospheric [CO_2] (eCO_2) and drought on leaf and whole-tree level C and water processes.

Increase of CO_2: a feast for trees?

Photosynthesis is the process by which CO_2 and water is converted into sugar and oxygen. Traditionally, photosynthesis is divided into two major processes: light reactions and C fixation

reactions (the Calvin cycle) (Bassham et al. 1956). Depending on the photosynthetic metabolic pathway, these two processes can co-occur (C3) or be separated in space (C4) or time (Crassulacean Acid Metabolism or CAM) (Ranson and Thomas 1960, Hatch and Slack 1966). Because the C3 pathway is the most common throughout plants worldwide (Yamori et al. 2014), including the one investigated along this PhD dissertation (*Populus tremula* L.), only the C3 pathway will further be explained. First, CO_2 diffuses from the atmosphere into the leaf (Figure 1.2, upper left-hand side). Leaf stomata are microscopic pores in the leaf surface formed by two specialized guard cells, which facilitate and regulate the CO_2 diffusion and uptake (Harrison et al. 2020). Subsequently, CO_2 diffuse through intercellular airspaces across the mesophyll, ultimately reaching the chloroplast (Figure 1.2, upper panels), where C fixation occurs, catalysed by enzyme RuBisCo (ribulose-1,5-bifosfaat carboxylase oxygenase), and carbohydrates are eventually assimilated (Yamori et al. 2014, Harrison et al. 2020). To acquire energy needed for growth and maintenance metabolism, assimilated carbohydrates are broken down in all living cells following respiratory metabolism, yielding energy by means of chemical compounds and emitting water and CO_2 as by-products. Respiration therefore occurs during night- and day-time regardless of light intensity, but is commonly measured under dark conditions as C assimilation (CO_2 uptake) can largely bias respiration (CO_2 efflux) estimates under light conditions (Yamori 2015). For this reason, photosynthetic rates are usually expressed as the net carbon assimilation (A_n), the difference between leaf level gross photosynthetic CO_2 uptake and leaf respiration (R_L).

The effects of eCO_2 on leaf level C processes, and in particular A_n, have been extensively studied over the last two decades (Figure 1.2, upper panels; reviewed e.g. Ainsworth and Rogers 2007, Norby and Zak 2011, Dusenge et al. 2019, Ainsworth et al. 2020, Allen et al. 2020). Today, stimulation of A_n under eCO_2 is no longer questioned, with an average A_n increase of 31 % in C3 plants exposed to free-air CO_2 enrichment (FACE) conditions (Ainsworth and Rogers 2007) (Text box 1.1). The reason for the enhanced C-fixation is two-fold. First, under ambient $[CO_2]$, photosynthesis is limited by substrate (i.e. CO_2) availability inside the sub-stomatal cavities. With rising atmospheric $[CO_2]$, higher internal $[CO_2]$ will lead to an increase of the carboxylation rate (Ainsworth and Rogers 2007, Ainsworth and Long 2020). Second, the chance of RuBisCo oxygenase activity (known as photorespiration) will lower under eCO_2 (Long et al. 2004). Photorespiration limits RuBisCo carboxylase efficiency, hereby limiting C fixation and further wasting some of the chemical compounds produced during the light reactions. Under current $[CO_2]$ and at 25 °C, approximately one third of RuBisCo functions as oxygenase (Ainsworth and Rogers 2007), and this fraction further increase with temperature (Long 1991). The higher $[CO_2]$ in sub-stomatal cavities, the higher

the RuBisCo efficiency as carboxylase, as a result of the lower oxygen - carbon dioxide ratio and RuBisCo oxygenase function (Long et al. 2004) (Text box 1.1).

Despite the widely observed eCO_2-induced stimulation of gross primary production (GPP), as the result of the A_n stimulation, it is still highly uncertain whether the C surplus will translate into an increase of net primary production (NPP) at the whole-tree level. Additional available C can also be allocated to alternative C sinks, including respiration, accumulation of non-structural carbohydrates (NSC), rhizodeposition or emission of volatile organic compounds (Körner 2006, Sala et al. 2012, Salomón et al. 2017b, Jiang et al. 2020). Initial eCO_2 studies on young fast growing trees suggested a parallel stimulation in tree growth and biomass production (Figure 1.2, lower panels; e.g. Pritchard et al. 1999, Moore et al. 2006, Dawes et al. 2014). Nonetheless, the effects of eCO_2 in closed stands composed by mature and large trees remain far less certain (e.g. Asshoff et al. 2006, Klein et al. 2016, Ellsworth et al. 2017, Jiang et al. 2020). For example, in an *Eucalyptus* woodland, GPP increased while NPP remained unaltered under FACE conditions. This discrepancy was attributed to parallel stimulation of respiratory fluxes under eCO_2 (Jiang et al. 2020), thereby highlighting two important knowledge gaps. First, current understanding of respiration under eCO_2 is comparatively limited and needs to be extended if we want to predict future tree's C sequestration potential (Dusenge et al. 2019). Second, homeostatic NPP under eCO_2 disputes the traditional view that growth is solely determined by the C availability (i.e. source driven) and stresses the importance of other co-drivers, such as nutrient and water availability or climatic conditions, determining the potential for tree development (i.e. sink driven) (Fatichi et al. 2014, Körner 2015).

Text box 1.1: A/C_i and light response curves under ambient and elevated CO_2

Carbon assimilation rates are driven by the [CO_2] in the sub-stomatal cavities (C_i), leaf light availability and prevailing temperature. A brief overview of the effects of C_i and light availability on carbon assimilation (A) rates based on eCO_2-induced shifts in the A/C_i and light response (LR) curves are given.

At low C_i levels, A is limited by the carboxylation rate of RuBisCo and increases with C_i until reaching a settling value determined by the leaf's capacity to regenerate RuBP (Text box figure 1.1, left-hand side panel, Von Caemmerer 2000). Stomatal

determines the ratio of intercellular to atmospheric $[CO_2]$ and thus the slope of the CO_2 supply curve and the final operating point (i.e. the intersection between the A/C_i and supply curve) (Von Caemmerer 2000, Ainsworth and Rogers 2007). Under current atmospheric $[CO_2]$, A is limited by RuBisCo carboxylation capacity for all C3 plants, including trees. Also under eCO_2 and assuming a constant slope of the supply curve, trees would still be operating at a RuBisCo limited stage of the A/C_i curve, indicating the large potential for stimulation of carbon assimilation under eCO_2 (Ainsworth et al. 2007). It must, however, be underlined that long term exposure to eCO_2 can induce plant acclimation (Ainsworth and Rogers 2007) or reduce the number and size of stomata shifting the slope of the supply curve (Xu et al. 2016, Engineer et al. 2016), lowering the potential stimulation of A under eCO_2.

Light is indispensable for photosynthesis. Increasing light availably enhances A until reaching maximal photosynthetic capacity (LR-curve Text box figure 1.1, right-hand side panel). As a result of the stimulated RuBisCo activity under eCO_2 (i) light saturation of A will occur at higher light intensity, and (ii) light saturated A will be higher under eCO_2 than aCO_2 (Ainsworth and Rogers 2007). For trees grown under FACE conditions, light saturated A is expected to be approximately 50 % higher relative to aCO_2 grown trees (Ainsworth and Rogers 2007). It must, however, be noted that the extent to which light saturated A is stimulated, is highly dependent on leaf characteristics and growing conditions. For instance, the relative stimulation of A in sun leaves was more than double compared to the eCO_2-induced stimulation in shade leaves as a likely effect of the leaf characteristics (including the leaf nitrogen and RuBisCo concentration) (Herrick and Thomas 1999).
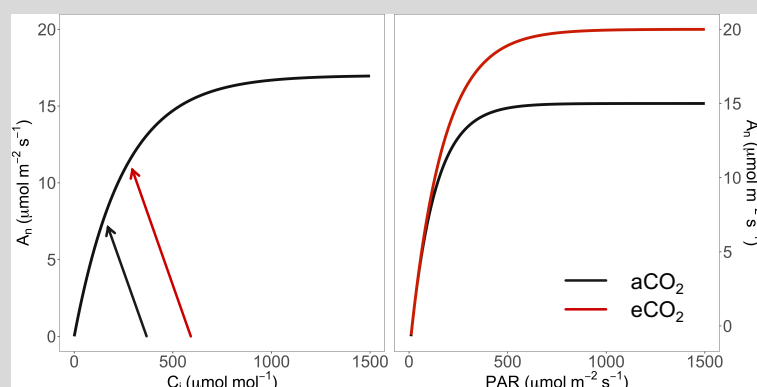
Text box figure 1.1 Theoretical A/C_i (left-hand side panel) and light response (LR, right-hand side panel) curve of C3 trees under ambient (black) and elevated (red) CO_2 growing conditions. Arrows show the supply curve and indicate the operating point under the corresponding atmospheric CO_2 concentration. With A_n net carbon assimilation, C_i CO_2 in sub-stomatal cavities and PAR photosynthetic active radiation.

Tree responses to eCO_2 are known to be variable within a single growing season. Highest leaf A_n stimulation is often found during the early season corresponding with the rapid vegetative growth phase followed by a down-regulation towards the end of the summer (Gamage et al. 2018). Seasonality in A_n stimulation can be substantial. For example in well-watered *Eucalyptus globulus* trees, A_n was stimulated up to 46 % during summer, but only 14 % during winter months (Quentin et al. 2015). Likewise, and at the whole-tree level, stem growth in *Larix kaempferi* trees was stimulated by eCO_2 only during the early season, after which stem growth stimulation under eCO_2 became insignificant (Yazaki et al. 2004). Seasonality is therefore expected to strongly alter C sink activity and consequently alter tree responses to eCO_2 (Gamage et al. 2018). Although long-term eCO_2 studies are still scarce, magnitude of the CO_2-induced stimulation in tree growth is also known to reduce after several years. This observed eCO_2 acclimation has been attributed to lowering of RuBisCo transcription, stoichiometric constraints (limitation of other required nutrients for tree development) or trees' inability to expand the C sink strength (e.g. Norby et al. 2010, Klein et al. 2016, Ellsworth et al. 2017 and reviewed by Gamage et al. 2018). Such dynamic behaviour of the eCO_2 response over time, in particular within a single growing season, is poorly understood and remains largely ignored in terrestrial biosphere models.

The necessity of water: there is no living without

Role of water in trees can be summarized in four core tasks: (i) It is an essential molecule for photosynthesis, (ii) it maintains living cells below lethal temperature thresholds by means of transpirational cooling, (iii) it maintains cell turgor pressure and metabolic functioning and (iv) it drives upward nutrient transport from soil to leaf and downward carbohydrate transport from leaf to roots (Bernacchi and Vanloocke 2015). By far, the largest fraction of water in trees, approximately 95 %, is merely transported upwards without being retained or used for any other function (McElrone et al. 2013). Xylem tissues are responsible for upward water transport and consists of stacked dead conductive elements forming hollow tubes, surrounded by living parenchyma cells. Xylem conduits are typically wide, long and heavily lignified, to minimize flow resistance and withstand large negative pressures once the cytoplasm is lost and only the lumen remains for water transport (Sperry et al. 2006, Pittermann 2010, Evert and Eichhorn 2013, Venturas et al. 2017). Cavities inside the secondary wall of conducting elements, known as conduit pits, allow water exchange between adjacent conduit lumen and create a connected hydraulic system. Inside the pits, modified primary cell walls, known as pit membranes, act as safety valves preventing rapid spread of air through the xylem, which may eventually lead to fatal hydraulic disruption (Pittermann 2010, Venturas et al. 2017).
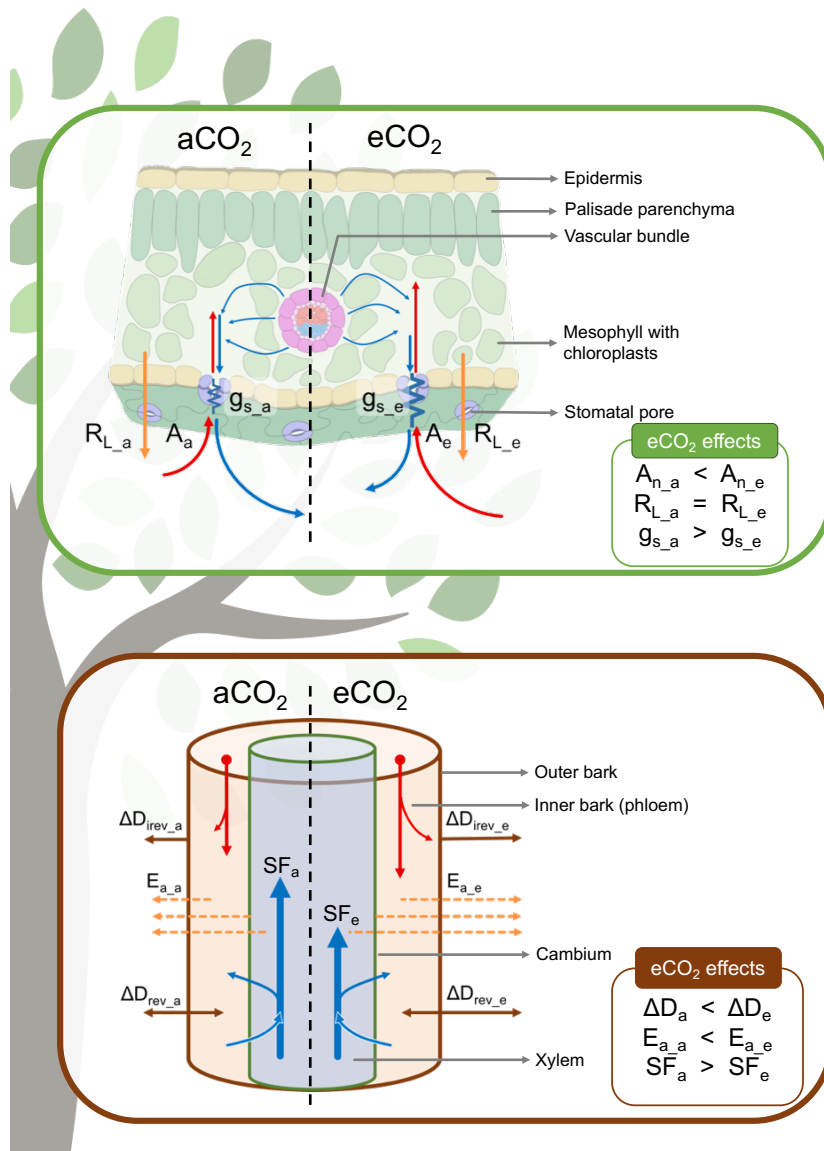
Figure 1.2 Schematic overview of pathways of water (blue) and carbon (red and dark orange) at leaf (top panels) and stem (lower panels) scale under ambient (aCO_2) and elevated (eCO_2) CO_2 growing conditions. Commonly assumed effects of eCO_2 on the three main processes at leaf (A_n, R_L and g_s) and stem (ΔD, E_a and SF) scale are indicated by arrow length and summarized in the inset.

With A carbon assimilation, A_n net carbon assimilation ($A - R_L$), g_s stomatal conductance, R_L leaf respiration, ΔD_{irrev} irreversible growth-driven stem diameter variations, ΔD_{rev} reversible water-driven stem diameter variations, ΔD total stem diameter variations ($\Delta D_{irrev} + \Delta D_{rev}$), E_a stem CO_2 efflux and SF sap flow as proxy of transpiration (upper panel modified from Harrison et al. 2020).

Upward water transport is driven by a passive process where water is pulled from the soil to the atmosphere as the result of leaf level (stomatal) water loss. As soon as water evaporates from the sub-stomatal cavities to the atmosphere, and as a result of the strong cohesion bonds between water molecules, water in the mesophyll cells moves towards the sub-stomatal cavity

(Figure 1.2, upper panels). Consequently, the tension exerted by the atmospheric water demand is transferred between adjacent water molecules throughout the entire tree, developing a vertical water potential gradient which drives continuous water movement from the soil to atmosphere, which is known as the cohesion-tension theory (Dixon and Joly 1895). The extent to which water is pulled upwards can be defined as a negative pressure (tension) or water potential (Ψ). Water moves according to potential gradients from less to more negative Ψ (Pittermann 2010). In addition to the axial water transport, water also flows radially between xylem and parenchymatic living tissues. In this way, stem living tissues serve as internal water pools. On a sub-daily basis, internal water pools are consecutively depleted and refilled, to bridge the time lag between leaf level water loss and water uptake by the roots, hereby buffering increases in xylem tension. As a result, shrinkage and swelling of stem elastic tissues can be found during morning and afternoon, respectively, according to the transpiration requirements imposed by the atmospheric demand (Zweifel et al. 2001, Meinzer et al. 2004, Steppe et al. 2006, De Swaef et al. 2015).

For most species, an increase of atmospheric [CO_2] induces stomatal closure, detected by a reduction in stomatal conductance (g_s) (Xu et al. 2016). For C3 species, an average 22 % reduction in g_s was measured under FACE conditions (Figure 1.2, upper panels; Ainsworth and Rogers 2007). For long, g_s reduction has been considered a consistent leaf response to eCO_2 (reviewed by e.g. Medlyn et al. 2001, Wullschleger et al. 2002, Long et al. 2004, Ainsworth and Rogers 2007). However, homeostatic g_s response to eCO_2 is not uncommon (review by Xu et al. 2016). Recent meta-analysis compiling data from over fifty FACE sites, even reported g_s increases under eCO_2 (Purcell et al. 2018). These observations therefore suggest a more complex stomatal behaviour under eCO_2 and call to revisit the widely accepted eCO_2-induced g_s inhibition (Xu et al. 2016). Uncertainty also exists on the effect of eCO_2 on the amount of transpired water at the whole-tree level (Figure 1.2, lower panels; Fatichi et al. 2016). Regardless of stomatal response to eCO_2, whole-tree transpiration is largely dependent on canopy leaf area (LA), which can be stimulated under eCO_2 (Pritchard et al. 1999). As a result, whole-tree transpiration has been observed to increase, despite potential reduction in leaf level water loss (Tricker et al. 2009, Fatichi et al. 2016).

Elevated CO_2 under drought: aggravation or mitigation?

When soil water content decreases, trees are forced to reduce their Ψ in the root system to take up water from the rhizosphere. Downstream (i.e. in stem, branches and leaves), Ψ must further reduce to maintain upward water transport to above-ground organs (Venturas et al. 2017). With increasing tension on the water column, conduits become more prone for the formation, spread and expansion of gas bubbles. As Ψ further declines, embolisms propagate

what could eventually lead to hydraulic failure (Venturas et al. 2017, Choat et al. 2018). Xylem vulnerability to embolism formation largely varies among tree species and is commonly expressed using the P_{50} value; i.e. the Ψ corresponding with 50 % loss of hydraulic conductivity (Choat et al. 2012). Wood anatomy, in particular xylem traits related to the ease of water exchange between xylem conduits (e.g. cell wall thickness, pit membrane porosity and conduit dimensions), largely determines the P_{50} value (Wheeler et al. 2005, Blackman et al. 2010, Christman et al. 2012, Rosner 2017, Olson 2020). Nonetheless, xylem vulnerability to embolism formation is just one feature determining overall tree drought tolerance, as the P_{50} value provides no information on the rate of Ψ reduction with decreasing soil water availability and atmospheric water demand. Two mechanisms involved in the modulation of Ψ reduction rate are stomatal regulation and the use of internal water pools (Epila et al. 2017, Venturas et al. 2017, Choat et al. 2018).

When facing drought, stomatal closure is the main mechanism to limit water loss and prevent lethal Ψ reductions (Martínez-Vilalta and Garcia-Forner 2017, Choat et al. 2018). However, as an inevitable effect of stomatal closure, CO_2 uptake and photosynthesis cease, so trees become dependent on carbohydrate pools to maintain metabolic activity. Drought stress therefore forces trees to balance risks of drought-induced hydraulic failure and carbon starvation (McDowell et al. 2008). It remains debatable whether carbon starvation can ultimately lead to tree death under drought conditions. A recent review showed xylem failure was omnipresent for 26 tree species at drought-induced mortality, while the carbohydrate status of dead trees were largely variable (Adams et al. 2017). During periods of low water availability, depletion of internal water pools enables short-term delay of stomatal closure, prolonging photosynthesis over time, and buffers the Ψ reduction to prevent onset of embolism formation (Choat et al. 2018, Fu et al. 2019). Despite the potential of capacitive water release to mitigate drought stress effects, the role of internal water pools during dehydration remains comparatively less studied than degradation of the hydraulic system's integrity under drought (Körner 2019, Martinez-Vilalta et al. 2019).

Effects of eCO_2 on drought vulnerability to embolism (i.e. shifts of P_{50}) under eCO_2 remain largely unknown (e.g. Tognetti et al. 1999, Gartner et al. 2003, Domec et al. 2010, Warren et al. 2011, Hao et al. 2018b, Newaz et al. 2018). Wood anatomy studies under eCO_2 suggest potential alterations in wood traits that could affect P_{50} values (Domec et al. 2017, Qaderi et al. 2019). An increase in average conduit diameter has been observed in parallel with the stimulated stem growth under eCO_2 (Domec et al. 2017). Wider conduits increase hydraulic efficiency, as conductivity is proportional to the fourth power of the conduit diameter (Hagen-Poiseuille law). However, increased conduit size has long been associated with a higher vulnerability to embolism as larger conduit surface area increases the chance of a failing pit

11

(e.g. Wheeler et al. 2005, Hacke et al. 2006, Christman et al. 2012). Nonetheless, a recent review found little evidence to support this trade-off between hydraulic efficiency and safety (Gleason et al. 2016) and appointed other wood characteristics, often related to mechanical strength, to determine to a greater extent hydraulic vulnerability to embolism (Mrad et al. 2018, Janssen et al. 2020). Some of these wood traits are expected to be altered under eCO_2 as increased C availability can stimulate cell wall deposition and increase wood density (e.g. Saxe et al. 1998, Atwell et al. 2003, Domec et al. 2010, 2016), possibly modifying pit membrane composition and enhance its ability to withstand xylem tension (Li et al. 2016).

When facing drought, eCO_2 is expected to alleviate some of the detrimental effects of drought on tree functioning (e.g. Wullschleger et al. 2002b, Avila et al. 2020, Birami et al. 2020). First, reduction of leaf level water loss via eCO_2-induced stomatal closure might result in an overall reduction of whole-tree water use, delaying the depletion of soil water and postponing suboptimal levels of water availability for hydraulic transport (Wullschleger et al. 2002b, Leuzinger and Körner 2007, Fatichi et al. 2016). Second, under moderate drought stress levels, eCO_2 facilitates CO_2 diffusion into the sub-stomatal cavities, which allows to maintain photosynthetic rates even when stomata are partially closed (Goodfellow et al. 1997, Herrick et al. 2004, Birami et al. 2020). However, with increasing drought and after full stomatal closure, mitigating effects of eCO_2 have been observed to progressively diminish (Birami et al. 2020). Furthermore, in some drought experiments, eCO_2 has been observed to exacerbate drought effects as stimulated growth and structural overshoot can accelerate depletion of soil water pools (e.g. Domec et al. 2010, Warren et al. 2011). It remains therefore highly uncertain whether trees' ability to withstand drought will be improved or deteriorated under eCO_2.

Dissertation outline: research questions and experimental set-up

Research questions

Previous research on the effects of eCO_2 on tree functioning has mainly focused on leaf level photosynthesis, g_s and whole-tree growth, while largely overlooking leaf and whole-tree respiration as well as whole-tree water use (Figure 1.3). Even today, despite numerous tools and approaches to monitor whole-tree responses (Jones 2004, Steppe et al. 2015), a substantial imbalance still exists between the number of studies conducted on leaf and whole-tree spatial scales under eCO_2. In particular for large trees, this discrepancy highlights an important knowledge gap, as leaf level responses to eCO_2 do not necessarily translate to the whole-tree level (e.g. Körner 2003, 2015, Palacio et al. 2014, Tor-ngern et al. 2015, Fatichi et

al. 2016) and potential mismatches between leaf and whole-tree level responses would induce biased predictions of future tree behaviour as climate changes.
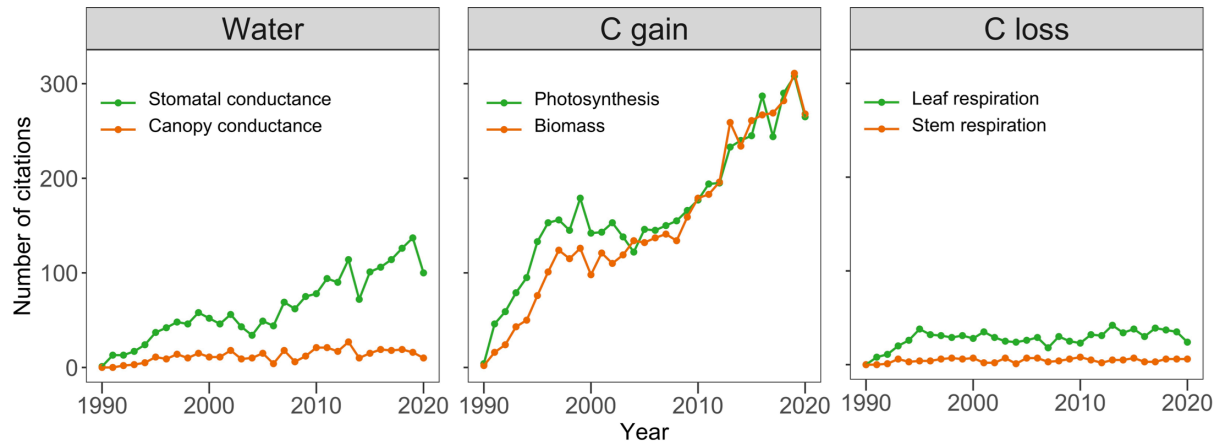

Figure 1.3 Comparison of *Web of Science* yearly citation reports on the number of conducted studies on leaf (green) and whole-tree (orange) responses of water, growth and respiration processes under elevated CO_2.

Basic topic search was conducted on 20 November 2020. *Elevated CO_2* was used as first keyword followed by the corresponding figure legend.

A second important knowledge gap in tree responses to eCO_2 is the high uncertainty regarding their temporal variability. In particular for long-living plants such as trees, down-regulation of the responses to eCO_2 is known to occur after multiple year of eCO_2 exposure (Norby et al. 2010, Klein et al. 2016, Ellsworth et al. 2017 and reviewed by Gamage et al. 2018). Furthermore, temporal dynamics of tree response to eCO_2 on a shorter timescale, i.e. within a single growing season, remain largely unknown and ignored (Gamage et al. 2018). The lack of a comprehensive understanding on the trend, magnitude and general occurrence of these temporal eCO_2 dynamics precludes reliable assessment by means of single point measurements. This is because, single measurements only provide a snapshot of dynamic tree responses and thus bias our understanding of the year-round effect of eCO_2.

Third, the effect of eCO_2 on tree responses to drought remains disputed, with reports of both mitigation (e.g. Goodfellow et al. 1997, Herrick et al. 2004, Birami et al. 2020) and aggravation (e.g. McCarthy et al. 2006, Bobich et al. 2010) of adverse drought effects under eCO_2. Uncertainty also remains on the effects of eCO_2 on hydraulic architecture and coupled hydraulic vulnerability. Despite a recent review on the effect of eCO_2 on the structure and functioning of plant hydraulic architecture (Domec et al. 2017), the number of studies focusing on possible alterations in hydraulic vulnerability (e.g. P_{50} value) under eCO_2 remain scarce

and contradictory (e.g. Tognetti et al. 1999, Gartner et al. 2003, Domec et al. 2010, Vaz et al. 2012, Newaz et al. 2018).

To address these three knowledge gaps, this PhD dissertation investigates the dynamic character of the eCO_2 response over time (early vs. late season), between spatial scales (leaf vs. whole-tree), and under both well-watered and drought conditions. For this, three research questions (Figure 1.4a) have been put forward, that we aim to answer along four research chapters (Figure 1.4b).

Experimental set-up

To test the temporarily dynamic nature of tree responses to eCO_2 on a temperate species (**Chapter 3 - 5**), we grew *Populus tremula* L. (European aspen) trees under ambient (aCO_2) and elevated (eCO_2) [CO_2]. *Populus tremula* was selected as it is a fast growing species, and thus highly susceptible to eCO_2, and because of its broad spatial distribution in Europe and important role as pioneer and keystone species widely used for recolonization of degraded areas (Myking et al. 2011, Caudullo et al. 2016, Rogers et al. 2020, Text box 1.2). At onset of the 2018 and 2019 growing seasons, approximately fifty one-year-old trees were acquired from a Belgian tree nursey (Sylva, Waarschoot). All trees were grown from wild seeds collected from same location in Europe. At the day of planting (day of year (DOY) 78-79), trees had an average diameter at stem base of 4.30 ± 0.20 mm. Trees were planted in 30 L pots with potting soil mixed with fertilizer (Osmocote Exact Standard 8-9M, ICL, Ipswich, UK), to allow optimal and individualized regulation of tree water availability and full randomization of well-watered and drought stressed treatment levels (see below), despite potential limiting effects of pots on tree biomass production (Poorter et al. 2012a, Campany et al. 2017).

Text box 1.2 *Populus tremula* L.

Populus tremula L. (European aspen) is a broadleaved, dioecious and diffuse-porous tree species native from cooler and temperate regions of Europe and Asia (von Wühlisch 2009). After Scots pine (*Pinus sylvestris* L.), European aspen has the widest distribution range, from north of the Arctic circle to Mediterranean regions (Spain and Turkey), indicating its high tolerance and plasticity for a wide variety of climatic and soil growing conditions (Caudullo et al. 2016). Nonetheless, moist and well-aerated soils with a high organic content (Kangur et al. 2021) and high light availability (von Wühlisch 2009, Caudullo et al. 2016) are the optimal conditions for the species.

Despite its limited commercial importance (Caudullo et al. 2016), European aspen trees are of high ecological value as they act as a keystone species to provide habitat for insects, birds and mammals and promoting biodiversity (Rogers et al. 2020). Furthermore, as a colonising pioneer, European aspen is considered an important facilitator for the (re)colonization of disrupted areas (e.g. after forest fires) (Caudullo et al. 2016). As a result, *P. tremula* was appointed as one of the six *Populus* species with a crucial role in promoting biodiversity, C sequestration and providing ecosystem services in the northern hemisphere (Rogers et al. 2020).

Until the age of 20 years, European aspen trees commonly show high growth rates, after which tree development slows down and tends to culminate at ca. 30 years, reaching a tree height of 30 m and a stem diameter of 1 m (Caudullo et al. 2016). Vegetative regeneration mainly occurs through the production of root suckers, and starting from the age of 10-15 years also seeds are produced for sexual reproduction (Myking et al. 2011). For young poplar trees, leaves emerge and develop from March to August, with a peak leaf biomass production in April. Stem volumetric growth occurs continuously from March to October, with highest rates at the end of spring and during early summer. Fine root production increases towards the end of the growing season, with a highest productivity in September, causing a shift in C allocation from aboveground to belowground biomass production in September and October (Text box figure 1.2; Broeckx et al. 2014).
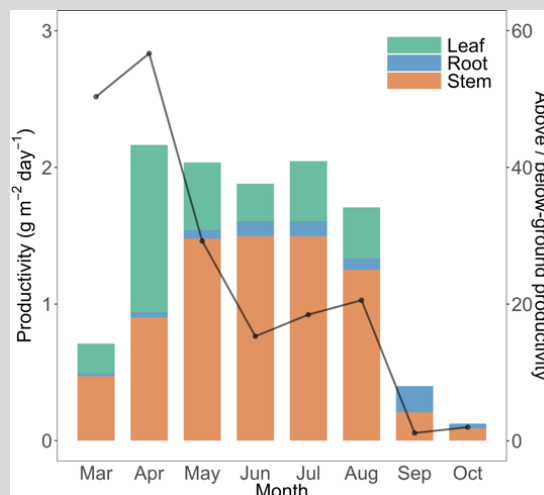
Text box figure 1.2 Time course of leaf (green), fine root (blue) and stem (orange – reflected by stem diameter increment) biomass production and the ratio of aboveground (stem + leaf) and belowground (fine root) productivity (black line, secondary y-axis) of a mixed *Populus* plantation during the 2011 growing season (one year after planting of unrooted hardwood cuttings) (modified from Broeckx et al. (2014)).
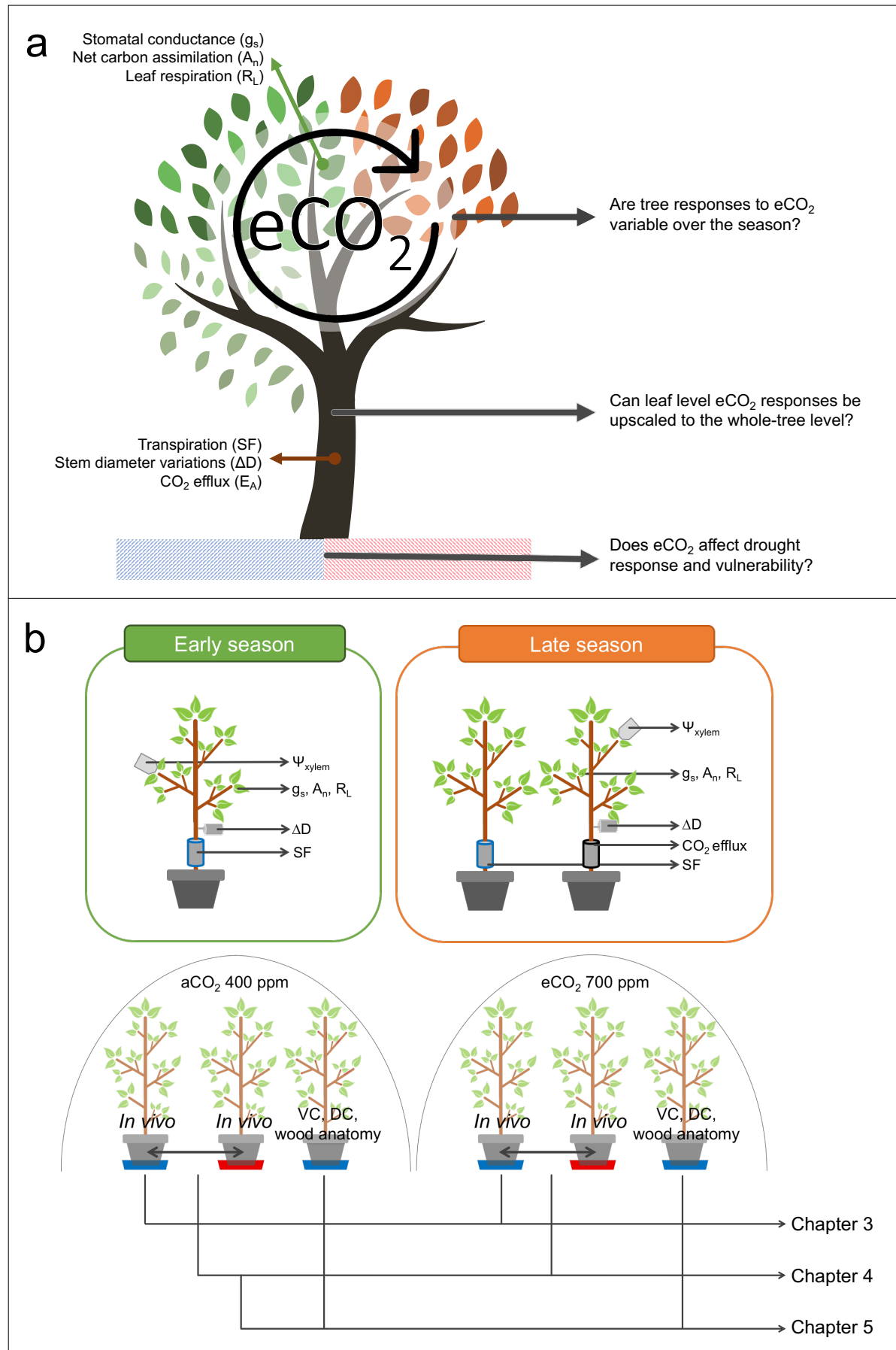
Figure 1.4 Visual overview of (a) the three main research questions of this PhD dissertation and (b) the conducted seasonal experiments with illustration of the monitored variables and experimental set-up to answer these questions along the PhD experimental chapters.

Two experiments were conducted during two subsequent growing seasons to study early (2019) and late (2018) leaf and whole-tree responses under ambient (400 ppm; aCO_2) and elevated (700 ppm; eCO_2) CO_2 concentration. Discrete (Ψ_{xylem}, A_n, g_s, R_L) and continuous (ΔD, SF, CO_2 efflux) measurements were performed during each seasonal experiment. Chapter 3 discusses the effect of the CO_2 treatment and experimental timing on *in vivo* leaf and whole-tree functioning in well-watered (blue coloured pots) *Populus tremula* L. trees. Chapter 4 expands this research to drought stressed trees (red coloured pots). Finally, chapter 5 combines and compares drought measurements *in vivo* with wood anatomical traits, hydraulic vulnerability and desorption curves (VC and DC, respectively) obtained from lab measurements.

Trees were distributed between two half-cylindrical treatment chambers (Figure 1.5a, based on a 4×4 m^2 square) located in an open grass field at the UGent campus Proefhoeve (Ghent University, Belgium, 50°58'N, 3°49'E), and constructed following the design of Wertin et al. (2010). Inside the treatment chambers, [CO_2] was continuously measured with a non-dispersive infrared sensor (GMT222, Vaisala, Helsinki, Finland) connected to a control unit and CO_2 tanks to maintain chamber [CO_2] at the targeted value. Target [CO_2] was set at 400 ppm (hereafter ambient [CO_2], aCO_2) and 700 ppm (hereafter elevated [CO_2], eCO_2). Ambient target [CO_2] was selected based on current measurements of global (NOAA 2021) and local atmospheric [CO_2] (414.75 ± 0.48 ppm and 411.64 ± 0.24 ppm during the 2018 and 2019 growing season, respectively). For eCO_2, 700 ppm was selected as target concentration to facilitate literature comparison (Chapter 2, Table 2.1 and Table 2.2). Note that the 700 ppm threshold will most likely be reached before 2150 (SSP4, Figure 1.1b).

The young trees were watered between 5:00 h and 6:00 h with an automatic irrigation system and the amount of water supplied was individually adjusted per pot throughout the season to avoid drought stress and soil-water saturation (Kangur et al. 2021). Soil water content was periodically (varying from once fortnightly to twice per week) measured using a ML3 ThetaKit (Delta-T Devices, Burnwell, UK) and maintained above 30 % and below 60 %. The microclimate was continuously monitored approximately 3.5 m above the soil level outside the treatment chamber and 0.5 m above the top foliage inside the treatment chamber. Air temperature (T; 10k thermistor, Epcos, Munich, Germany), relative humidity (RH; hygroclip probe, Rotronic, Basserdorf, Switzerland), both mounted inside a radiation shield, and photosynthetically active radiation (PAR; JYP PAR sensor, SDEC, Rousset, France) were measured. Vapor pressure deficit (VPD) inside each treatment chamber was calculated from T and RH as a measure of the atmospheric water demand (Allen et al. 1998). Chamber

temperature was programmed to mimic outside temperature using two cooling units (Midea, Foshan City, Guangdong, China) and a heater (AEG, Nurnberg, Germany) per chamber.

Figure 1.5 Pictures of the experimental set-up. (a) Outside and (b) inside of the two treatment chambers, and detailed image of the plant sensors: (c) linear variable displacement transducer to monitor stem diameter variations and stem cuvette to estimate stem CO_2 efflux (covered with aluminium foil during measurement period) and (d) sap flow sensor (type heat balance).

To limit possible pseudo-replication issues (i) trees were randomly distributed between the two treatment chambers the day of planting to maximize phylogenetic randomization, and (ii) possible differences in abiotic conditions between treatment chambers were limited. To this aim, the potting soil and irrigation water was identical in both treatment chambers, and differences in sunlight availability were avoided by using identical plastic foil for chamber construction and by building treatment chambers on the north-south axis relative to each other. For experimental feasibility, trees were not switched between treatment chambers during the growing season, as wiring connections between the plant sensors and the datalogger (as well as tubing between stem cuvettes, multiplexer and buffer tank) may have complicated continuous data collection.

To assess whether the tree seasonal stage affects tree responses to eCO_2 and drought, experiments were conducted during two consecutive growing seasons, allowing to study early (spring and early summer – 2019, hereafter ESE) and late (late summer and autumn – 2018, hereafter LSE) seasonal responses. Early during the growing season (April), woody biomass productivity is expected to start and to increase consistently until early July. After this peak is reached, productivity gradually decreases towards the onset of autumn (Figure 1.6, Cuny et al. 2015). Therefore, and according to this seasonality, drought was imposed when tree productivity was expected to be highest during ESE (2019), i.e. early July (DOY 183). Contrastingly, late season drought (2018) was imposed when tree carbon demand was expected to be reduced but not completely ceased, i.e. mid-August (DOY 222).
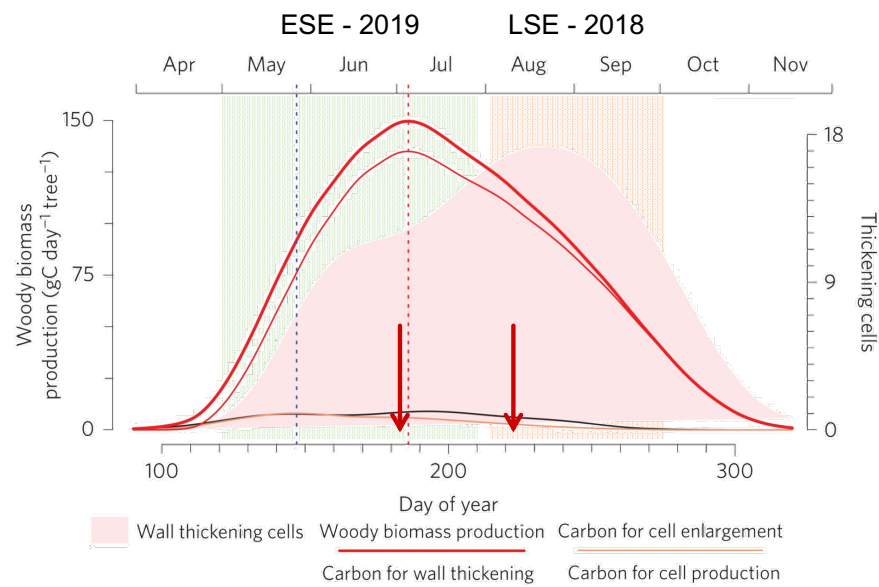
Figure 1.6 Timing of the conducted early (green, ESE - 2019) and late (orange, LSE - 2018) seasonal experiments in relation to the seasonality in plant woody biomass production as measured in a temperate conifer forest.

Vertical blue and red dashed lines indicate time of highest xylem volumetric increase and woody biomass production. Red arrows indicate the time of onset of drought stress during ESE and LSE. Figure modified from Cuny et al. (2015).

In vivo leaf and whole-tree responses were monitored using an array of discrete (A_n, g_s, R_L and Ψ) and continuous (radial stem diameter variation, sap flow as a proxy for transpiration and stem CO_2 efflux) measurements (Figure 1.5c,d). Monitored trees were harvested at the end of each seasonal experiment for dry biomass determination. Additionally, tree responses to drought were evaluated by establishing hydraulic vulnerability curves (VCs; i.e. relative

reduction in functional conduits with lowering Ψ) and stem desorption curves (DCs; the reduction in stem water content with lowering Ψ) by means of bench dehydration. During LSE, samples of bark, xylem and foliar tissues were collected before, during and after the drought event and analysed to determine NSC concentration.

Dissertation outline

Chapter 2 reviews current knowledge on the temporal variability of the effect of eCO_2 on C and water processes at leaf and whole-tree levels. By compiling previous studies which monitored eCO_2 responses along a single growing season, we aim at improving our understanding and suggest possible drivers of such potential seasonality. Additionally, an overview of FACE studies incorporating both leaf and whole-tree level measurements is given. By comparing responses between these two spatial scales, we assess the appropriateness of upscaling leaf measurements to the whole-tree level.

Data from the two seasonal experiments is analysed in Chapters 3 to 5. **Chapter 3** focuses on the effect of the [CO_2] treatment on the leaf and whole-tree responses under well-watered conditions. The effect of the [CO_2] treatment is assessed over time and spatial scales. We expect eCO_2 to stimulate A_n, leading to an increased stem growth, biomass production and respiration, while lowering leaf and whole-tree water use. We hypothesize leaf scale processes to be more susceptible to eCO_2 in comparison to the whole-tree scale, and expect down-regulation of the eCO_2 effects from the early to the late season.

In **Chapter 4**, data from the drought stressed trees is incorporated into the analyses. Effects of the drought treatment over time and with increasing drought stress levels is evaluated for both spatial scales (leaf vs. whole-tree) and seasonal periods (early vs. late season). Independent of the [CO_2] treatment, monitored variables during the late season are expected to be more susceptible to the drought event as a result of the increasing relative importance of water with leaf age (Pantin et al. 2012). We predict an eCO_2-induced alleviation of drought effects on leaf and tree functioning under moderate levels of drought stress, followed by a progressive diminution of mitigating effects as drought becomes more severe.

Chapter 5 relates tree drought avoidance strategies *in vivo* (i.e. stomatal regulation and use of internal water pools) with wood anatomical traits, hydraulic drought vulnerability and capacitance under aCO_2 and eCO_2 and during the early and late season. Vulnerability and desorption curves were determined by bench dehydration and using the acoustic method. As a result of potentially increased C availability under eCO_2 and consequently higher growth rate, we predict lower wood quality (i.e. reduction of wood density due to thinner cell walls and

larger vessels) in eCO_2 grown trees, leading to higher xylem vulnerability and hydraulic capacitance.

To conclude, **Chapter 6** summarizes and integrates all findings of the PhD dissertation. Here I aim to answer our three original research questions (Figure 1.4a) and suggest future research to tackle open questions in eCO_2 studies to come.

2

Temporal variability in tree responses to elevated CO$_2$

Abstract

At leaf level, elevated atmospheric CO_2 concentration (eCO_2) results in stimulation of carbon net assimilation and reduction of stomatal conductance. However, a comprehensive understanding of the impact of eCO_2 at larger temporal (seasonal and annual) and spatial (from leaf to whole-tree) scales is still lacking. Here, we review overall trends, magnitude, and drivers of dynamic tree responses to eCO_2, including carbon and water relations at the leaf and the whole-tree scale. Spring and early season leaf responses are most susceptible to eCO_2, and are followed by a down-regulation towards the onset of autumn. At whole-tree scale, CO_2 fertilization causes consistent biomass increments in young seedlings only, whereas mature trees show a variable response. Elevated CO_2-induced reductions in leaf stomatal conductance do not systematically translate into limitation of whole-tree transpiration due to the unpredictable response of canopy area. Reduction in the end-of-season carbon sink demand and water-limiting strategies are considered the main drivers of seasonal tree responses to eCO_2. These large temporal and spatial variabilities in tree responses to eCO_2 highlight the risk of predicting tree behaviour to eCO_2 based on single leaf level point measurements as they only reveal snapshots of the dynamic responses to eCO_2.

Introduction

Atmospheric carbon dioxide (CO_2) concentration ([CO_2]) has been rising since pre-industrial times (NOAA 2020) and is expected to keep increasing in the future (IPCC 2018). Over the past four decades, studies on the effect of elevated atmospheric CO_2 concentration (eCO_2) on plant growth and functioning have been numerous (reviewed e.g. by Norby and Zak 2011, De Kauwe et al. 2013, Xu et al. 2016, Dusenge et al. 2019, Allen et al. 2020). At leaf scale, free-air CO_2 enrichment (FACE) experiments have shown an average 31 % increase in carbon net assimilation (A_n) and 22 % reduction in stomatal conductance (g_s) (Ainsworth and Rogers 2007, Dusenge et al. 2019). Although useful for global modelling purposes, simplification of a general tree response to eCO_2 (hereafter 'eCO_2 effects') includes great risk for misjudging complex and dynamic eCO_2 effects, especially in long-living plant forms (Körner 2006, Fatichi et al. 2016, Paschalis et al. 2017). Trees, unlike other plant growth forms such as crops and grasses, develop slowly during multiple years and are able to grow for centuries. During tree life spans, eCO_2 effects are known to vary with size and age (temporal variability), and to depend on the spatial scale (leaf or whole-tree level) of the measurement (Long et al. 2004, Paschalis et

al. 2017, Jiang et al. 2020). Nonetheless, a comprehensive understanding of the dynamic character of eCO$_2$ responses is still lacking (Paschalis et al. 2017).

Over a single growing season, variability in the magnitude of eCO$_2$ effects has been observed for more than 35 years. A pioneering study in bean (*Phaseolus vulgaris*) reported a decline in the eCO$_2$-induced enhancement on leaf growth (Jolliffe and Ehret 1985). This observation was later confirmed in four poplar (*Populus* spp.) clones with eCO$_2$ effects on leaf area and overall growth being limited to the early growth phase (Radoglou and Jarvis 1990). Seasonal variability in eCO$_2$ effects has been consistently observed in several tree species ever since (Table 2.1). Most observations indicate acclimation in leaf responses to eCO$_2$ towards the end of the growing season, which may additionally be affected by abiotic or biotic co-variables (e.g. Goodfellow et al. 1997, Yazaki et al. 2004, Uddling and Wallin 2012, Urban et al. 2019). The seasonal down-regulation of the eCO$_2$ effects can be related to the limited need of carbon (C) for tree development at the end of the season and subsequent accumulation of sugars in the leaf, thereby causing reduction in RuBisCo (ribulose-1,5-bisphosphate carboxylase) activity and down-regulation of the photosynthetic activity (Ainsworth et al. 2007, Galmés et al. 2013, Gamage et al. 2018, Dusenge et al. 2019).

Temporal down-regulation of eCO$_2$ has also been observed at longer (annual) temporal scales due to the inability of mature trees to develop new C sinks (e.g. for growth or reproduction) to allocate the C excess. This agrees with the growing body of evidence indicating that tree biomass production does not merely rely on C availability (Muller et al. 2011, Sala et al. 2012, Körner 2015). As A_n is a key driver for tree biomass production and g_s controls whole-tree water use, leaf responses to eCO$_2$ can be expected to impact whole-tree C and water relations (Figure 2.1). However, eCO$_2$ studies integrating both leaf and whole-tree level measurements have reported discrepancies in the magnitude and timing of eCO$_2$ effects and in their evolution over time between spatial scales (e.g. Wullschleger et al. 2002a, Fatichi et al. 2016, Paschalis et al. 2017). Indirect effects of eCO$_2$, including soil water-savings due to reduced stomatal conductivity, stimulation of the canopy leaf area (LA) development and faster soil nutrient depletion, are assumed to partially explain discrepancies in eCO$_2$ effects between leaf and whole-tree levels (Fatichi et al. 2016). Absence of a straightforward translation from the leaf to the whole-tree level (Steppe et al. 2015), especially under eCO$_2$ conditions, hinders the prediction of a general tree response to climate change based on leaf level observations (Fatichi et al. 2016; Li et al. 2018; Paschalis et al. 2017; Wullschleger et al. 2002).
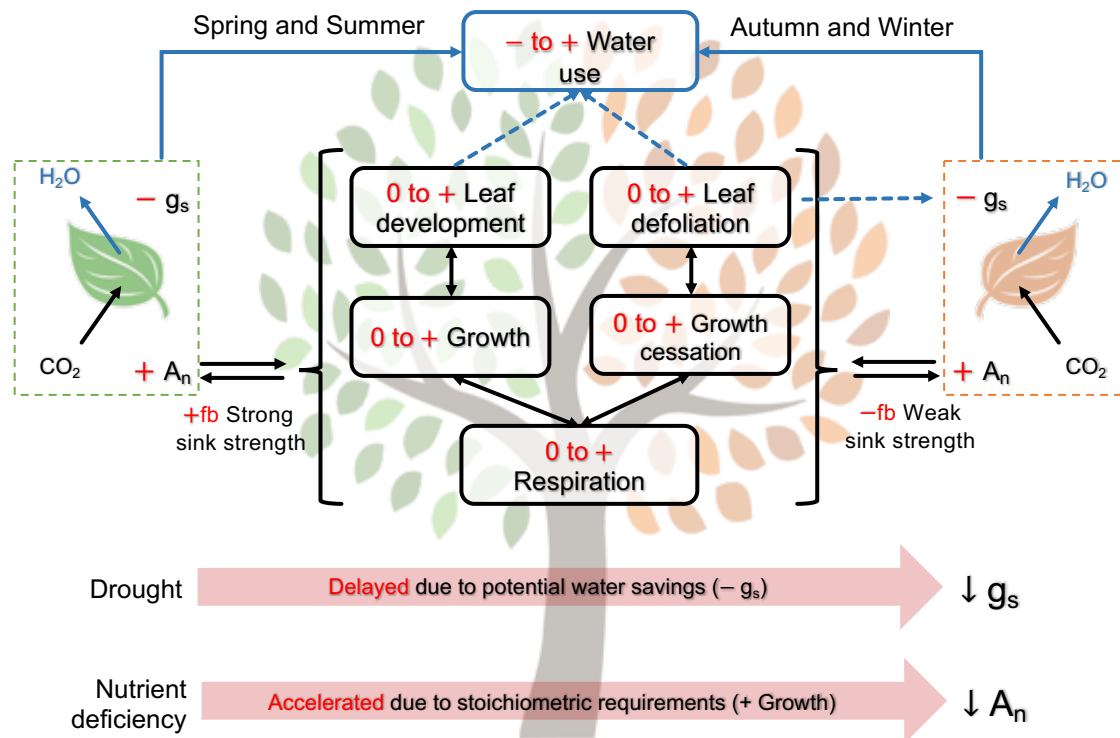
Figure 2.1 Schematic representation of the carbon (C, black) and water (blue) processes at leaf (left and right-hand side) and whole-tree (central) scale during spring and summer (green, left-hand side) and during autumn and winter (orange, right-hand side), including the effects of elevated atmospheric CO_2 concentration (eCO_2, in red) under non-limited water and nutrient conditions. Red arrows indicate the effects of drought and nutrient deficiency at the leaf scale.

Leaf and whole-tree responses to eCO_2 (- inhibition, 0 neutral effect, + stimulation), and feedbacks (fb) across spatial scales are displayed in red. Solid and dashed lines show direct and indirect interactions among responses to eCO_2, respectively. Leaf scale responses include stomatal conductance (g_s) and net carbon assimilation (A_n). Two horizontal red arrows at the bottom display the effects of commonly studied environmental co-factors on leaf level responses.

The dynamic character of tree responses to eCO_2 highlight the importance of monitoring leaf and whole-tree performance during the entire season and in the long-term (over several years) because single point observations will only reveal a partial snapshot of a complex and time-dependent tree response to eCO_2. This temporal and spatial dependence of tree responses to eCO_2 is, however, poorly understood and mostly ignored in terrestrial biosphere models (Paschalis et al. 2017), limiting our ability to predict the trend and magnitude of tree responses to eCO_2. In this review, we therefore aimed at (i) describing the temporal dynamics of eCO_2 effects at leaf scale C gain (A_n) and water loss (g_s), (ii) compiling studies in which leaf scale responses are compared to whole-tree growth and water use, and (iii) discussing the potential drivers for the temporal and the spatial variability found in eCO_2 responses. Because eCO_2 effects are expected to be stronger at the leaf than at the whole-tree scale, A_n and g_s responses are reviewed first before leaf

scale observations are upscaled and compared with whole-tree biomass and water use. In this review, we focus on trees because differences in the eCO$_2$ effects across spatial scales are expected to be stronger than in smaller-sized plant growth forms such as annual grasses and crops (recently reviewed by Ainsworth and Long 2020). Compared to grasslands and croplands, tree-dominated systems allocate most biomass into woody tissues (Poorter et al. 2012b). Because of this difference, grasslands and croplands may differ from trees in the link between leaf and whole-plant response to eCO$_2$.

Seasonal eCO$_2$ effects at the leaf scale

Dynamics in net carbon assimilation and stomatal conductance

As leaves develop in deciduous tree species, A$_n$ and g$_s$ rapidly increase, reaching highest rates at full expansion followed by a steady decrease towards the end of the growing season and leaf senescence (Riikonen et al. 2003, Xu and Baldocchi 2003, Pantin et al. 2012, Greer 2015, Way et al. 2017). A constant A$_n$ stimulation or g$_s$ inhibition under eCO$_2$ would simply lead to baseline vertical shifts of these A$_n$ and g$_s$ curves over time. However, this is rarely the case for A$_n$ (Table 2.1; only 2 out of 29 cases). For instance, eCO$_2$ stimulation in *Tilia americana* foliage was largely dependent on leaf age. As for late bud-break (July) leaves, eCO$_2$ stimulation remained significant until the end-of-season, while early bud-break (June) leaves showed acclimation to eCO$_2$ stimulation upon senescence (Li et al. 2019b). Likewise, the high relative abundance of young leaves, most responsive to eCO$_2$, during early and mid-summer contributed to the corresponding peak of A$_n$ stimulation at this time in several deciduous species (e.g. Curtis et al. 1995, Epron et al. 1996, Li et al. 2019b). As leaves senesce, the decreasing number of leaves susceptible to eCO$_2$ stimulation resulted in limited whole-tree photosynthetic stimulation at the end-of-season (Figure 2.1), as consistently observed in *Populus* x *euramericana* (Curtis et al. 1995)*, Betula pendula* (Rey and Jarvis 1998)*, Fagus sylvatica* (Epron et al. 1996), *Liquidambar styraciflua* (Herrick and Thomas 2003) and *Tilia americana* (Li et al. 2019b) (Table 2.1). Therefore, the magnitude of eCO$_2$-induced stimulation of A$_n$ in deciduous species is not constant but varies over time and with leaf age (Figure 2.2a).

Table 2.1 Overview of studies evaluating time dependent (dynamic) or independent (non-dynamic, ND) tree responses to elevated atmospheric CO_2 concentration (eCO_2) at leaf and whole-tree scale. Dynamic responses are classified into end-of-season down-regulation (seasonal acclimation, A), or environmental induced seasonality (S).

A series of carbon-related (net carbon assimilation A_n, leaf area $_{LA}$, leaf area index $_{LAI}$, leaf growth rate $_{LGR}$, projected leaf area $_{PLA}$, leaf or tree dry weight $_{DW}$, tree volumetric growth rate $_{VGr}$, stem basal area $_{BA}$, tree volume $_V$, net ecosystem carbon exchange $_{NEE}$) and water-related (stomatal conductance g_s, whole-tree transpiration Tr, canopy conductance $_{gc}$, sap flow $_{Sf}$, sap flux density $_{Sfd}$, evapotranspiration $_{ET}$) variables are compiled (subscript). Overall stimulation ($^+$), inhibition ($^-$) or neutral effect (^{0}) of eCO_2 is indicated (superscript). Imposed CO_2 levels for the ambient (aCO_2) and highest eCO_2 treatment are shown and expressed in ppm ($^†CO_2$ levels were converted from Pa to ppm at standard atmospheric pressure, na when no concentration available). Tree age or size and growing conditions (in closed container or pot (P) or in open soil (S)) are indicated.

Tree characteristics			CO$_2$	Leaf		Tree			Remarks	Reference
				A$_n$	g$_s$	Leaf	Growth	Tr		
Four *Populus* clones	15 cm	P	350 – 700			A_{LA}^+	A_{DW}^+			Radoglou and Jarvis (1990)
Populus grandidentata	0 yr	P	361 – 707	A^+	ND^-	ND_{LA}^+	ND_{DW}^+		Delayed senescence suggested by lack of late season A_n decline	Curtis and Teeri (1992)
Liriodendron tulipifera	1-4 yr	S	348 – 653	A^+	ND^0					Gunderson et al. (1993)
Quercus alba	1-4 yr	S	348 – 653	A^+	ND^0					Gunderson et al. (1993)
***Picea rubens* Sarg.**	0 yr	P	374 – 714	A^+	ND^0				Includes different nutrient and water regimes	Samuelson and Seiler (1994)
Castanea sativa	2 yr	P	350 – 700	A^+		ND_{LA}^+	A_{An}^+		Includes different nutrient regimes	El Kohen and Mousseau (1994)
Populus x euramericana	5.2 gram	S	340 – 684	A^+		ND_{LA}^+	ND_{DW}^+		Includes different nutrient regimes	Curtis et al. (1995)

Species	Duration	P/S	CO_2 range					Comments	Reference
Fagus sylvatica	2 yr	P	$aCO_2 - aCO_2 +350$	A^+	ND^0	ND^+_{LA}	ND^+_{DW}		Epron et al. (1996)
Pinus radiata	1 yr	S	$375 - 632^†$	ND^+					Hogan et al. (1996)
Nothofagus fusca	1 yr	S	$375 - 632^†$	A^+					Hogan et al. (1996)
Pinus taeda	1-2 yr	P	$361 - 657^†$	A^+					Lewis et al. (1996)
Mangifera indica	1-4 yr	S	$na - 700$	S^+	S^-	ND^0_{DW}	ND^+_{DW}	VPD regulates eCO_2 effects	Goodfellow et al. (1997)
Pinus taeda	9 yr	S	$358 - 741$	A^+	ND^0			Includes leaf age effect and different nutrient and water regimes	Murthy et al. (1997)
Pinus taeda	0-4 yr	S	$361 - 657^†$	A^+	A^-	ND^+_{LA}	ND^+_{DW}		Tissue et al. (1997)
Fagus sylvatica	2-3 yr	S	$370 - 570$	A^+	A^-	ND^0_{DW}	ND^+_{DW}		Egli et al. (1998)
Picea abies	4 yr	S		A^+	A^-	ND^+_{DW}	ND^+_{DW}		
Betula pendula	4 yr	S	$350 - 700$	A^+	ND^-				Rey and Jarvis (1998)
Pinus sylvestris	5 yr	S	$350 - 750$	A^+				$eCO_2 \times$ needle age interaction	Jach and Ceulemans (2000)
Three *Populus* species	na	S	$na - 544$			A^+_{LGR}			Ferris et al. (2001)
Three *Quercus* species	2 yr	S	$379 - 704$	A^+				Relative eCO_2 response is species dependent	Ainsworth et al. (2002)

	Age	S/P	CO_2						Notes	Reference
Scrub-oak ecosystem	3-5 yr	S	360 – 710			A^+_{LAI}				Hymus et al. (2002)
Liquidambar styraciflua	12 yr	S	394 – 538		A^-			S^-_{gc}	VPD and soil water content regulate eCO_2 effects	Wullschleger et al. (2002)
Fourteen deciduous forest trees	80-120 yr	S	365 – 520		ND^-			S^-_{Sfd}	VPD and soil water content regulate eCO_2 effects	Cech et al. (2003)
Liquidambar styraciflua	8-12 m	S	379 – 574	A^+	ND^0	ND^0_{LA}			eCO_2 × leaf age and eCO_2 × leaf location interactions	Herrick and Thomas (2003)
Citrus aurantium	14 yr	S	aCO_2 + 300	A^+	A^+					Adam et al. (2004)
Liquidambar styraciflua	15-16 m	S	362 – 556	A^+						Sholtis et al. (2004)
Larix kaempferi	2 yr	P	360 – 720	ND^+			A^+_{VGr}		Incudes different nutrient regimes	Yazaki et al. (2004)
Pinus sylvestris	30-33 yr	S	na – 730			A^+_{PLA}		A^-_{Sf}	LA x g_c interaction regulates eCO_2 effects	Wang et al. (2005)
Picea mariana	0 yr	P	365 – 700[†]	A^+			A^+			Bigras and Bertrand (2006)
Pinus taeda	14 m	S	386 – 582				A^+_{BA}			Moore et al. (2006)
Four understory tree saplings		S	380 – 580	A^+						Springer and Thomas (2007)

| Species									Notes	Reference
Picea Abies	> 6.5 m	S	365 – 700	A^+					Temperature regulated A_n stimulation	Uddling and Wallin (2012)
Eucalyptus globulus	9.5 m	S	390 – 630	A^+	ND^0	ND_{DW}^+	A_V^+		No eCO₂ × temperature interaction	Quentin et al. (2015)
Fagus sylvatica	3 yr	S	400 - 700	A^+	ND^-				eCO₂ × ultraviolet radiation interaction changes over season	Urban et al. (2019)
Tilia americana	2 yr	P	400 – 800	A^+	ND^0	A_{LA}^+	A_{An}^+		Advanced senescence under eCO₂ and eCO₂ × leaf age interaction	Li et al. (2019)
Coffea arabica	4 yr	S	400 – 550	A^+	ND^0					Sanches et al. (2020)
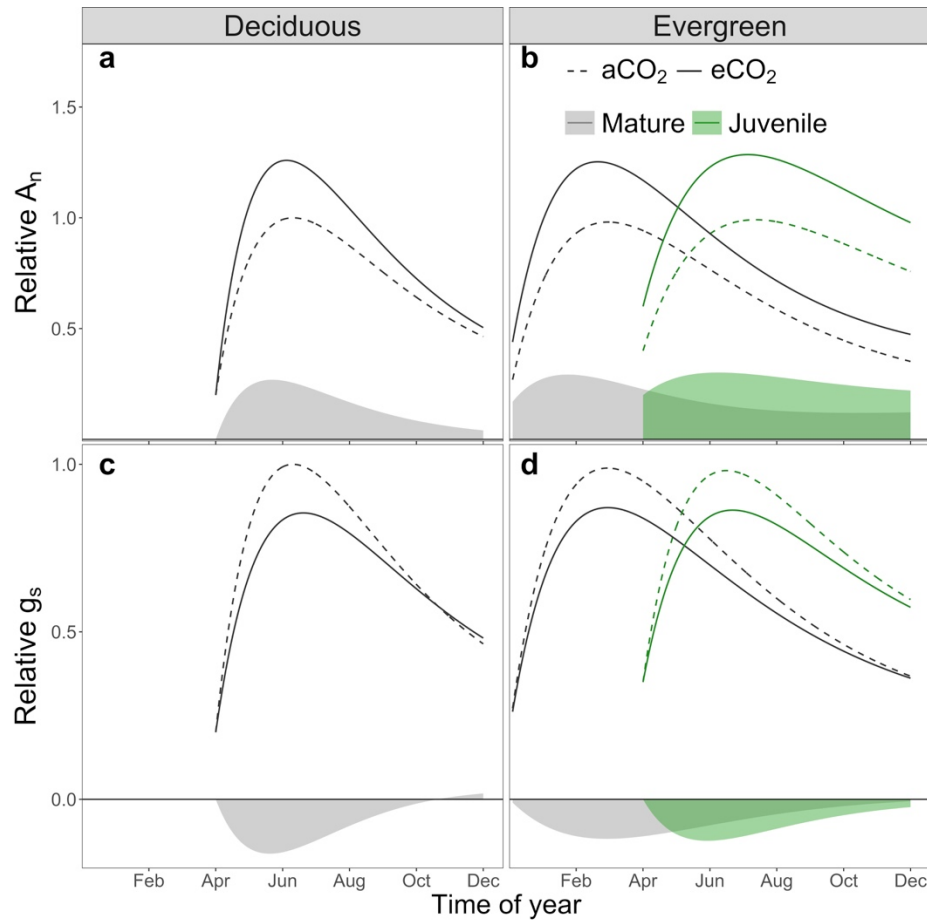
Figure 2.2 Relative seasonal leaf scale dynamics of (a-b) net carbon assimilation rate (A_n) and (c-d) stomatal conductance (g_s) of deciduous (left hand-side panels) and evergreen (right hand-side panels) tree species under ambient (aCO_2) and elevated (eCO_2) atmospheric CO_2 concentration.

Distinction between mature (black) and juvenile (green) foliage is made for evergreen species. The eCO_2 effect over time (defined as the difference between the eCO_2 and aCO_2 values) in the northern hemisphere is shown by the filled area. This schematic does not match seasonality in southern hemisphere forests. Trends in A_n, g_s, and subsequent eCO_2 effect give a schematic overview summarizing observations on seasonal leaf scale dynamics under eCO_2 (Table 2.1). A_n and g_s dynamics are represented with a non-rectangular hyperbola following Xu et al. (2019) and scaled with maximal A_n and g_s under aCO_2.

Evergreen tree species also show a seasonal and age-dependent A_n response to eCO_2 (Figure 2.2b). For mature (one-year old) *Pinus taeda* foliage, the rate of A_n monthly increase was stimulated with increasing atmospheric [CO_2] during winter months (January – March in the northern hemisphere) (Figure 2.3a). A_n rates subsequently declined during spring (March – June) and summer (June – September) in all [CO_2] treatments. Even though eCO_2 stimulation remained significant until September, the A_n reduction was faster under highest eCO_2 in spring and in both eCO_2 treatments during summer (Murthy et al. 1997). A different seasonal pattern was observed in juvenile (current-year) foliage

(Figure 2.3a): A_n gradually increased during late spring and summer under all $[CO_2]$ treatments, with a faster and stronger stimulation with increasing $[CO_2]$ (Murthy et al. 1997). In all needles and measurement periods, eCO_2 stimulated A_n, but A_n stimulation was largest in May for mature needles whereas maximal stimulation for juveniles was observed in September (Jach and Ceulemans 2000). When measurements were conducted after multiple-year exposure to eCO_2, lack of A_n acclimation was observed over three (Lewis et al. 1996) and four (Tissue et al. 1997, Turnbull et al. 1998) years in juvenile *P. taeda* and *P. radiata* needles. In mature needles, however, down-regulation of A_n stimulation under eCO_2 did occur, supporting the idea that in evergreen conifer trees eCO_2 stimulation reduces with needle age, rather than with tree age (Figure 2.2b) (Turnbull et al. 1998). Stimulation of A_n in two evergreen broadleaf trees, *Nothofagus fusca* and *Eucalypus globulus*, showed high resemblance with deciduous species. Maximum stimulation was registered in summer and early-autumn, followed by a decrease, or complete cessation of eCO_2 stimulation in winter (Hogan et al. 1996, Quentin et al. 2015). Likewise, in mature *Coffea arabica* leaves, the eCO_2 induced stimulation in A_n was stronger in summer (121 %) than in winter (45 %) (Sanches et al. 2020).

In concert with eCO_2 stimulation of A_n, the commonly observed g_s reduction also varies throughout the season (Figure 2.2c,d), although a constant response of g_s to eCO_2 is not uncommon (Table 2.1; 13 out of 19 cases). In deciduous tree species, largest g_s inhibition in *Liquidambar styraciflua* was observed trees in early and mid-summer, when A_n reached highest rates, followed by a reduction in eCO_2 effect in late summer and autumn (Figure 2.3b; Wullschleger et al. 2002). In evergreen tree species, the limiting effect of eCO_2 on g_s is commonly maintained for longer periods even though its magnitude is smaller (Figure 2.2d; Tissue et al. 1997). This difference in stomatal eCO_2 response between deciduous and evergreen species was also observed in *Fagus sylvatica* and *Picea abies* trees: in spruce, the g_s reduction in the current-year shoots was only observed in late summer, while g_s in beech reduced during late summer and autumn (Egli et al. 1998).

Regardless of evergreen or deciduous leaf type, the magnitude of the eCO_2 response on g_s is highly dependent on the environment as both soil and atmospheric drought influence the stomatal response to eCO_2 (Purcell et al. 2018). With increasing vapor pressure deficit (VPD) or decreasing soil water content, trees reduce g_s to limit water loss and prevent hydraulic failure (e.g., Grossiord et al. 2020; Menezes-Silva et al. 2019). The magnitude of g_s reduction under eCO_2 depends on the intensity of drought stress to which the tree is exposed. Mild stomatal response to eCO_2 might be expected when absolute g_s rates are low due to water shortage (Ainsworth and Rogers 2007). Under hot and dry conditions, g_s

can even increase under eCO_2, possibly as a result of prior water-savings, challenging the well-established idea of consistent g_s reduction under eCO_2 (Purcell et al. 2018).
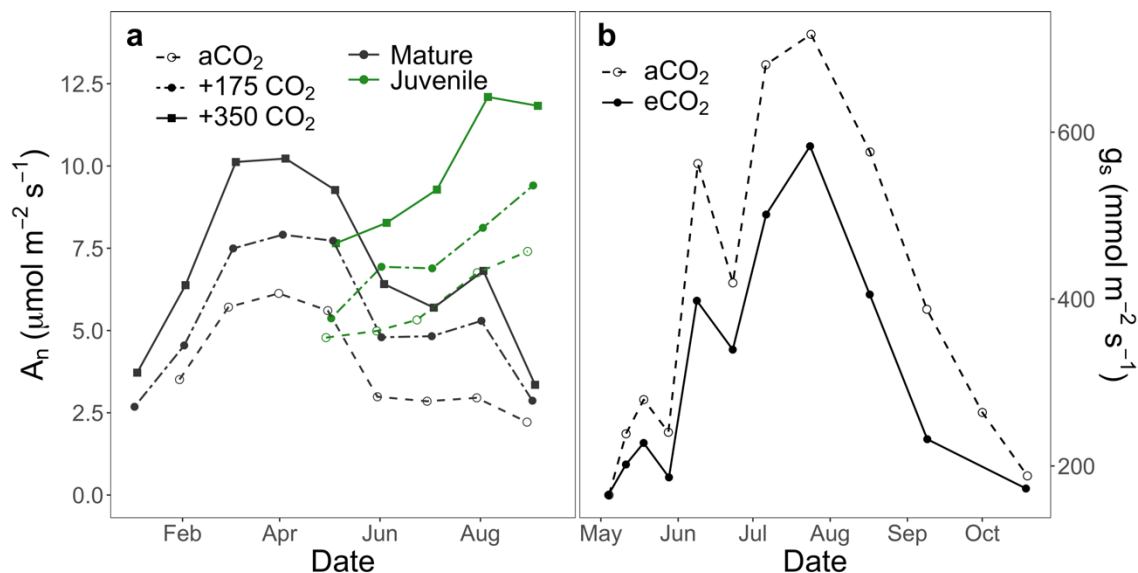

Figure 2.3 Seasonal measurements of (a) net assimilation rate (A_n) of mature (one-year-old, black) and juvenile (current year, green) *Pinus taeda* needle cohorts under three CO_2 treatments (with aCO_2 being 385 ppm) and (b) stomatal conductance (g_s) of *Liquidambar styraciflua* under ambient (aCO_2, 394 ppm) and elevated (eCO_2, 538 ppm) CO_2 growing conditions.

Figures modified from Murthy et al. (1997) and Wullschleger and Norby (2001).

Leaf development under eCO_2

Leaf development is crucial for light capturing, photosynthetic assimilation, and thus tree growth and survival. Despite some degree of discrepancy among studies, eCO_2 commonly stimulates development of canopy LA following a greater number of leaves, an increased area per individual leaf, or a combination of both (reviewed by Pritchard et al. 1999; Table 2.1; 12 out of 15 cases). Stimulation of foliar growth by eCO_2 is especially pronounced in early stages of leaf development. For instance, three *Populus* species showed a 13 to 30 % increase in foliar growth rate during the first week of leaf development under eCO_2 relative to aCO_2 (Figure 2.4; Ferris et al. 2001). The subsequent stage of leaf development was characterized by lower growth rates under both [CO_2] treatments, with a limited stimulation and even reduced leaf growth under eCO_2 relative to aCO_2 (from +16 % to -25 %) (Ferris et al. 2001). Also in evergreen *Quercus suber* seedlings, leaf area, leaf dry weight and leaf thickness was only stimulated during the first six months of exposure to eCO_2 conditions, after which differences in leaf morphology between [CO_2]

treatments disappeared (Vaz et al. 2012). In a natural stand of 30-year old *Pinus sylvestris* trees, eCO_2 increased the total projected foliage area by 5.7 %, 2.8 % and 2.2 % during three consecutive years due to an increase in needle size and number (Wang et al. 2005). Differences in canopy LA in this pine stand between $[CO_2]$ treatments varied over the year, with largest and smallest differences being observed in early summer and autumn, respectively.

During the course of leaf ontogeny, leaf growth constraints are expected to switch from being metabolically (C) to hydraulically (water) controlled (Pantin et al. 2012). The relatively strong early season eCO_2 effect on leaf size might be partly explained by stimulated A_n and subsequent cell division promoted by C surplus. The modest late season stimulation of leaf size might be driven by reduced g_s and leaf water loss, improving cell water status and facilitating turgor-driven cell expansion (Steppe et al. 2015). Cell wall properties may, however, also be altered under eCO_2 (Pantin et al. 2012) consequently affecting cell expansion. In general, an increase in cell wall extensibility is expected under eCO_2 via expression of cell-wall loosening genes and down-regulation of secondary wall construction enzymes (Gamage et al. 2018). Increased cell wall extensibility was, however, only observed in young but not in old *Populus* × *euramericana* leaves under eCO_2 (Taylor et al. 2003). The absence of late season eCO_2-induced stimulation of leaf growth, despite the above-mentioned improved cell water status, might be the result of a decrease in cell wall extensibility, precluding turgor-driven cell expansion (Lockhart 1965).
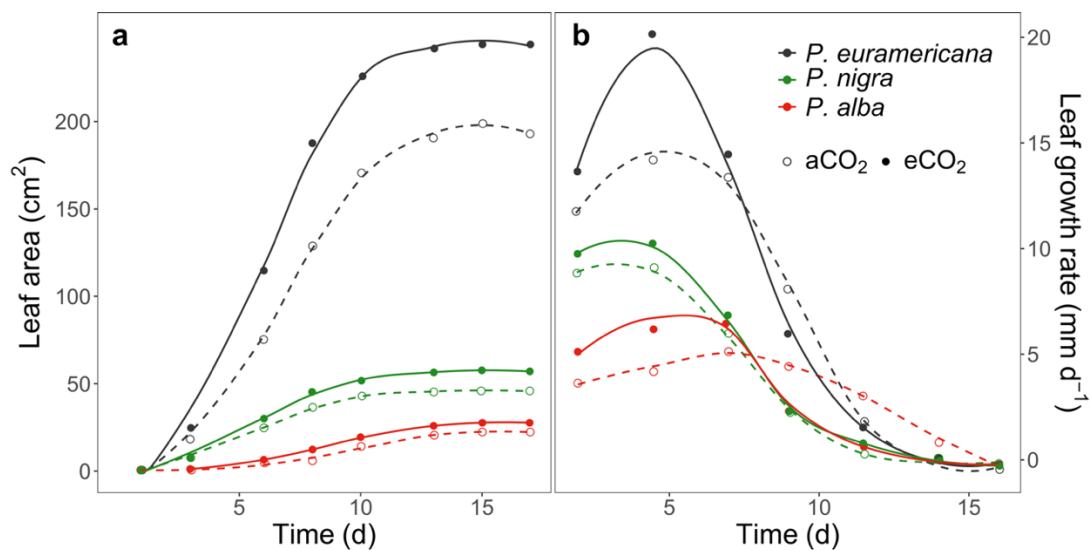

Figure 2.4 Individual (a) leaf area and (b) leaf growth rates of *Populus euramericana*, *P. nigra*, and *P. alba* over time under ambient (aCO_2) and elevated (eCO_2, 550 ppm) CO_2 growing conditions.

Modified from Ferris et al. (2001).

From leaf to whole-tree scale under eCO$_2$

Canopy area

Scaling leaf observations to the whole-tree and ecosystem scale is crucial to predict global C exchange in terrestrial biosphere models (Fatichi et al. 2016, Wu et al. 2016). This requires detailed information on canopy LA development and its dependence on biotic and abiotic conditions including CO$_2$ levels (Ewert 2004). Canopy LA generally increases under eCO$_2$ (Figure 2.1 and 2.5a; Table 2.1; 12 out of 15 cases). However, most of these observations have been obtained from growing seedlings planted in growth chambers or greenhouses, where atmospheric [CO$_2$] can be easily manipulated. Methodological feasibility has therefore resulted in a biased understanding of leaf and canopy development under eCO$_2$, which might hinder extrapolation to natural forests (Becklin et al. 2017). In the few cases where natural mature systems have been studied, the magnitude of the leaf area index (LAI) response to eCO$_2$ is smaller and observations are contradictory (Figure 2.5b, Table 2.2). Leaf area index increased under eCO$_2$ in two hardwood forests (McCarthy et al. 2007, Uddling et al. 2008), a scrub-oak ecosystem (Hymus et al. 2002) and in *Populus* spp. (Liberloo et al. 2006) and *Citrus* spp. (Kimball et al. 2007) plantations. Contrastingly, a neutral eCO$_2$ effect on LAI has been reported in a deciduous *L. styraciflua* forest (Norby et al. 2003) and a native evergreen *Eucalypus* woodland (Duursma et al. 2016), whereas even LAI reductions were transiently observed in a mixed temperate forest (Asshoff et al. 2006) (Table 2.2, Figure 2.5a,b). Correct estimation of LAI remains therefore essential to determine light interception throughout different canopy layers and thus whole-tree dynamics under eCO$_2$ (Duursma and Mäkelä 2007). In this line, and for experimental simplicity, substantial literature regarding the effect of eCO$_2$ on leaf photosynthesis is performed under light saturating conditions independed of leaf light availability (e.g. Ainsworth and Rogers 2007, Reich et al. 2018, Crous et al. 2021) hence resulting in highest values of potential photosynthetic simulation. Nevertheless, stimulation in leaves located in lower canopy layers might be substantially smaller, as photosynthetic rates might be limited to a greater extent by the rate of light reactions, required for the regeneration of Ribulose 1,5-bisphosphate (RuBP). For instance, the relative stimulation of A$_n$ in shade leaves of 7-11 m tall *Liquidambar styraciflua* trees was only half of the stimulation in sun leaves (Herrick and Thomas 1999). Likewise, for two *Populus* clones, stimulation of whole canopy photosynthesis under eCO$_2$ could largely be attributed to the increase of LAI rather than by enhanced leaf-level stimulation (Chen et al. 1997). Correspondingly for plant water use, increased LAI resulted in higher self-shading in *Quecus myrtifolia* trees and a consequent inhibition of whole-tree

36

transpiration as an indirect effect of eCO$_2$ while stomatal regulation remain unaltered (Li et al. 2003).
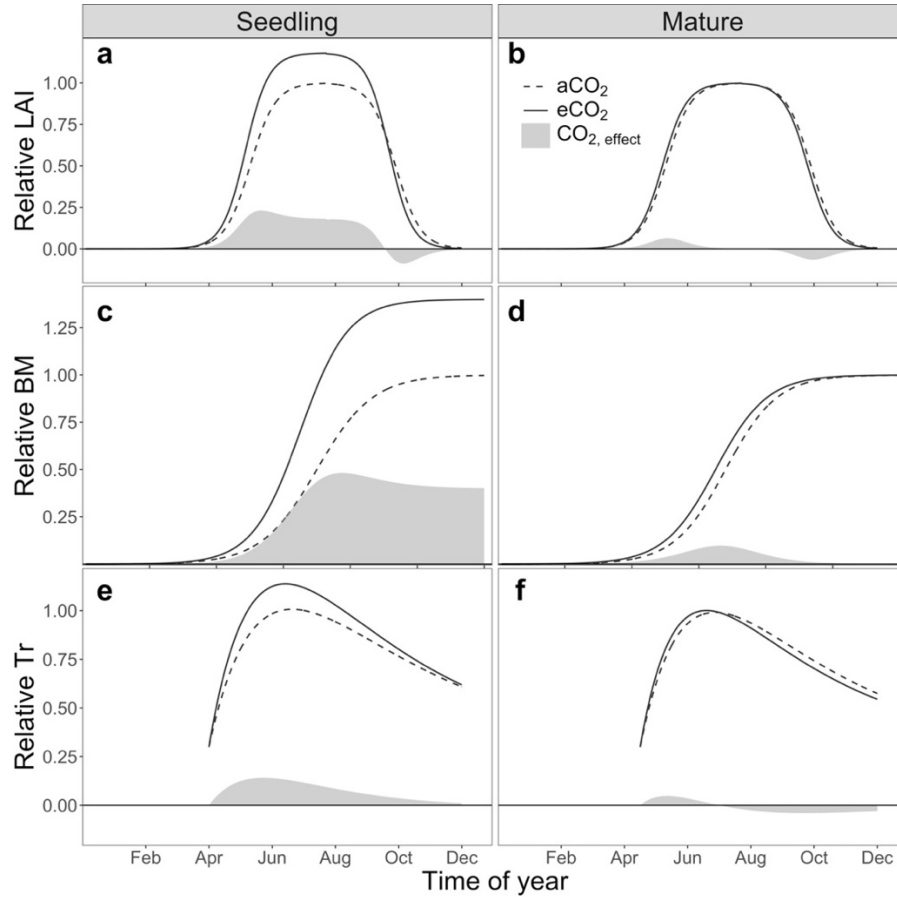

Figure 2.5 Relative whole-tree seasonal dynamics of the (a-b) leaf area index (LAI), (c-d) tree biomass (BM), and (e-f) tree transpiration (Tr) under ambient (aCO$_2$) and elevated (eCO$_2$) atmospheric CO$_2$ concentration for relatively CO$_2$-susceptible (seedling, left hand-side panels) and less susceptible (mature, right hand-side panels) deciduous tree species.

The eCO$_2$ effect over time (i.e., difference between eCO$_2$ and aCO$_2$ values) in the northern hemisphere is shown by the filled area. This schematic does not match seasonality in southern hemisphere forests. Trends in LAI, BM, and T illustrate a simplified and schematic overview, recapitulating observations on seasonal whole-tree dynamics under eCO$_2$ (Tables 2.1 and 2.2). LAI and BM dynamics are represented with a single (BM) or combined sigmoid growth curve, T dynamics are represented with a non-rectangular hyperbola following Xu et al. (2019). All variables are scaled relative to maximal values under aCO$_2$.

Under changing climate conditions, leaf phenology (i.e. leaf unfolding, senescence, and life span) might also be altered, affecting the relationship between leaf scale measurements and whole-tree annual performance (Sigurdsson 2001a). Three decades of satellite data from a large part of the northern hemisphere suggests lengthening of the

growing season due to an earlier spring leaf unfolding and a delayed autumn senescence (Piao et al. 2019). Increased temperature is assumed to be the most important regulator, but also soil nutrient availability, precipitation shifts and atmospheric $[CO_2]$ are used to explain changes in canopy phenology (Cleland et al. 2007, Ge et al. 2015, Gill et al. 2015, Piao et al. 2019). In any case, current understanding of the response of canopy phenology to eCO_2 remains limited. Only a mild or neutral effect of eCO_2 on bud-break timing has been observed (e.g. Epron et al. 1996, Jach and Ceulemans 1999, Cavender-Bares et al. 2000, Sigurdsson 2001a, Bigras and Bertrand 2006), while the onset of autumn leaf senescence can be either delayed (Cavender-Bares et al. 2000, Taylor et al. 2008, Duursma et al. 2016) or accelerated (Figure 2.5a,b; Li et al. 2019b; Sigurdsson, 2001a) under eCO_2.

Tree biomass production and water use

While there is general consensus that gross primary production (GPP) is enhanced by eCO_2 at leaf and tree canopy scale (Table 2.1 and 2.2), parallel increases in net primary production (NPP) in mature trees and in environments with nutrient and water limitations are far less certain (Norby et al. 2016), with only five of the seventeen eCO_2 experiments compiled in Table 2.2 reporting an overall NPP stimulation. As a result of stimulated photosynthesis and carbohydrate availability under eCO_2, most studies performed on seedlings and young growing trees found an increase in stem or branch growth (Pritchard et al. 1999, Moore et al. 2006, Dawes et al. 2014). Growth can be stimulated under eCO_2 throughout the growing season (Moore et al. 2006, Quentin et al. 2015), but especially during spring and early summer (Figure 2.5c), when photosynthetic stimulation is stronger (Figure 2.2a,b) (Radoglou and Jarvis 1990, Yazaki et al. 2004).

However, discrepancies between leaf A_n stimulation and the wide range of growth responses in mature trees under eCO_2 (Table 2.2) suggest that assimilated C can be allocated to different sinks, with C sequestration (biomass production) being just one of them (De Lucia et al. 2007, Collalti and Prentice 2019). For example, eCO_2 had a neutral effect on stem basal area of five 35-m tall deciduous tree species (Asshoff et al. 2006); 110-year-old *Picea abies* did not show eCO_2-induced stimulation in tree growth or foliar and fine root production (Klein et al. 2016); and aboveground NPP in *Eucalyptus* trees, integrating foliar and wood growth, did not change under eCO_2 (Ellsworth et al. 2017) (Figure 2.5b,d). Because eCO_2 commonly stimulates foliar photosynthetic capacity, GPP did increase in these eCO_2 experiments (Table 2.2) pointing towards a missing C sink. The fate of this C surplus, taken up by the tree but not invested in growth metabolism, remains largely unknown (De Kauwe et al. 2014). Only recently, the first ecosystem C-

budget has been closed after a four-year FACE experiment performed in *Eucalyptus* trees. This indicated that despite the GPP stimulation at the canopy scale, parallel enhancement of ecosystem respiratory fluxes resulted in homeostatic ecosystem NPP (Jiang et al. 2020). Enhanced C transport belowground and rapid soil C turnover (Drake et al. 2011) resulted in greater soil (mostly heterotrophic) respiration, which accounted for half of the C surplus. In addition, autotrophic respiration could also constitute a significant sink of the C surplus (reviewed by Dusenge et al. 2019). Tree respiration consumes a large portion of total tree C gain, with NPP:GPP ratios ranging from 0.22 to 0.79 (Collalti and Prentice 2019), and largely determining tree and ecosystem C use efficiency (Valentini et al. 2000, Piao et al. 2010, Drake et al. 2016, 2019). Notwithstanding, we poorly understand how respiration responds to eCO_2 at the whole-tree scale, which seems to be highly variable in relation to abiotic and biotic drivers determining overall tree metabolism, supply of respiratory substrates and demand for respiratory products (Smith 2017, Dusenge et al. 2019, Salomón et al. 2019). Therefore, studies in mature forests suggest C-saturation (possibly induced by nutrient or water limitation; Fatichi et al. 2014) for tree growth under eCO_2 and question the commonly accepted predominance of C supply as a controlling driver for biomass production (Körner 2015, Jiang et al. 2020).

Predictions of limited whole-tree water use under eCO_2 conditions are endorsed by observations of reduced g_s at the leaf scale (Table 2.1). Nonetheless, no straightforward translation exists between leaf and whole-tree water use, since the latter is largely affected by canopy LA (Figure 2.1; Fatichi et al. 2016; Tor-ngern et al. 2015). A modelling study on eCO_2 effects across a variety of ecosystems, highlighted the contrast between leaf scale g_s reductions (-5 to -15 %) and the roughly homeostatic whole-tree water use (0 to -5 %) under eCO_2 (Fatichi et al. 2016). Only when eCO_2 induces a sufficiently strong reduction in leaf g_s, which outweighs the potential stimulation in canopy LA or potentially greater atmospheric evaporative demand, a water-saving effect can be expected at the whole-tree scale (Norby and Zak 2011, Fatichi et al. 2016). From the eCO_2 experiments compiled in Table 2.2, four, four and three studies reported increased, neutral and reduced whole-tree water use, respectively. This highlights the current uncertainty regarding the effect of eCO_2 on tree water use (i.e. canopy transpiration quantified as sap flow), which might be largely dependent on site-specific conditions. For instance, in an *Eucalyptus* woodland, canopy LA did not respond to eCO_2 (Duursma et al. 2016), g_s reduction was limited to non-drought-stress periods (Gimeno et al. 2016), but tree transpiration on yearly basis remained unaffected (Gimeno et al. 2018). In a mixed *P. tremuloides* and *B. papyrifera* forest, eCO_2 had a highly variable effect on g_s (Darbah et al. 2010) and LAI stimulation led to an overall increase in whole-tree water use (Uddling et al. 2008).

Table 2.2 Overview of leaf (stomatal conductance g_s, net carbon assimilation A_n) and whole-tree (canopy area L, growth and transpiration Tr) responses (neutral response 0, inhibition -, stimulation +) under elevated atmospheric [CO_2] (eCO_2). The compiled dataset consists of free soil CO_2 enrichment experiments of more than one year in duration, for which leaf and whole-tree measurements are available. Experimental eCO_2 target concentrations (eCO_2, ppm) and species or ecosystem under investigation are indicated. Three experimental set-ups are distinguished: closed treatment chambers (CTC), free-air CO_2 enrichment (FACE) and open-top treatment chambers (OTC).

Site	Species or ecosystem	Set-up and eCO2		Leaf		Tree			References
				A_n	g_s	L	G	Tr	
Aspen FACE	Mixed northern hardwood plantation	FACE	560 ppm	+ [2]	- to + [2]	+ [1]	+ [1]	+ [1]	[1]Uddling et al. (2008), [2]Darbah et al. (2010)
Birmensdorf	*Fagus sylvatica* and *Picea abies*	OTC	590 ppm	+ [1]	- [1]	0 to + [1,2]	- to + [1,2,3]	-[1] to + [2]	[1]Egli et al. (1998), [2]Sonnleitner et al. (2001), [3]Spinnler et al. (2003)
EucFACE	Native evergreen *Eucalyptus* woodland	FACE	aCO2 +150 ppm (≈ 540 ppm)	0 to + [2]	- to 0 [2]	0 [1]	0 [4]	0 [3]	[1]Duursma et al. (2016), Gimeno et al. [2](2016), [3](2018), [4]Ellsworth et al. (2017)
Duke FACE	Mixed hardwood forest	FACE	aCO2 +200 ppm (≈ 572 ppm)	+ [3]	- [1,4]	+ [2,5]		0 [5]	[1]Herrick et al. (2004), [2]McCarthy et al. (2007), [3]Ellsworth et al. (2012), [4]Ward et al. (2013), [5]Tor-ngern et al. (2015)
Flakaliden	*Picea abies*	CTC	700 ppm	+ [2]	0 [1,2]	+ [2]	0 [2]	0 to + [1,2]	[1]Hasper et al. (2016), [2]Klein et al. (2016)

Site	Species	Type	CO₂						References
Glendevon	*Alnus glutinosa*	OTC	700 ppm	+ [1]		0 [1]	+ [1]		Temperton et al. (2003)[1]
Gunnarsholt	*Populus trichocarpa*	CTC	700 ppm	+ [2,3]	0 [2,3]	0 to + [1]	0 to + [4]		Sigurdsson, [1](2001a), [2](2001b), [3](2002), [4]Sigurdsson et al. (2001)
Mekrijärvi	*Pinus sylvestris*	CTC	600 ppm	+ [2]	- [3]		+ [1]		Peltola et al. (2002), Wang et al. [2](1995), [3](1997)
Merritt Island	Shrub-Oak ecosystem	OTC	+ 350 ppm	0 to +[1,5]	-[6]	+[3,6]	0 to + [2,4,7]		Ainsworth et al. (2002)[1], [2]Dijkstra et al. (2002), Hymus et al. [3](2002), [4](2003), Li et al. [5](1999), [6](2003), Seiler et al. [7](2009)
ORNL FACE	*Liquidambar styraciflua*	FACE	565 ppm (day) 645 ppm (night)	0 to + [3,4]	- to 0 [1]	0 [2]		- [1]	[1]Wullschleger et al. (2001), [2]Norby et al. (2003), [3]Sholtis et al. (2004), [4]Warren et al. (2015)
POP- and EUROFACE	*Populus* plantation	FACE	550 ppm	+ [3,4]	- [5,6]	+ [1,2,3]	0 to + [2,3]	+ [6]	[1]Ferris et al. (2001), Liberloo et al. [2](2005), [3](2006), [4](2007), Tricker et al. [5](2005), [6](2009)
SCBG	Subtropical forest	OTC	700 ppm	+ [2]	- [2]		+ [1,3]		[1]Deng et al. (2010, [2]Li et al. (2013), [3]Liu et al. (2011)
Suonenjoki	*Betula pendula*	OTC	2 x aCO₂ (≈ 700 ppm)	+ [2]	- [3]	0 to + [1]	0 to + [1]		Riikonen et al. [1](2004), [2](2005), [3](2008)
UMBS	*Populus* species	OTC	720 ppm	+ [1]		0 [1]	0 [1]		[1]Kubiske et al. (1998)

USDA	*Pinus ponderosa* and *P. taeda*	OTC	aCO_2 +350 ppm (≈ 700 ppm)	+[4]	0[2]	0 to +[2,3]	0 to +[1,3]		[1]Johnson et al. (1998), [2]Maherali et al. (2000), [3]Tingey et al. (1996), [4]Tissue et al. (1999)
USDA	*Citrus aurantium*	OTC	aCO_2 +300 ppm	+[1]	0 to +[1]	+[2]	+[1,2]		[1]Adam et al. (2004), [2]Kimball et al. (2007)
Web-FACE	100-yr-old mixed forest stand	FACE	550 ppm	+[1]	0[3]	- to +[2]	0 to +[2]	-[4]	[1]Zotz et al. (2005), [2]Asshoff et al. (2006), [3]Keel et al. (2007), [4]Leuzinger et al. (2007)

Likewise, transpiration in *Populus* trees increased as a result of enhanced canopy LA despite a g_s reduction observed at the leaf scale (Tricker et al. 2009). In a mixed hardwood forest, g_s reduction compensated canopy LA increase, leaving tree transpiration unaffected under eCO_2 (Ward et al. 2013, Tor-ngern et al. 2015). In a *L. styraciflua* stand, eCO_2 reduced both g_s and tree transpiration (Wullschleger and Norby 2001).

Adding further complexity, the response of g_s, tree transpiration and canopy LA to eCO_2 varies over time (Figure 2.2 and 2.5; Wullschleger et al. 2002a, Wang et al. 2005, Tor-ngern et al. 2015). During a single growing season, g_s and canopy conductance g_c (calculated from the Penman–Monteith equation) in *L. styraciflua* trees showed different behaviour, with relatively stronger eCO_2-induced reductions in g_s and a more variable g_c response, largely dependent on environmental factors (Wullschleger et al. 2002a). Inter-annual variability has also been reported: transpiration in *P. sylvestris* was enhanced during the first year of eCO_2 exposure as a result of an increase in canopy LA, but during the two following years transpiration was reduced as result of a relatively larger reduction in g_s and g_c (Figure 2.5e,f; Wang et al. 2005). Attenuation or alteration of leaf scale responses at the whole-tree scale highlight the importance of combining measurements at different spatial scales to realistically predict tree hydraulic regulation under eCO_2 (Wullschleger et al. 2002a, Norby and Zak 2011).

Drivers of temporal variability in eCO_2 responses

Carbon balances drive patterns under well-watered conditions

Under unlimited water availability, two drivers can be identified to explain temporal variability in the CO_2-fertilization effects on tree functioning. Firstly, eCO_2 shifts the balance between C sources and C sinks throughout the season (Figure 2.1, see seasonal positive and negative feedbacks in relation to C sink strength). Increased atmospheric CO_2 availability promotes photosynthesis providing additional C to the tree. During the early season vegetative stages, growth and development of different tree organs (leaves, stem, roots and seeds) increase C sink activity (Gamage et al. 2018). Carbon costs associated to reproductive processes, especially in fruiting trees, can also result in a seasonal increase in C sink demand, which largely varies throughout plant ontogeny (e.g. Fujii and Kennedy 1985, Ribeiro et al. 2012, Mund et al. 2020, Tixier et al. 2020). As a result, the intensity of the eCO_2-induced A_n stimulation in *Jatropha curcas* (Kumar et al. 2014) and *Coffea arabica* (Rakocevic et al. 2020) increased during flowering and fruit ripening. When C sink demand is reduced, e.g. by stoichiometric constraints or environmental drivers, tree growth ceases and sugar accumulation, especially under eCO_2, will trigger down-regulation of RuBisCo activity (Körner,

2015; Li et al. 2019b) resulting in a negative feedback (Figure 2.1). Carbon sink limitation to growth is more likely to occur at the end of the season, for instance due to cooler temperatures or after completion of genetically controlled phenological phases of wood formation, hereby resulting in attenuated eCO_2 stimulation of photosynthesis along the season (Figure 2.1).

Secondly, attenuation of the CO_2-fertilization effect might result from acclimation to new developing conditions when other factors become more limiting for photosynthesis and growth, particularly nutrient deficiency (Sigurdsson et al. 2013), possibly induced or accelerated under eCO_2 by the stimulated growth and hence nutrient demand (Figure 2.1). Down-regulation of A_n stimulation under eCO_2 may result from decreasing nitrogen (N) content in the leaf (Long et al. 2004), as photosynthetic proteins constitute a large fraction of leaf N, with RuBisCo accounting for 20 % of it (Evans and Clarke 2019). Along the season, especially under eCO_2 conditions, leaves can accumulate a disproportionate amount of sugars, leading to a C:N imbalance and potentially limiting A_n (Long et al. 2004, Agüera and De la Haba 2018). Down-regulation of A_n can therefore be more pronounced in soil N-limited conditions (Reddy et al. 2010, Dusenge et al. 2019). Reduced N availability will also trigger N relocation from mature to young leaves, as reflected by a decrease in chlorophyll and carotenoid mass-based concentration with leaf aging, and a higher efficiency of new leaves in utilizing absorbed photons to yield chemical energy (Wujeska-Klause et al. 2019). However, soil N content might not be the most important factor determining tree nutrient limitation, since symbiotic association with fungi may determine to a larger extent tree´s capacity to take up N and P available in the soil in different forms. Accordingly, it has been observed that trees with ectomycorrhizal fungi increase N uptake, hereby enabling CO_2 fertilization and enhancing biomass production despite low soil N availability (Terrer et al. 2016). Although comparatively less studied, leaf phosphorus (P) content is also a key determinant of photosynthetic performance. Compiled data from 314 species suggests that the positive slope of the photosynthetic capacity with increasing soil N content will be affected by P availability, with a flatter slope under low P levels (Reich et al. 2009). This is because P limitation will reduce RuBisCo carboxylation activity, regeneration of ribulose-1,5 bisphosphate (RuBP), CO_2 diffusion across stomata and mesophyll and the energy transfer to photosystem II (Pandey et al. 2015). According to this observation, stimulation of tree growth (in terms of canopy LA and dry biomass) by eCO_2 in *Eucalyptus* seedlings was positively correlated with the increasing treatment levels of soil P supply (Duan et al. 2019).

Water-restraining strategies take over under drought

When facing drought, trees need to balance the risk of drought-induced hydraulic failure and C starvation to survive (McDowell et al. 2008, Körner 2019), inevitably affecting all leaf and

tree C related processes. Any potential CO$_2$ fertilization effect on tree physiology can therefore drastically change when water becomes limiting (e.g. Warren et al. 2011, Birami et al. 2020). Water, along with C, is necessary to regulate leaf development and growth (Pantin et al. 2012). Especially mature leaves are highly dependent on water availability, as these are relatively prone to wilt when the tree is exposed to drought stress. In comparison, young leaves appear to be more drought-tolerant and maintain high levels of cell turgor under moderate drought stress as a result of better osmotic adjustment (Pantin et al. 2012).

Since stomatal closure is the main mechanism for trees to limit water losses and avoid hydraulic failure (Martínez-Vilalta and Garcia-Forner 2017), drought stress commonly results in g$_s$ reduction (Sperry 2000). Stomatal closure reduces gas exchange and lowers [CO$_2$] in sub-stomatal cavities, hence imposing C restrictions to A$_n$ (Flexas and Medrano 2002). When facing drought under eCO$_2$, stomatal limitations to A$_n$ might be alleviated under eCO$_2$ as higher sub-stomatal [CO$_2$] will be maintained for a given g$_s$ in comparison to aCO$_2$ conditions (Menezes-Silva et al. 2019). As a result, relative eCO$_2$-induced stimulation of A$_n$ can increase under moderate drought stress as observed in *Mangifera indica* trees, where A$_n$ stimulation was greatest during the dry season (Goodfellow et al. 1997). Nevertheless, eCO$_2$ could be a disadvantage as drought stress proceeds. Due to structural overshoot (Jump et al. 2017) or altered xylem characteristics (e.g. increased vessel diameter or reduced wood density) (Domec et al. 2017), eCO$_2$ grown trees might be more susceptible to xylem embolism and hydraulic failure than trees grown under aCO$_2$ (Menezes-Silva et al. 2019). In *P. tremula* seedlings, the reduction in canopy conductance with increasing VPD was faster under eCO$_2$, suggesting higher embolism vulnerability to atmospheric drought stress (De Roo et al. 2020a). In 19-year-old *L. styraciflua* trees, extreme summer drought lowered whole-tree transpiration under both aCO$_2$ and eCO$_2$, but reductions in hydraulic conductance following xylem embolism occurred faster under eCO$_2$, leading to stronger limitations in g$_c$ and GPP, and premature leaf senescence (Warren et al. 2011). Similarly, under moderate drought stress, eCO$_2$ improved leaf scale water use efficiency in *P. halepensis* seedlings, but any favorable effect of eCO$_2$ vanished as drought stress progressed (Birami et al. 2020). Improving the characterization of the role of eCO$_2$ in mitigating or amplifying drought stress responses remains therefore critical to assess future tree behaviour and survival (Menezes-Silva et al. 2019).

Conclusion and future research

This review highlights the variability in magnitude and direction of the eCO$_2$ effect on tree functioning over time (from seasons to years) and between spatial scales (from leaf to whole-

tree scale) as a result of complex interactions among tree C source-sink balance, nutrient and water availability, as well as developmental, reproductive and ontogenetic processes. The widespread temporal variability in the response to eCO_2 across a variety of tree species (Table 2.1), clearly indicates that assessment of leaf and tree behaviour under eCO_2 cannot be limited to single point measurements as these only provide a snapshot of the dynamic tree functioning under future $[CO_2]$ growing conditions. Future studies that aim to better capture tree responses to eCO_2 in the longer term should therefore cover different seasons and developmental stages, preferably at a high temporal resolution. Moreover, large discrepancies between leaf and whole-tree eCO_2 effects (Table 2.2) indicate the limited ability of g_s and A_n measurements to describe whole-tree responses to eCO_2. To improve predictions of vegetation C storage under climate change scenarios, temporal and spatial variability in eCO_2 effects should be considered in tree and ecosystem models. For this, representation of different leaf developmental stages, with different photosynthetic susceptibility to eCO_2, would improve estimates of leaf A_n and whole-tree GPP stimulation in the long term. Moreover, refinement of algorithms determining dynamic C allocation patterns (rather than constant fractions) would be necessary to better constrain the fate of the eCO_2-induced C surplus.

3

Leaf and whole-tree responses of young European aspen trees to elevated atmospheric CO$_2$ vary over the season

Abstract

Elevated atmospheric CO_2 concentration (eCO_2) commonly stimulates net leaf assimilation, decreases stomatal conductance and has no clear effect on leaf respiration. However, effects of eCO_2 on whole-tree functioning and its seasonal dynamics remain far more uncertain. To evaluate temporal and spatial variability in eCO_2 effects, one-year-old European aspen trees were grown in two treatment chambers under ambient (aCO_2, 400 ppm) and elevated (eCO_2, 700 ppm) CO_2 concentrations during an early (spring 2019) and late (autumn 2018) season experiment. Leaf (stomatal conductance, net carbon assimilation and leaf respiration) and whole-tree (stem growth, transpiration and stem CO_2 efflux) responses to eCO_2 were measured. Under eCO_2, carbon assimilation was stimulated during both the early (1.63-fold) and late (1.26-fold) season. Stimulation of carbon assimilation changed over time with largest increases observed in spring when stem volumetric growth was highest, followed by late season down-regulation, when the increase in stem volumetric growth ceased. The neutral eCO_2 effect on stomatal conductance and leaf respiration measured at leaf scale paralleled the unresponsive canopy conductance (derived from sap flow measurements) and stem CO_2 efflux measured at tree scale. Our results highlight that the seasonal variability in carbon demand for tree growth substantially affects the magnitude of the response to eCO_2 at both leaf and whole-tree scale.

Introduction

Atmospheric CO_2 concentration ($[CO_2]$) has been rising rapidly since the industrial revolution (NOAA 2020), causing an overall increase in global mean air temperature and more irregular patterns in the hydrological cycle, hence challenging forests to grow and survive in increasingly harsh environments (Menezes-Silva et al. 2019). Forests are however expected to partially mitigate climate change effects (IPCC 2018) as ~30 % of the anthropogenically emitted CO_2 is taken up through plant photosynthesis (Pugh et al. 2019). To better predict ongoing climate change, it is therefore essential to understand forests' ability to sequester carbon (C) and survive under future climate conditions (Cernusak et al. 2019, Anderegg et al. 2020).

Elevated atmospheric $[CO_2]$ (eCO_2) commonly stimulates net carbon assimilation (A_n) and decreases stomatal conductance (g_s) at the leaf scale (Ainsworth and Rogers 2007, Ainsworth and Long 2020). More uncertainty exists on the response of leaf respiration (R_L) under eCO_2 conditions (Dusenge et al. 2019), precluding closure of leaf C budgets. Studies on R_L have been contradictory, with reports of a positive (e.g. Wang et al. 2001), negative (da Silva et al. 2017) or neutral (e.g. Hamilton et al. 2001, Aspinwall et al. 2017) response to eCO_2. The effect

of eCO_2 on leaf scale processes (A_n, g_s and R_L) has been the main focus of eCO_2 research over the past three decades. Nevertheless, whole-tree responses to eCO_2 determine ecosystem C and water fluxes to a greater extent, and have been comparatively overlooked (Figure 1.3, Becklin et al. 2017). Predictions of whole-tree behaviour under eCO_2 based on leaf scale observations have resulted in large discrepancies (Chapter 2, Table 2.2). For instance, eCO_2-induced stimulation of A_n does not consistently translate into greater biomass production, especially in mature forests, suggesting C availability is not necessarily the most limiting factor for tree growth (Körner 2003, 2015, Palacio et al. 2014). Along the same line, regulation of the respiratory metabolism at the whole-tree scale under eCO_2 remains quite uncertain (Smith 2017, Dusenge et al. 2019) despite its crucial role to determine tree and ecosystem net primary production (Valentini et al. 2000, De Lucia et al. 2007, Collalti and Prentice 2019). For instance, increase in gross primary production in a dry *Eucalyptus* woodland free air CO_2 enrichment (FACE) experiment did not increase net primary production due to parallel stimulation of ecosystem respiratory fluxes (Jiang et al. 2020). Similarly, four years of eCO_2 exposure in a 100-year-old mixed forest did not result in an increased stem growth (Asshoff et al. 2006) despite stimulation of A_n at the leaf scale (Zotz et al. 2005). The same idea applies to water relations. Reductions in g_s under eCO_2 do not necessarily result in water use limitations at the whole-tree scale due to large dependence of whole-tree water use on canopy leaf area (LA), where potential LA stimulation under eCO_2 can offset the decrease in leaf scale water loss (Tor-ngern et al. 2015, Fatichi et al. 2016). As a result, whole-tree water use might decrease (Wullschleger and Norby 2001), increase (Tricker et al. 2009) or remain unaffected (Ward et al. 2013, Tor-ngern et al. 2015) under eCO_2 regardless of the stomatal behaviour at the leaf scale.

Besides the spatial variability, leaf and tree responses to eCO_2 (hereafter 'eCO$_2$ effects') are also dynamic over time. The magnitude and direction of eCO_2 effects vary with leaf age and over a single growing season (Chapter 2). Seasonal canopy and root development, stem biomass production, reproduction, leaf senescence and growth cessation shift the balance between C sources and sinks year-round, affecting tree responsiveness to eCO_2 and feedback mechanisms. As a result, in well-watered *Eucalyptus globulus* trees, eCO_2-induced stimulation of A_n was stronger in summer (+46 %) than in winter (+14 %) (Quentin et al. 2015), and in *Tilia americana* trees A_n stimulation was variable with leaf age and across the season, with strongest eCO_2 effect during spring and in young leaves (Li et al. 2019b). Time-dependent stimulation of A_n under eCO_2 also translated into a dynamic stimulation of stem and whole-tree growth, with stronger eCO_2 effects during spring and summer compared to autumn and winter (e.g. Yazaki et al. 2004, Bigras and Bertrand 2006). Similarly, the magnitude of g_s reduction under eCO_2 has also been observed to vary over the season with strongest g_s

reductions during early and mid-summer, after which the eCO_2 effect dwindled towards the onset of autumn (Tissue et al. 1997, Wullschleger et al. 2002a). Nonetheless, g_s reduction under eCO_2 is not always observed (Xu et al. 2016) and the effect of eCO_2 on g_s can substantially differ depending on the exposure time to eCO_2 (Medlyn et al. 2001), the functional plant type (evergreen vs. deciduous plant species; Medlyn et al. 2001, Dusenge et al. 2019) and the environmental conditions, in particular water availability (Goodfellow et al. 1997), making stomatal behaviour under eCO_2 more difficult to predict.

Further exploration of eCO_2 effects at a fine temporal resolution (on a sub-daily basis) reveals complex interactions among plant water and C relations (Steppe et al. 2015). At leaf scale, highly resolved measurements under eCO_2 have shown sub-daily variability in leaf expansion rate of *Populus* (Walter et al. 2005) and species-specific (for *P. tremula*, *P. tremuloides* and *Sambucus racemosa*) temporal shifts of the daily maximum g_s during the day (Batke et al. 2020), all affecting sub-daily water and C budgets. Nonetheless, sub-daily dynamics in whole-tree processes under eCO_2 remain relatively unexplored (Wullschleger and Norby 2001, Tricker et al. 2009, Dawes et al. 2014). In 36-year-old *Larix decidua* trees, daily stem shrinkage measured with point dendrometers was reduced under eCO_2, presumably as a result of altered stem water flow and storage under eCO_2 (Dawes et al. 2014). In *Liquidambar styraciflua* trees, a general sap flow (SF, as proxy of transpiration) reduction was observed under eCO_2 throughout diurnal hours (Wullschleger and Norby 2001). Contrastingly, in a *P.* x *euramericana* stand and on days with high atmospheric water demand, increased canopy LA under eCO_2 resulted in stimulation of SF, but effects were larger before noon than during the afternoon (Tricker et al. 2009). Although largely unexploited to date, sub-daily dynamics in stem diameter variations, whole-tree water use as a proxy for transpiration and stem CO_2 efflux under current and future CO_2 regimes might provide novel insights in eCO_2-induced alterations in tree C and water relations.

The objective of this study was to assess variability in eCO_2 effects on leaf and whole-tree physiology during two seasonal stages: start and end of the growing season. To this end, one-year-old European aspen (*Populus tremula* L.) trees were subjected to ambient (aCO_2) and elevated (eCO_2) atmospheric [CO_2] in two subsequent growing seasons. Point leaf measurements (A_n, g_s and R_L) and continuous stem measurements (stem diameter variations, SF and stem CO_2 efflux) were used to evaluate the temporal and spatial variability in leaf and tree responses to eCO_2. We hypothesized that (i) eCO_2 will stimulate leaf A_n and overall respiration as a consequence of increased tree growth, and will reduce leaf g_s and hence whole-tree water use, (ii) leaf scale processes will be more susceptible to eCO_2 than whole-tree processes, and (iii) stronger eCO_2 effects will be observed at the beginning of the growing season, followed by a down-regulation towards the onset of autumn.

Material and methods

Plant material and experimental set-up

Approximately fifty one-year-old European aspen (*Populus tremula* L.) trees were planted before onset of the 2018 and 2019 growing seasons (day of year (DOY) 78-79). Trees were randomly distributed between two treatment chambers and grown under ambient (400 ppm, hereafter aCO$_2$) or elevated (700 ppm, hereafter eCO$_2$) [CO$_2$]. Additionally, temperature (T), relative humidity (RH) and photosynthetic active radiation (PAR) inside the treatment chamber were continuously monitored (see Chapter 1 for a detailed overview of the experimental set-up).Early and late season responses to eCO$_2$ were studied in 2019 and 2018, respectively. During the 2019 growing season, measurements were conducted from the onset of leaf development (early May, DOY 121) until leaves were fully mature in mid-summer (late July, DOY 209) (hereafter early season experiment "ESE"). During the 2018 growing season, measurements were conducted from mid-summer (late July, DOY 211) to leaf senescence (late September, DOY 273) (hereafter late season experiment "LSE"). After the measurement period, trees were harvested (DOY 209 and 288 for ESE and LSE, respectively). Stems were cut above pot soil level and leaves and stems (including branches) were manually separated. Roots were manually dug out and the remaining soil fraction was removed by rinsing of the roots. All tissues were air dried for three months to quantify leaf, root and stem (including branches) dry biomass.

Point measurements

Point measurements were conducted on five trees per treatment chamber. A young fully developed leaf from the middle canopy was randomly selected for measurement of light-saturated net carbon assimilation (A$_n$) and stomatal conductance (g$_s$), with PAR of 1500 μmol m^{-2} s^{-1} according to the maximal midday PAR registered on sunny days, and leaf respiration (R$_L$) under dark conditions. Note that values of light saturated A$_n$ better reflect estimates of photosynthetic capacity rather than actual photosynthetic rates. Measurements were registered after stabilization of CO$_2$ exchange rates (5 to 10 minutes), and were conducted using a portable gas exchange system (Li-6400, Li-Cor Inc., Lincoln, Nebraska, USA) set at treatment chamber [CO$_2$] (400 or 700 ppm for aCO$_2$ and eCO$_2$, respectively) and at prevailing chamber temperature. Additionally, xylem water potential (Ψ$_{xylem}$) of the same trees was measured using a pressure chamber (Model 600, PMS Instrument Company, Corvallis, OR, USA) in one mid-canopy leaf loosely covered with aluminium foil for at least one hour to allow hydraulic equilibrium (Begg and Turner 1970). Point measurements were

performed around midday (between 11:00 h and 15:00 h). Frequency of the measurements varied from once fortnightly (DOY 130 to 167) to once weekly (DOY 168 to 209) along the course of ESE, and twice per week (DOY 214 to 257) during LSE followed by a final measurement on DOY 270. In addition, pre-dawn water potential (Ψ_{pd}) was measured four and five times during ESE and LSE, respectively.

Continuous measurements

Water and C relations of the same trees selected for point measurements were monitored using plant sensors. Radial stem volumetric diameter variation (ΔD) was measured with linear variable displacement transducers (LVDT, model DF5.0, Solartron Metrology, Leicester, UK) installed on the bark at an approximate height of 30 cm above (pot) soil level. At the time of LVDT installation, initial stem diameter was 4.98 ± 0.50 mm and 4.44 ± 0.28 mm during ESE (DOY 121) and 9.18 ± 0.57 mm and 10.67 ± 0.72 mm during LSE (DOY 211) under aCO_2 and eCO_2, respectively (n = 5). Daily radial stem volumetric growth (DG) was calculated as the difference in maximum stem diameter, commonly registered at predawn, between two consecutive days. Daily radial stem shrinkage (DS) was defined as the difference between daily maximum and minimum stem diameter, commonly registered at predawn and during high-transpiration hours (between 10:00 h and 18:00 h), respectively.

Sap flow (SF) rate in three (ESE) and four (LSE) trees per treatment chamber was measured using EXO-Skin sensors (SGEX9/10, EXO-Skin, Dynagage, Dynamax, Houston, TX, USA) applying the heat balance method (Smith and Allen 1996). Sensors were installed approximately 10 cm above (pot) soil level. During ESE, SF sensors were installed on trees equipped with ΔD sensors and installation was delayed until the young trees reached the required minimum stem diameter (DOYs 173 and 188 for eCO_2 and aCO_2 seedlings, respectively). During LSE, SF was measured during the entire surveyed period, with SF and ΔD being monitored on different individuals. To compare whole-tree water use while accounting for potential differences in vapor pressure deficit (VPD) between treatment chambers (calculated following Allen et al. (1998) using chamber T and RH), canopy conductance (g_c = SF / VPD; Morris et al. 1998) was calculated for every time stamp and integrated on a daily basis (g_{c_daily}).

During LSE, stem CO_2 efflux rates to the atmosphere (E_A) were monitored on four trees per treatment equipped with ΔD sensors. Note that E_A was used as a proxy of stem respiration for treatment comparison, as the limited contribution of xylem CO_2 transport to stem respiration in small-sized stems minimizes misestimation of respiratory rates of underlying tissues in seedlings, which can be substantial in mature trees (Teskey et al. 2008). The relative

contribution of internally transported CO_2 to stem respiration lowered with decreasing stem size in *Liriodendron tulipifera* L. trees (Fan et al. 2017) and accounted for less than 15 % of the stem respiration in 3-year-old *Populus* x *canadensi* trees with stem diameter of 3.1 cm (Salomón et al. 2018a). Since stem size of the European Aspen under study was even smaller, we expect limited contribution of the internal transported CO_2. Custom-made cuvettes, surrounding a 7 – 8.5 cm length stem segment, were made from flexible polycarbonate film and sealed with adhesive closed-cell foam gaskets and non-caustic silicone to prevent air leakage. Cuvettes were covered with aluminium foil to prevent woody tissue photosynthesis (De Roo et al. 2020b). Inside each treatment chamber, cuvettes were connected to an infrared gas analyser (IRGA, Li-840, Li-Cor) with plastic tubing in open through-flow configuration. Ambient air (400 or 700 ppm) was mixed in a 50 L container to buffer short term $[CO_2]$ variations and pumped through the cuvettes. Airflow was measured with flow meters (model 5860S; Brooks Instruments, Ede, Netherlands) installed within the inlet tubing. A custom-built multiplexer automatically switched air flow from each cuvette to the IRGA every 5 min. The difference in $[CO_2]$ between incoming air and the air leaving the cuvette (ΔCO_2) was measured. A tightly closed plastic bag served as reference chamber and was integrated within the setup to account for IRGA drift. ΔCO_2 measurements were recorded every minute and averaged over the last three minutes of each measurement cycle to allow ΔCO_2 stabilization. Measurements of E_A per seedling were generated every 45 minutes and time series were smoothed to avoid artefactual peaks following sharp variations in $[CO_2]$ within each treatment chamber (ca. ± 25 ppm) after CO_2 flushing to maintain $[CO_2]$ target levels. E_A on a surface basis ($\mu mol\ m^{-2}\ s^{-1}$) was calculated following the standard method (Long and Hällgren 1993) and E_A values were integrated to estimate daily E_A (E_{A_daily}, $\mu mol\ m^{-2}\ day^{-1}$). E_A sensitivity to temperature (Q_{10}) was estimated on a daily basis for each seedling according to the exponential relationship between E_A and chamber temperature (T):

$$Log(E_A) = a + bT \qquad\qquad\qquad \text{Equation 3.1}$$

$$Q_{10} = e^{(10b)} \qquad\qquad\qquad \text{Equation 3.2}$$

where a is the slope and b the intercept of the regression between $Log(E_A)$ and T.

Data analyses

Continuous microclimate, ΔD and SF data were registered every minute and averaged every five minutes. All continuous data was collected using a datalogger (CR1000, Campbell Scientific, Logan, UT, USA) and data was retrieved and visualized in real-time using the

PhytoSense software (Phyto-IT, Gent, Belgium). Data analyses was performed using R software (R Core Team, 2018). Measurements were pooled on a fortnightly basis to harmonize data to the same time window, resulting in two time frames per month. The effect of the [CO_2] treatment (and its temporal variability) on leaf scale measurements was assessed using linear mixed effects models (*nlme* package), including data point correlation due to the repeated measurement design of the experiment and considering the [CO_2] treatment (aCO_2 and eCO_2) and time frame (fortnight period) as fixed effects, while tree was considered as a random factor. Comparison between CO_2 treatments and across time frames was performed by calculation of least squared means and pairwise-comparison with Tukey contrasts (multcomp package). The effect of eCO_2 on continuous stem scale measurements was assessed over time by applying two sample t-tests on a daily basis. Sub-daily dynamics in highly-resolved stem measurements were averaged on a monthly basis. To account for temporal within-subject variability, *summarySEwithin* (*Rmisc* package) function was applied as described by Morey (2008). Note that focus is on treatment comparisons within the same experiment and comparisons between ESE and LSE are avoided, as inter-annual differences in trees and microclimatic conditions could bias seasonal comparisons. Given the small sample size (n = 3 - 5), statistically strong ($P < 0.05$) and moderate ($P < 0.10$) differences are reported. Reported values refer to mean ± SE (standard error).

Results

Chamber microclimate and tree biomass

Average microclimate during daytime (PAR > 5 µmol m^{-2} s^{-1}) in each treatment chamber is shown in Figure 3.1. Along the measurement period, aCO_2 was 458.41 ± 3.38 ppm and 432.20 ± 4.89 ppm, and eCO_2 was 706.81 ± 5.84 ppm and 696.79 ± 5.61 ppm during ESE and LSE, respectively. The [CO_2] treatment did not affect the daytime T (24.57 ± 0.32 °C and 24.41 ± 0.35 °C during ESE and LSE, respectively) or PAR (590.17 ± 13.95 µmol m^{-2} s^{-1} and 484.68 ± 14.12 µmol m^{-2} s^{-1} during ESE and LSE, respectively). Daytime VPD (1.20 ± 0.3 kPa) did not differ between chambers during ESE. During LSE differences in VPD were observed between treatment chambers ($P < 0.001$; 1.54 ± 0.07 kPa and 1.22 ± 0.06 kPa under aCO_2 and eCO_2, respectively), presumably caused by the moderate stimulation of canopy development under eCO_2 ($P < 0.1$; Figure 3.2) and, hence, greater whole-tree transpiration and chamber RH. In addition to the moderate increase in leaf dry biomass, eCO_2 increased stem and root ($P < 0.01$) dry biomass during LSE after almost 7 treatment months. Contrastingly, dry biomass of leaf, stem and root was left unaffected by eCO_2 during ESE after

almost 4.5 months of treatment application (P = 0.3, 0.4 and 0.3 for leaf, stem and root, respectively) (Figure 3.2).
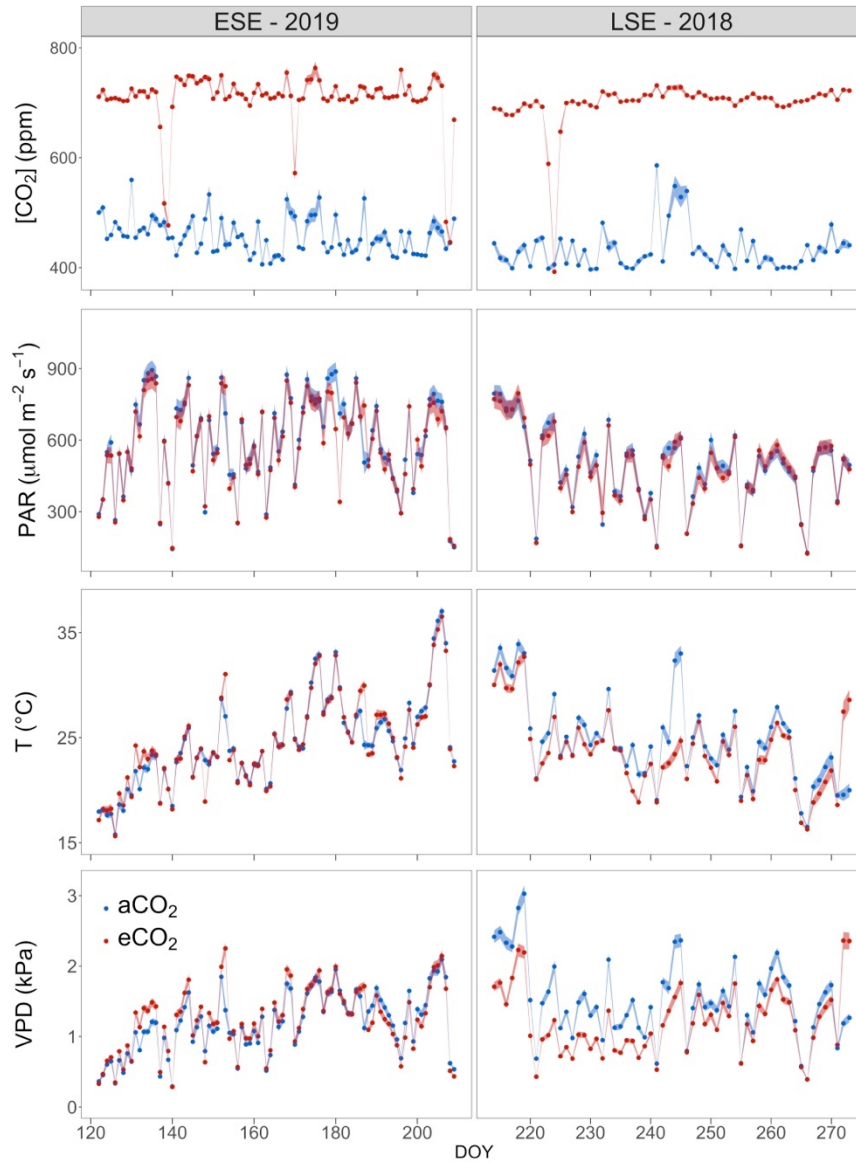

Figure 3.1 Daily mean CO$_2$ concentration ([CO$_2$]), photosynthetically active radiation (PAR), air temperature (T), and vapor pressure deficit (VPD) in the ambient (aCO$_2$, blue) and elevated (eCO$_2$, red) [CO$_2$] treatment chamber during daytime (PAR > 5 µmol m^{-2} s^{-1}) along the course of the early (ESE – 2019, left-hand side panels) and late (LSE – 2018, right-hand side panels) season experiment.
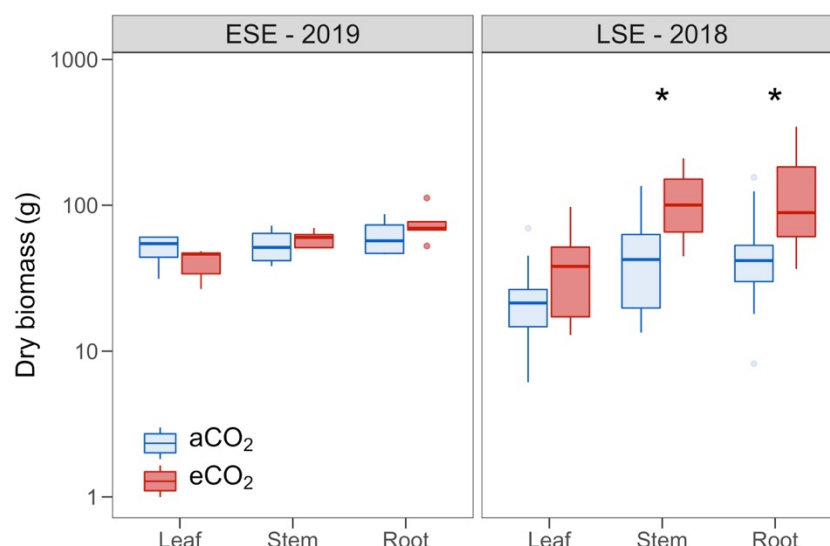
Figure 3.2 Leaf, stem (including branches) and root dry biomass under ambient (aCO_2) and elevated (eCO_2) [CO_2] at the end of the early (ESE – 2019) and late (LSE – 2018) season experiments.

Asterisks indicate significant differences between aCO_2 and eCO_2 (parametric t-test with $P < 0.05$). With $n = 4$ (aCO_2) and 5 (eCO_2) during the ESE and $n = 12$ (aCO_2) and 11 (eCO_2) during LSE. Note log scale of y-axis.

Leaf photosynthesis and tree growth

During ESE, A_n stimulation under eCO_2 was observed during June and early July ($P < 0.05$; Figure 3.3, upper panels). The effect of eCO_2 on A_n (as the ratio between eCO_2 and aCO_2 mean values) increased from May (1.60-fold increase) to June (1.91-fold increase), and later decreased in July (1.56-fold increase). During LSE, A_n stimulation under eCO_2 was uniquely observed in early September ($P < 0.01$; 1.49-fold increase). Within a single [CO_2] treatment, highest A_n rates were observed from May to June during ESE, while remaining stable (for both aCO_2 and eCO_2) during LSE.

At the stem scale, DG was stimulated under eCO_2 from early June to mid-July during ESE, whereas DG ceased faster under eCO_2 at the end of LSE (Figure 3.3, middle panels). Overall, cumulative stem diameter increment over the measurement period was higher under eCO_2 during ESE ($P < 0.05$; increment of 7.82 ± 1.24 mm and 12.16 ± 0.99 mm under aCO_2 and eCO_2, respectively), whereas during LSE cumulative stem growth was not affected by the [CO_2] treatment ($P > 0.1$; increment of 3.79 ± 0.22 and 4.15 ± 1.07 mm under aCO_2 and eCO_2, respectively). Over time and during ESE, stem shrinkage decreased from May to July under aCO_2 ($P < 0.1$) and eCO_2 ($P < 0.05$) (Figure 3.3, lower panels). When pooling data separately for each seasonal experiment, a moderate ($P < 0.1$; from 70.53 ± 2.75 μm day^{-1} under aCO_2 to 42.26 ± 1.80 μm day^{-1} under eCO_2) and strong ($P < 0.05$; from 104.77 ± 4.35 μm day^{-1}

under aCO_2 to 56.09 ± 3.27 µm day^{-1} under eCO_2) reduction in stem shrinkage under eCO_2 was observed during ESE and LSE, respectively.
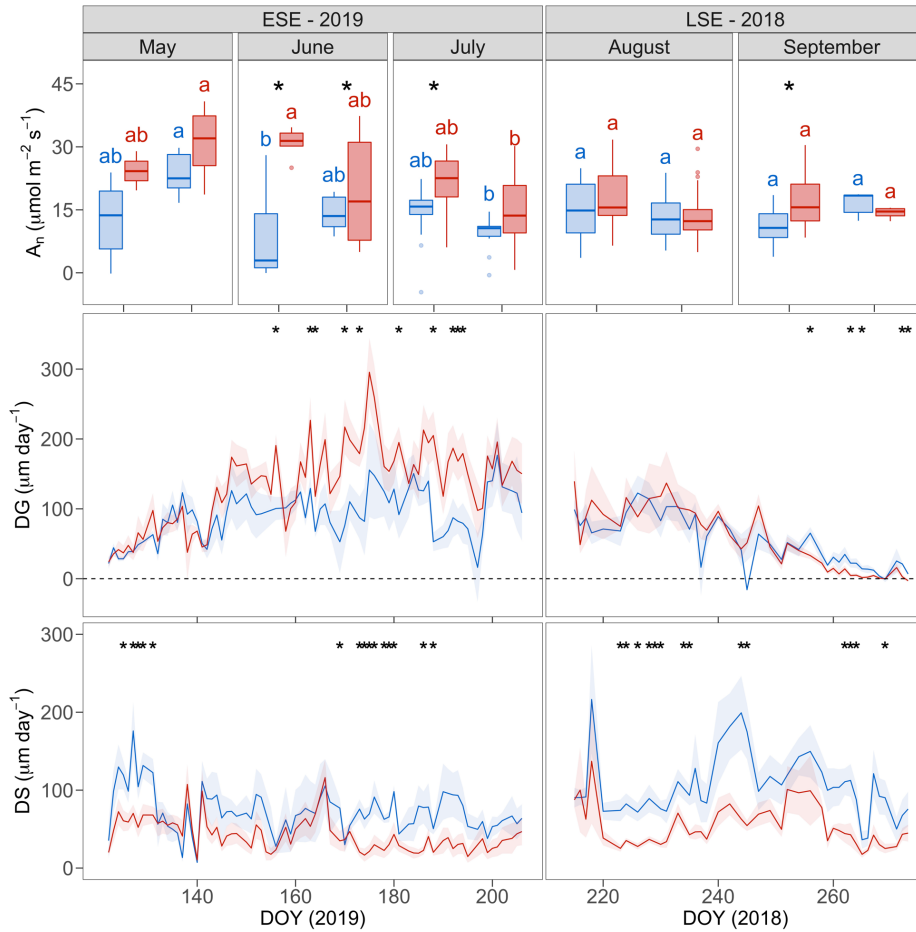

Figure 3.3 Temporal variability in leaf net carbon assimilation (A_n, upper panels), daily stem radial growth (DG, middle panels) and daily stem shrinkage (DS, lower panels) under ambient (aCO_2) and elevated (eCO_2) [CO_2] and during the early (ESE - 2019) and late (LSE - 2018) season experiments.

A_n was pooled on a fortnightly basis. Letters indicate significant differences among time frames within each [CO_2] treatment and seasonal experiment (mixed effect model). Asterisks indicate significant differences between aCO_2 and eCO_2 ($P < 0.05$) for a given time frame (A_n, mixed effect model) or on daily (DG and DS, parametric t-test) basis.

Stomatal and canopy conductance and plant water status

A decrease in g_s under eCO_2 was limited to late May during ESE ($P < 0.05$) and to late September during LSE ($P < 0.05$) (Figure 3.4, upper panels). Overall, eCO_2 did not affect g_s when pooling measurement campaigns within a season experiment ($P > 0.1$), with eCO_2/aCO_2 ratios of 0.85 and 0.99 for ESE and LSE, respectively. Within each [CO_2] treatment, g_s did not

substantially vary over time in any season experiment. Also, at the whole-tree scale, g_{c_daily} was not significantly affected by the $[CO_2]$ treatment during ESE or LSE (Figure 3.4, lower panels), with overall eCO_2/aCO_2 ratios of 0.87 and 0.64, respectively. In both $[CO_2]$ treatments, g_{c_daily} was relatively high during ESE (July, 415.95 ± 9.07 g kPa^{-1} day^{-1}) and during the first month of LSE (August, 280.64 ± 14.69 g kPa^{-1} day^{-1}), followed by a substantial decrease ($P < 0.001$) along September (113.22 ± 9.35 g kPa^{-1} day^{-1}).
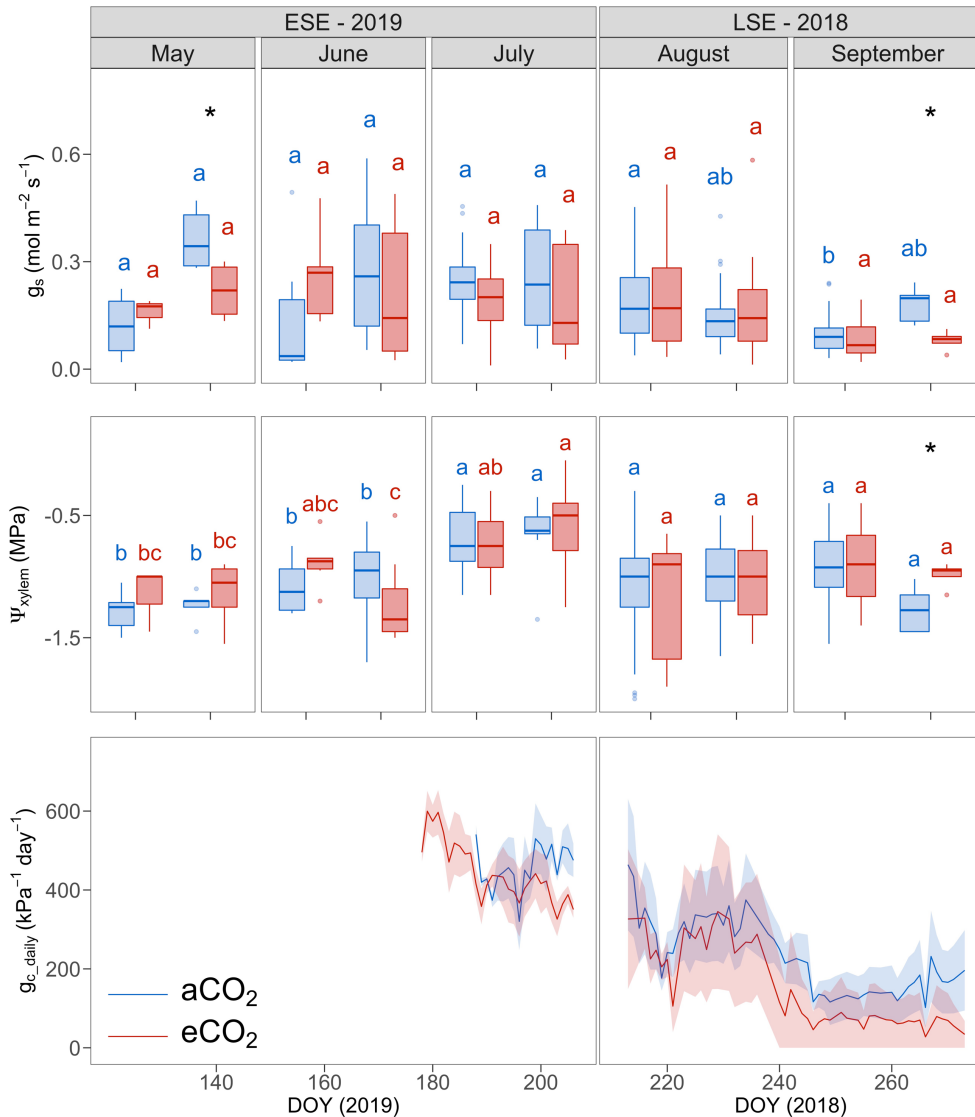

Figure 3.4 Temporal variability in stomatal conductance (g_s, upper panels), xylem water potential (Ψ_{xylem}, middle panels) and daily canopy conductance (g_{c_daily}, lower panels) over time under ambient (aCO_2) and elevated (eCO_2) $[CO_2]$ and during the early (ESE - 2019) and late (LSE - 2018) season experiment.

g_s and Ψ_{xylem} were pooled on a fortnightly basis. Letters indicate significant differences among time frames within each $[CO_2]$ treatment and seasonal experiment (mixed effect model). Asterisks indicate significant differences between aCO_2 and eCO_2 ($P < 0.05$) for a given time frame (g_s and Ψ_{xylem}, mixed effect model) or on a daily basis (g_{c_daily}, parametric t-test).

In both season experiments, [CO$_2$] treatment did not consistently affect Ψ_{xylem} (P > 0.1; -0.91 ± 0.03 MPa and -1.01 ± 0.02 MPa for ESE and LSE, respectively) (Figure 3.4, middle panels) and Ψ_{pd} (P > 0.1; -0.15 ± 0.02 MPa and -0.46 ± 0.03 MPa for ESE and LSE, respectively). Only in late September, Ψ_{xylem} was more negative under aCO$_2$ than under eCO$_2$ (P < 0.05). When comparing within [CO$_2$] treatments, Ψ_{xylem} generally increased over time during ESE as a likely result of the increase of soil water content (Supplementary Figure S1). During LSE, Ψ_{xylem} did not change over time under any of the [CO$_2$] treatments.

Leaf and stem CO$_2$ efflux

Leaf respiration was not affected by the [CO$_2$] treatment during ESE (P > 0.1) and showed no clear seasonal pattern (Figure 3.5, upper panels). During LSE, averaged R$_L$ showed a small, yet significant, decrease under eCO$_2$ compared to aCO$_2$ (P < 0.05; 3.32 ± 0.23 µmol m^{-2} s^{-1} and 2.74 ± 0.12 µmol m^{-2} s^{-1}, for aCO$_2$ and eCO$_2$, respectively). This difference was significant in early September (P < 0.05). During LSE, an apparent decrease of R$_L$ occurred along the course of the experiment under both [CO$_2$] treatments. Variability among time frames in both season experiments was mostly driven by prevailing chamber temperature (P < 0.001). At stem scale, E$_{A\_daily}$ was not affected under eCO$_2$ (P > 0.1) (Figure 3.5, lower panels). Again, temporal variability in E$_{A\_daily}$ was largely driven by chamber temperature (P < 0.001).

Sub-daily variability in stem measurements over the season

Sub-daily fluctuations in stem diameter averaged per month are shown in Figure 3.6 (upper panels). During ESE and under aCO$_2$, no difference in end-of-day stem diameter was observed from May to July (P > 0.1). Under eCO$_2$, a moderate decrease in end-of-day diameter was observed from June (167.15 ± 5.28 µm) to July (147.09 ± 5.29 µm) (P < 0.01). During LSE, end-of-day stem diameter variation decreased from August (47.35 ± 6.21 µm and 87.90 ± 9.32 µm under aCO$_2$ and eCO$_2$, respectively) to September (28.11 ± 2.47 µm and 27.22 ± 4.36 µm under aCO$_2$ and eCO$_2$, respectively) (P < 0.001) under both [CO$_2$] treatments. A stimulation in end-of-day diameter under eCO$_2$ was uniquely observed in June (P < 0.05). Timing of maximal pre-dawn stem diameter, and therefore timing of the onset of stem shrinkage and depletion of internal water pools, was delayed under eCO$_2$ compared to aCO$_2$ in June by 44 ± 9 min (P < 0.1) and in August by 44 ± 7 min (P < 0.05).
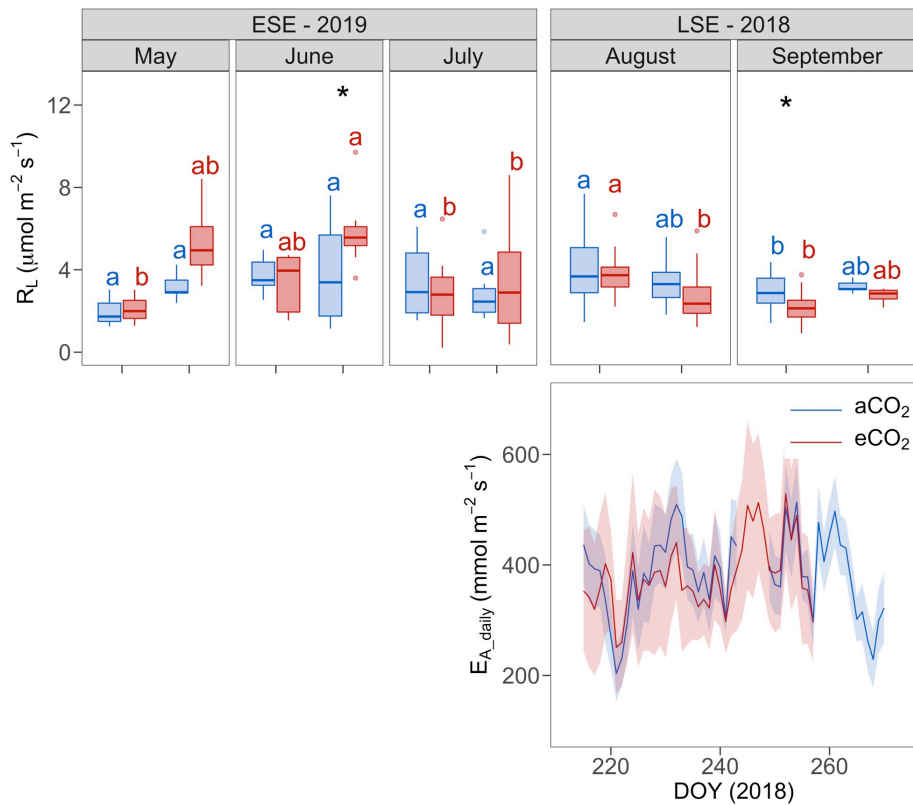
Figure 3.5 Temporal variability in leaf respiration (R_L, upper panels) and daily stem CO_2 efflux (E_{A_daily}, lower panels) under ambient (aCO_2) and elevated (eCO_2) [CO_2] and during the early (ESE - 2019) and late (LSE - 2018) season experiment.

R_L was pooled on a fortnightly basis. Letters indicate significant differences among time frames within each [CO_2] treatment and seasonal experiment (mixed effect model). Asterisks indicate significant differences between aCO_2 and eCO_2 ($P < 0.05$) for a given time frame (R_L, mixed effect model) or on a daily basis (E_{A_daily}, parametric t-test).

Sub-daily g_c patterns showed little effect of the [CO_2] treatment (Figure 3.6, middle panels). Maximum sub-daily g_c was observed during morning hours (on average 9:40 h ± 17 min and 10:55 h ± 12 min during ESE and LSE, respectively), and timing of the daily onset of g_c remained unaffected by the [CO_2] treatment in every month during both season experiments ($P > 0.1$). The reduction observed in g_{c_daily} during LSE from August to September was mainly attributed to the reduction in afternoon (after 12:00 h) rather than pre-noon (before 12:00 h) g_c. Sub-daily E_A patterns (Figure 3.6, lower panels) largely mimicked those of temperature. Despite the neutral effect of eCO_2 on E_A, eCO_2 increased E_A sensitivity to temperature ($P < 0.01$; Q_{10} = 1.63 ± 0.02 and 1.95 ± 0.06 for aCO_2 and eCO_2, respectively) more markedly in September, hereby resulting in larger sub-daily E_A fluctuations.
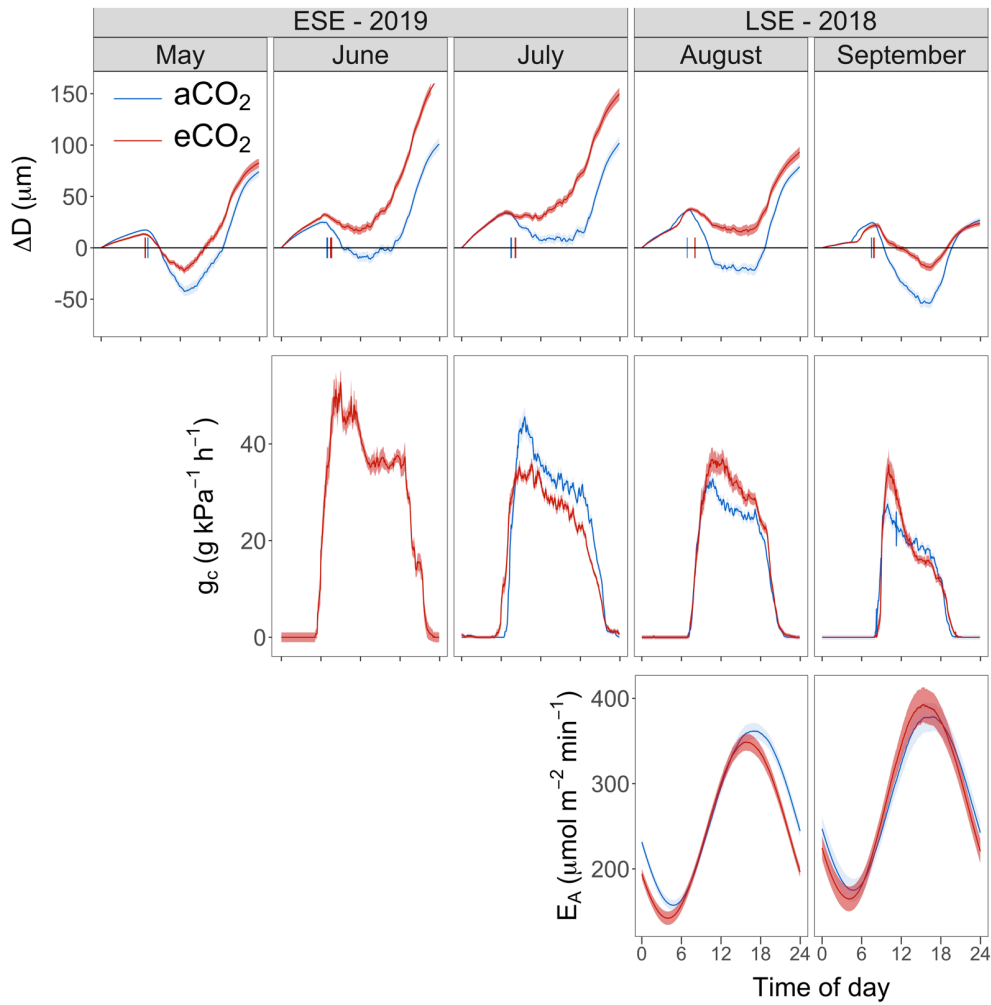
Figure 3.6 Sub-daily patterns of stem diameter variation (ΔD, upper panels, with vertical lines indicating the time when maximal pre-dawn stem diameter was registered), canopy conductance (g_c, middle panels) and stem CO_2 efflux (E_A, lower panels) under ambient (aCO_2) and elevated (eCO_2) [CO_2] averaged on a monthly basis for the early (ESE - 2019) and late (LSE - 2018) season experiments.

Discussion

Corresponding and diverging eCO₂ effects at leaf and tree scale

Average leaf A_n was 63 and 26 % higher under eCO_2 in comparison to aCO_2 during ESE and LSE, respectively. This leaf photosynthetic stimulation is in accordance with the average increase of 31 % compiled over C3 plants grown in FACE experiments (Ainsworth and Rogers 2007, Ainsworth and Long 2020), and with previous eCO_2 studies in *Populus* spp. in which A_n stimulation varied from 31 to 49 % (Liberloo et al. 2007, 2009), and from 33 % to 38 % (Noormets et al. 2001). During ESE, leaf scale A_n stimulation (1.63-fold) resulted in a parallel increase in radial stem diameter increment (1.55-fold) over the course of the experiment.

61

Contrastingly, leaf and whole-tree responses to eCO$_2$ diverged during LSE, as there was a 1.26-fold increase in A$_n$ while stem diameter increment remained unaffected under eCO$_2$. This remarkable observation suggests that enhanced C supply at the end of the growing season was not invested in stem volumetric growth. Although mismatches between leaf and whole-tree responses are not uncommon in large trees (Chapter 2, Table 2.2), they might be unexpected in young and fast growing seedlings (Wertin and Teskey 2008). It is worth noting that eCO$_2$-stimulation of stem volumetric growth registered during ESE did not translate into increased aboveground woody biomass. In contrast, biomass production was stimulated under eCO$_2$ during LSE, when eCO$_2$-induced stimulation of stem volumetric growth was no longer registered. This apparent discrepancy between stem diameter size and biomass production can be explained by two reasons. Firstly, harvest time may affect comparisons of biomass production because any potential stimulation is more likely to be detected towards the end of the season after completion of the annual growth cycle. Secondly, stem volumetric increment does not immediately translate into an increase in stem biomass, according to their substantial time lag. Across boreal, temperate, subalpine and Mediterranean forests, stem biomass production lagged behind stem volumetric growth for over one month (Cuny et al. 2015). Since additional C supply due to A$_n$ stimulation under eCO$_2$ can alter both cell size and cell wall thickness (Watanabe et al. 2010, Richet et al. 2012, Lotfiomran et al. 2015, Liu et al. 2020), early season C surplus might have stimulated cambial division and cell production (hence stem volumetric growth) to a greater extent, while late season C surplus might be partly allocated to cell wall thickening, thereby increasing stem biomass for a relatively constant size. Nevertheless, we acknowledge that stem height and branch length, not measured here, may also play a role in the increase of stem biomass observed under eCO$_2$ during LSE, following a potential shift from radial to axial growth.

In contrast to the expected eCO$_2$-induced decrease in g$_s$ (average reduction of 22 % across FACE experiments; Ainsworth and Rogers 2007), leaf g$_s$ remained largely unaffected under eCO$_2$ during both seasonal experiments. Stomatal behaviour largely depends on microclimatic conditions (particularly VPD) and water availability (Xu et al. 2016) and the wide range of g$_s$ responses to eCO$_2$ observed across a variety of biomes questions the commonly accepted reduction of g$_s$ under eCO$_2$ (Purcell et al. 2018). Therefore, even though g$_s$ reduction under eCO$_2$ has previously been observed in *Populus* spp. (Tricker et al. 2009, Hao et al. 2018b, De Roo et al. 2020a), unresponsive g$_s$ is not uncommon in this genus (Bernacchi et al. 2003, Bobich et al. 2010). The invariability of leaf g$_s$ between [CO$_2$] treatments upscaled to the whole-tree scale as g$_{c\_daily}$ also remained homeostatic during both seasonal experiments. Previous studies in a poplar plantation under FACE conditions showed the large dependence of whole-tree water use on canopy LA, since transpiration increased as a result of enhanced leaf area

index despite reductions in leaf g_s (Liberloo et al. 2007, Tricker et al. 2009). Here, although we do not have direct measurements of canopy LA, leaf dry biomass was unaffected under eCO_2 during ESE and moderately increased during LSE. The absence of the expected g_{c_daily} increase during LSE, despite the increase in leaf biomass with a homeostatic stomatal behaviour, might be explained by the limited statistical power to detect significant differences (n = 4) given the large variability in g_{c_daily} observed among individuals. Moreover, potential discrepancy between canopy LA and leaf biomass can be mediated by increase in leaf thickness under eCO_2 (Oksanen et al. 2001), which may contribute to the homogenisation of leaf transpiring area and hence whole-tree water loss.

At both leaf and stem scale, only small or no changes in leaf respiration and stem CO_2 efflux were observed under eCO_2. In comparison with previous studies conducted across species (Atkin et al. 2015), including *Populus* spp. (Hovenden 2003), leaf respiration was remarkably high under both [CO_2] treatments and seasonal experiments as a likely combination of three factors: (i) high leaf temperature at midday, quite often exceeding 25 ºC (Tjoelker et al. 2001, Aspinwall et al. 2017), (ii) the addition of growth respiration to overall R_L (Amthor 1984), as highest rates were measured during May and June, and (iii) a systematic bias related to the short stabilization time under dark conditions, as respiratory processes may peak after illumination (Azcón-Bieto and Osmond 1983). Previous studies reported an overall reduction of 15 – 20 % in R_L under eCO_2 (Drake et al. 1999, Jahnke 2001), which is in agreement with the R_L decrease observed during LSE. Effects of eCO_2 on R_L remain, however, under debate (Smith 2017, Dusenge et al. 2019) as methodological artefacts might be partially responsible for such reductions (Jahnke 2001). At whole-tree scale, stem CO_2 efflux is expected to increase with stem growth (Edwards et al. 2002, Saveyn et al. 2007, Wertin and Teskey 2008, Acosta et al. 2010) according to the maintenance and growth respiration paradigm (reviewed by Amthor 2000). Enhanced photosynthetic activity and carbohydrate supply could therefore lead to increased whole-tree respiration (Gifford 2003), especially in young seedlings (Wertin and Teskey 2008). Here, carbohydrate supply and stem volumetric growth remained largely unaffected under eCO_2 during LSE, and similar E_A between [CO_2] treatments was therefore in line with the expectations. Accordingly, previous studies found that E_A remained unaffected under eCO_2 when stimulation in stem volumetric growth was absent in different species (Mildner et al. 2015, Salomón et al. 2019) including *Populus* spp. (Gielen et al. 2003, Liberloo et al. 2008).

Early and late season dynamics in the eCO_2 response

Seasonal dynamics in both magnitude and direction of eCO_2 effects in leaf and whole-tree functioning were observed. During ESE, leaf A_n was overall larger in May and June and

progressively decreased towards the end of July. Early season dynamics in leaf C uptake upscaled to the whole-tree scale, as the rate of stem volumetric growth increased during ESE, reaching highest rates in late June. During LSE, A_n variation over time in each $[CO_2]$ treatment was limited and stem volumetric growth (unaffected by eCO_2) slowed down from August to the end of September, as a likely result of the onset of autumnal leaf senescence triggered by microclimatic conditions (e.g. reduced T, PAR and photoperiod). Likewise, in a previous experiment conducted on even-sized European aspen trees using the same experimental setup, stem volumetric growth was not affected under eCO_2 during the end of the summer season, and stimulation of stem size was limited to early spring (De Roo et al. 2020a). This seasonality of the eCO_2 effect on C dynamics at leaf and whole-tree scale is not limited to young *Populus* spp. trees, as it has been observed in a variety of tree species and across tree ages (Chapter 2, Table 2.1). For instance, in evergreen *Eucalyptus globulus* trees, A_n stimulation varied from 46 % in summer to 14 % in winter, with a parallel seasonal fluctuation in stem volumetric growth dynamics (Quentin et al. 2015). Also in deciduous *Fagus sylvatica* saplings, the magnitude of A_n stimulation varied over time, as A_n stimulation was only significant in July followed by a limited response in August and September (Urban et al. 2019).

This temporal variability in the magnitude of the eCO_2 effect on A_n and DG throughout ESE and LSE can be explained by the seasonality in whole-tree C sink strength. During spring and early summer (June and July) tree productivity in *Populus* spp. is relatively high, with a peak in the production of aboveground (leaves and stems) and below ground (coarse and fine roots) biomass (Block et al. 2006, Broeckx et al. 2014). During this period, tree development may be C limited, triggering rapid allocation of C from source to sink organs, hereby developing a positive feedback which amplifies the fertilization effect. Towards the end of the growing season, tree productivity declines and the magnitude of the eCO_2 effect decreases as C supply is no longer the most limiting factor for growth and availability of water and nutrients gain relative importance (Pantin et al. 2012). Reduction in C demand for the development of plant organs may lead to leaf C accumulation, affecting the carbon-to-nitrogen balance, hence limiting RuBisCo concentration and activity (Gamage et al. 2018) and ultimately triggering leaf senescence. It is worth noting that the duration of the growing period was shortened under eCO_2 in our study, as denoted by the relatively low stem volumetric growth towards the end of LSE. Earlier autumnal cessation of stem volumetric growth under eCO_2 might be related to the overall end of season downregulation of leaf and whole-tree activity. This would explain g_s reduction under eCO_2 during late September, likely causing the observed relaxation in Ψ_{xylem}. We therefore suggest that the early season eCO_2-induced stimulation of stem volumetric growth advanced the completion of the potential annual stem girth development, triggering an earlier autumn leaf senescence. Nevertheless, it must be noted that the effects of eCO_2 on

autumn phenology remain under debate as leaf senesce has also been observed to delay (Taylor et al. 2008, Reyes-Fox et al. 2014), likely ascribed to a prolongation of wood formation phenophases (Lupi et al. 2010) as a result of eCO_2-stimlated cell production.

eCO_2 affects sub-daily C and water processes

Sub-daily dynamics in C and water relations reveal that stem diameter variations (ΔD) were altered under eCO_2 throughout the growing season, while g_c and E_A sub-daily dynamics remained mostly unaffected. The sub-daily ΔD pattern is the combined result of (i) irreversible (plastic) stem volumetric growth and (ii) reversible (elastic) fluctuations following depletion and refilling of internal stem water pools. Therefore, eCO_2-driven changes in sub-daily ΔD dynamics result from both water and C relations. Overall, stem shrinkage varied over the season, partly related to the evaporative water demand, and was smaller under eCO_2. Three potential causes might contribute to the limited stem shrinkage observed under eCO_2: (i) alteration of radial hydraulic resistance (Dawes et al. 2014) (ii) modification of cell wall properties (Le Gall et al. 2015) and (iii) stimulated radial stem volumetric growth. First, the radial hydraulic resistance regulating the water flow between bark and xylem tissues may increase under eCO_2. Reduced stem contractions under eCO_2 were first reported for large *Larix decidua* trees (Dawes et al. 2014), and the authors suggested that radial hydraulic resistance increased under eCO_2, hereby limiting bark dehydration. Increased radial hydraulic resistance might be caused by a reduction in aquaporin activity (Steppe et al. 2012) or by xylem anatomy alterations, such as reductions in abundance of radial conductive tissues (ray parenchyma) (Dawes et al. 2014). Delayed timing in stem diameter contraction under eCO_2 during part of the season, while the onset of transpiration remained unaffected, indicates temporal limitations to radial water exchange, further supporting this first hypothesis. Second, cell wall plasticity and rigidity (depending on cell wall expansin proteins and rates of hemicellulose and lignin deposition) are dynamic throughout the tree's lifespan and can adapt to environmental stress elicitors (Le Gall et al. 2015). Therefore, changing atmospheric $[CO_2]$ may affect cell wall properties, as previously observed in well-watered birch seedlings (*Betula populifolia*; Morse et al. 1993) and in late season cut roses (*Rosa hybrida*; Urban et al. 2002) for which eCO_2 increased cell elastic modulus and thus reduced tissue elasticity. More rigid cell walls of elastic water pools may contribute to the limited shrinkage observed in our young European aspen trees grown under eCO_2. Third, increased C availability under eCO_2 can stimulate stem volumetric growth, hereby counteracting elastic and water-driven stem shrinkage (De Swaef et al. 2015). Nonetheless, reduced shrinkage under eCO_2 at the end of the growing season, when stem size increases ceased earlier, suggests limited influence of

stem size volumetric growth on stem shrinkage patterns, and reinforces the possibility that eCO_2-grown trees limited the use of stem elastic water pools.

In contrast to earlier studies (Wullschleger and Norby 2001, Tricker et al. 2009), sub-daily dynamics in canopy conductance were not affected under eCO_2 in our study. In *Liquidambar styraciflua* trees, SF rates were reduced on all daytime hours (between 11:00 h and 18:00 h) under eCO_2, as a likely consequence of g_s reduction (Wullschleger and Norby 2001). In contrast, hybrid poplar *P*. x *euramericana* under FACE conditions showed an increase in daily tree water use under eCO_2 mainly as result of stimulated transpiration before noon (Tricker et al. 2009). Because Tricker et al. (2009) observed these differences between $[CO_2]$ treatments only on sunny days with high atmospheric water demand, they were partly explained by transpiration dependence on VPD. The invariability in sub-daily g_c patterns in our young European aspen trees, despite high T, PAR and VPD during the summer months, was in agreement with the homeostatic behaviour of leaf scale g_s and whole-tree g_{c_daily} under eCO_2 observed throughout the season.

Although E_A showed little differences between $[CO_2]$ treatments, E_A sensitivity to temperature (Q_{10}) increased under eCO_2 at the end of the late season. Previous research has shown contrasting results regarding the effect of eCO_2 on Q_{10}. For instance, eCO_2 had no effect on Q_{10} averaged across the growing season in 14-year-old and 110-year-old *Picea abies* trees (Acosta et al. 2010, Mildner et al. 2015). In contrast, end-of-summer Q_{10} in *Pinus ponderosa* saplings increased under eCO_2 (Carey et al. 1996), whereas in *Liquidambar styraciflua* tree stems, Q_{10} was reduced and stimulated under eCO_2 during the growing and dormant season, respectively (Edwards et al. 2002). Further research in this line would be necessary to understand how respiratory physiology responds to combined effects of eCO_2 and increasing temperatures to better constrain predictions of whole-tree respiration (and hence net primary productivity) under climate change scenarios.

Conclusions

Combination of leaf (A_n, g_s and R_L) and whole-tree (DG, g_c and E_A) measurements in young *Populus tremula* trees indicates that leaf scale responses to eCO_2 largely upscaled to the whole-tree scale. However, eCO_2-induced photosynthetic stimulation led to an increase in stem volumetric growth only during springtime, while radial stem volumetric growth was not stimulated during autumn despite enhanced A_n. Thus, the magnitude of C-related responses to eCO_2 were dynamic over time, and most likely driven by seasonality in C-sink strength. The C demand was relatively high in spring during periods of high plant productivity (reflected by increases in stem diameter size), and progressively diminished during autumn, when C is

mostly allocated to cell wall thickening (reflected by increases in dry biomass). Leaf g$_s$ and whole-tree g$_c$ were not affected under eCO$_2$. Similarly, leaf respiration stem CO$_2$ efflux, serving as a proxy of stem respiration, were also not substantially affected under eCO$_2$. Stem sub-daily shrinkage was significantly reduced under eCO$_2$, suggesting changes in tissue and cell traits (radial hydraulic conductance and cell wall elastic modulus) limiting the use of internal stem water pools, even under well-watered conditions. Taken together, these observations underline the importance of the C source-sink interactions under future [CO$_2$] regimes.
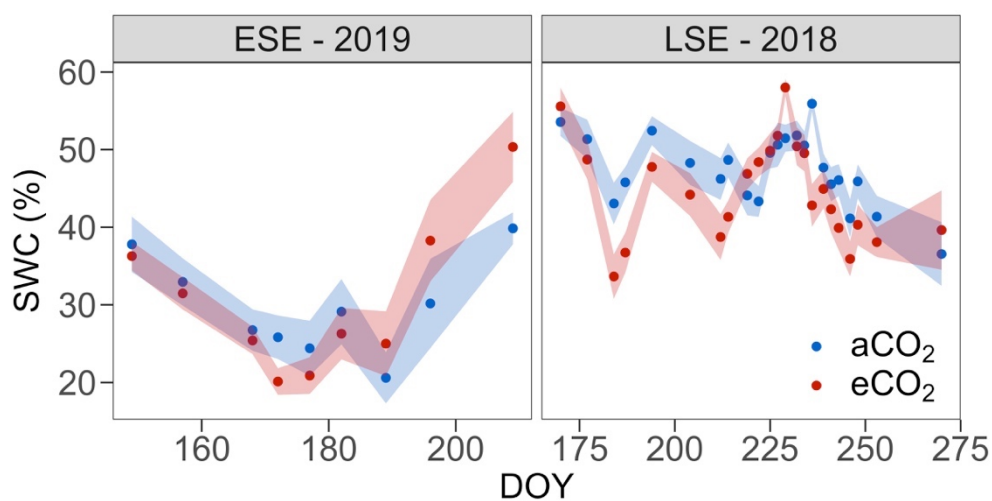
Supplementary material

Figure S3.1 Soil water content (SWC) under ambient (aCO$_2$) and elevated (eCO$_2$) during the early (ESE - 2019) and late (LSE - 2018) season experiments. Points and ribbons indicate the averaged values and corresponding standard error, respectively.

4

Limited mitigating effects
of elevated CO$_2$ in young aspen trees
to face drought stress

Abstract

Elevated atmospheric CO_2 concentration (eCO_2) is expected to mitigate negative effects of moderate drought on leaf and whole-tree functioning. However, tree responses to eCO_2 under severe drought and throughout the growing season remain largely unknown. One-year-old *Populus tremula* L. trees were grown in two controlled growth chambers under ambient and elevated CO_2 conditions, while progressive drought was imposed early (spring/summer 2019) and late (summer/autumn 2018) in the growing season. Stomatal conductance, leaf carbon assimilation and leaf respiration were monitored in concert with whole-tree canopy conductance derived from sap flow measurements, radial stem volumetric growth, stem CO_2 efflux, xylem water potential and non-structural carbohydrates (NSC). During late season drought, eCO_2 delayed drought-induced reduction in leaf carbon assimilation and lowered g_s drought susceptibility. Drought effects on whole-tree functioning and NSC depletion remained unaltered under eCO_2. Stem volumetric growth ceased earlier than photosynthesis, while leaf and stem respiratory metabolism were maintained at 30 % of well-watered levels even under severe drought, independent of the CO_2 treatment and the timing of drought. The ability of eCO_2 to mitigate drought was limited to leaf processes, mainly stomatal conductance, during the late season and under moderate drought (> -2 MPa) levels. Contrastingly for whole-tree processes (i.e. water use, stem volumetric growth and stem CO_2 efflux), drought offset any beneficial effect of eCO_2.

Introduction

Forests are exposed to a rapid changing climate. Unprecedented emission of greenhouse gases, including carbon dioxide (CO_2), led to global warming and alteration of the hydrological cycle, with more frequent and longer drought events (IPCC 2018). When facing drought, trees close their stomata to reduce water loss and balance the risk of drought-induced hydraulic failure and carbon (C) starvation (McDowell et al. 2008, Lin et al. 2015). CO_2 fertilization has been suggested to alleviate some of the detrimental effects of drought on tree functioning (e.g. Wullschleger et al. 2002b, Avila et al. 2020, Birami et al. 2020). The explanation is twofold. First, the reduction of stomatal conductance (g_s) under eCO_2 improves water use efficiency at the leaf scale (Menezes-Silva et al. 2019). This potentially leads to an overall water-saving effect, delaying soil water depletion over time (Wullschleger et al. 2002b, Leuzinger and Körner 2007, Fatichi et al. 2016). Second, drought-induced g_s reduction imposes C limitations to photosynthetic activity. CO_2 fertilization may partially alleviate C shortage, as CO_2 concentration ([CO_2]) in the sub-

stomatal cavities will be higher under eCO$_2$ compared to current atmospheric [CO$_2$]. As a result, and relative to well-watered conditions, a stronger eCO$_2$ induced stimulation of net C assimilation (A$_n$) has been commonly found during drought periods in different tree species (e.g. Goodfellow et al. 1997, Herrick et al. 2004, Birami et al. 2020).

Contrarily, adverse effects of drought on tree functioning might also be exacerbated under eCO$_2$ (e.g. Domec et al. 2010, Warren et al. 2011). Stimulated canopy development under eCO$_2$ might result in a mismatch between water supply and demand when water becomes limiting ("structural overshot") (McCarthy et al. 2006, Bobich et al. 2010, Fatichi et al. 2016, Jump et al. 2017). Likewise, rapid increase of stem size may affect wood quality and result in wider vessels and a reduction of wood density (Ceulemans et al. 2002, Bobich et al. 2010, Kostiainen et al. 2014, Kim et al. 2015), which would increase xylem vulnerability to embolism formation and hydraulic failure (Mrad et al. 2018, Janssen et al. 2020). This wide range of eCO$_2$ effects under drought, from mitigation to aggravation, was recently observed in young *Pinus halepensis* trees, for which eCO$_2$-induced drought effects varied with drought intensity (Birami et al. 2020). At moderate drought levels, A$_n$ and water use efficiency increased under eCO$_2$. Nonetheless, mitigating eCO$_2$ effects disappeared when drought became more severe (Birami et al. 2020). Conflicting observations denote a limited understanding of tree performance and survival under interacting drought and eCO$_2$ conditions. Research integrating multiple stress elicitors (e.g. Warren et al. 2011, Bauweraerts et al. 2013, Duan et al. 2015, Birami et al. 2020) are therefore crucial to predict tree behaviour as climate changes (reviewed in Becklin et al. 2017, Menezes-Silva et al. 2019).

Although, the effects of drought under ambient [CO$_2$] (aCO$_2$) on tree development and survival have been extensively studied, research has mainly focused on drought intensity, while the timing of drought remains largely unexplored despite its crucial role (Granda et al. 2013, Lévesque et al. 2013, Camarero et al. 2015, D'Orangeville et al. 2018, Forner et al. 2018). Also tree responses to eCO$_2$ (hereafter 'eCO$_2$ effect') can vary over time and depend on the tree's development stage (Chapter 2). Leaf and tree development during spring and early summer is largely sensible to CO$_2$ fertilization, as a result of high C-demand for the development of above- and belowground biomass production at this time (Pantin et al. 2012). Maximal eCO$_2$-induced stimulation is therefore regularly reported during the early season vegetative developmental stage (e.g. Quentin et al. 2015, Li et al. 2019b, Urban et al. 2019, Sanches et al. 2020). As the growing season progresses and phenological controlled changes in growth occur, the tree C sink strength reduces while water becomes the primary driver for tree development (Pantin et al. 2012). As a result, non-structural carbohydrates (NSC) accumulate throughout tree organs (Li et al. 2018b),

71

including foliar tissues, increasing the carbon-to-nitrogen balance (Long et al. 2004). This eventually triggers down-regulation of the RuBisCo (Ribulose-1,5-bisphosphate carboxylase-oxygenase) activity, reducing the eCO_2 effect at the leaf scale (Gamage et al. 2018).

The magnitude of the eCO_2 effect also depends on the spatial scale under study (leaf vs. whole-tree) (Chapter 2). Especially in mature trees, mismatches between leaf and whole-tree responses to eCO_2 may occur. For example, increased C availability as a result of A_n stimulation does not necessarily enhance whole-tree biomass production. This is because the C surplus can be diverted to alternative tree C sinks, such as NSC storage, respiratory metabolism, emission of volatile organic compounds (VOCs), rhizodeposition, or synthesis of skeleton intermediates for reproductive or defensive functions (Körner 2006, Sala et al. 2012, Salomón et al. 2017b, Jiang et al. 2020). Likewise, no straightforward translation exists from leaf to whole-tree water use, as the latter is dependent on both leaf g_s and canopy leaf area. Only when eCO_2-induced g_s reduction is strong enough to compensate for the potential stimulation of canopy leaf area, whole-tree water use may decrease under eCO_2 (Fatichi et al. 2016). As a result, whole-tree water use has been observed to either decrease (Wullschleger and Norby 2001), increase (Uddling et al. 2008, Tricker et al. 2009) or remain unaffected (Ward et al. 2013, Tor-ngern et al. 2015, Gimeno et al. 2018) under eCO_2.

Potential mitigation or aggravation of drought effects under eCO_2 highlight the uncertainty to predict tree behaviour in future climates. Temporal and spatial dynamic tree responses to eCO_2 further question whether the interacting effects of drought and eCO_2 vary over time and are scalable from leaf to whole-tree scale. This study therefore focusses on leaf and whole-tree water and C relations in one-year-old European aspen (*Populus tremula* L.) trees subjected to combined treatments of eCO_2 and drought. Leaf scale measurements included g_s, A_n and leaf respiration, whereas whole-tree scale measurements included canopy conductance (derived from sap flow measurements), stem diameter variations, stem CO_2 efflux (as a proxy of stem respiration) and xylem water potential. Additionally, NSC concentrations were measured in leaf, bark and xylem tissues. To assess potential eCO_2 mitigation to drought at different seasonal developmental stages, two sets of trees were planted in consecutive years to evaluate leaf and whole-tree responses to early and late season drought (both under ambient and elevated [CO_2]). We hypothesize that (i) drought-driven down-regulation of leaf processes will be faster during the late in comparison to the early season due to the increasing relative importance of water over C for leaf development as the season progresses (Pantin et al. 2012), (ii) eCO_2 will alleviate detrimental effects of moderate drought, but mitigating effects will

72

disappear as drought intensifies, and (iii) the magnitude of eCO$_2$-induced drought mitigation will reduce from leaf to whole-tree scale, as similarly observed under well-watered conditions (Chapter 2 and 3).

Material and methods

Plant material and experimental set-up

Approximately fifty one-year-old European aspen (*Populus tremula* L.) trees were planted before the onset of the 2018 (DOY 79) and 2019 (DOY 78) growing season in 30 L pots with potting soil mixed with fertilizer (Osmocote Exact Standard 8-9M, ICL, Ipswich, UK). Trees were randomly distributed into two growth chambers (see Chapter 1 for detailed overview of the treatment chamber set-up), allowing continuous monitoring and regulation of the chamber microclimate. Target [CO$_2$] was controlled to 400 ppm (hereafter ambient [CO$_2$], aCO$_2$) and 700 ppm (hereafter elevated [CO$_2$], eCO$_2$). Half of the trees within each chamber (ca. 25) were randomly assigned to a well-watered or a drought stressed group. This 2x2 factorial experimental design resulted in four treatment groups: well-watered trees under aCO$_2$ (aW) and eCO$_2$ (eW), and drought stressed trees under aCO$_2$ (aD) and eCO$_2$ (eD). Well-watered trees were irrigated at pre-dawn (between 05:00 h to 06:00 h) with an automated irrigation system and the amount of water supplied was adjusted per pot and throughout the season based on point measurements of soil water content (SWC; ThetaKit, Delta-T Devices, Burnwell, UK).

During the 2018 growing season, trees were subjected to drought during late August and September (hereafter "late season drought experiment" or LSE). Drought was induced by lowering irrigation to 50 % relative to the well-watered trees from DOY 222 (10 August), after which water supply was completely stopped from DOY 229 (17 August). During the 2019 growing season, irrigation was ceased on DOY 183 (2 July) (hereafter "early season drought experiment" or ESE). After each seasonal experiment (DOYs 288 and 209 for the LSE and ESE, respectively), trees were harvested for determination of dry biomass of roots, stem and leaves. The stem was cut above pot soil level and leaves and stems (including branches) were manually separated. Roots were manually dug out and the remaining soil fraction was removed by rinsing of the roots. All tissues were air dried for three months to quantify leaf, root and stem (including branches) dry biomass. The root:shoot ratio was calculated as the ratio of the dry weight of the roots and the sum of the leaves and stems.

Point measurements

Point measurements were conducted on ten trees per chamber (five per treatment group), and spanning a period from before the onset of drought until measurements of xylem water potential (Ψ_{xylem}) were no longer possible in drought stressed trees due to leaf wilting (DOY 121-209 and DOY 211-253 during ESE and LSE, respectively). Measurements were performed around midday (between 11:00 h and 15:00 h), two to three times a week during LSE and once a week during ESE. A mid-canopy leaf was randomly selected for measurements of A_n and g_s at saturation light (PAR 1500 µmol m^{-2} s^{-1}; according to the maximal PAR measured inside the treatment chamber on sunny days), and leaf respiration (R_L) under dark conditions (PAR 0 µmol m^{-2} s^{-1}). Measurements were taken with a portable photosynthesis system (Li-6400, Li-Cor Inc., Lincoln, Nebraska, USA) set at chamber [CO_2] (400 or 700 ppm) and prevailing temperature (T) and after stabilization of the CO_2 exchange rates (5 to 10 minutes). A pressure chamber (Model 600, PMS Instrument Company, Corvallis, OR, USA) was used to measure midday Ψ_{xylem} in mid-canopy leaves loosely covered with aluminum foil for at least one hour to allow hydraulic equilibrium (Begg and Turner 1970). In addition, pre-dawn water potential (Ψ_{pd}) was measured three to four times across each drought experiment.

Continuous measurements

In the same time span as the point measurements, trees were equipped with stem sensors and cuvettes to monitor stem diameter variations (ΔD), sap flow (SF) and stem CO_2 efflux (E_A). Stem diameter variation was measured with linear variable displacement transducer (LVDT, model DF5.0, Solartron Metrology, Leicester, UK) installed over the bark of the same ten trees selected for point measurements at an approximate height of 30 cm above pot soil level. At time of installation, initial stem diameter was 4.44 ± 0.50 mm (aCO_2) and 4.98 ± 0.28 mm (eCO_2) during ESE, and 9.18 ± 0.57 mm (aCO_2) and 10.67 ± 0.72 mm (eCO_2) during LSE. Daily stem volumetric growth (DG) was calculated as the difference between stem diameter maxima of two consecutive days. The heat balance method (Smith and Allen 1996) was applied to monitor SF. Six (ESE) and eight (LSE) trees per chamber (i.e. three to four per irrigation group) were equipped with EXO-Skin SF sensors (type SGEX9/10, Dynamax, Houston, TX, USA). During ESE, ΔD and SF measurements were conducted on the same trees, and SF measurements started when trees reached the girth required for sensor installation (DOY 188 and 173 for aCO_2 and eCO_2, respectively). During LSE, SF was measured during the entire course of the experiment, but ΔD and SF sensors were installed on different trees due to spatial constraints (see stem CO_2 efflux measurements below). To account for potential differences in chamber vapor pressure

74

deficit (VPD, calculated from chamber T and relative humidity (RH) following Allen et al. (1998)), canopy conductance (g_c = SF / VPD) was calculated at fine temporal resolution (equal to SF records) and integrated on a 24 h-basis for comparison of whole-tree water use (g_{c_daily}).

Stem CO_2 efflux to the atmosphere was measured as a proxy of stem respiration, as the contribution of internal transport of respired CO_2 with the transpiration stream has been reported to be minor in small-sized trees (Chapter 3; Fan et al. 2017, Salomón et al. 2018a). Stem CO_2 efflux was only measured during LSE, in eight trees per chamber (four per irrigation group) that were also equipped with LVDT sensors. Custom-made stem cuvettes were installed around 7 to 8.5 cm long stem segments, approximately 5 cm below the LVDT sensor. Cuvettes were made of flexible polycarbonate film and sealed with adhesive closed-cell foam gaskets and non-caustic silicone to prevent air leakage. An additional reference cuvette was included within each chamber to account for potential measurement drift. Plastic tubing connected the cuvettes to an infrared gas analyzer (IRGA, Li-840, Li-Cor) in open through-flow configuration. Cuvettes were covered with aluminum foil to prevent woody tissue photosynthesis (De Roo et al. 2020b). Inside each growth chamber, ambient air was mixed in a 50 L container to buffer [CO_2] fluctuations and air was pumped through the cuvettes. Airflow was measured with flowmeters (model 5860S; Brooks Instruments, Ede, Netherlands). A custom-built multiplexer switched between monitored cuvettes every five minutes. Difference in [CO_2] between ambient air and air exiting the cuvette (ΔCO_2) was measured with the IRGA. Measurements were recorded every minute and averaged over the last three minutes of each measurement cycle to allow for reading stabilization. Stem CO_2 efflux to the atmosphere was calculated on a surface basis following the standard procedure (McGuire and Teskey 2004, Salomón et al. 2018b). Therefore, measurements of E_A were generated for each tree every 45 minutes (9 cuvettes per chamber × 5 minutes) and E_A time series were smoothed to avoid peaks following sharp variations in chamber [CO_2] after CO_2 flushing to maintain target levels. Values of E_A were integrated on a 24 h-daily basis for comparison (E_{A_daily}).

Non-structural carbohydrate analysis

During LSE, eight non-instrumented trees per [CO_2] treatment (four per irrigation group) were selected to repeatedly measure non-structural carbohydrate concentration ([NSC]) before (DOY 221), during (three weeks after onset of drought; DOY 243) and after (at harvest; DOY 288) the drought period. Samples were taken from mid-canopy full grown leaves and from xylem and bark tissues of lignified branches. Bark and xylem tissues were separated manually. Samples were placed in liquid nitrogen to stop metabolic activity and

stored at -80 °C. Before analysis, samples were oven dried (70 °C, 72 h) and grinded (Ultra Centrifugal Mill ZM 200, Retsch, Haan, Germany). A modified protocol from Maness (2010) was used to determine [NSC]. Soluble sugars (SS) were extracted by incubating 20 mg of dried tissues in 1 mL of 80 % ethanol at 80 °C. This process was repeated twice, and extracts were combined and stored at -20 °C until analysis. The insoluble material was used for starch determination. Starch was transformed into glucose monomers using amyloglucosidase from *Aspergillus niger* at 50 U mL^{-1} (Sigma-10115) and α-amylase from *Bacillus licheniformis* at 500 U mL^{-1} (Sigma-A4582) in 0.1 M NaAc (pH 4.5). The mix was incubated for 2 h at room temperature and for 24 h at 55 °C. Sugar monomers from the ethanolic extract or starch enzymatic digestion were quantified by the anthrone–sulfuric acid colorimetric microassay, based on Laurentin and Edwards (2003), using 96-well microplates. The values were quantified according to a standard curve with known concentrations of glucose, fructose and galactose in the case of SS (0–10–50–100–250– 500–750–1000 ppm), and glucose (0–10–50–100–250–500–750–1000 ppm) in the case of starch. Standards and samples were measured at 630 nm in an ELx808™ Absorbance Microplate Reader (BioTek Instruments, Inc., Winooski, VT, USA). Total [NSC] was calculated by adding the concentrations of SS and starch.

Data analyses

Microclimate and continuous stem (ΔD and SF) measurements were registered every minute and averaged every five minutes using a datalogger (CR1000, Campbell Scientific, Logan, UT, USA). Data was retrieved, stored and visualized using the PhytoSense software (Phyto-IT, Gent, Belgium). Statistical analyses were performed using R software (R Core Team, 2018). Pre-drought differences and treatment effects over time during drought on leaf (g_s, A_n, R_L) and whole-tree (g_{c_daily}, DG, E_{A_daily}) functioning were assessed using linear mixed effects models (*nlme* package) including an autoregressive temporal correlation structure, with [CO_2] treatment (aCO_2 or eCO_2), irrigation treatment (well-watered or drought stressed) and their interaction as fixed effects and tree as random factor. Stepwise backward selection was applied for model selection. When significant, post-hoc multiple comparison among treatment groups were evaluated by Tukey tests (*multcomp* package). The effect of eCO_2 and drought on dry biomass, [SS], [starch] and [NSC] for each tissue and sampling period was assessed using linear models including the [CO_2] treatment, the irrigation treatment and their interaction, followed by stepwise backward selection and post-hoc analysis. Normality and homogeneity of variances were tested, and data was log transformed when necessary.

The evolution of leaf and whole-tree variables across a gradient of drought was evaluated according to Muller et al. (2011). The normalized value of each variable per individual drought stressed tree (as the percentage of the well-watered average) was regressed against the corresponding reduction in Ψ_{xylem} ($\Delta\Psi$; as the difference from the well-watered average). A sigmoidal curve was then fitted using the *nls* function:

$$y = \frac{1}{1 + \exp^{a(\Delta\Psi+b)}} + \left(1 - \frac{1}{1 + \exp^{a(\Delta\Psi+b)}}\right) s \qquad \text{Equation 4.1}$$

where y is the normalized value of the dependent variable (%), a defines the reduction rate of the curve, b is the inflection point (MPa), and s is the settling plateau (%) determining the maximum y reduction across the surveyed drought gradient. Note that the first term of the right-hand side represents a classic vulnerability curve, while the second term allows for a settling plateau different from zero. A lower limit was set to force the initial point of the sigmoidal curve (at $\Delta\Psi = 0$) above 95 % of the control average. Effects of the seasonal timing (early and late season), [CO₂] treatment, and spatial level (leaf and whole-tree) were assessed for each of the curve parameters (a, b and s) by fitting linear models. Goodness of fit was determined by calculated of the correlation between measured and predicted values (*stats* package). Strong ($P < 0.05$) and moderate ($P < 0.10$) statistical differences are reported for those tests with small sample size (n = 3-5). Values refer to mean ± standard error.

Results

Chamber microclimate and treatment effectiveness

Average chamber [CO₂] during daytime (PAR > 5 µmol m^{-2} s^{-1}) was 458.41 ± 3.38 ppm (aCO₂) and 706.81 ± 5.84 ppm (eCO₂) during ESE and 435.94 ± 6.67 ppm (aCO₂) and 691.61 ± 8.08 ppm (eCO₂) during LSE (Supporting Information Figure S4.1). Average daytime PAR did not differ between [CO₂] treatment chambers and was 590.17 ± 13.95 µmol m^{-2} s^{-1} and 500.18 ± 17.94 µmol m^{-2} s^{-1} during ESE and LSE, respectively. Average T and VPD was 24.57 ± 0.32 °C and 1.20 ± 0.04 kPa during ESE and 25.45 ± 0.40 °C and 1.39 ± 0.06 kPa during LSE. Average T was similar between [CO₂] chambers. VPD did not differ between [CO₂] treatment chambers during ESE. Contrastingly, during LSE differences in VPD were observed between treatment chambers ($P < 0.001$; 1.62 ±

0.09 and 1.17 ± 0.07 for aCO_2 and eCO_2), as a likely consequence of stimulated canopy area development and transpiration under eCO_2, hereby increasing chamber RH.

During ESE, dry biomass of leaves, roots and stems (Figure 4.1) were consistently reduced under drought ($P < 0.001$), while eCO_2 uniquely resulted in moderate increases of root dry biomass ($P < 0.1$). During LSE, root and stem dry biomass increased under eCO_2 ($P < 0.001$), while drought lowered leaf ($P < 0.05$) and root ($P < 0.01$) dry biomass. Root:shoot ratio was not affected by any treatment during ESE ($P > 0.1$), but was reduced under drought during LSE ($P < 0.05$, Figure S4.2). Interaction between eCO_2 and drought had no significant effect on dry biomass of any organ or the root:shoot ratio during ESE or LSE ($P > 0.1$). The drought treatment reduced Ψ_{xylem} at midday ($P < 0.001$, Figure 4.2) and pre-dawn ($P < 0.01$ Figure S4.3) over time. No significant interaction between the $[CO_2]$ and irrigation treatment was detected and eCO_2 did not alter Ψ_{xylem} or Ψ_{pd} among well-watered or drought stressed trees during any of the seasonal experiments ($P > 0.1$).
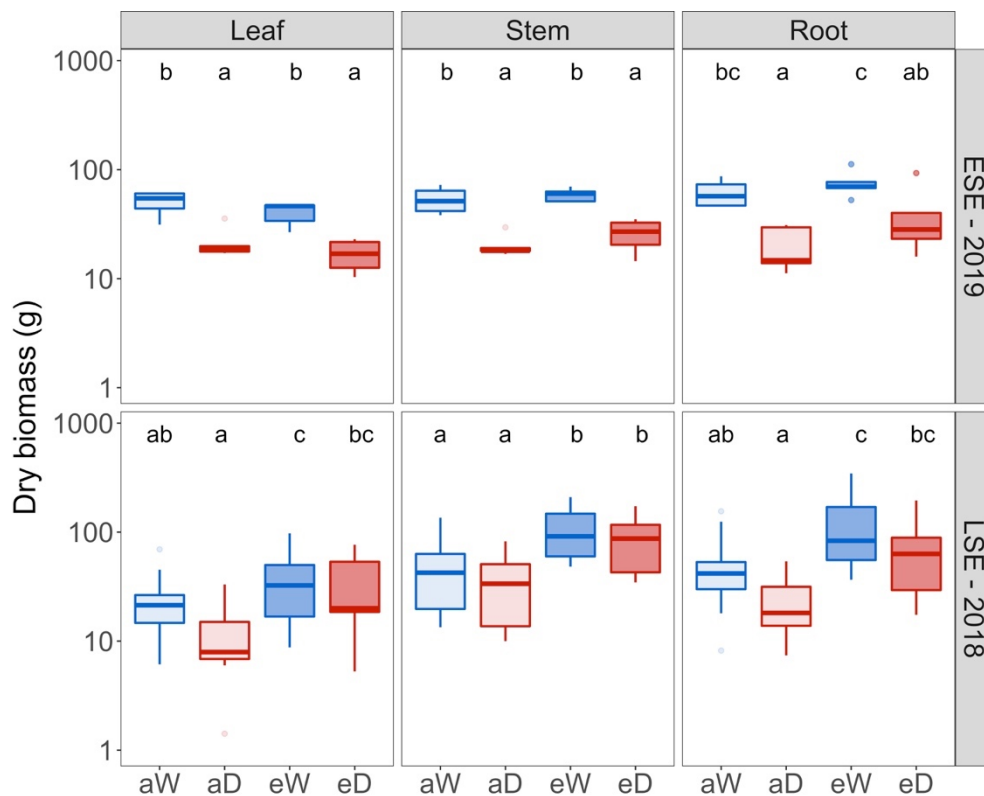

Figure 4.1 Leaf, stem (including branches) and root dry biomass at the end of the early (ESE - 2019) and late (LSE - 2018) season drought experiment.

One-year-old European aspen trees were subjected to combined treatments of $[CO_2]$ (a and e for ambient and elevated $[CO_2]$, respectively) and drought stress (W and D for well-watered and drought stress, respectively). Letters indicate statistical differences in dry biomass among treatment combinations (linear model, $P < 0.05$, n = 4-5 and 9-12 for ESE and LSE, respectively). Note log scale of y-axis.

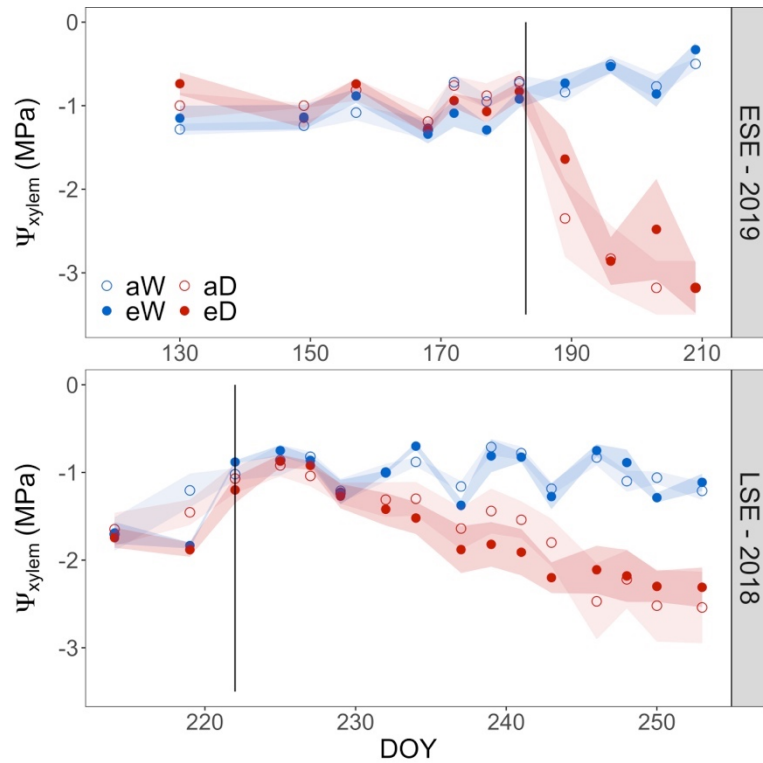Figure 4.2 Midday stem xylem water potential (Ψ_{xylem}) over time during the early (ESE - 2019) and late (LSE - 2018) season drought experiment.

One-year-old European aspen trees were subjected to combined treatments of [CO_2] (a and e for ambient and elevated [CO_2], respectively) and drought stress (W and D for well-watered and drought stressed, respectively). Vertical lines indicate the start of the drought treatment. With DOY day of year.

Leaf and whole-tree responses over time

Leaf responses to drought over time are shown in Figure 4.3 for LSE, with higher temporal resolution and coverage, and Figure S4.4 for ESE, whereas tree responses are shown in Figure 4.4 and S4.5, respectively. At leaf scale and during the well-watered period (Figure 4.3 and S4.4, left-hand side panels), g_s remained unaffected under eCO_2 during both seasonal experiments ($P > 0.1$), A_n was stimulated during ESE and LSE ($P < 0.001$), while R_L remained unaffected during LSE ($P > 0.1$), but was stimulated during ESE ($P < 0.01$). Pre-drought differences between irrigation groups were not observed for any of the leaf variables during any of the seasonal experiments ($P > 0.1$). When facing drought (Figure 4.3 and S4.4, right-hand side panels), the effects of the [CO_2] treatment were limited to an overall reduction of R_L during LSE ($P < 0.05$) and an increase of A_n during ESE ($P < 0.01$), while g_s remained unaltered ($P > 0.1$). Contrastingly, the drought treatment led to an evident decline in g_s ($P < 0.01$ during both ESE and LSE), A_n ($P < 0.01$ and 0.001 during ESE and LSE, respectively) and R_L ($P < 0.05$ and 0.01 during ESE and LSE,

respectively). The interaction between the $[CO_2]$ and irrigation treatment was not significant for any of the leaf variables or seasonal experiments (P > 0.1).
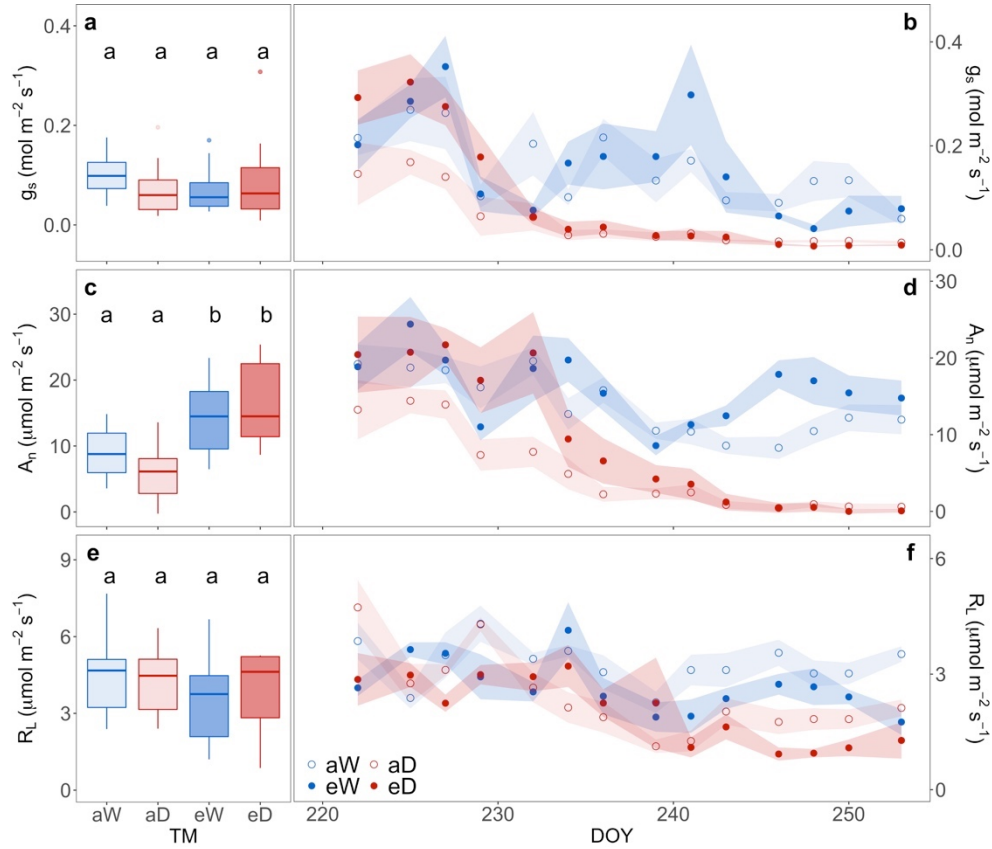

Figure 4.3 Comparison of leaf stomatal conductance (g_s, a-b), net carbon assimilation (A_n, c-d) and leaf respiration (R_L, e-f) in the late season experiment (2018) during the pre-drought period (left-hand side panels) and over time during the drought period (right-hand side panels).

One-year-old European aspen trees were subjected to combined treatments of $[CO_2]$ (a and e for ambient and elevated $[CO_2]$, respectively) and drought stress (W and D for well-watered and drought stressed, respectively). Letters indicate statistical differences (linear mixed model, P < 0.05) among treatment combinations. With DOY day of year.

Whole-tree responses (g_{c_daily}, DG and E_{A_daily}) during the well-watered period (Figure 4.4 and S4.5, left-hand side panels) were not affected by the $[CO_2]$ or irrigation treatment (P > 0.1), with the exception of a moderate DG stimulation in well-watered trees during LSE (P < 0.1). After onset of drought (Figure 4.4 and S4.5, right-hand side panels), eCO_2 resulted in an apparent short-term increase of g_{c_daily} among drought stressed trees during LSE (P > 0.1 during the first 5 days of LSE). With progressing drought, g_{c_daily} lowered under both $[CO_2]$ treatments and seasonal experiments (Figure 4.4b and S4.5b), with a significant reduction of g_{c_daily} during the last 17 days among the drought stressed trees (P

< 0.05). Regarding stem volumetric growth, drought stress reduced DG under both [CO$_2$] treatments and seasonal experiments (P < 0.01), while CO$_2$ induced a moderate stimulation of DG during ESE (P < 0.1) but not during LSE (P > 0.1). Stem CO$_2$ efflux was not affected by the [CO$_2$] treatment (P > 0.1) but reduced under drought during the last 4 days of LSE (P < 0.01, Figure 4.4f).
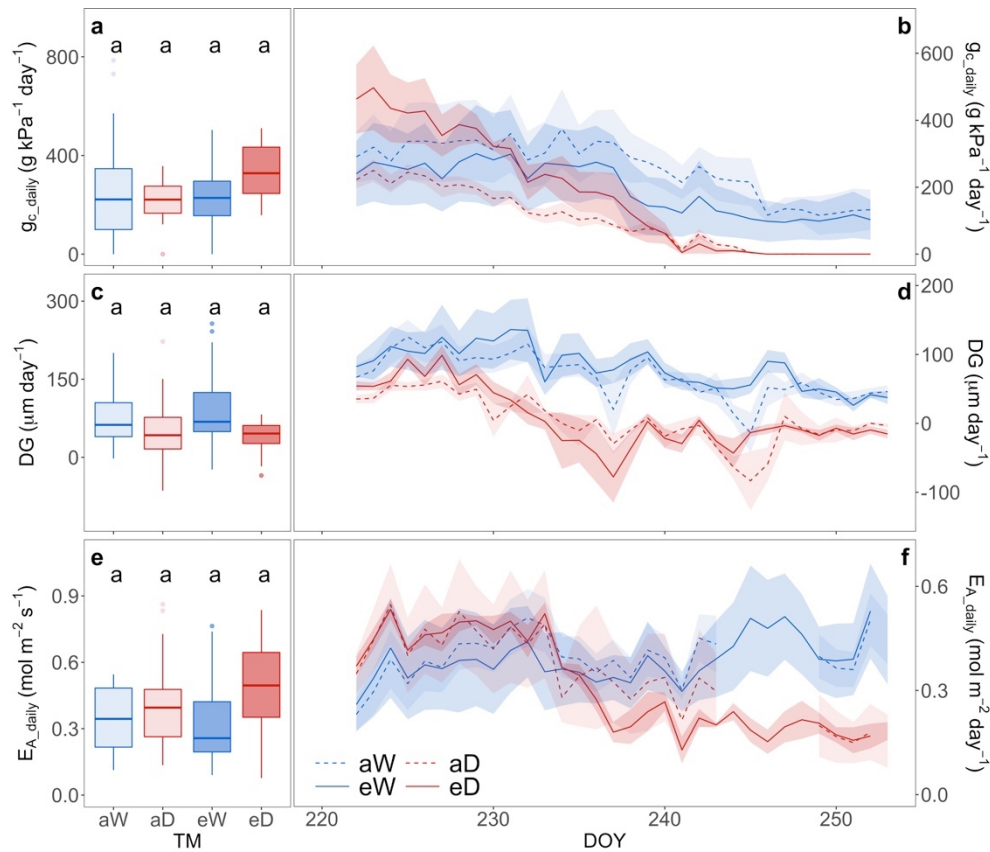

Figure 4.4 Comparison of whole-tree canopy conductance (g$_{c\_daily}$, a-b), daily stem volumetric growth (DG, c-d) and stem CO$_2$ efflux (E$_{A\_daily}$, e-f) in the late season experiment (LSE - 2018) during the pre-drought period (left-hand side panels) and over time during the drought period (right-hand side panels).

One-year-old European aspen trees were subjected to combined treatments of [CO$_2$] (a and e for ambient and elevated [CO$_2$], respectively) and drought stress (W and D for well-watered and drought stressed, respectively). Letters indicate statistical differences (linear mixed model, P < 0.05) among treatment combinations. The data gap in E$_{A\_daily}$ in the aCO$_2$ growth chamber was caused by a malfunction of the air pumping system. With DOY day of year.

NSC analysis

During the well-watered period (Figure 4.5, left-hand side panels), eCO_2 increased [NSC] in leaf ($P < 0.01$) and xylem ($P < 0.05$) tissues, while the increase in bark tissues was only moderate ($P < 0.1$). Differences in leaf [NSC] were attributed to higher [starch] and [SS], whereas enhanced xylem [NSC] was solely attributed to increased [SS]. There were no pre-drought differences between irrigation groups ($P > 0.1$).
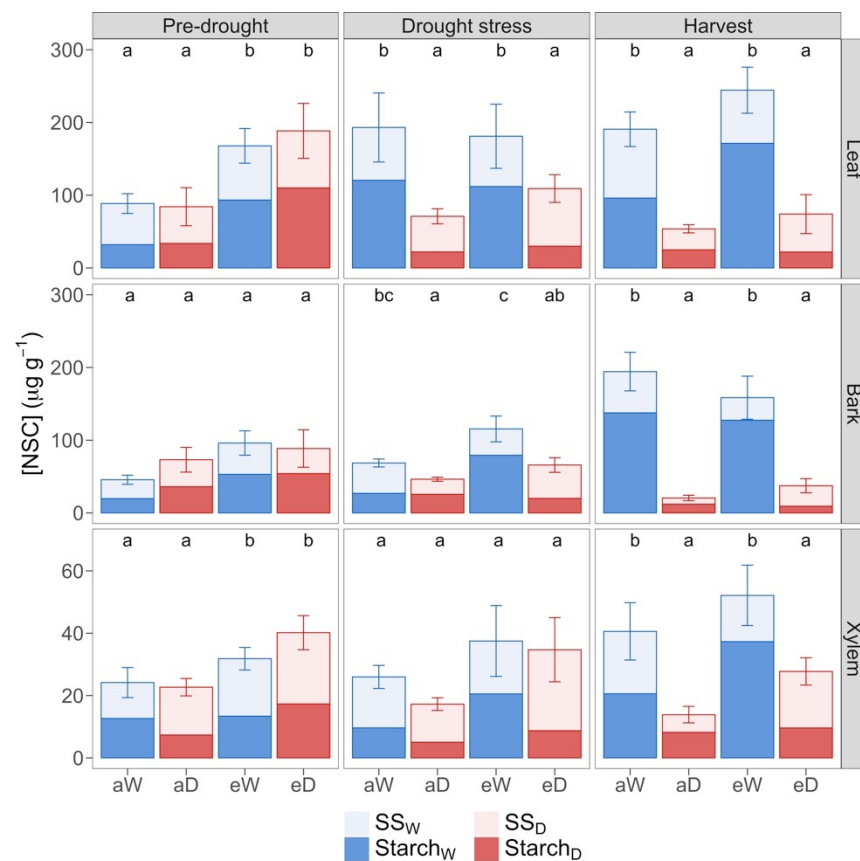

Figure 4.5 Concentration of soluble sugars (SS, light coloured bars) and starch (dark coloured bars) before the start of the drought period (DOY 221, left-hand side panels), after three weeks of drought (DOY 243, middle panels) and at the end of the experiment at harvest (DOY 288, right-hand side panels) in leaf, bark and xylem tissues during the late season experiment (2018).

One-year-old European aspen trees were subjected to combined treatments of [CO_2] (a and e for ambient and elevated [CO_2], respectively) and drought stress (W and D for well-watered and drought stress, respectively). Non-structural carbohydrate concentration ([NSC]) is the sum of [SS] and [starch]. Error bars indicate the standard error (SE) of total [NSC]. Letters indicate statistical differences in [NSC] among treatment combinations (linear model, $P < 0.05$).

Three weeks into the drought period (Figure 4.5, middle panels) [NSC] in drought stressed trees was reduced in leaf ($P < 0.05$) and bark ($P < 0.01$), mainly as a result of lower [starch]. No significant differences in xylem [NSC] were detected between irrigation groups ($P > 0.1$). At this time, the effect of eCO_2 was limited to an overall increase in bark ($P < 0.05$), as a result of higher bark [starch], and a moderate increase in xylem NSC ($P < 0.1$). At harvest, after nine weeks of drought treatment application (Figure 4.5, right-hand side panels), [starch] and [NSC] were reduced in all tissues ($P < 0.01$) by drought stress, while eCO_2 only led to a moderate overall increase in xylem [NSC] ($P < 0.1$).

Dynamics in tree responses to progressing drought

To assess leaf and whole-tree responses under progressing drought, relative reductions in water use (g_s, g_{c_daily}), C gain (A_n, DG) and C loss (R_L, E_A) during ESE and LSE (Figure 4.6 and S4.6) were compared by means of the parameters of fitted sigmoidal curves (Table 4.1). Early season drought-induced reduction in leaf scale water use was only moderately affected under eCO_2, as the inflection point was shifted to smaller $\Delta\Psi$ ($P < 0.1$) while other curve parameter were left unaltered ($P > 0.1$). During LSE, however, the g_s drought response was highly affected by eCO_2: the inflection point was shifted to larger $\Delta\Psi$ ($P < 0.001$), the reduction rate slowed down ($P < 0.01$) and the settling plateau lowered ($P < 0.01$) under eCO_2. For leaf C gain, A_n reduction with progressing drought did not differ between eCO_2 and aCO_2 during ESE ($P > 0.1$). During LSE, reduction rate was left unaltered while the settling plateau of A_n was lowered under eCO_2 ($P < 0.05$). The inflection point was apparently shifted to larger $\Delta\Psi$ under eCO_2, however, the effect of the [CO_2] treatment being not significant ($P = 0.11$, Figure S4.6). Leaf C loss was not affected by the [CO_2] treatment during the early or late season ($P > 0.1$). At the whole-tree scale, [CO_2] treatment did not alter any of the surveyed variables during any of the seasonal experiments (g_c, DG or E_{A_daily}; Figure 4.6, right-hand side panels, Table 4.1). This observation indicates that differences in leaf responses to drought under eCO_2, did not directly translate into whole-tree responses.
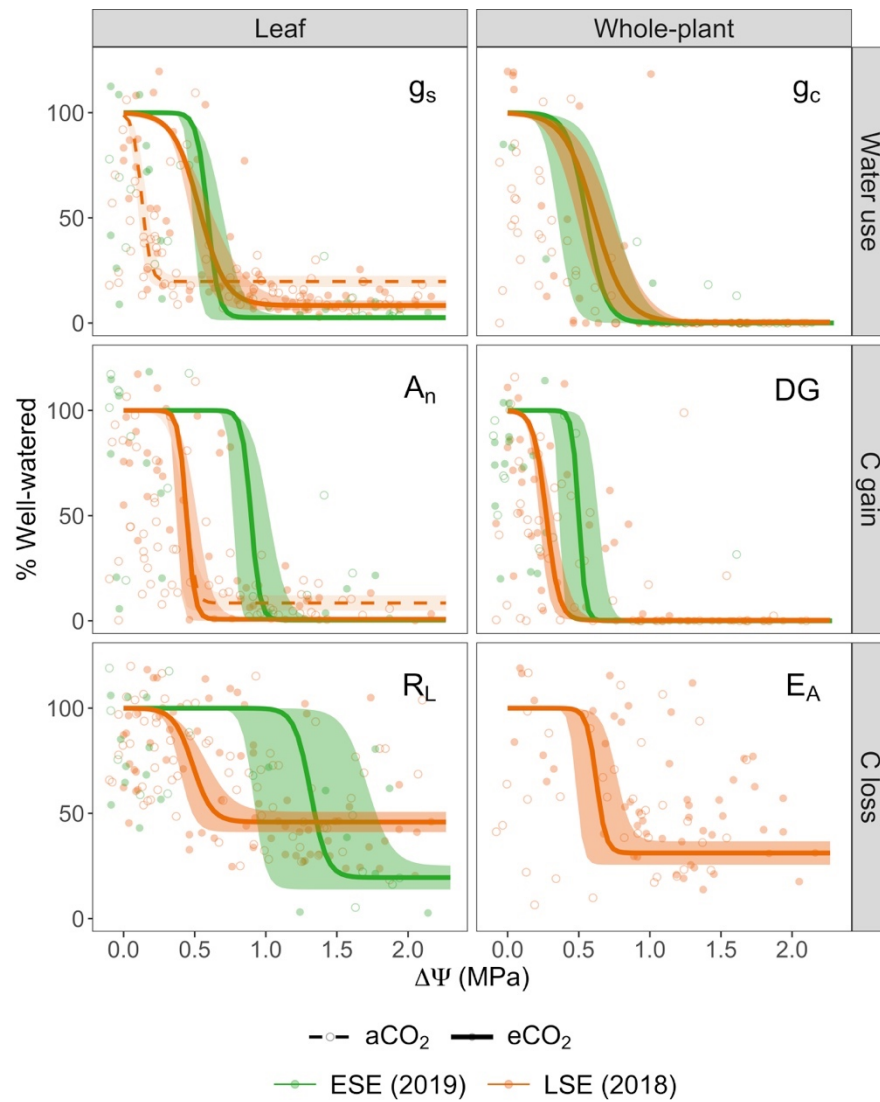
Figure 4.6 Normalized value (as percentage of the well-watered average) of leaf (left-hand side panels) and whole-tree (right-hand side panels) measurements with increasing drought stress ($\Delta\Psi$ = well-watered – drought stressed xylem water potential) along the course of the early (green, ESE – 2019) and late (orange, LSE - 2018) season experiments, in which one-year-old European aspen trees were subjected to combined treatments of $[CO_2]$ and drought stress. Measurements include stomatal conductance (g_s) and daily canopy conductance (g_c) to describe water use (upper panels), leaf net carbon assimilation (A_n) and daily stem volumetric growth (DG) to describe carbon gain (middle panels), and leaf respiration (R_L) and daily stem CO_2 efflux (E_A) to describe carbon respiratory losses (lower panels).

Open and closed points indicate trees subjected to ambient (aCO_2) and elevated (eCO_2) $[CO_2]$, respectively. Average curve parameters (a, b and s) and corresponding standard error were calculated across parameters individually adjusted per tree and used to display the average drought response curve and error band. Curve parameters were averaged across all trees when no differences ($P > 0.05$) were observed between $[CO_2]$ treatments for any parameter. Different curves for aCO_2 and eCO_2 are shown when differences ($P < 0.05$) were observed for at least one parameter, with different curves being built considering uniquely differential parameters.

Table 4.1 Mean values and standard error of fitted parameters (reduction rate a, inflection point b and settling plateau s) of the sigmoidal curves defining relative reductions in stomatal conductance (g_s), daily canopy conductance (g_c), leaf net carbon assimilation (A_n), daily stem volumetric growth (DG), leaf respiration (R_L) and stem CO_2 efflux (E_A). Measurements were conducted during an early (ESE - 2019) and late (LSE - 2018) season experiment and under ambient (aCO_2) and elevated (eCO_2) [CO_2] growing conditions.

Different letters indicate significant differences (• $P < 0.1$, * $P < 0.05$, t.test or wilcox.test) between [CO_2] treatment levels (aCO_2 and eCO_2) for each parameter of the fitted curve. Mean value and standard error of the correlation between measured and predicted values is shown as proxy of the goodness of fit (GF) of the sigmoidal curves and differences between spatial scales (leaf vs. whole-plant) within each flux-type (water use (g_s, g_c) , carbon gain (A_n, DG) and carbon loss (R_L, E_A)) are also indicated (• $P < 0.1$, * $P < 0.05$, linear mixed model). Daily canopy conductance under aCO_2 during ESE represents one tree only due to delayed onset of SF measurements.

			Reduction rate (a)		Inflection point (-b, MPa)		Settling plateau (s, %)		GF	
			aCO_2	eCO_2	aCO_2	eCO_2	aCO_2	eCO_2	aCO_2	eCO_2
ESE (2019)	Water	g_s	11.05 ± 5.13 a	38.8 ± 20.59 a	0.78 ± 0.13 a	0.44 ± 0.13 b•	0.02 ± 0.02 a	0.03 ± 0.02 a	0.78 ± 0.08	0.78 ± 0.07
		g_c	3.49 a	18.46 ± 4.20 a	0.84 a	0.46 ± 0.25 a	0.00 a	0.00 ± 0.00 a	0.75	0.99 ± 0.01
	C gain	A_n	50.81 ± 30.82 a	13.46 ± 5.68 a	0.90 ± 0.20 a	0.89 ± 0.17 a	0.01 ± 0.01 a	0.00 ± 0.00 a	0.73 ± 0.14	0.78 ± 0.07
		DG	46.28 ± 29.75 a	40.70 ± 19.57 a	0.70 ± 0.27 a	0.34 ± 0.10 a •	0.00 ± 0.00 a	0.00 ± 0.00 a	0.80 ± 0.05	0.82 ± 0.05
	C loss	R_L	21.78 ± 10.01 a	13.65 ± 7.46 a	1.11 ± 0.28 a	1.52 ± 0.79 a	0.23 ± 0.09 a	0.16 ± 0.07 a	0.82 ± 0.04	0.73 ± 0.13
		E_A								
LSE (2018)	Water	g_s	35.98 ± 4.42 a	10.34 ± 2.81 b*	0.11 ± 0.03 a	0.53 ± 0.07 b*	0.21 ± 0.02 a	0.08 ± 0.02 b*	0.46 ± 0.15	0.72 ± 0.11
		g_c	7.09 ± 1.58 a	10.82 ± 1.98 a	0.47 ± 0.21 a	0.55 ± 0.31 a	0.01 ± 0.01 a	0.00 ± 0.00 a *	0.80 ± 0.08	0.57 ± 0.24
	C gain	A_n	22.42 ± 9.02 a	47.97 ± 34.14 a	0.33 ± 0.10 a	0.56 ± 0.08 a	0.08 ± 0.04 a	0.01 ± 0.01 b*	0.72 ± 0.05	0.89 ± 0.06
		DG	16.90 ± 7.10 a	28.23 ± 11.54 a	0.32 ± 0.06 a	0.23 ± 0.06 a •	0.00 ± 0.00 a	0.00 ± 0.00 a *	0.58 ± 0.13	0.52 ± 0.07
	C loss	R_L	9.81 ± 2.74 a	18.65 ± 9.30 a	0.56 ± 0.10 a	0.44 ± 0.15 a	0.54 ± 0.10 a	0.33 ± 0.07 a	0.74 ± 0.11	0.71 ± 0.03
		E_A	17.12 ± 9.23 a	42.23 ± 15.21 a	0.60 ± 0.25 a	0.65 ± 0.20 a	0.24 ± 0.05 a	0.39 ± 0.08 a	0.70 ± 0.19	0.80 ± 0.01

When comparing leaf and whole-tree drought responses within a single seasonal experiment and flux type (i.e. left- versus right-hand side panels in Figure 4.6), differences in drought-induced reductions between spatial scales were assessed for water use (g_s vs. g_{c_daily}), C gain (A_n vs. DG) and C loss (R_L and E_{A_daily}) responses (Table 4.1). For water processes, difference between spatial scales was limited to a higher settling plateau for g_s in comparison to g_{c_daily} ($P < 0.01$) during the LSE. For C gain, the inflection point was moderately smaller for DG than for A_n during ESE ($P < 0.1$) and LSE ($P < 0.01$), indicating an earlier drought-driven reduction in DG than A_n. Additionally, a small, yet significant, difference was found between the settling plateau of A_n and DG during the LSE ($P < 0.05$). This residual leaf activity (in g_s and A_n) relative to whole-tree activity cessation (in g_{c_daily} and DG) under severe drought likely reflects sampling bias towards functional greener leaves. No differences in the fitted parameters were observed between R_L and E_A curves during LSE ($P > 0.1$).

Early and late season drought responses were compared by pooling data from both [CO_2] treatments. Differences between seasonal experiments were limited to leaf scale g_s ($P < 0.05$), A_n ($P < 0.01$), with a shift of the inflection point to smaller $\Delta\Psi$ during LSE. Also, inflection point of R_L was moderately shifted to smaller $\Delta\Psi$ during the late compared to the early season ($P < 0.1$). All reduction rates and inflection points of whole-tree g_{c_daily} and DG remained unaffected by the seasonal timing of drought ($P > 0.1$).

To explore the sequential down-regulation of different processes (A_n, g_s, R_L, DG, g_{c_daily} and E_{A_daily}) under progressive drought independent of the [CO_2] conditions and the seasonal timing of the drought event, curve parameters from both ESE and LSE and aCO_2 and eCO_2 were combined (Figure 4.7). Overall, stem volumetric growth was the first process to decline, with the DG inflection point ($\Delta\Psi = 0.38 \pm 0.07$ MPa) being smaller ($P < 0.05$) than that of A_n (0.67 ± 0.09 MPa), E_{A_daily} (0.62 ± 0.14 MPa) and R_L (0.98 ± 0.25 MPa). However, no differences was found ($P > 0.1$) between the inflection point of DG and that of g_s (0.45 ± 0.07 MPa) or g_{c_daily} (0.55 ± 0.11 MPa). At maximal drought levels, the settling plateau was highest for C loss (respiratory) fluxes (28.83 ± 5.00 and 31.12 ± 5.59 % for R_L and E_{A_daily}, respectively), reflecting substantial maintenance of respiratory metabolism. The reduction rate did not statistically differ among variables ($P > 0.1$).
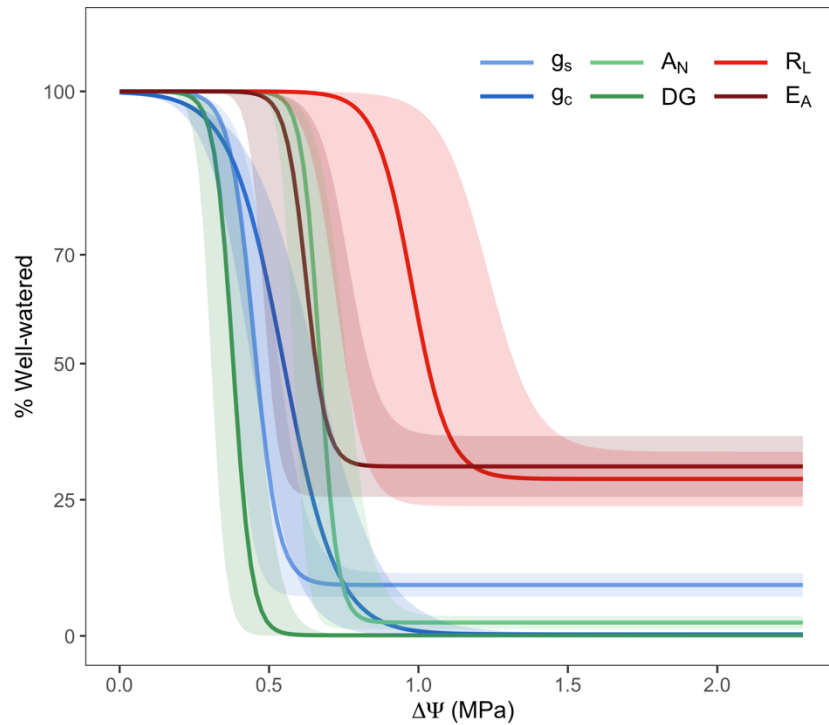
Figure 4.7 Normalized value (as a percentage of the well-watered average) of leaf and whole-tree measurements with increasing drought stress ($\Delta\Psi$ = well-watered – drought stressed xylem water potential). Measurements include stomatal conductance (g_s), daily canopy conductance (g_c), leaf net carbon assimilation (A_n), daily stem volumetric growth (DG), leaf respiration (R_L) and daily stem CO_2 efflux (E_A).

Average curve parameters and corresponding standard error were calculated across parameters individually adjusted per tree, independent of the [CO_2] treatment and seasonal experiment, and used to display the averaged drought response curve and error band. Line colours differentiate among flux-types (with blue, green and red representing water use (g_s, g_c), carbon gain (A_n, DG) and carbon loss (R_L, E_A), respectively. Light and dark lines indicate leaf and whole-tree measurements, respectively.

Discussion

Different responses during early and late season drought

Dry biomass was differently affected by the drought and [CO_2] treatments during the early and the late season (Figure 4.1). Dry biomass remained unaffected under eCO₂ in the early season but reduced under drought. Contrastingly, dry biomass increased under eCO₂ in the late season, while remaining unaltered by the drought treatment. Timing of drought events on whole-tree development only gained interest over the last decade (Granda et al. 2013, Lévesque et al. 2013, Camarero et al. 2015, D'Orangeville et al. 2018, Forner et al. 2018). Previous studies agree with our observations on the young *Populus* trees that the early season drought event altered current year growth. For example, a study including 346 temperate forest stands in North America showed that early season drought effectively reduced stem

volumetric growth, while stem volumetric growth remained largely unaltered when drought occurred later in the season (D'Orangeville et al. 2018). The root:shoot ratio (Figure S4.2) was unaffected by eCO_2 during ESE and LSE. This observation indicates proportional stimulation of above- and below-ground biomass production, as similarly observed in short-rotation *Populus* plantation (Calfapietra et al. 2003). During LSE, root:shoot ratio was higher for well-watered trees as a result of the relatively stronger drought-driven inhibition of root growth during the last month of LSE (DOY 253 – 288) as root productivity may increase under well-watered conditions as the growing season progresses (Broeckx et al. 2014).

Differences between early and late season drought responses were also observed at leaf scale with increasing drought ($\Delta\Psi$). Independently of the $[CO_2]$ treatment, drought-induced reduction of A_n, g_s and R_L occurred at smaller $\Delta\Psi$ during the late season in comparison with the early season, confirming our first hypothesis (Figure 4.6). Early season leaf development is largely dependent on C availability for new cell differentiation and development. As the season progresses, leaf growth will be mainly driven by cell enlargement and thus turgor pressure and water availability (Pantin et al. 2012). According to the high C sink strength of young leaves, Pantin et al. (2012) suggested that leaf drought tolerance decreases with leaf age since reduced C allocation towards old leaves will result in a limited ability for osmotic adjustement to face drought. We suggest that high C requirements during the early season for the development of both aboveground and belowground tissues could trigger a less conservative behavior in water use, with prolonged leaf scale activity despite potentially larger reductions in Ψ_{xylem}. Oppositely, lower C requirements during the late season may have resulted in a comparatively rapid down-regulation of leaf gas exchange to improve plant water status. In any case, our observations should be interpreted with caution as inter-annual differences in tree sets and climatic conditions (summer 2018 was extremely warm in central Europe) could bias comparisons between early and late season experiments.

Drought mitigation under elevated CO_2 at leaf and whole-tree scale

During the drought period and over time, effects of the $[CO_2]$ treatment were limited to an overall increase in A_n and a reduction in R_L during ESE and LSE, respectively (Figure 4.3f and S4.4d). Stomatal conductance remained, however, unaffected by the $[CO_2]$ treatment over time, suggesting no mitigation or aggravation of drought under eCO_2 (Figure 4.3b). Despite the neutral effect of eCO_2 on Ψ_{xylem} (Figure 4.2), discrepancies in eCO_2 mitigating effects arose when comparing drought responses over time (Figure 4.3; drought responses were not affected by eCO_2) and along $\Delta\Psi$ gradients (Figure 4.6; delayed and slowed down stomatal closure under eCO_2). We suggest that assessment of drought responses against the corresponding $\Delta\Psi$ measured *in situ* (rather than over time) might provide more accurate

88

insights on the potential leaf acclimation to eCO_2 over the surveyed drought gradient. With declining water status eCO_2 delayed and slowed the reduction of g_s during LSE, counter to expectations of an earlier stomatal closure based on stomatal behaviour under well-watered conditions (Ainsworth and Rogers 2007, Walker et al. 2020). In parallel, an apparent delay in A_n reduction was noticed under eCO_2 (Figure S4.6), likely masked by the limited statistical power of our test (n = 5). When drought was moderate ($\Delta\Psi < 0.5$ MPa), stomata remained open in eCO_2 grown leaves, allowing leaf gas exchange under greater xylem tension. This less conservative behaviour under eCO_2 may transiently mitigate drought in terms of C uptake. An eCO_2-induced delay of photosynthetic inhibition has previously been observed in different tree species (Goodfellow et al. 1997, Herrick et al. 2004, Birami et al. 2020), and it is usually attributed to the alleviation of C limitation to RuBisCo carboxylation activity after partial stomatal closure (Menezes-Silva et al. 2019). In the young *P. tremula* trees surveyed here, however, the apparent prolonged A_n activity under eCO_2 can most likely be attributed to the delayed stomatal closure. When drought was most severe ($\Delta\Psi > 1$ MPa), final settling plateaus of g_s and A_n were lower under eCO_2, indicating lower residual water loss to the detriment of limited C fixation. The dependency of the settling plateaus for both g_s and A_n on the [CO_2] treatment partly refutes our second hypothesis, as the effects of the [CO_2] treatment did not completely vanished at highest levels of drought severity.

Supporting our third hypothesis, none of the whole-tree responses to drought (g_c, DG and E_A) were altered by eCO_2 along the surveyed gradient of water potential (Figure 4.6). In terms of water use, delayed g_s reduction under eCO_2 with increasing drought did not lead to parallel alterations in whole-tree water use (g_{c_daily}). In their review, Choat et al. (2018) suggested that stomatal response curves under drought can be used as a proxy for xylem hydraulic vulnerability, as stomatal closure will delay critical xylem tension than might result in embolism formation. Following this reasoning, later onset of stomatal closure under eCO_2 would imply later onset of drought-induced embolism and thus delayed g_{c_daily} reduction (Venturas et al. 2017, Choat et al. 2018). Nonetheless, unresponsive canopy conductance to the [CO_2] treatment does not support this idea, highlighting the likelihood for misjudgement when effects of eCO_2 on hydraulic functioning are solely based on eCO_2-induced alterations of drought responses measured at the leaf scale. Stimulation of leaf A_n under eCO_2 before the onset of drought for both ESE and LSE (Figure 4.3 and S4.4) and consequent initial increases in leaf and xylem [NSC] (Figure 4.5) did not mitigate detrimental effects of drought on stem volumetric growth, as DG similarly ceased under both [CO_2] treatments after relatively small drop in water potential. Likewise, the drought-driven reduction of E_A and its settling plateau, as a proxy of stem respiration, remained unaltered by the [CO_2] treatment, suggesting that other factors

(rather than leaf C availability) govern the regulation of stem growth and respiratory metabolism when facing drought stress.

Sequential down-regulation of leaf and whole-tree carbon processes

Over the past two decades, the traditional perspective of C (source) driven plant growth has been challenged by the growing body of studies evidencing the major role of the C sink strength (Körner 2003, 2015, Sala et al. 2012, Fatichi et al. 2014, 2019, Steppe et al. 2015, Peters et al. 2020b). Although this revisited view of sink driven tree growth does not dispute the relevance of C availability, its importance is downgraded as it no longer outranks other key drivers, including nutrient and water availability, and other environmental conditions as temperature (Körner 2015). When one of the key drivers becomes limiting, tree growth would immediately decline, despite possible and temporal preservation of A_n (Fatichi et al. 2014). Accordingly, this sequential drought response over time has been observed in different tree species (Muller et al. 2011, Mitchell et al. 2014, Lin et al. 2018) including *Populus* spp. (Bogeat-Triboulot et al. 2007). Here, in the young *Populus* trees under study, earlier reductions in stem volumetric growth were also observed when facing drought despite the continued C gain (A_n) (Figure 4.7).

During the period of zero stem volumetric growth and continued C gain at early drought stages, tree C balance could improve, leading to potential accumulation of NSC (Mitchell et al. 2014, Lin et al. 2018) if C respiratory expenditures do not exceed C uptake. Here, when facing moderate drought (three weeks into the drought period; $\Psi_{xylem} < -2$ MPa), NSC measurements did, however, not indicate any improvement in the C status in any of the sampled tissues (Figure 4.5). On the contrary, drought lowered [NSC] in leaf and bark tissues, whereas [NSC] levels remained unaffected in the xylem. The reason for the absence of C accumulation is twofold. First, the delay in A_n reduction compared to DG cessation (i.e. the carbon safety margin; as defined in Mitchell et al. 2014) was relatively small, with a difference in inflection points of 0.30 MPa. A small C safety margin limits the time window during which C accumulation is possible (Mitchell et al. 2014), hereby making young *P. tremula* trees rapidly dependent on their NSC pools, as similarly observed in young *P. deltoides* trees (Wertin and Teskey 2008). Second, and according to the growth and maintenance respiration paradigm (Amthor 1984), growth respiration is expected to cease in parallel to growth rates. However, basal respiration rates should be maintained to meet metabolic requirements as long as the tree is alive (maintenance respiration). Therefore, potential C accumulation during zero stem volumetric growth and moderate drought levels was counterbalanced as leaf respiration and stem CO_2 efflux did not decrease before leaf C gain did, hereby resulting in the observed

partial depletion of NSC pools throughout tree organs (Adams et al. 2013, Hartmann and Trumbore 2016).

With increasing drought, maintenance respiratory metabolism decreased, but remained active in both foliar and woody tissues, stabilizing at approximately 30 % of well-watered conditions. CO_2 efflux in drought stressed trees was fuelled by remaining NSC pools, explaining the progressive depletion of NSC throughout tissues as drought intensity increased from moderate to severe. It is worthy to note that only under well-watered conditions (during the pre-drought period), as a likely consequence of stimulated A_n, [NSC] increased under eCO_2 in foliar and xylem tissues. However, the progressive depletion of NSC pools with drought was not affected by the [CO_2] treatment, as pre-drought differences between aCO_2 and eCO_2 grown trees disappeared under moderate and severe drought levels. These observations suggest non prioritized allocation of C surplus for storage, as it could be expected in young and fast growing trees (Wertin and Teskey 2008, Salomón et al. 2018b, Gattmann et al. 2020). Taken together, our observations highlight complex NSC dynamics under drought, and question the ability of eCO_2 to mitigate drought.

Conclusions

In conclusion, four insights can be gained from this study. First, drought-induced down-regulation of leaf gas exchange occurred faster during the late than during the early season. A greater C demand during the early season may have triggered this less conservative behaviour in water use. Water conservation might become more important as the season progresses and turgor pressure driving cell enlargement gains relative importance for leaf volumetric growth. Second, the [CO_2] treatment had limited effects on leaf responses to drought in young *Populus tremula* trees and effects were restricted to the late season only. With increasing levels of drought (greater $\Delta\Psi$), g_s reduction was less susceptible under eCO_2. Likewise, an apparent delay in the reduction of A_n occurred under eCO_2, with the effect being not significant. Third, despite the limited alterations in leaf scale drought dynamics, whole-tree drought responses remained unaltered under eCO_2 with decreasing water potential. This highlights the complexity of the interaction between leaf and whole-tree responses under combined drought stress and eCO_2. Fourth, when combining data across [CO_2] treatments and seasonal experiments, stem volumetric growth ceased earlier than A_n under drought stress, while leaf respiration and stem CO_2 efflux (as proxy for stem respiration) were maintained at 30 % of pre-drought levels, even under most severe drought. This sequential down-regulation of physiological processes resulted in a progressive depletion of NSC pools in leaf, bark and xylem tissues, regardless any effect of the [CO_2] treatment. Taken together,

results suggest that the ability of eCO_2 to mitigate drought stress is small and limited to leaf processes and moderate drought stress levels during the late season.
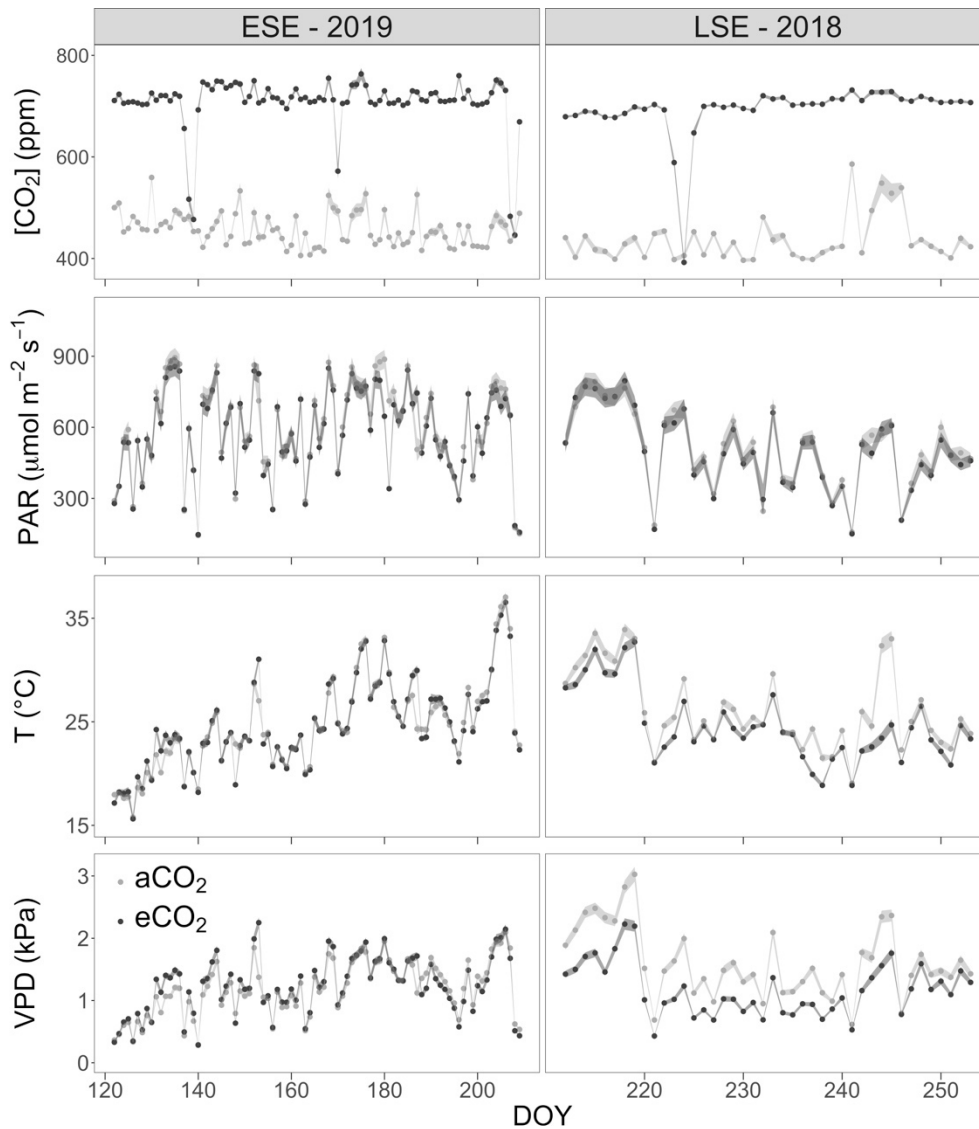
Supplementary material

Figure S4.1 Average chamber CO_2 concentration ($[CO_2]$) during daytime (PAR > 5 µmol m^{-2} s^{-1}), photosynthetically active radiation (PAR), temperature (T) and vapor pressure deficit (VPD) in the ambient (aCO_2, light grey) and elevated (eCO_2, dark grey) $[CO_2]$ growth chamber and along the course of the early (ESE - 2019, left-hand side panels) and late (LSE - 2018, right-hand side panels) season experiment (with DOY day of year).
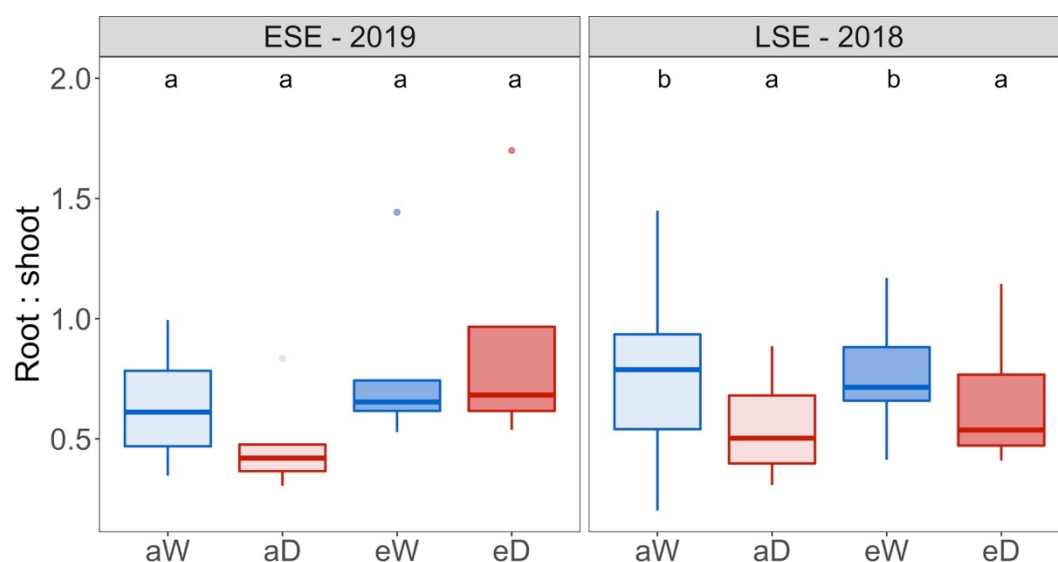
Figure S4.2 Root-to-shoot ratio at the end of the early (ESE - 2019) and late (LSE - 2018) season drought experiment.

One-year-old European aspen trees were subjected to combined treatments of $[CO_2]$ (a and e for ambient and elevated $[CO_2]$, respectively) and drought stress (W and D for well-watered and drought stress, respectively). Letters indicate statistical differences among treatment combinations (linear model, $P < 0.05$, n = 4-5 and 9-12 for ESE and LSE, respectively).
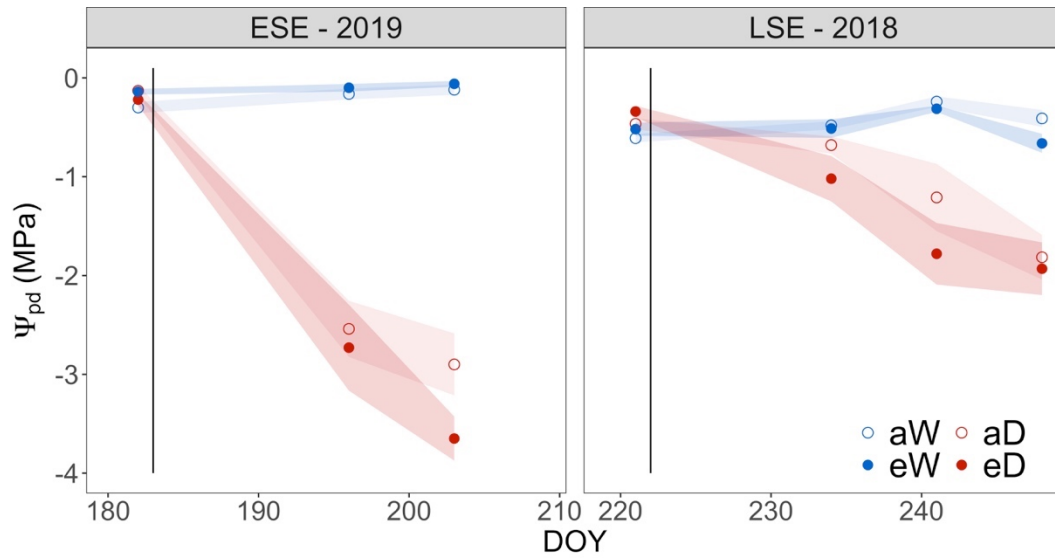
Figure S4.3 Pre-dawn water potential (Ψ_{pd}) over time during the early (ESE - 2019) and late (LSE - 2018) season experiments.

One-year-old European aspen trees were subjected to combined treatments of [CO_2] (a and e for ambient and elevated [CO_2], respectively) and drought stress (W and D for well-watered and drought stressed, respectively). Vertical lines indicate the start of the drought treatment. With DOY day of year.
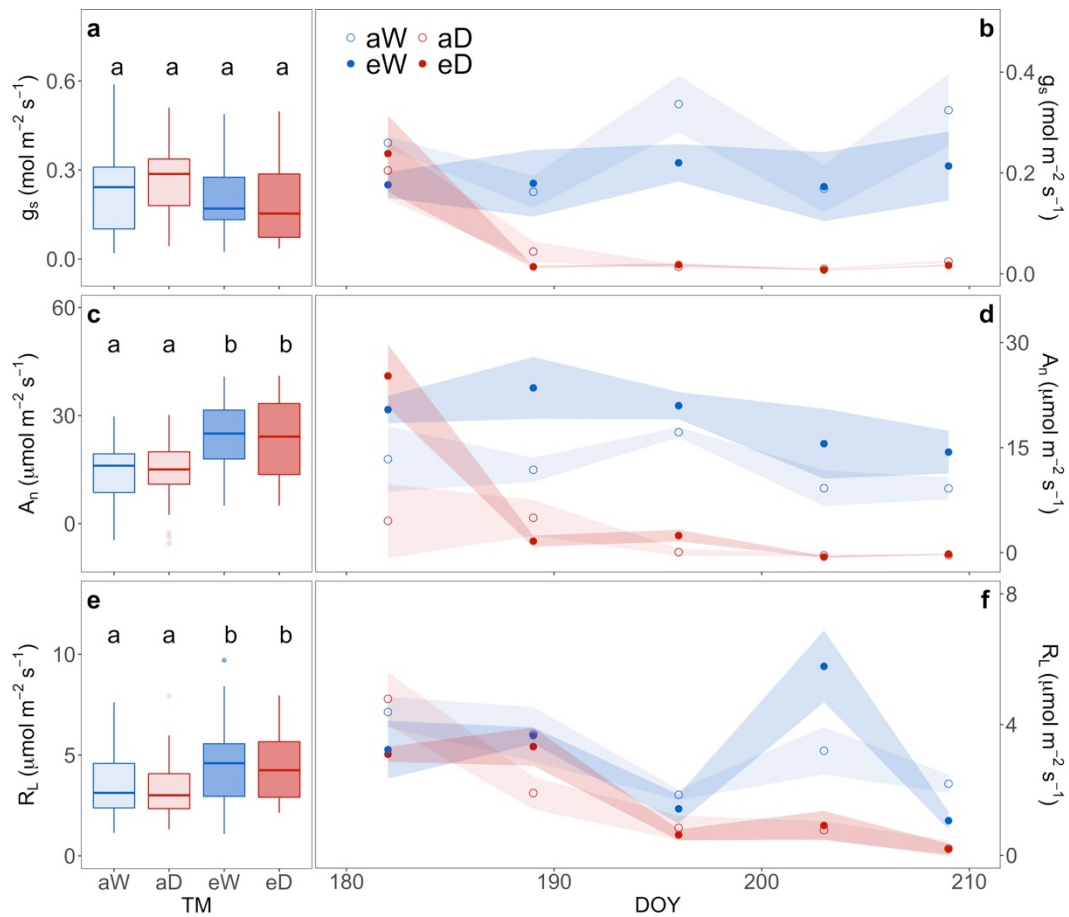
Figure S4.4 Comparison of leaf stomatal conductance (g_s, a-b), net carbon assimilation (A_n, c-d) and respiration (R_L, e-f) in the early season experiment (2019) during the pre-drought period (left-hand side panels) and over time during the drought period (right-hand side panels).

One-year-old European aspen trees were subjected to combined treatments of $[CO_2]$ (a and e for ambient and elevated $[CO_2]$, respectively) and drought stress (W and D for well-watered and drought stressed, respectively). Letters indicate statistical differences (linear mixed model, $P < 0.05$) among treatment combinations. With DOY day of year.

Figure S4.5 Comparison of whole-tree canopy conductance (g$_c$, a-b) and daily stem volumetric growth (DG, c-d) in the early season experiment during the pre-drought period (left-hand side panels) and over time during the drought period (right-hand side panels).

One-year-old European aspen trees were subjected to combined treatments of [CO₂] (a and e for ambient and elevated [CO₂], respectively) and drought stress (W and D for well-watered and drought stressed, respectively). Letters indicate statistical differences (linear mixed model, $P < 0.05$) among treatment combinations. With DOY day of year.
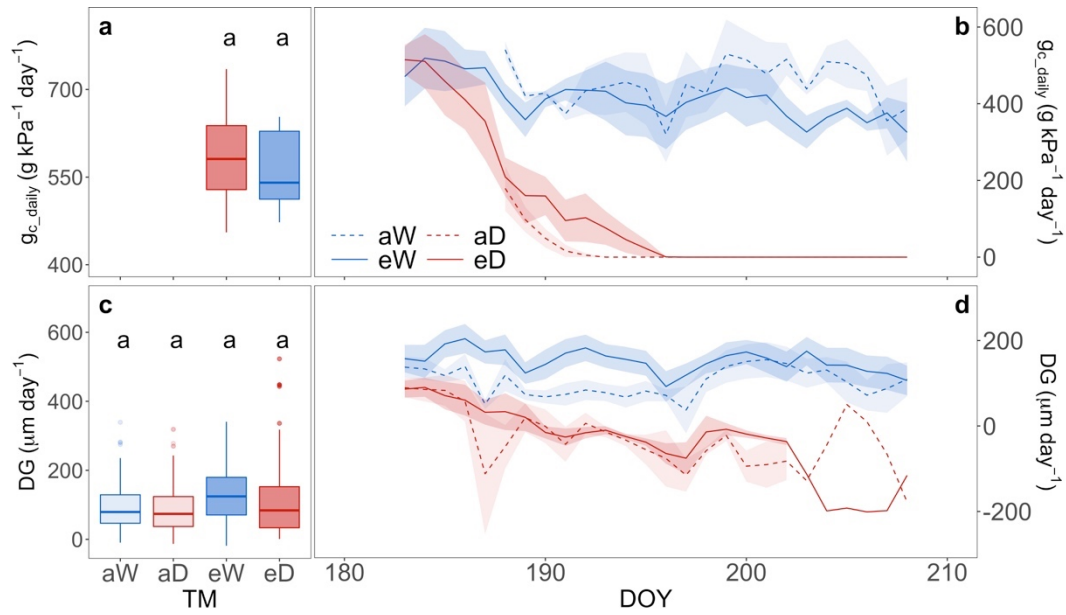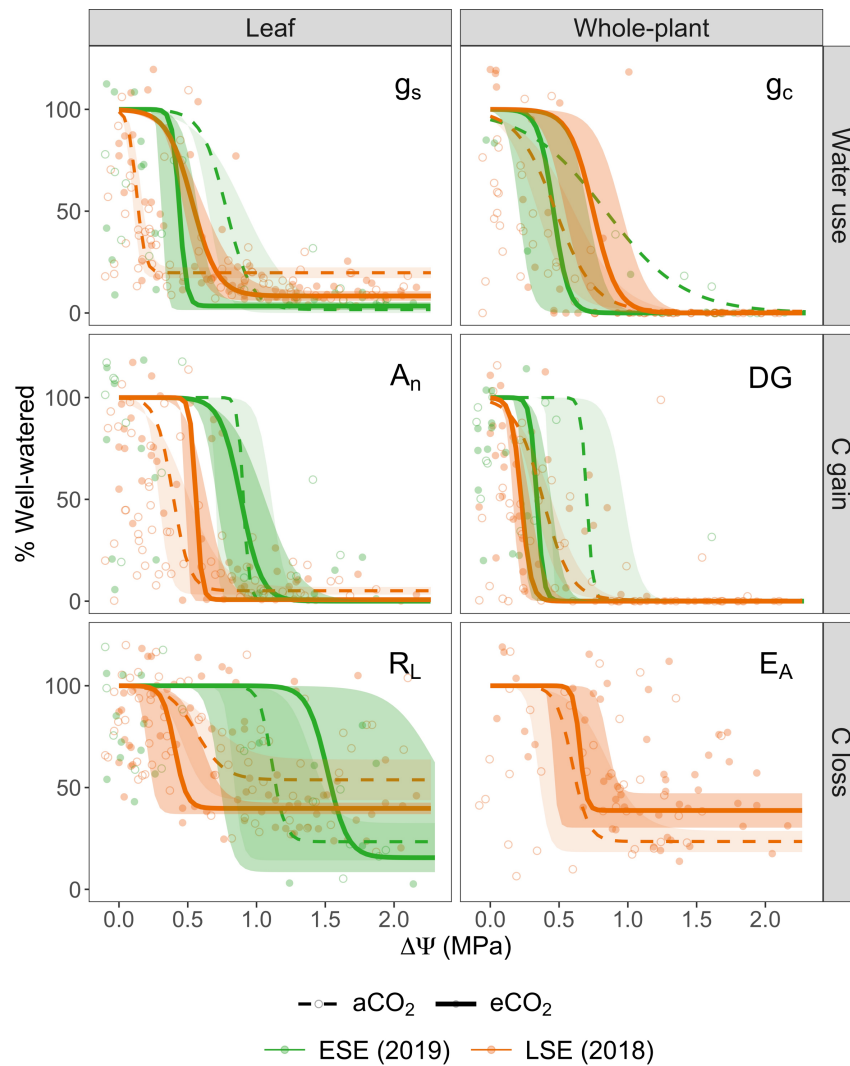
Figure S4.6 Normalized value (as percentage of the well-watered average) of leaf (left-hand side panels) and whole-tree (right-hand side panels) measurements with increasing drought stress ($\Delta\Psi$ = well-watered – drought stressed xylem water potential) along the course of the early (green, ESE - 2019) and late (orange, LSE - 2018) season experiments, in which one-year-old European aspen trees were subjected to combined treatments of $[CO_2]$ and drought stress. Measurements include stomatal conductance (g_s) and daily canopy conductance (g_c) to describe water use (upper panels), leaf net carbon assimilation (A_n) and daily stem volumetric growth (DG) to describe carbon gain (middle panels), and leaf respiration (R_L) and daily stem CO_2 efflux (E_A) to describe carbon respiratory losses (lower panels).

Open and closed points indicate one-year-old European aspen trees subjected to ambient (aCO_2) and elevated (eCO_2) $[CO_2]$, respectively. Average curve parameters (a, b and s) and corresponding standard error were calculated across parameters individually adjusted per tree and used to display the average drought response curve and error band. Curve parameters were averaged across all trees per $[CO_2]$ treatment and seasonal experiment. Daily canopy conductance under aCO_2 during ESE represents one tree only due to delayed onset of measurements.

5

Elevated CO_2 increases hydraulic vulnerability in young European aspen trees during early but not late season drought

Abstract

The timing of abiotic stress elicitors on wood formation largely affect xylem traits that determine xylem efficiency and vulnerability. Nonetheless, seasonality in effect of elevated atmospheric carbon dioxide concentration (eCO$_2$) on tree drought responses remains largely unknown. To address this knowledge-gap, one-year-old *Populus tremula* L. trees were grown under ambient and elevated CO$_2$ and exposed to early (spring/summer 2019) and late (end of summer 2018) season drought events. Stomatal conductance and stem shrinkage were monitored *in vivo* as xylem water potential decreased. Additional trees were harvested for characterization of wood anatomical traits and to determine vulnerability and desorption curves via bench dehydration. The abundance of narrow vessels decreased under eCO$_2$ only during the early season. At this time, xylem vulnerability to embolism formation and hydraulic capacitance during severe drought increased under eCO$_2$. Contrastingly, stomatal closure was delayed during the late season, while hydraulic vulnerability and capacitance remained unaffected under eCO$_2$. Independently of the CO$_2$ treatment, elastic and inelastic water pools depleted simultaneously after halfway of complete stomatal closure. Our results suggest that the effect of eCO$_2$ on drought physiology and wood traits varies during the season, and questions a sequential capacitive water release from elastic and inelastic pools as drought proceeds.

Introduction

Forests are exposed to unprecedented climate changes driven by a rapid rise in atmospheric CO$_2$ concentration ([CO$_2$]). As a consequence, air temperature is rapidly increasing and precipitation patterns are altering, often leading to longer and more intense drought episodes (IPCC 2018). Drought, in particular when exacerbated by high temperature and vapor pressure deficit, has far-reaching effects on tree functioning and vitality (Choat et al. 2018, Hartmann et al. 2018, Brodribb et al. 2020). Across a wide variety of species and biomes, hydraulic failure has been suggested as the predominant underlying cause of drought-induced mortality (Adams et al., 2017; McDowell, 2011). Although tree hydraulic architecture is largely genetically determined (Pritzkow et al. 2020, Challis et al. 2020), resource availability and environmental conditions can alter tree allometry and xylem traits (Diaconu et al. 2016, Deslauriers et al. 2017). Therefore, exposure to elevated [CO$_2$] (eCO$_2$) may also affect anatomical traits and determine the tree's response to drought (Tognetti et al. 1999, Domec et al. 2017, Bartlett et al. 2019).

When facing drought, stomatal closure limits water losses (Choat et al. 2018). Although necessary to prevent a rapid decline of xylem water potential (Ψ_{xylem}), stomatal closure hampers CO_2 uptake for photosynthesis and negatively affects the tree carbon balance (McDowell et al. 2008, Drake et al. 2017). Residual water losses through leaf (Kerstiens 1996) and bark (Oren and Pataki 2001) further reduce tree water status (Choat et al. 2018, Körner 2019, Machado et al. 2020). When reaching the critical Ψ_{xylem} threshold for drought-induced embolism formation, tension developed in xylem conduits may disrupt the continuous water column leaving an inactive air-filled conduit (Sperry 2000, Venturas et al. 2017). Propagation of embolism events throughout the xylem may cause systemic failure of the vascular system and ultimately tree death (Adams et al. 2017, Hammond et al. 2019). Different techniques have been developed to assess the relationship between loss of xylem hydraulic conductivity (k_h) and Ψ_{xylem}, commonly referred to as the vulnerability curve and useful to obtain the P_{50} value, i.e. the Ψ_{xylem} corresponding with 50 % loss of k_h (Cochard et al. 2013, Nolf et al. 2015, De Baerdemaeker et al. 2019a, Sergent et al. 2020). Although seemingly easy to interpret, vulnerability curves contain no information on the rate of Ψ_{xylem} reduction and hence k_h loss as drought proceeds (Meinzer et al. 2009). More complex approaches have therefore attempted to assess drought responses under natural conditions, often by integrating the role of stomatal regulation on xylem functioning (Li et al., 2019). Examples of these approaches are evaluation of the hydraulic safety margin, i.e. the difference between midday Ψ_{xylem} and hydraulic vulnerability thresholds (Meinzer et al. 2009, Delzon and Cochard 2014, Skelton et al. 2015), or the hydroscape area, i.e. the Ψ_{xylem} range that stomata are still able to regulate leaf gas exchange (e.g. Johnson et al., 2018; Li et al., 2019; Meinzer et al., 2016). For long, the P_{50} value, as a proxy of xylem vulnerability for drought-induced embolism formation, has been considered a static parameter. A recent study on grapevine (*Vitis vinifera*) leaves, however, contradicted this assumption as P_{50} decreased from the early to the late season, suggestsing that xylem vulnerability to embolism is variable over time, as a likely result of seasonal changes in wood anatomical traits (Sorek et al. 2020).

Capacitive release of internal water pools to fulfil the evaporative demand buffers Ψ_{xylem} reductions, and therefore delays (or possibly avoids) drought-induced embolism (Tyree and Ewers 1991, Meinzer et al. 2009, Choat et al. 2018). Desorption curves describe the relation between water content and Ψ_{xylem}, with the hydraulic capacitance being defined as the corresponding slope (Zweifel et al. 2001, Steppe et al. 2006, Steppe 2018). Since trees store water in different organs and tissues, desorption curves are commonly partitioned into different phases, each one characterized by its corresponding capacitance (Tyree and Yang 1990, Pratt and Jacobsen 2017, Choat et al. 2018, Steppe 2018).

Capillary water pools, i.e. intercellular spaces or lumen of previous embolized conduits, largely deplete at relatively high Ψ_{xylem} (> -0.5 MPa) and are therefore expected to be physiologically irrelevant under drought (Tyree and Yang 1990, Tyree and Ewers 1991). Elastic water pools, i.e. living cells mostly located in the bark and in xylem parenchyma rays, deplete and refill on a daily basis contributing to the transpiration stream (e.g. Tyree and Yang 1990, Zweifel et al. 2000, 2001, Steppe et al. 2006, De Swaef et al. 2015). Finally, water can be released from inelastic pools, i.e. embolized conduits, which is inevitably accompanied by reduction in k_h (Tyree and Yang 1990, Hölttä et al. 2009, Vergeynst et al. 2015).

The daily contribution of elastic water to the transpiration stream can be approached with highly-resolved measurements of stem diameter variations (De Swaef et al. 2015, Steppe et al. 2015, Zweifel 2016). Sub-daily depletion and refilling of stem water pools result in sub-daily dynamics of radial stem shrinkage and swelling. The difference between the maximal pre-dawn stem diameter and the minimal diameter during high-transpiration hours, known as maximum daily stem shrinkage, has been commonly used as a proxy for tree water status (e.g. De Swaef et al. 2009, Ortuño et al. 2009, Puerto et al. 2013). However, daily shrinkage largely depends on the diurnal atmospheric evaporative demand and does not account for the cumulative water loss under extended drought periods (De Swaef et al. 2009), which progressively limits stem hydraulic capacitance (Salomón et al. 2017a). To circumvent this issue, tree water deficit was introduced as a measure of stem water depletion (Zweifel 2016) and has proven to be a reliable indicator for water status in several tree species (Dietrich et al. 2018, Krejza et al. 2020). Briefly, tree water deficit is defined as the absolute stem shrinkage in relation to the previously registered diameter maximum (Zweifel 2016), hereby accounting for both seasonal stem dehydration and daily water release and refill (see Figure 5.1 from Zweifel (2016) for a visual illustration of this concept).

Drought tolerance is determined by both wood anatomical traits (e.g. conduit diameter and pit membrane thickness) and physiological functioning (e.g. stomatal regulation and hydraulic capacitance) (Choat et al. 2018, McCulloh et al. 2019), which both can acclimate to changing environmental conditions, including [CO_2] (Domec et al. 2017, Qaderi et al. 2019). Exposure to eCO_2 commonly results in photosynthetic stimulation and stomatal closure (Ainsworth and Rogers 2007), consequently increasing carbon availability (Norby et al. 2005) and altering hydraulic conductivity throughout tree organs (Hao et al. 2018b). Increased carbon availability may result in faster growth rates with development of wider conduits, favouring k_h and thus hydraulic efficiency (e.g. Domec et al. 2010, Kostiainen et al. 2014, Kim et al. 2015). Enhanced carbon availability may also result in stimulated cell
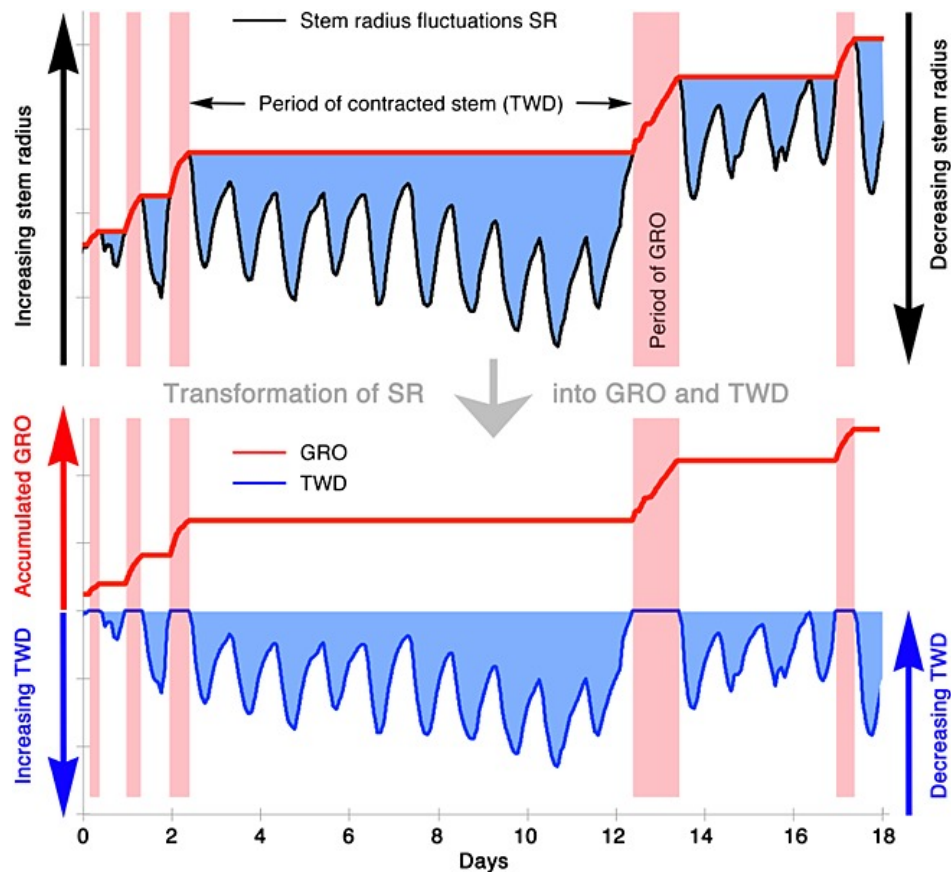
102

Figure 5.1 Determination of the irreversible growth-induced expansion (GRO, red lines) and the reversible and tree water deficit-induced shrinkage (TWD, blue lines) of the stem radius (SR, black lines). Time periods in which volumetric growth occurred and elastic water pools were depleted are indicated with the red and blue areas, respectively. Stem volumetric growth (i.e. cell division and elongation) is assumed to be zero during periods of stem shrinkage (Figure 1 from Zweifel (2016)).

wall deposition, thereby densifying wood and favouring mechanical strength (Saxe et al. 1998, Atwell et al. 2003, Domec et al. 2010, 2016). For long, it has been assumed that hydraulic efficiency is inversely linked with hydraulic vulnerability. The mechanism behind this assumption is that the chance of a failing pit triggering embolism propagation increases in larger conduits due to larger vessel surface area (e.g. Wheeler et al. 2005, Hacke et al. 2006, Christman et al. 2012). However, meta-analysis only detected a weak trade-off between hydraulic efficiency and vulnerability (Gleason et al. 2016). It is therefore expected that other xylem anatomical traits (e.g. conduit wall reinforcement and pit morphology) determine to a large extent xylem vulnerability to drought-induced embolism (Mrad et al. 2018, Janssen et al. 2020). Additional thickening of xylem cell walls under eCO₂ is expected to improve hydraulic resistance, as enhanced mechanical strength and robustness of the pit membranes decrease the risk of embolism propagation (Li et al.

2016). During the early 1990s, Tyree and Alexander (1993) already called for much-needed research on drought vulnerability under eCO_2. Nevertheless, the effects of eCO_2 on hydraulic vulnerability remain largely unexplored. To the best of our knowledge, only seven eCO_2 studies established vulnerability curves in tree species under eCO_2 so far (Table 5.1). Results are inconclusive, as greater xylem vulnerability (Domec et al. 2010, Warren et al. 2011) and no response (Tognetti et al. 1999, Gartner et al. 2003, Domec et al. 2010, Vaz et al. 2012, Hao et al. 2018b, Newaz et al. 2018) have been reported under eCO_2.

To assess the effects of eCO_2 on tree physiology under drought, we integrated measurements of leaf stomatal behaviour, stem shrinkage, vulnerability to embolism formation and stem water content along gradients of drought stress (Ψ_{xylem}) with wood anatomical traits. For this, young European aspen (*Populus tremula* L.) trees were grown in treatment chambers under ambient (aCO_2) or elevated (eCO_2) [CO_2]. Drought was imposed early and late during the growing season to further assess seasonality in the hydraulic response to eCO_2. *In vivo* drought responses were measured at leaf (stomatal conductance) and whole-tree (tree water deficit) scale. Xylem anatomical traits (including vessel diameter and tissue density), vulnerability to drought-induced vessel embolism formation and hydraulic capacitance were additionally determined. To this end, the bench dehydration method was used and simultaneous measurements of Ψ_{xylem}, embolism-related acoustic emissions (Nolf et al. 2015, De Roo et al. 2016) and stem volumetric water content were carried out (Vergeynst et al. 2015a). We hypothesize that the effect of eCO_2 on xylem vulnerability is dependent on the timing of the drought event, with higher xylem vulnerability to embolism formation during the early season. This as a result of the stimulation of stem volumetric growth by CO_2 fertilization leading to the development of large and thin-walled vessels which may offer limited resistance to run-away embolism. By contrast during the late season, stimulated cell wall deposition under eCO_2 might enhance wood mechanical strength (Chapter 3) and counteract detrimental effects of rapid growth on hydraulic safety. Independent of the [CO_2] treatment, we expect drought responses to be sequential, with limitation of leaf scale water loss followed by consecutive water release from elastic and inelastic tree water pools, the latter in concert with embolism propagation.

Table 5.1 Compilation of studies investigating the effect of elevated CO_2 concentration (eCO_2) on the xylem vulnerability of stems and branches in trees. The species under study, tree age or height, eCO_2 experimental set-up, applied method, and the main effects of eCO_2 are summarized.

The eCO_2 setup specifies whether free-air carbon dioxide enrichment (FACE) or treatment chambers (TC) were applied, and the CO_2 concentration to which trees were subjected (ppm). Details on the applied methods are explained in [1]Sperry and Tyree 1988b; [2]Salleo et al. (1992) and Sperry and Saliendra (1994); [3]Alder et al. 1997; [4]Cochard et al. (1992).

Species	Tree age	eCO₂ set-up	Method	eCO₂ effect on vulnerability	Reference
Five broadleaved tree species	3 - 9 m	Natural eCO_2 spring (500 - 1000)	Hydraulic method[1]	Vulnerability was not affected	Tognetti et al. (1999)
Quercus ilex L.	16 to 17-moths-old	TC (750 – 700)	Air-injection[2]	Vulnerability was not affected	Gartner et al. (2003)
Pinus taeda	13.7 - 19.6 m	FACE (aCO_2 + 200)	Centrifugal force[3]	Vulnerability increased in *L. styraciflua* and *C. florida* Vulnerability was not affected in *P. taeda* and *U. alata*	Domec et al. (2010)
Liquidambar styraciflua L. *Cornus florida* L. *Ulmus alata*	4.1 - 7.8 m				
Liquidambar styraciflua	19-years-old	FACE (525 – 555)	Air-injection[2]	Vulnerability increased	Warren et al. (2011)
Quercus suber	18-months-old	TC (700)	Hydraulic method[1]	Vulnerability was not affected	Vaz et al. (2012)
Six broadleaved trees	1-year-old	TC (600)	Centrifugal force[3]	Vulnerability was not affected	Hao et al. (2018b)
Pinus banksiana	1-year-old	TC (900)	Air pressure[4]	Vulnerability was not affected	Newaz et al. (2018)

Material and methods

Plant material and experimental set-up

During two consecutive years (DOY 79 2018 and DOY 78 2019), one-year-old European aspen (*Populus tremula* L.) trees were planted in 30 L pots filled with potting soil and fertilizer (Osmocote Exact Standard 8-9M, ICL, Ipswich, UK). Young trees were randomly distributed between treatment chambers, where relative humidity (RH) and photosynthetically active radiation (PAR) were continuously monitored, while temperature (T) and atmospheric $[CO_2]$ were regulated (for detailed overview of the set-up see Chapter 1). Target atmospheric $[CO_2]$ inside the treatment chambers was 400 ppm (hereafter ambient CO_2, aCO_2) and 700 ppm (hereafter elevated CO_2, eCO_2). Young trees were watered with an automated irrigation system at predawn (between 5:00 h and 6:00 h). The amount of water provided was adjusted for each pot and throughout the season following point measurements of soil water content (ML3 ThetaKit, Delta-T Devices, Burnwell, UK). For the *in vivo* drought measurements (see below), trees inside each chamber were randomly assigned to a well-watered (control) or a drought stress group. This 2×2 factorial experimental design resulted in four treatment groups (n = 5 per treatment group): well-watered trees under aCO_2 (aW) and eCO_2 (eW) and drought stressed trees under aCO_2 (aD) and eCO_2 (eD). During the 2018 growing season, trees were first subjected to moderate drought by reducing irrigation to 50 % of the well-watered trees (DOY 222, 10 August). One week later, irrigation was completely ceased (DOY 229, 17 August). During the 2019 growing season, irrigation was ceased completely on DOY 183 (2 July). Onset of the drought events was hence imposed early (hereafter "early season experiment" or ESE) and late (hereafter "late season experiment" or LSE) during the growing season to study potential seasonality in the tree hydraulic response to eCO_2.

Vulnerability and desorption curves

For the construction of vulnerability (VC) and desorption (DC) curves, four well-watered trees per $[CO_2]$ treatment were transported to the lab (DOYs 183 and 240 for ESE and LSE, respectively) in their pots. Before cutting, stems were divided into two equal halves. Approximately forty leaves on branches of the upper stem part were loosely covered with aluminium foil to ensure hydraulic equilibrium with the stem (Begg and Turner 1970). Remaining leaves were cut at the petiole scale and wounds were covered with petroleum jelly. Likewise, all leaves on branches of the lower stem part were removed and wounds were covered with petroleum jelly to ensure similar dehydration rates between stem halves. Next, stems were cut just above the pot soil level after root soil removal and at mid-height separating

the two stem halves. To avoid air-entry artefacts, cuts were executed under water followed by two additional recuts of 3 cm (Cochard et al. 2013, Wheeler et al. 2013). Cut ends were covered with wet paper towels during sensor installation (see below) to avoid water loss prior to bench dehydration. To further avoid air-entry artefacts, sample preparation was performed in the dark with low intensity green operating light (PAR = 0 µmol m^{-2} s^{-1}) to limit transpiration.

To construct VCs, embolism formation was measured using a broadband point contact acoustic emission (AE) sensor (KRNBB-PC, KRN Services, Richland, WA, USA) in the upper stem halves. A rectangular section of the bark (1.5 × 0.5 cm^2) was removed to establish better acoustic coupling with AEs originating from xylem embolisms. A droplet of vacuum grease (High-Vacuum Grease, Dow Corning, Seneffe, Belgium) was applied between the sensor tip and the xylem. The AE sensor was mounted and pressed against the xylem using a custom-made PVC tubular frame and a compression spring (D22050, Tevema, Amsterdam, The Netherlands). The pencil lead break test was performed to ensure good contact between the AE sensor and the xylem (Tyree and Sperry 1989, Sause 2011, Vergeynst et al. 2015b). Acoustic signals were amplified by 35.6 dB (AMP-1BB-J, KRN Services, Richland, WA, USA), waveforms of 7168 samples length were acquired at 10 MHz sample rate and signals were collected using two 2-channel PCI boards and redirected to the AEwin software (PCI-2, AEWIN E4.70; Mistras Group BV, Schiedam, the Netherlands). Acoustic emission signals with amplitude below 34 dB were discarded (20 –1000 kHz electronic band pass filter) to remove noise unrelated to vessel embolism events (Beall 2002, Steppe et al. 2009, Vergeynst et al. 2016).

To obtain continuous Ψ_{xylem} data, the linear relationship between discrete Ψ_{xylem} measurements and relative xylem shrinkage was established for the upper halves of each stem (with average R^2 = 0.87 ± 0.01 (ESE) and R^2 = 0.79 ± 0.04 (LSE)). Measurements of Ψ_{xylem} were performed on wrapped leaves using a pressure chamber (Model 600, PMS Instrument Company, Corvallis, OR, USA). Frequency of Ψ_{xylem} measurements varied from once to twice per hour depending on the rate of AE signal registration. When leaves for Ψ_{xylem} measurements were cut from the stem, registration of AE signals was put on hold to avoid acoustic noise. In addition, absolute xylem diameter shrinkage (ΔD_{xylem}) was continuously measured in the upper stem halves using a dendrometer (DD-S, Ecomatik, Dachau, Germany) pressed against the xylem and located approximately 7 cm apart from the AE sensor. For this, a rectangular section of the bark (1.5 × 0.5 cm^2) was removed and petroleum jelly was applied to prevent local water loss (Vergeynst et al. 2015a). Relative xylem shrinkage was estimated as the ratio of ΔD_{xylem} and the initial stem diameter.

To construct DCs, lower stem halves were placed on a weighing scale (0.01 g accuracy; DK 6200, Henk Maas, Veen, The Netherlands) for continuous measurements of fresh mass during dehydration. Stem mass was monitored, from initial stem mass (M_i) at onset of dehydration to final stem mass (M_f) when complete vessel embolization was detected in the upper counterparts (approximately after 24 and 48 h of bench dehydration during the ESE and LSE, respectively). Fresh stem mass (M_{fresh}) and volume (V) was also measured on a 3-cm-length wood sample collected before and after bench dehydration. Wood samples were then oven dried (80 °C) until constant mass (M_{dry}) to estimate fresh volumetric water content (VWC = (M_{fresh} – M_{dry})/V) and stem wood density (ρ_{stem} = M_{dry}/V). Continuous VWC data were obtained by rescaling weighing scale measurements from initial (VWC_i) to final (VWC_f) VWC during the course of the bench dehydration experiment (Vergeynst et al. 2015a). Similar dehydration rates were assumed between upper and lower parts, so that continuous Ψ_{xylem} data obtained to construct VCs was used likewise to construct DCs.

Xylem anatomical traits

After bench dehydration an additional set of wood samples of 3-cm-length (four per [CO_2] treatment for both ESE and LSE) were cut from the stem segments used to construct VCs and stored in an ethanol/glycerol/water (70/20/10 %vol) solution until analysis of wood anatomical traits. Wood samples were transversely cut into 35-μm-thick sections using a sledge microtome (Jung Hn-40, JUNG, Germany). Samples were stained using a standard colouring mix (0.5 % w/v astra blue, 0.5 % w/v chrysoidin and 0.5 % w/v acridine red) for 5 minutes, dehydrated in 2-propanol and mounted in (Carl Roth, Germany). Slides were observed and imaged using a Nikon Ni-U light microscope (Nikon Instruments) equipped with a Nikon DS-Fi3 digital camera.

Wood anatomical images were processed using the image-processing software FIJI (www.fiji.sc; ImageJ) with implementation of the *Biovoxxel* toolbox. For each stem section, xylem area (A_{xylem}, i.e., cross-section area without bark and pit) was selected for analysis of anatomical traits related with hydraulic efficiency and spatial vessel arrangement. Note that A_{xylem} integrated two growth rings, with the second one being formed under experimental conditions. Given the limited contribution of the first growth ring to A_{xylem} (Figure 5.2a), both growth rings were analysed as a whole for comparison with the VCs and DCs. Extended particle analysis was applied to select vessels within the 200 – 1500 μm^2 range (Cai and Tyree 2010, Johnson et al. 2018) and lumen area was individually estimated per vessel. Individual vessel diameter (d_v) was approximated assuming a circular vessel lumen area, and distributed into four 10 μm classes. Total number of vessels per cross-section (N_{v_all}) and per vessel size

class (N_{v_class}) was determined, and individual vessel lumen area was integrated to estimate total vessel conducting area (A_{v_all}). As a measure of mechanical strength and in addition to ρ_{stem}, the non-lumen area fraction (F_{nv}) was determined as the inverse of the lumen fraction ($F_{nv} = (A_{xylem} - A_{v\_all})/A_{xylem}$). Vessel grouping index (v_g), defined as the ratio of total number of vessels and the sum of solitary vessels and vessels clusters (Scholz et al. 2013), was determined with the imaging software using *Neighbor Analysis*. Vessels were considered of the same cluster applying a distance threshold of 10 μm. The average hydraulic weighted vessel diameter (d_h) was calculated (Scholz et al. 2013) for the entire xylem area (d_{h_all}) and for each vessel diameter class (d_{h_class}) following:

$$d_h = \sqrt[4]{\frac{1}{n} \sum_{i=1}^{n} d_{v,i}^4}$$

Equation 5.1

For calculation of d_{h_all}, n equalled to the total number of vessels (N_{v_all}) and d_v to their corresponding diameter. For calculation of d_{h_class}, n was equal to the number of vessels within a single vessel size class (N_{v_class}) with corresponding diameter d_v. Theoretical hydraulic conductivity of the whole cross-section (k_{h_all}) and of each vessel size class (k_{h_class}) was calculated as the proportionally constant derived from the Hagen-Poiseuille law (Equation 5.2) (Steppe and Lemeur 2007, Poorter et al. 2010, Scholz et al. 2013).

$$k_h = \frac{\pi \rho \, VD}{128 \, \eta} \, d_h^4$$

Equation 5.2

With the ρ water density (998.2 kg m^{-3}) and η the water viscosity (1.002 10^{-9} MPa s), both at 20 °C. For calculation of k_{h_all}, vessel density (VD) was calculated as the ratio of N_{v_all} and A_{xylem} and d_h equalled to d_{h_all}. For class-specific k_{h_class}, VD was calculated as the ratio of N_{v_class} and A_{xylem} and d_h equalled to d_{h_class}.

Drought stress responses *in vivo*

The effects of the drought event under aCO₂ and eCO₂ were assessed on ten trees per [CO₂] treatment (i.e. five per irrigation group). Discrete leaf measurements (Ψ_{xylem} and stomatal conductance (g_s)) were conducted around midday (11:00 h – 15:00 h) once (ESE) or 2-3 times (LSE) per week on fully developed leaves located in the mid-canopy. A pressure chamber (Model 600, PMS Instrument Company, Corvallis, OR, USA) was used to measure Ψ_{xylem} in leaves loosely covered with aluminium foil at least one hour prior to the measurement to allow hydraulic equilibrium (Begg and Turner 1970). Stomatal conductance of the same trees was measured using a portable photosynthesis system (Li-6400, Li-Cor Inc., Lincoln, Nebraska,

109

USA) set at chamber [CO_2] (400 or 700 ppm), prevailing T and light saturated PAR (1500 µmol m^{-2} s^{-1}). Measurements were registered after stabilization of the CO_2 exchange rates.

Depletion of stem elastic water pools was assessed in the same ten trees selected for discrete measurements by monitoring stem diameter variations (ΔD). A linear variable displacement transducer (LVDT, model DF5.0, Solartron Metrology, Leicester, UK) was installed on the stem at an approximate height of 30 cm above pot soil level. Tree water deficit (TWD) was calculated in drought stressed trees by applying the "zero growth concept" (Zweifel et al. 2016); i.e. stem growth was assumed zero during periods of stem shrinkage. Midday TWD was estimated on a daily basis as the difference between the last maximum stem diameter and the daily minimal stem diameter measured around midday (i.e. TWD4 as defined in Dietrich et al. 2018). Measurements ceased when Ψ_{xylem} could no longer be measured in drought stressed trees (DOYs 209 and 253 for ESE and LSE, respectively).

Data analyses

Continuous ΔD and mass data from the bench dehydration experiment were registered every minute using custom-built acquisition board. Continuous microclimate and ΔD data from the *in vivo* drought experiment were registered every minute and averaged over five minutes using a data logger (CR1000, Campbell Scientific, Logan, UT, USA). Continuous data from both approaches was collected and visualized using the PhytoSense software (Phyto-IT, Gent, Belgium). All data and statistical analyses were performed using R software (R Core Team, 2018).

For the construction of the acoustic VC (VC$_{AE}$), AE activity was determined as the first derivative of the cumulative number of AE signals. The end-point of the VC$_{AE}$ (Ψ_{xylem} corresponding to 100 % of embolized vessels) was determined as the point of strongest decrease in AE activity following highest AE activity. Mathematically, this end-point corresponds with the maximum of the third derivative of the cumulative AE curve (Vergeynst et al. 2016). To approximate relative k$_h$ loss, absolute cumulative AE values were rescaled between zero and the end-point. Water potentials corresponding with onset of embolism formation (Ψ_{xylem} at 12 % of the embolism related AE signals; AE$_{12}$), 50 % of the embolism AE signals (AE$_{50}$) and almost complete hydraulic failure (Ψ_{xylem} at 88 % of the embolism related AE signals; AE$_{88}$) were calculated. For the DCs, continuous VWC was regressed against Ψ_{xylem} and two different phases of the desorption curve were determined by segmented linear regression (*segmented* package). Elastic (C$_{el}$) and inelastic (C$_{inel}$) capacitance were determined as the corresponding slopes of the linear segments.

To describe the relative change in g_s and TWD with Ψ_{xylem} during the *in vivo* drought experiment, a sigmoidal fit (Equation 5.3) was applied:

$$y = \frac{1}{1 + \exp^{a(\Psi+i)}}$$
Equation 5.3

where y is the relative variation in g_s or TWD, a defines the steepness of the curve and i is the inflection point. Loss in g_s was defined relative to the average g_s across well-watered trees during the same day and within the same [CO$_2$] treatment. Increase in TWD was defined relative to the individual-specific maximal TWD (TWD registered on the last day of Ψ_{xylem} measurement). Thresholds of Ψ_{xylem} corresponding with 12, 50 and 88 % of g_s reduction (g_{s_12}, g_{s_50} and g_{s_88}) or TWD increase (TWD$_{12}$, TWD$_{50}$ and TWD$_{88}$) were calculated.

To evaluate the effect of eCO$_2$ on tree hydraulic functioning, parametric and non-parametric tests (depending on data normality) were applied on wood anatomical traits (d_v, d_{h_all}, VD, k_{h_all}, v_g, F_{nv} and ρ_{stem}) and thresholds of embolism-related acoustic emissions (AE$_{12}$, AE$_{50}$ and AE$_{88}$), hydraulic capacitances (C_{el} and C_{inel}), stomatal conductance (g_{s_12}, g_{s_50} and g_{s_88}) and tree water deficit (TWD$_{12}$, TWD$_{50}$ and TWD$_{88}$) during ESE and LSE. Differences in relative vessel size class abundancy (N_{rel}) and contribution to the overall k_h (k_{h_rel}) were determined using a non-parametric Kruskal-Wallis test followed by post-hoc multiple comparison (Wilcoxon) among vessel size classes for each [CO$_2$] treatment. Timing of xylem embolism formation (bench dehydration), stomatal closure and stem dehydration (*in vivo*) with declining tree water status were compared using a linear mixed effect model (*nlme* package), including data point correlation due to the repeated measurement design of the experiment and with plant response type (g_s, TWD and AE) as fixed effect and tree as a random factor. Post-hoc Tukey tests were applied for multiple comparison (multcomp package) among plant response types. Since inter-annual differences in trees and microclimate conditions could bias comparison between seasonal experiments, we intentionally focus on treatment comparisons within a single growing season, while avoiding seasonal comparisons for a given treatment. Strong ($P < 0.05$) and moderate ($P < 0.10$) statistical differences are reported for those tests with small sample size (n = 3 - 5) and statistical power to detect significant differences. Reported values refer to mean ± SE.

Results

Wood anatomical characteristics

Examples of transverse stem sections of *Populus tremula* L. trees grown under different [CO_2] treatments and harvested during different seasonal experiments are shown in Figure 5.1a. Average vessel diameter (d_v) was larger under eCO_2 during ESE, while the opposite was found during LSE ($P < 0.0001$; Table 5.2). However, changes in d_v under eCO_2 did not substantially affect vessel efficiency since no differences in overall hydraulic vessel diameter (d_{h_all}), vessel conductivity (k_{h_all}) or vessel grouping index (v_g) were detected ($P > 0.1$). Also wood anatomical traits related to mechanical strength, i.e. vessel density (VD), non-vessel fraction (F_{nv}), and stem wood density (ρ_{stem}), were not significantly affected by the [CO_2] treatment ($P > 0.1$; Table 5.2). The [CO_2] treatment had a limited impact on the relative frequency of vessel diameters (Figure 5.1b, upper panels), as a moderate decrease in relative vessel abundancy was only observed for narrow vessels within the 20 - 30 µm class under eCO_2 during ESE ($P < 0.1$). Vessels with diameters within the 20 - 40 µm were more frequent during ESE ($P < 0.05$), and the 30 - 40 µm size category contributed to the greatest extent to overall k_h (Figure 5.1b, lower panels). The relative contribution of each vessel size class to k_h (k_{h_class}) was not affected by eCO_2 ($P > 0.1$).

Table 5.2 Mean value and standard error of the wood anatomical characteristics measured during the early (ESE- 2019) and late (LSE- 2018) season experiment under different [CO_2] treatments (aCO_2 and eCO_2 for ambient and elevated [CO_2] treatment, respectively).

With d_v the average vessel diameter, d_{h_all} the hydraulic vessel diameter, VD the vessel density, k_{h_all} the vessel hydraulic conductivity, v_g the vessel grouping index, F_{nv} the non-vessel fraction and ρ_{stem} the stem wood density. Differences between aCO_2 and eCO_2 are indicated (parametric t.test, * $P < 0.05$).

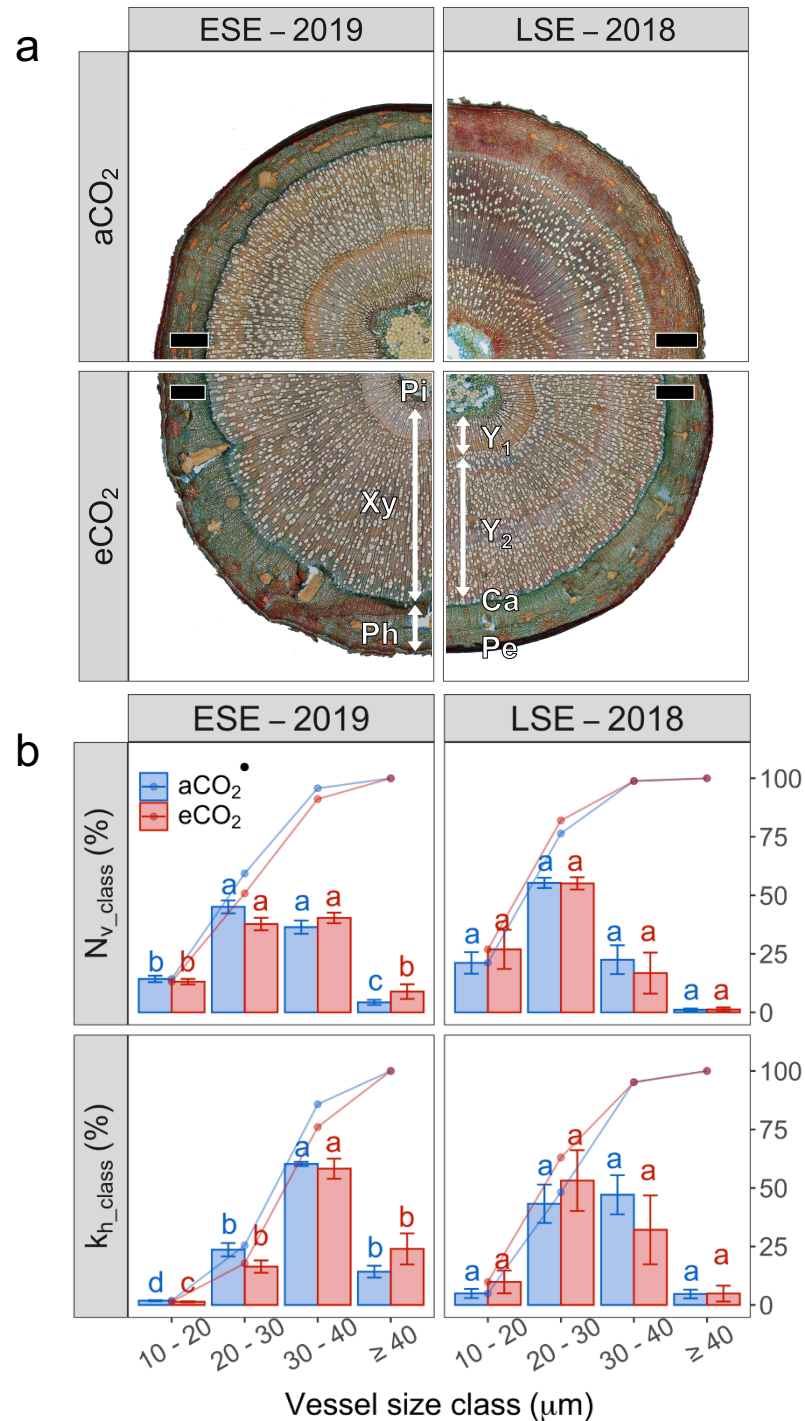|		ESE (2019)		LSE (2018)	
		aCO_2	**eCO_2**	**aCO_2**	**eCO_2**
d_v	µm	28.16 ± 0.04	29.55 ± 0.05 *	26.44 ± 0.04	25.64 ± 0.05 *
d_{h_all}	µm	30.40 ± 0.62	31.98 ± 0.73	27.35 ± 1.23	25.88 ± 2.05
VD	mm^{-2}	206.3 ± 26.2	157.6 ± 14.3	266.4 ± 28.5	229.0 ± 19.0
k_{h_all}	kg m^{-1} MPa^{-1} s^{-1}	4.26 ± 0.41	4.00 ± 0.29	3.88 ± 0.95	2.72 ± 0.78
v_g	-	1.38 ± 0.03	1.45 ± 0.09	1.52 ± 0.11	1.34 ± 0.05
F_{nv}	-	0.86 ± 0.01	0.89 ± 0.01	0.85 ± 0.02	0.89 ± 0.02
ρ_{stem}	kg m^{-3}	362.82 ± 7.39	339.31 ± 17.98	294.03 ± 22.88	322.81 ± 11.31

Figure 5.2 (a) Transverse stem sections of studied *Populus tremula* L. trees and (b) relative (bar plot) and cumulative (line plot) abundancy of vessels classified by four size classes (N$_{v\_class}$, upper panels) and their contribution to overall hydraulic conductance (k$_{h\_class}$, lower panels) during the early (ESE - 2019) and the late (LSE - 2018) season experiment.

Trees were subjected to different levels of atmospheric [CO$_2$] (ambient (aCO$_2$) and elevated (eCO$_2$)). In (a), scale bars correspond to 1 mm. Lignified and non-lignified cell walls are coloured red and blue, respectively, with distinction of cambium (Ca), periderm (Pe), phloem (Ph), pith (Pi) and xylem (Xy) from the 1st year (Y$_1$) and the 2nd year (Y$_2$). In (b), letters indicate differences in N$_{v\_class}$ and k$_{h\_class}$ contributions for a given [CO$_2$] treatment and seasonal experiment (Wilcoxon test, P < 0.05). Moderate differences between aCO$_2$ and eCO$_2$ within each diameter class are also indicated (linear model, • P < 0.1).

Stem vulnerability and desorption curves

Acoustic vulnerability curves (VC_{AE}; Figure 5.3, upper panels) and corresponding thresholds (AE_{12}, AE_{50} and AE_{88}; Table 5.3) indicate that eCO_2 resulted in an earlier AE_{88} during ESE ($P < 0.05$). Although this trend of increased xylem vulnerability under eCO_2 during ESE seemingly held for AE_{12} and AE_{50}, differences between $[CO_2]$ treatments were not statistically significant ($P = 0.14$ and 0.12 for AE_{12} and AE_{50}, respectively). During LSE, VC_{AE} and corresponding thresholds were not affected by the $[CO_2]$ treatment ($P > 0.1$). Accordingly, desorption curves (DC; Figure 5.3, lower panels) were only altered under eCO_2 during ESE. Although elastic capacitance (C_{el}) did not differ between $[CO_2]$ treatments ($P > 0.1$; Table 5.3), C_{inel} was larger under eCO_2 ($P < 0.05$) indicating greater capacitive water release from embolized vessels. During LSE, the $[CO_2]$ treatment did not affect C_{el} or C_{inel} ($P > 0.1$).

Table 5.3 Mean value and standard error of the hydraulic vulnerability thresholds and capacitances measured during the early (ESE - 2019) and late (LSE - 2018) season experiment under different $[CO_2]$ treatments (aCO_2 and eCO_2 for ambient and elevated $[CO_2]$ treatment, respectively).

Hydraulic vulnerability is defined by the threshold water potentials corresponding with 12 % (AE_{12}), 50 % (AE_{50}) and 88 % (AE_{88}) of the embolism related acoustic emission (AE) signals. Hydraulic capacitance is characterized by capacitance of the elastic (C_{el}) and inelastic (C_{inel}) water pools. Differences between aCO_2 and eCO_2 are indicated (parametric t.test, • $P < 0.1$, * $P < 0.05$).

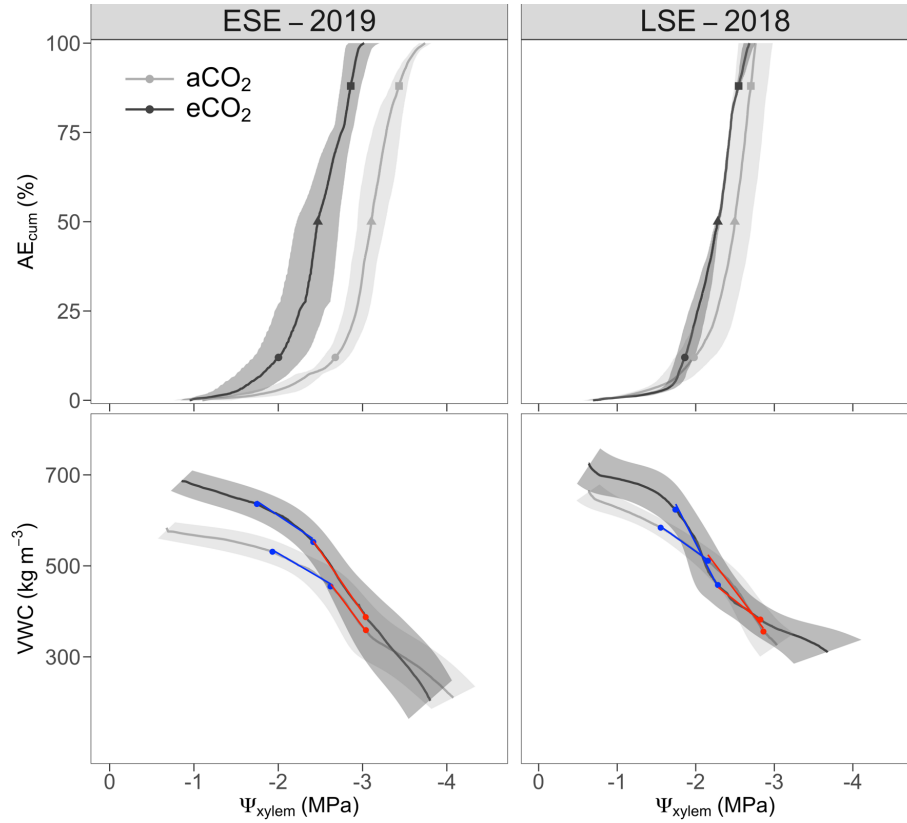|		ESE - 2019			LSE - 2018		
		aCO_2	eCO_2		aCO_2	eCO_2	
Vulnerability curves							
AE_{12}	MPa	-2.60 ± 0.13	-1.99 ± 0.31		-1.97 ± 0.25	-1.86 ± 0.11	
AE_{50}	MPa	-3.02 ± 0.14	-2.47 ± 0.25		-2.50 ± 0.22	-2.28 ± 0.03	
AE_{88}	MPa	-3.39 ± 0.08	-2.86 ± 0.12	*	-2.70 ± 0.21	-2.54 ± 0.02	
Desorption curves							
C_{el}	kg m^{-3} MPa^{-1}	206.1 ± 71.4	147.1 ± 32.6		119.4 ± 25.0	265.2 ± 148.7	
C_{inel}	kg m^{-3} MPa^{-1}	136.1 ± 22.0	341.4 ± 43.5	*	175.9 ± 24.4	279.6 ± 66.3	

Figure 5.3 Acoustic vulnerability curves (VC_{AE}, upper panels) and desorption curves (DC, lower panels) during the early (ESE - 2019) and the late (LSE - 2018) season bench dehydration experiments.

Trees were subjected to different levels of atmospheric $[CO_2]$ (ambient (aCO_2) and elevated (eCO_2)). Xylem water potential (Ψ_{xylem}) at which 12, 50 and 88 % of the embolism-related acoustic emission occur (AE_{12} (●), AE_{50} (▲), AE_{88} (■), respectively) are shown (upper panels). Blue and red lines on the DCs display the Ψ_{xylem} range of elastic and inelastic water release, respectively. Corresponding hydraulic capacitances (elastic and inelastic) are calculated as the slope of the linear relationship between volumetric water content (VWC) and Ψ_{xylem}.

Microclimate and effectiveness of the *in vivo* drought stress treatments

Averages of microclimatic variables during daytime (PAR > 5 µmol m^{-2} s^{-1}) and along the duration of the *in vivo* seasonal drought treatments are shown in Figure S5.1. Chamber $[CO_2]$ was 448.16 ± 5.00 ppm (aCO_2) and 698.86 ± 13.48 ppm (eCO_2) during ESE, and 440.41 ± 8.67 ppm (aCO_2) and 694.29 ± 10.75 ppm (eCO_2) during LSE. Daytime PAR and T did not differ between $[CO_2]$ treatment chambers and averaged 568.76 ± 24.20 µmol m^{-2} s^{-1} and 27.08 ± 0.54 °C during ESE, and 463.12 ± 16.65 µmol m^{-2} s^{-1} and 24.10 ± 2.65 °C during LSE. Chamber VPD did not differ between chambers during ESE (P > 0.1; 1.34 ± 0.06 kPa), but was reduced under eCO_2 during LSE (P < 0.0001; 1.44 ± 0.07 kPa and 1.05 ± 0.08 kPa under aCO_2 and eCO_2, respectively), presumably as a result of enhanced transpiration related to stimulated leaf area development under eCO_2 (Chapter 4). Variability in midday Ψ_{xylem} over time (Figure S5.1) was small under well-watered conditions with an average Ψ_{xylem} of

-0.67 ± 0.04 MPa and -0.98 ± 0.02 MPa during ESE and LSE, respectively. Drought stress reduced Ψ_{xylem} over time under both aCO_2 and eCO_2. The [CO_2] treatment did not affect Ψ_{xylem} under well-watered or drought conditions ($P > 0.1$).

Stomatal conductance and tree water deficit responses to in vivo drought stress

Drought stress reduced g_s under both aCO_2 and eCO_2 and during both seasonal experiments ($P < 0.001$; Figure 5.4, left-hand side panels). The sigmoidal fits between relative g_s loss and Ψ_{xylem} are shown in Figure 5.4 (right-hand side panels) with corresponding parameters in Table 5.4. During ESE, eCO_2 slightly flattened the slope of the g_s curve ($P < 0.1$), but did not affect its inflection point ($P > 0.1$), denoting a moderately earlier onset of stomatal closure followed by a more gradual drought-induced g_s reduction. In contrast and during LSE, eCO_2 did not affect the slope of the g_s curve ($P > 0.1$) but the inflection point was shifted to more negative Ψ_{xylem} ($P < 0.05$), denoting a delayed stomatal closure.
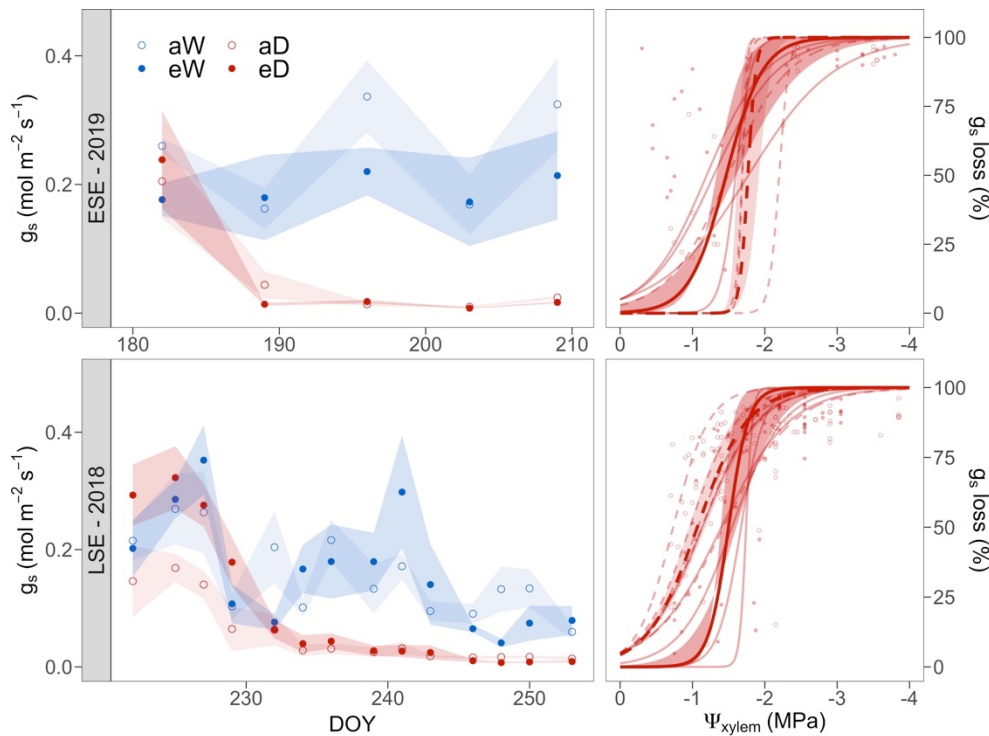

Figure 5.4 Stomatal conductance (g_s) over time (left-hand side panels) and relative g_s loss with decreasing xylem water potential (Ψ_{Xylem}) (right-hand side panels) during the early (ESE - 2019) and late (LSE - 2018) season *in vivo* drought experiment.

Trees were subjected to combined treatments of atmospheric [CO_2] (ambient (a) and elevated (e)) and drought stress (well-watered (W) and drought stressed (D)). Thin red lines show the sigmoidal relation between relative g_s loss and Ψ_{xylem} for individual seedlings. Dashed and solid lines illustrate aCO_2 and eCO_2, respectively. Bold lines and shaded areas indicate model fit applying average ± SE parameter for aCO_2 and eCO_2 (n = 4 and 5 for ESE and LSE, respectively). With DOY day of year.
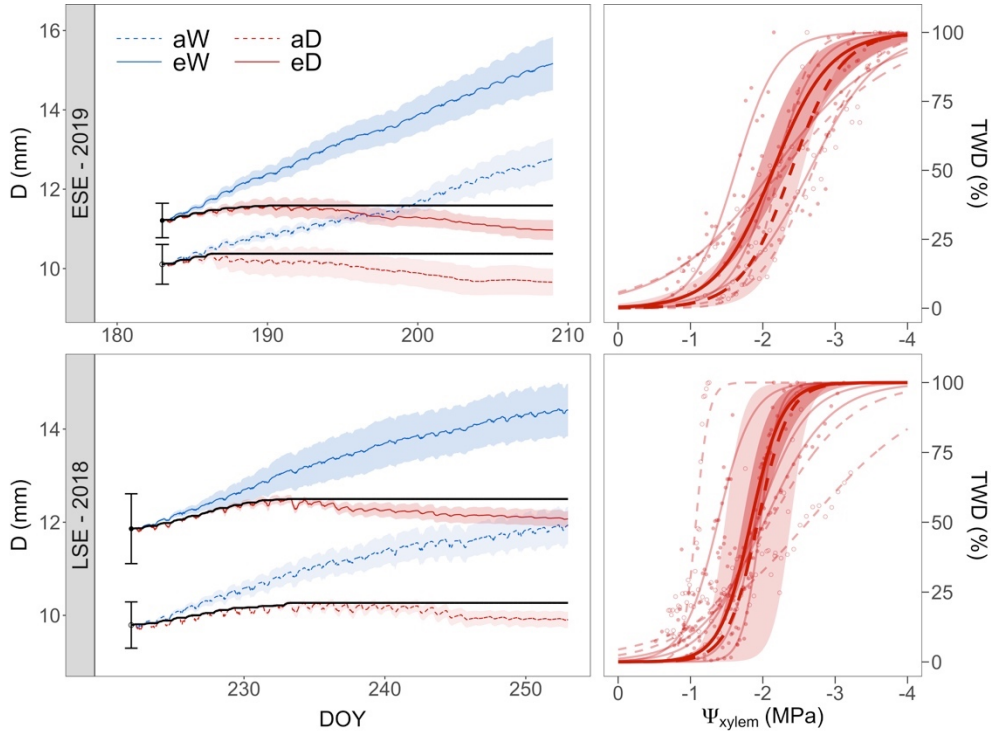
Figure 5.5 Stem diameter (D) over time (left-hand side panels) and relative increase of tree water deficit (TWD) with decreasing xylem water potential (Ψ_{xylem}) (right-hand side panels) during the early (ESE - 2019) and the late (LSE - 2018) season *in vivo* drought experiment.

Trees were subjected to combined treatments of atmospheric CO_2 (ambient (a) and elevated (e)) and drought stress (well-watered (W) and drought stressed (D)). Discrete Ψ_{xylem} measurements were linearly regressed over time to match temporal resolution (on a daily basis) of TWD and Ψ_{xylem} (average R^2 = 0.71 ± 0.04). Error bars indicate the standard error on the mean stem diameter size per [CO_2] treatment at the onset of the drought treatment. Black lines show the preceding maximum stem diameter of the drought stressed trees as reference to estimate TWD. Thin red lines show sigmoidal relation between TWD and Ψ_{xylem} for individual trees. Dashed and solid lines illustrate aCO_2 and eCO_2, respectively. Bold lines and shaded areas indicate model fit applying average ± SE parameter values for aCO_2 (n = 3 for ESE and LSE) and eCO_2 (n = 4 and 5 for ESE and LSE, respectively). With DOY day of year.

Stem diameter at onset of drought did not significantly differ between [CO_2] treatments during ESE (P > 0.1), and was larger under eCO_2 during LSE (P < 0.05, Figure 5.5, left-hand side panels). Throughout both surveyed seasonal periods and for both [CO_2] treatments, well-watered trees kept growing until the end of the experiment while drought-stressed trees start to shrink 6.5 ± 1.2 and 16.1 ± 1.9 days after onset of the drought event for ESE and LSE, respectively. The sigmoidal fits between tree water deficit (TWD) and Ψ_{xylem} (Figure 5.5, right-hand side panels) were not affected by the [CO_2] treatment during any of the seasonal experiments (P > 0.1; Table 5.4).

117

Table 5.4 Average value and standard error of the parameters (a and i) of the sigmoidal curve adjusted to define the relative change in stomatal conductance (g_s) and tree water deficit (TWD) with decreasing xylem water potential (Ψ_{xylem}) during the early (ESE - 2019) and late (LSE - 2018) season experiments under different [CO_2] treatments (aCO_2 and eCO_2 for the ambient and elevated CO_2 treatment, respectively).

Goodness of fit (GF) is calculated as the mean (±SE) correlation between the measured and predicted values of the tree specific sigmoidal curves. Differences between aCO_2 and eCO_2 are indicated (linear model, • P < 0.1, * P < 0.05).

		Rate (a, MPa^{-1})		Inflection point (i, MPa)		GF	
		aCO_2	eCO_2	aCO_2	eCO_2	aCO_2	eCO_2
g_s	ESE	17.85 ± 6.27	3.95 ± 1.82 •	-1.77 ± 0.15	-1.46 ± 0.13	0.83 ± 0.08	0.54 ± 0.05
	LSE	2.90 ± 0.32	7.27 ± 3.89	-1.07 ± 0.11	-1.50 ± 0.11 *	0.41 ± 0.14	0.70 ± 0.12
TWD	ESE	2.89 ± 1.05	2.55 ± 0.50	-2.39 ± 0.15	-2.14 ± 0.21	0.97 ± 0.01	0.95 ± 0.01
	LSE	4.74 ± 3.27	4.62 ± 1.05	-1.93 ± 0.45	-1.83 ± 0.12	0.88 ± 0.07	0.94 ± 0.06

Comparison of hydraulic thresholds

Figure 5.6 shows the sequential pattern of the tree dehydration processes (top panels) and comparison of corresponding threshold values among surveyed variables (g_s, TWD and AE) and between [CO_2] treatments (lower panels). At relatively high Ψ_{xylem} (> -1.5 MPa), and during both ESE and LSE, the first response to drought was the reduction of leaf scale water loss by stomatal closure (g_{s_12}), followed by depletion of stem elastic water pools (TWD_{12}) and, later start of embolism formation (AE_{12}). Initial depletion of inelastic water pools denoted by the onset of embolism formation was thus preceded by decreased leaf-scale water loss (P < 0.01) and depletion of elastic water storage pools (P < 0.01). With decreasing Ψ_{xylem} (from -1.5 MPa to -2.5 MPa), differences (P < 0.05) between TWD_{50} and AE_{50} disappeared. Nonetheless during ESE, TWD_{50} was still moderately less negative than AE_{50} (P < 0.1), while during LSE no differences were measured (P > 0.1). This denotes only slight (ESE) or even no (LSE) differences in Ψ_{xylem} were measured when elastic and inelastic stem water pools were half depleted. When approximating full hydraulic failure (approximately -3.0 MPa), TWD_{88} and AE_{88} did not differ during ESE or LSE (P > 0.1), suggesting simultaneous full depletion of elastic and inelastic water pools ,when hydraulic conductivity was mostly lost. Remarkably, AE_{12} did not significantly differ from g_{s_88} (under both [CO_2] treatments and during both seasonal experiments; P > 0.1), indicating that drought-induced stomatal closure was almost complete

when drought-induced embolism started. Regarding [CO_2] treatment differences, and in addition to the earlier (less negative) AE_{88} under eCO_2 observed during ESE (Table 5.2), the [CO_2] treatment also altered some of the TWD and g_s thresholds. During ESE, g_{s_12} was moderately shifted to the left (less negative Ψ_{xylem}) under eCO_2 ($P < 0.1$). Contrastingly, during LSE, g_{s_12}, TWD_{12} (both $P < 0.1$) and g_{s_50} ($P < 0.05$) were shifted to the right (more negative Ψ_{xylem}) under eCO_2.
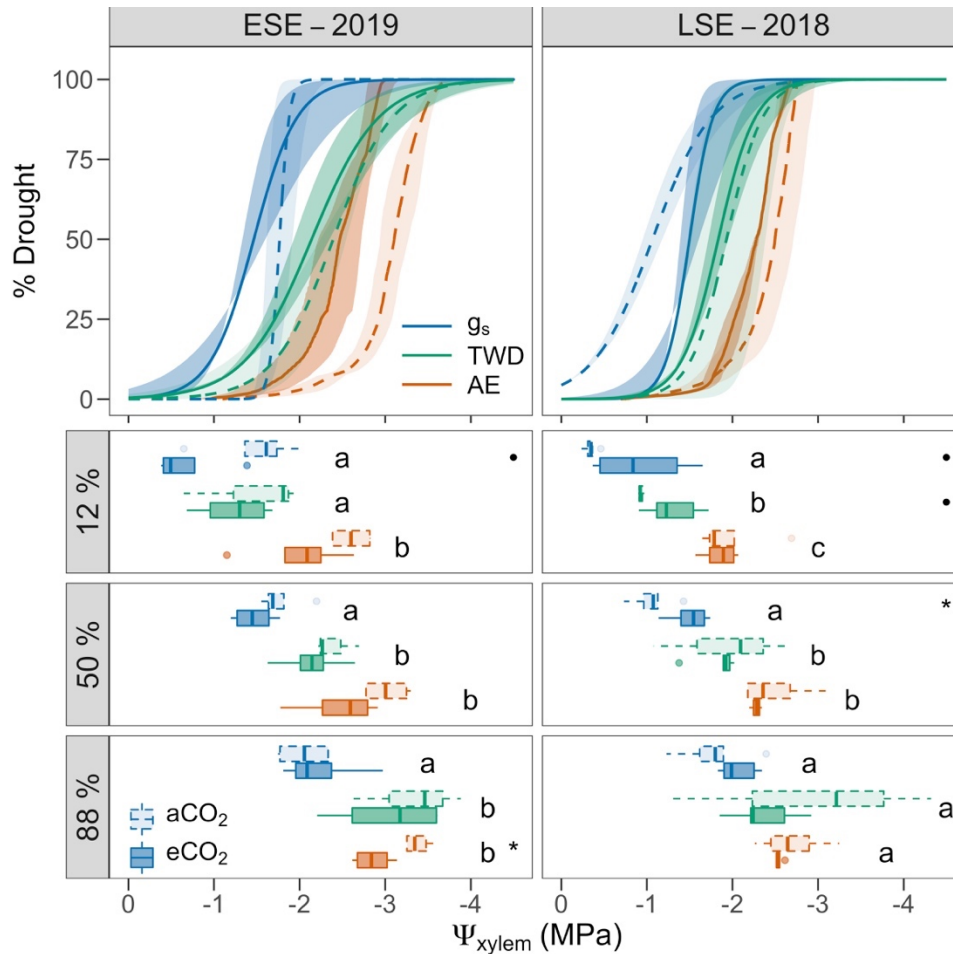

Figure 5.6   Relative variation of the stomatal conductance (g_s), tree water deficit (TWD) and embolism-related acoustic emissions (AE) with decreasing xylem water potential (Ψ_{xylem}) during the early (ESE - 2019) and the late (LSE - 2018) season drought experiment (upper panels) and pairwise comparison of their corresponding hydraulic thresholds (lower panels).

Trees were subjected to different levels of atmospheric [CO_2] (aCO_2 and eCO_2 for ambient and elevated [CO_2], respectively). Lines and shades areas show model fit applying average ± SE parameter values under aCO_2 (dashed lines) and eCO_2 (solid lines). Boxplots show hydraulic thresholds corresponding with 12, 50 and 88 % loss of each of the variables for aCO_2 (light coloured) and eCO_2 (dark coloured). Letters indicate difference between variables (linear mixed effect model, $P < 0.05$, pooling aCO_2 and eCO_2 data). Differences between [CO_2] treatments for each threshold are also indicated (linear model, • $P < 0.1$, * $P < 0.05$).

Discussion

Effects of eCO_2 on wood anatomy and hydraulic vulnerability

Exposure to eCO_2 commonly stimulates leaf photosynthesis and increases carbon availability (Ainsworth et al. 2007), which in young and fast growing trees often leads to an initial increase of growth rates (Pritchard et al. 1999). At the wood anatomical scale, rapid stem growth is often positively related to wider vessels to meet tree water needs for transpiration and negatively related to wood density to maximize volumetric growth for a given carbon cost (e.g. Poorter et al. 2010, Martínez-Cabrera et al. 2011). Accordingly, recent reviews confirm an overall increase in conduit diameter and xylem conductivity in woody species exposed to eCO_2 to improve hydraulic efficiency (Domec et al. 2017, Qaderi et al. 2019). Here, in the young European aspen trees under study, eCO_2-induced stimulation of A_n and radial stem growth were observed during the early season (Chapter 3), which may partly explain the overall wider vessel diameter under eCO_2 at this time. However, despite the increase of average vessel diameter, vessel hydraulic diameter and conductivity as proxies of hydraulic efficiency were not affected by the $[CO_2]$ treatment during ESE. In concert with the effect of eCO_2 on vessel width during the early season, (i) vulnerability curves apparently shifted towards less negative Ψ_{xylem}, with significant differences being found for AE_{88} values and (ii) inelastic capacitive water release from embolized vessels also increased under eCO_2 during ESE. Taken together, these comparisons suggest eCO_2 increased hydraulic vulnerability while hydraulic conductivity remained relatively unaltered. Such observation might be partly explained by wood features not surveyed here. Pit membrane thickness has been suggested to be a key trait to prevent rapid spread of air throughout the xylem (Li et al. 2016, Venturas et al. 2017, Kaack et al. 2021), hence determining xylem resistance to drought-induced embolism. Taking into account the direct relationship between wood density and pit membrane thickness (Jansen et al. 2009), we speculate that greater hydraulic vulnerability under eCO_2 during ESE could also be related to the non-significant reduction in wood density, and potentially thinner pit membranes.

During the late season treatment differences in vessel diameter were reversed, as vessels were overall wider under aCO_2 than eCO_2. Two factors might explain this unexpected and opposite effect of eCO_2 on vessel width during LSE. First, after cell division and enlargement during the early season, cell wall deposition and thickening occurs during late phenological phases of wood formation (Cuny et al. 2015). During this period, increased carbon availability under eCO_2 might therefore result in enhanced secondary cell wall thickening and lignification (e.g. Domec et al. 2010, 2016) at the expense of reduced vessel lumen, as hinted here by

non-significant increases in the non-vessel fraction and wood density under eCO_2 during LSE. Secondly, stimulated development of late-wood vessels under eCO_2 may also contribute to a reduction of the average vessel diameter, as suggested here by the relative vessel abundance by size classes (Figure 5.2). In any case, any potential alteration in wood traits during LSE did not affect xylem vulnerability to drought-induced embolism according to similar vulnerability curves and inelastic capacitance for both $[CO_2]$ treatments. Our results therefore highlight that wood phenology should be considered when studying possible alterations in wood traits and their relationship with hydraulic vulnerability, which merits further effort to better predict plant hydraulic functioning in future climates.

Regardless of the effect of eCO_2 on xylem vulnerability, 50 % of embolism-related acoustic emissions (AE_{50}) occurred at -2.74 ± 0.17 MPa and -2.39 ± 0.11 MPa during ESE and LSE, respectively. Drought vulnerability to embolism formation in the young trees under study was therefore at the lower end of reported P_{50} values across *Populus* spp. (from -1.1 to -3.0 MPa; (Fichot et al. 2015, Guet et al. 2015, Pivovaroff et al. 2016, De Baerdemaeker et al. 2017, Venturas et al. 2019, Zhang et al. 2020). Large variability in P_{50} among studies can be explained by differences in hydraulic vulnerability across plant organs (Choat et al. 2005) and differences between measurement techniques. For instance, in branches *of Populus trichocarpa* trees, P_{50} values spanned a 2 MPa range among four widely used approaches, namely the optical method, the hydraulic method, the centrifuge method and X-ray-computed microtomography (microCT) (Venturas et al. 2019), the latter providing P_{50} values similar to those obtained via the acoustic method (De Baerdemaeker et al. 2019b). Differences between measurement techniques are often attributed to measurement artefacts. Nonetheless, they may also result from differences in the way k_h losses are quantified. For example, the optical and acoustic method focus on the number of embolism events, which is not necessarily proportional with the loss of k_h as this is dependent on the size of the embolized conduit according to Equation 5.2. Comparison of P_{50} values determined using different measurement techniques, however, could provide valuable information on plant hydraulic characteristics (Venturas et al. 2019).

Stomatal regulation and tree water deficit under drought and elevated CO_2

Hydraulic thresholds are widely used for assessment and comparison of plant performance under drought stress. The "gold standard" for comparison (i.e. the P_{50} value) informs about xylem vulnerability for embolism formation (Meinzer et al. 2009, Li et al. 2019a). However, this approach narrows our perspective of plant behaviour under water limiting conditions, as any other functional strategy to limit or delay increases in xylem tension remains ignored (Epila et al. 2017). To limit increases in xylem tension, trees reduce leaf scale water loss by stomatal

closure. Residual water loss through the leaf cuticle or through the stem bark further impoverish tree water status, and internal water pools progressively deplete to buffer Ψ_{xylem} reductions (Epila et al. 2017, Choat et al. 2018). To gain a more comprehensive understanding on tree drought susceptibility, it is therefore crucial to integrate several drought-related thresholds informing about *in vivo* stomatal behaviour and plant dehydration rates (Bartlett et al. 2016).

During the early and late season drought events, the [CO_2] treatment affected the onset and rate of stomatal closure with declining tree water status (Ψ_{xylem}). In addition, eCO_2 effects differed between seasonal drought experiments. During the ESE, g_s reduction started earlier and was more gradual under eCO_2, as it could be expected from stomatal behaviour under well-watered conditions (Ainsworth and Rogers 2007). High atmospheric [CO_2] facilitates maintenance of relatively high [CO_2] in the sub-stomatal cavities despite partial stomatal closure. When facing moderate drought, this advantage of CO_2 fertilization might gain importance as an earlier and more gradual stomatal closure favours water savings, thereby limiting detrimental effects of reduced carbon availability (e.g. Goodfellow et al. 1997, Herrick et al. 2004, Robredo et al. 2007, Drake et al. 2017, Pathare et al. 2017, Birami et al. 2020). As drought proceeds, advanced stomatal closure can help to maintain the integrity of the hydraulic system, as an earlier stomatal closure is often associated with higher xylem vulnerability to drought-induced embolism (Brodribb et al. 2014, 2017), which is consistent with the shift of the VC_{AE} observed here. Contrastingly, stomatal closure was delayed under eCO_2 during LSE, highlighting that stomatal responses to drought are seasonal-dependent (Chapter 2). Limited sensitivity of g_s to soil drought under eCO_2 has previously been observed in beech, chestnut and oak trees (Heath 1998), as well as in tomato (Liu et al. 2019) and other crop species (Haworth et al. 2016). It is likely mediated by an eCO_2-induced disruption of the ABA (abscisic acid) signal transduction pathway (Li et al. 2020), which might in turn be affected by leaf development (Mcadam and Brodribb 2015). In any case, delayed stomatal closure under eCO_2 during LSE did not compromise xylem integrity at this time, as denoted by similar hydraulic vulnerability curves for both [CO_2] treatments.

Capacitive water release is another relevant strategy to face drought and delay embolism formation (Epila et al. 2017, Körner 2019, Martinez-Vilalta et al. 2019, Hammond et al. 2021). However, possible eCO_2-induced alteration of the capacity to store water in stem tissues remains largely unexplored. *In vivo* measurements of stem shrinkage suggest that the progressive depletion of elastic water pools (TWD) was unaffected by eCO_2. Accordingly, estimates of elastic capacitance (C_{el}) derived from desorption curves via bench dehydration did not differ between [CO_2] treatments. Independent of the [CO_2] treatment, C_{el} in the young European aspen trees surveyed here varied from 119 to 265 kg m^{-3} MPa^{-1}, which is in

agreement with the elastic hydraulic capacitance previously measured in ten small-sized (≤ 3 m height) angiosperm trees (20 - 280 kg m^{-3} MPa^{-1}; Scholz et al. 2011). Reliance on stored water to maintain transpiration requirements and stem hydraulic capacitance commonly increase with stem size (Phillips et al. 2003, Scholz et al. 2011). However, despite the observed stimulation of stem volumetric growth (ESE) and stem mass growth (LSE) for the surveyed trees under eCO₂ (Chapter 3 and 4), eCO₂-induced differences in stem size might still be insufficient to significantly affect the size of stem elastic water pools and C_{el}. Long-term experiments would be necessary to detect eCO₂-induced differences in elastic hydraulic capacitance. Nevertheless, we speculate that potential differences would result from biophysical responses to eCO₂ rather than from physiological acclimation.

Sequential down-regulation of tree water losses and depletion of water pools

Stomatal closure was the first response to declining tree water status under both aCO₂ and eCO₂. Remarkably, almost complete stomatal closure (g_{s_88}) and onset of embolism formation (AE_{12}) occurred at a similar Ψ_{xylem} for the surveyed trees. The reduction of leaf scale water loss to delay further increases in xylem tension as an attempt to avoid lethal drought-driven embolism reveals a strict stomatal regulation, even in the young trees under study which cannot rely to a great extent on previously stored carbohydrates (Wertin and Teskey 2008). Such conservative hydraulic behavior prioritizes the safeguarding of the vascular system integrity to the detriment of a limited carbon uptake to fulfil metabolic requirements (Brodribb et al. 2017, Choat et al. 2018), a strategy already observed in several plant species (Hochberg et al. 2017, Choat et al. 2018, Li et al. 2018b, Blackman et al. 2019).

Less studied is the timing and coordination of the progressive depletion of capillary, elastic and inelastic stem water pools leading to lethal tissue dehydration (Körner 2019, Martinez-Vilalta et al. 2019). Capacitive water release from capillary spaces and elastic pools buffers daily fluctuations in Ψ_{xylem} (Zweifel et al. 2001, Steppe et al. 2012, 2015, De Swaef et al. 2015), while further seasonal depletion of elastic living cells delays Ψ_{xylem} reductions when facing prolonged drought stress (Vergeynst et al. 2013, Salomón et al. 2017a). Only when Ψ_{xylem} exceeds critical thresholds, inelastic water release from embolized conduits is expected to occur, transiently reducing the risk of runaway embolism (Hölttä et al. 2009). This widely accepted sequential dehydration pattern results in the theoretical desorption curve and its three discrete phases (Tyree and Yang 1990, Vergeynst et al. 2015a, Pratt and Jacobsen 2017, Choat et al. 2018, Steppe 2018). Accordingly, stems started to shrink before onset of embolism formation ($TWD_{12} > AE_{12}$). However, with declining tree water status (when stomatal closure reached 50 %), differences between $TWD_{50} - AE_{50}$ and $TWD_{88} - AE_{88}$ thresholds diminished. Therefore, comparison of TWD and AE trends after halfway of complete stomatal

closure indicate a parallel rather than sequential depletion of stem elastic and inelastic water pools. This dehydration pattern is consistent with recent microCT studies performed to assess temporal and spatial variability in xylem dehydration. In *Castanea dentata* (Knipfer et al. 2019), *Eucalyptus camaldulensis* (Nolf et al. 2017) and *Laurus nobilis* L. (Nardini et al. 2017), dehydration of non-conducting xylem tissues (i.e. living cells and dead fibbers) occurred simultaneously or even after onset of embolism formation. In two-year-old *C. dentata* trees, current-year xylem, closely located to the cambium layer, remained hydrated at a lower water potential than that in the older xylem, more distant from the cambium. These observations suggest prioritization of cambial survival over maintenance of the vascular functionality since living cambial cells are crucial for drought recovery and growth resumption (Knipfer et al. 2019). The parallel depletion of elastic and inelastic water pools observed here at Ψ_{xylem} below g_{s_50} highlights that depletion of stem water pools does not simply switch from elastic to inelastic tissues and further questions the classic sequential dehydration pattern merely based on the water source type. While the initial slope of the desorption curve might be an adequate proxy of the elastic capacitance at full tissue hydration (Steppe et al. 2006), with increasing levels of drought stress, capacitive water release might be simultaneously released from elastic and inelastic pools. The slope of the final part of the segmented DC might therefore represent an integrated hydraulic capacitance of partly depleted elastic and inelastic water pools. When aiming to disentangle the relative contribution of both elastic and inelastic water pools throughout the complete gradient of drought stress, combined measurements of stem shrinkage and proxies of conduit embolism would be helpful.

Conclusion

The [CO_2] treatment differently affected average vessel diameter in young *Populus tremula* trees depending on wood phenological phases. During the early season, stimulated stem volumetric growth under eCO_2 might have resulted in wider vessels and marginal reductions in wood density. Accordingly, xylem was more vulnerable to drought-induced embolism under eCO_2 and hydraulic capacitance increased during severe drought stress. Hydraulic efficiency, however, remained unaltered by the [CO_2] treatment, as estimated from average vessel hydraulic diameter and conductivity. Drought-driven stomatal closure was accelerated under eCO_2, which might help to maintain vascular integrity of a more vulnerable hydraulic system. Contrastingly, and during the late season, carbon surplus under eCO_2 might have been allocated to cell wall thickening, hereby narrowing vessel lumen. This alteration did not affect xylem hydraulic vulnerability or capacitance. Depletion of stem elastic water pools (detected with high-resolution dendrometers) remained unaffected by the [CO_2] treatment during both of the *in vivo* seasonal drought experiments. Limitation of leaf scale water losses was the first

tree response when facing drought, and stomatal closure was almost complete at the onset of embolism formation. Such conservative hydraulic behaviour denotes prioritized maintenance of vascular integrity over carbon uptake. Despite earlier onset of the depletion of stem elastic pools relative to the inelastic ones, differences levelled off after halfway of complete stomatal closure. This underlines that the relative contribution of elastic water pools to the overall hydraulic capacitance remained significant even during vessel embolism formation. We therefore urge to revisit the idea of a simplified sequential depletion of elastic and inelastic water pools, as simultaneous dehydration suggests otherwise.
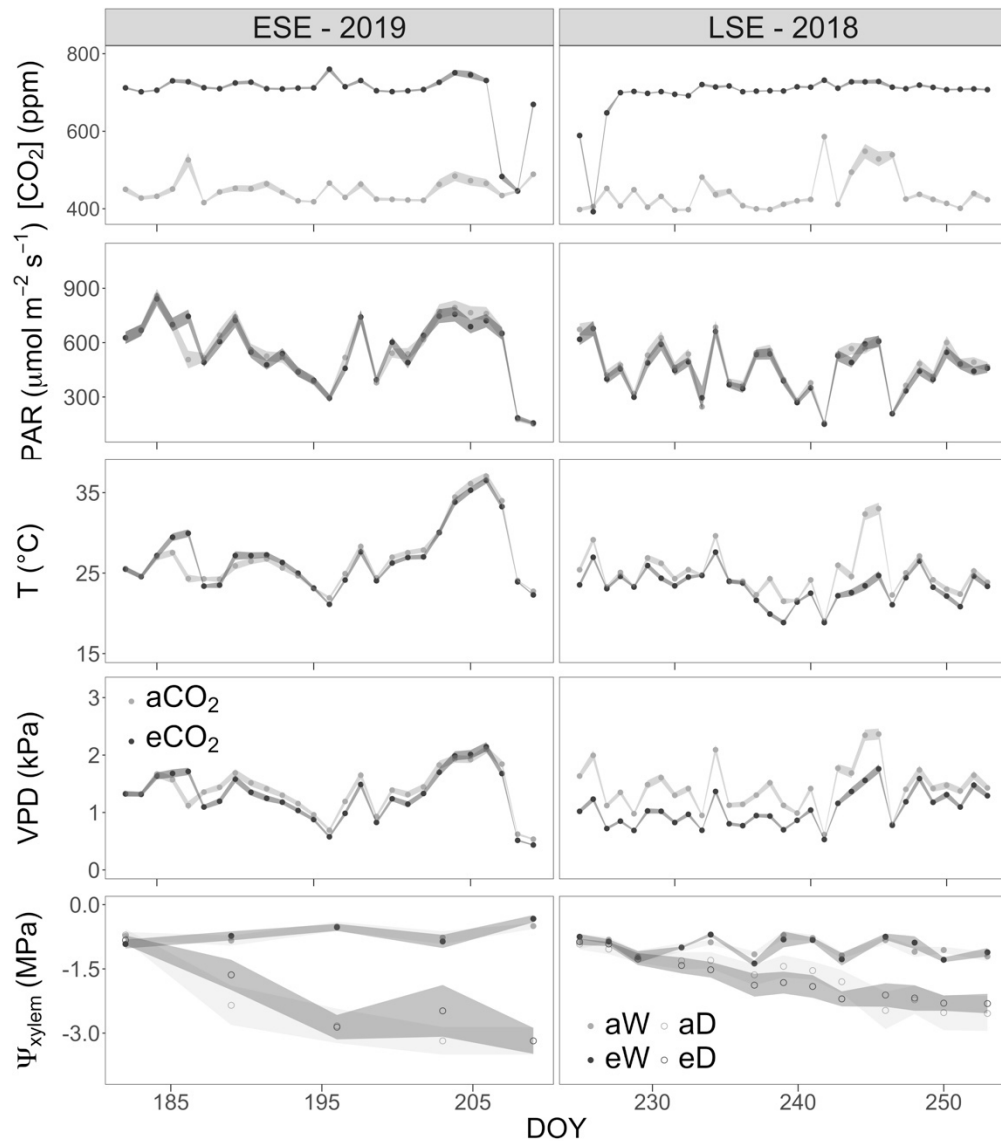
Supplementary material

Figure S5.1 Average daytime (PAR > 5 µmol m^{-2} s^{-1}) chamber CO_2 concentration ([CO_2]), photosynthetically active radiation (PAR), temperature (T), and vapor pressure deficit (VPD) in the ambient (aCO_2, light grey) and elevated (eCO_2, dark grey) [CO_2] treatment chambers and average xylem water potential (Ψ_{Xylem}) along the early (ESE - 2019, left-hand side panels) and late (LSE - 2018, right-hand side panels) season *in vivo* drought experiments.

Trees were subjected to combined treatments of atmospheric [CO_2] (ambient (a) and elevated (e)) and drought stress (well-watered (W) and drought stressed (D)). With DOY day of year.

6

General conclusions and outlook

Rapid climate change is placing forests under unprecedented stress (McDowell et al. 2020). Drought events, often in combination with high temperatures, have increased in frequency, duration and intensity (IPCC 2018). Despite substantial research efforts over the last decades, the question remains if increasing atmospheric carbon dioxide concentration ($[CO_2]$) mitigates or aggravates adverse effects of drought stress on tree functioning (Menezes-Silva et al. 2019). Nonetheless, current widespread forest dieback (Allen et al. 2015, Hartmann et al. 2018) does not suggest that CO_2 fertilization is capable of preventing tree mortality. In turn, forests are able to mitigate the threads of climate change, as they are responsible for the uptake of 30 % of the anthropogenic emitted CO_2 (Friedlingstein et al. 2019, Pugh et al. 2019). Accurate understanding of forests' behaviour and potential for carbon (C) sequestration under future climates is therefore crucial to predict global C budgets under changing climate scenarios (Cernusak et al. 2019, Anderegg et al. 2020). Terrestrial biosphere models remain inconclusive towards future forests' C sink strength and ecosystem functioning (Schurgers et al. 2018, Krause et al. 2019, Pugh et al. 2019), because model assumptions to simulate forest behaviour do not accurately reflect underlying mechanisms of tree physiology under different stress elicitors. Improving our understanding on tree responses to eCO_2, drought and their interaction remains therefore crucial to predict forest development and enable science-based decision making.

To advance knowledge in this line, this PhD dissertation focused on the temporal dynamics of leaf and whole-tree responses to eCO_2 under well-watered and drought conditions. Temporal

variability in eCO$_2$ responses have long been reported, with a pioneering study in bean (*Phaseolus vulgaris*) being published 35 year ago (Jolliffe and Ehret 1985), yet effects of eCO$_2$ are often simplified by a temporally static value thereby precluding a comprehensive understanding of complex and variable eCO$_2$ effects on tree functioning. To ascertain the general occurrence of dynamic eCO$_2$ responses over time (within a single growing season and across multi-annual developmental stages) and spatial scales (leaf vs. whole-tree scale), a review was conducted (**Chapter 2**). *In vivo* effects of elevated [CO$_2$], and of the experimental timing of drought events (early vs. late season), were assessed at both leaf and whole-tree scale in one-year-old *Populus tremula* L. (European aspen) trees under well-watered (**Chapter 3**) and drought (**Chapter 4**) conditions. Finally, drought strategies monitored *in vivo* were compared with hydraulic vulnerability and stem dehydration, respectively, assessed in the lab with embolism-related acoustic emissions and hydraulic capacitances (**Chapter 5**).

To gain more insight in the dynamic nature of tree eCO$_2$ responses over time (early vs. late season) and spatial scales (leaf vs. whole-tree) under well-watered and drought conditions, young European aspen trees were grown in treatment chambers allowing straightforward manipulation of environmental conditions and of the timing of imposed drought events. Nonetheless, studies in growth chambers inevitably limit the number and size of trees under survey. Such spatial constraints precluded to study early and late seasonal responses to the [CO$_2$] treatment on the same set of trees during a single growing season. Consequently, comparison between early and late season datasets might be biased by different annual environmental conditions (a heat wave occurred in 2018), so that the effects of the [CO$_2$] treatment in this dissertation focused on [CO$_2$] treatment differences observed within a single seasonal development stage (as independent experiments), being more cautious regarding seasonal comparisons. Moreover, legacy effects derived from different time exposure to eCO$_2$ (7 and 4 months for LSE and ESE, respectively) likely led to relatively larger NSC pools in eCO$_2$ trees at the onset of the drought event. Given the coupling between hydraulic performance and NSC status (Tomasella et al. 2020), legacy effects might also affect the interaction between seasonality and hydraulic functioning. Finally, and as a result of the limited number of treatment chambers, pseudo-replication issues could not be completely avoided, lowering the statistical confidence of the comparison between [CO$_2$] treatments. Despite these experimental drawbacks, combination of the results from the four research chapters, allows a cautious reply to our three original research questions (Figure 1.4 in **Chapter 1**)

Are tree responses to elevated CO$_2$ dynamic over time?

Although tree responses to eCO$_2$ are often summarized using a single static value, dynamic leaf and whole-tree responses to eCO$_2$ have been observed in a variety of tree species and during different developmental stages (**Chapter 2**). Overall, the magnitude of the [CO$_2$] treatment is commonly largest during the early season (i.e. from spring to early summer), while down-regulation occurs towards the end of the growing season (from onset of autumn to winter). These observations highlight the importance of phenological-driven variations in tree C-sink strength to meet seasonal C requirements. When C demand is high as a result of aboveground and belowground biomass production, rapid allocation of carbohydrates from leaves towards sink organs triggers a positive feedback up-regulating tree responses to eCO$_2$. In contrast, as the season progresses and tree C sink strength declines, leaf C accumulation in foliar tissues down-regulates the leaf response to eCO$_2$. Also, in the young European aspen trees surveyed here, stimulation of net carbon assimilation (A$_n$) under eCO$_2$ increased from the onset of leaf development and peaked during stages of extensive stem volumetric growth (June and early July), after which A$_n$ stimulation diminished towards the onset of leaf senescence (**Chapter 3**). Increased leaf C fixation rates translated to the whole-tree scale, resulting in a stimulation of stem volumetric growth during the early season and dry biomass production during the late season, when cell wall thickening typically leads to C sequestration but not to volumetric growth. Responses to eCO$_2$ in stomatal and canopy conductance or in leaf and stem respiratory physiology were not dynamic over time, as a likely result of the limited overall impact of eCO$_2$ on leaf and whole-tree water use and respiration.

The effects of elevated [CO$_2$] on tree drought responses (**Chapter 4**) and xylem vulnerability to embolism (**Chapter 5**) were dependent on the seasonal timing of the drought event. Strong significant effects of the [CO$_2$] treatment on *in vivo* drought responses at the leaf scale were observed when drought was imposed during the late season (mid-August). Contrastingly, vulnerability to drought-induced embolism formation and corresponding hydraulic capacitance differed between [CO$_2$] treatments during the early season, while remaining unaffected during the late season. This discrepancy in the effects of eCO$_2$ on tree's stomatal regulation under drought (**Chapter 4**) and hydraulic vulnerability (**Chapter 5**), underline the need to further unravel possible shifts in tree vulnerability to drought-induced embolism formation under eCO$_2$. In particular, since drought-induced stomatal closure only provides a fraction of tree's drought responses (Choat et al. 2018).

Can leaf scale responses to elevated CO_2 be upscaled to the whole-tree scale?

Compilation of tree C (i.e. A_n and daily stem volumetric growth) and water (i.e. stomatal and canopy conductance) processes under free-air CO_2 enrichment (FACE) conditions showed that both magnitude and direction of the eCO_2 responses can substantially vary depending on the spatial scale under study (**Chapter 2**). For C processes, stimulation of leaf A_n does not necessarily result in parallel increases in tree volumetric or mass growth. In free soil eCO_2 studies, A_n was consistently stimulated under eCO_2. Nonetheless, growth was stimulated in only six of the eighteen compiled studies (**Chapter 2**). These observations suggests that additional available C could be alternatively diverted to respiration processes, storage of non-structural carbohydrates (NSC), root exudates or emission of volatile organic compounds lowering growth stimulation. In particular in mature trees, growth is expected to be C-saturated, since nutrient or water limitation might govern tree dynamics in closed stands.

In the young European aspen trees, stimulation of A_n was observed throughout the entire growing season (**Chapter 3**). However, stimulated A_n did not result in an increase of dry biomass by the end of July, and stem volumetric increment remained unaffected from August to September. We hypothesize that increased C availability in the young trees under survey stimulated growth year-long, but C allocation shifted over time: from cell division and enlargement during the early season, to cell wall thickening and lignification during the late season. The study of wood anatomical traits partially confirmed this hypothesis (**Chapter 5**). Early season wood was characterized by a wider average vessels when exposed to eCO_2. Contrastingly, no differences in vessel diameter between [CO_2] treatments were detected during the late season, likely as a consequence of the increased cell wall thickening and abundance of narrow late-wood vessels under eCO_2.

Also, for water processes (i.e. stomatal (g_s) and canopy conductance), effects of eCO_2 at the leaf scale do not systematically translate to whole-tree responses. Elevated [CO_2] commonly lowers leaf scale water loss (Ainsworth and Rogers 2007). Nonetheless, potential stimulation of total canopy area can nullify g_s reduction, and even enhance whole-tree water use depending on the magnitude of these eCO_2-induced alterations (Fatichi et al. 2016; **Chapter 2**). In contrast with our expectations, we did not find consistent reductions in leaf water loss under eCO_2 during the seasonal experiments. This neutral effect of eCO_2 at leaf scale upscaled to the whole-tree scale as water use remained unaltered (**Chapter 3**).

Discrepancies between leaf and whole-tree responses to eCO_2 were also found when surveyed trees were subjected to drought. Despite the limited effects of eCO_2 at leaf-scale

drought responses *in vivo*, whole-tree drought responses (in terms of tree water use, stem volumetric growth and respiration) all remained unaltered under eCO_2 (**Chapter 4**). This observation highlights the risk of predicting whole-tree responses to eCO_2 solely based on leaf scale measurements. We therefore urge scientists to incorporate stem-based measurements and whole-tree responses in future eCO_2 experiments to gain a balanced understanding of leaf and whole-tree scale behaviour as climate changes (**Chapter 1**).

Does elevated CO_2 mitigate adverse drought effects and alter drought vulnerability?

Increasing atmospheric [CO_2] has been suggested to improve tree water status and mitigate adverse effects of drought stress. However, in the young European aspen trees under survey, mitigating effects of eCO_2 were limited to the leaf-scale and the late season (**Chapter 4**). During the early season, *in vivo* drought responses remained mainly unaffected by eCO_2 over time. The difference between [CO_2] treatments was limited to a moderate advance (shift in inflection point; **Chapter 4**) or more gradual (i.e. lower reduction rate; **Chapter 5**) stomatal closure with increasing drought stress gradient or decreasing xylem water potential (Ψ_{xylem}), respectively, both hinting towards an earlier onset of stomatal closure under eCO_2. In their review, Choat et al. (2018) hypothesized stomatal closure occurs to avoid high-risk xylem tensions leading to conduit embolism formation. Onset of stomatal closure at less negative Ψ_{xylem} could thus denote an increase in xylem vulnerability towards drought-induced embolism formation. In agreement with this hypothesis, corresponding xylem vulnerability and hydraulic capacitance was higher under eCO_2 during ESE, with an apparent shift of the vulnerability curve to less negative Ψ_{xylem} and an increase in hydraulic capacitance when drought was most severe, likely related to the development of wider vessels during the period of fast stem volumetric growth (**Chapter 5**).

Contrastingly, during the late season drought event, eCO_2 delayed and slowed-down stomatal closure with increasing levels of drought stress, enabling gas exchange at more negative Ψ_{xylem} and possibly prolonging A_n over time (**Chapter 4**). In contrast, vulnerability curves and hydraulic capacitance were not altered by eCO_2 during the late season (**Chapter 5**). We therefore suggest year-long exposure to eCO_2 delayed leaf scale drought responses, as a possible result of disrupted stomatal regulation.

Hydraulic failure is considered the predominant cause of drought-induced tree mortality (Adams et al. 2017). Nonetheless, stomatal closure to avoid embolism for extended periods can induce an imbalance between C demand and supply leading to C starvation, a possible co-driver of tree morality. Before onset of drought, eCO_2 increased the concentration of NSC

(starch and soluble sugars) in leaf and xylem tissues (**Chapter 4**). Despite the enlarged pre-drought NSC pool, respiratory C expenditures as drought proceeded offset all differences in [NSC] between [CO_2] treatments. These results highlight the complex interactions between NSC, drought, and the [CO_2] treatment. Although possible mitigating effect of enhanced pre-drought NSC pools under eCO_2 deserve further investigation, our results do not indicate alleviating effects of CO_2 treatment for C starvation under severe drought stress.

Future perspectives

Although the *in vivo* research was limited to young trees, seasonal variability in eCO_2 responses might also be scalable to mature forests (**Chapter 2**), which would alter their capacity to act as terrestrial C sinks year-round (recently reviewed in Walker et al. (2020)). Nonetheless, the extent to which early and late season eCO_2 responses are expected to differ across mature forests remains far less certain and will be likely dependent on nutrient availability (in particular nitrogen (N) and phosphorous (P)), forest microclimate (e.g. temperature and light intensity) and water availability. For instance, a recent study showed that under current [CO_2] aboveground biomass was 95 % higher near the forest edge in comparison to inner forest areas as a likely result of increased N deposition and higher light availability (Meeussen et al. 2021). As a result of the spatial variability in the C sink strength of the forest, CO_2 fertilization might also be stronger at the forest edge, amplifying current differences in biomass productivity. Among others, future research questions should focus on the effects of nutrient deficiency and its ability to initiate or amplify discrepancies between leaf and whole-tree responses under eCO_2. Recent meta-analyses underlined that the magnitude of eCO_2 effects is largely determined by the N and P availability (Terrer et al. 2019) and mycorrhizal associations facilitating nutrient uptake (Terrer et al. 2016). Also, air temperature and light intensity, two climatic variables that remained unexplored in this PhD dissertation, should be included in future analyses. Despite the general stimulation of C fixation rates following a moderate temperature increase (Long 1991) and the species-specific dependency of plant performance on the daily light integral (Poorter et al. 2019), accurate translation to the whole-tree scale, in particular during the late season when relative C demand reduces (Pantin et al. 2012, Cuny et al. 2015), remains crucial (Teskey et al. 2015). Finally, our results indicate seasonality of tree responses to eCO_2 might cause a shift in tree drought responses and vulnerability throughout the growing season (**Chapter 4 and 5**). Although seasonal differences in drought vulnerability is increasingly gaining interest (e.g. D'Orangeville et al. 2018, Sorek et al. 2020), this relatively novel research topic deserves further investigation to refine predictions of the effects of more frequently occurring drought events under current and future [CO_2].

It is a natural response to think bigger, but answers might also be hidden in the details. Despite decades of research on the effects of eCO_2 on wood anatomy, dynamic effects of increased $[CO_2]$ over multi-annual developmental stages remain largely unexplored. High frequency wood sampling or non-invasive methods adding a time stamp to the wood sample (e.g. cambial pinning; Van Camp et al. 2018), allow the determination of wood traits at well-chosen moments during the growing season. Not only would this provide valuable information on the evolution of the eCO_2 effect over time, combination of anatomical and ecophysiological data, including *in vivo* drought responses and hydraulic vulnerability, could bridge the still-existing knowledge gap between these two research fields (as highlighted by Steppe et al. (2015)).

"Trees are wonderful things" (McCarroll and Loader 2004). Trees are appreciated for their ability to evolve and to adapt to face adverse and seasonally changing environmental conditions. For instance, trees cope with both cold winters and hot dry summers in temperate forests. As a result of environmental year-round changes, it is not surprising that tree responses to eCO_2 are also dynamic over time. Along this PhD dissertation, we strived to underline how seasonality of tree C sink strength can drive temporal eCO_2 dynamics at different spatial scales under well-watered and drought conditions. Although we realize our results might have raised more questions than they were able to answer, it would almost be a shame if they did not. We hope our results convince scientists to no longer ignore temporal and spatial eCO_2 dynamics to further unravel them in eCO_2 experiments to come.

B
Bibliography

Acosta M, Pokorný R, Janouš D, Marek M V. (2010) Stem respiration of Norway spruce trees under elevated CO_2 concentration. Biol Plant 54:773–776.

Adam NR, Wall GW, Kimball BA, Idso SB, Webber AN (2004) Photosynthetic down-regulation over long-term CO_2 enrichment in leaves of sour orange (*Citrus aurantium*) trees. New Phytol 163:341–347.

Adams HD, Germino MJ, Breshears DD, Barron-Gafford GA, Guardiola-Claramonte M, Zou CB, Huxman TE (2013) Nonstructural leaf carbohydrate dynamics of *Pinus edulis* during drought-induced tree mortality reveal role for carbon metabolism in mortality mechanism. New Phytol 197:1142–1151.

Adams HD, Zeppel MJB, Anderegg WRL, Hartmann H, Landhäusser SM, Tissue DT, Huxman TE, Hudson PJ, Franz TE, Allen CD, Anderegg LDL, Barron-Gafford GA, Beerling DJ, Breshears DD, Brodribb TJ, Bugmann H, Cobb RC, Collins AD, Dickman LT, Duan H, Ewers BE, Galiano L, Galvez DA, Garcia-Forner N, Gaylord ML, Germino MJ, Gessler A, Hacke UG, Hakamada R, Hector A, Jenkins MW, Kane JM, Kolb TE, Law DJ, Lewis JD, Limousin JM, Love DM, Macalady AK, Martínez-Vilalta J, Mencuccini M, Mitchell PJ, Muss JD, O'Brien MJ, O'Grady AP, Pangle RE, Pinkard EA, Piper FI, Plaut JA, Pockman WT, Quirk J, Reinhardt K, Ripullone F, Ryan MG, Sala A, Sevanto S, Sperry JS, Vargas R, Vennetier M, Way DA, Xu C, Yepez EA, McDowell NG (2017) A multi-species synthesis of physiological mechanisms in drought-induced tree mortality. Nat Ecol Evol 1:1285–1291.

Agüera E, De la Haba P (2018) Leaf senescence in response to elevated atmospheric CO_2 concentration and low nitrogen supply. Biol Plant 62:401–408.

Ainsworth EA, Davey PA, Hymus GJ, Drake BG, Long SP (2002) Long-term response of photosynthesis to elevated carbon dioxide in a Florida scrub-oak ecosystem. Ecol Appl 12:1267–1275.

Ainsworth EA, Lemonnier P, Wedow JM (2020) The influence of rising tropospheric carbon dioxide and ozone on plant productivity. Plant Biol 22:5–11.

Ainsworth EA, Long SP (2020) 30 years of free-air carbon dioxide enrichment (FACE): What have we learned about future crop productivity and its potential for adaptation? Glob Chang Biol:gcb.15375. https://onlinelibrary.wiley.com/doi/10.1111/gcb.15375

Ainsworth EA, Rogers A (2007) The response of photosynthesis and stomatal conductance to rising $[CO_2]$: Mechanisms and environmental interactions. Plant, Cell Environ 30:258–270.

Ainsworth EA, Rogers A, Leakey ADB, Heady LE, Gibon Y, Stitt M, Schurr U (2007) Does elevated atmospheric $[CO_2]$ alter diurnal C uptake and the balance of C and N metabolites in growing and fully expanded soybean leaves? J Exp Bot 58:579–591.

Alder NN, Pockman WT, Sperry JS, Nuismer S (1997) Use of centrifugal force in the study of xylem cavitation. J Exp Bot 48:665–674.

Allen CD, Breshears DD, McDowell NG (2015) On underestimation of global vulnerability to tree mortality and forest die-off from hotter drought in the Anthropocene. Ecosphere 6:1–55.

Allen LH, Kimball BA, Bunce JA, Yoshimoto M, Harazono Y, Baker JT, Boote KJ, White JW (2020) Fluctuations of CO_2 in Free-Air CO_2 Enrichment (FACE) depress plant photosynthesis, growth, and yield. Agric For Meteorol 284

Allen CD, Macalady AK, Chenchouni H, Bachelet D, McDowell N, Vennetier M, Kitzberger T, Rigling A, Breshears DD, Hogg EH (Ted., Gonzalez P, Fensham R, Zhang Z, Castro J, Demidova N, Lim JH, Allard G, Running SW, Semerci A, Cobb N (2010) A global overview of drought and heat-induced tree mortality reveals emerging climate change risks for forests. For Ecol Manage 259:660–684.

Allen RG, Pereira LS, Raes D, Smith M (1998) Crop evapotranspiration — guidelines for computing crop water requirement. FAO Irrig Drain Pap 56. http://www.fao.org/docrep/x0490e/x0490e00.htm (1 July 2020, date last accessed).

Amthor JS (1984) The role of maintenance respiration in plant growth. Plant Cell Environ 7:561–569.

Amthor JS (2000) The McCree-de Wit-Penning de Vries-Thornley respiration paradigms: 30 Years later. Ann Bot 86:1–20.

Anderegg WRL, Anderegg LDL, Kerr KL, Trugman AT (2019) Widespread drought-induced

tree mortality at dry range edges indicates that climate stress exceeds species' compensating mechanisms. Glob Chang Biol 25:3793–3802.

Anderegg WRL, Prall JW, Harold J, Schneider SH (2010) Expert credibility in climate change. Proc Natl Acad Sci U S A 107:12107–12109.

Anderegg WRL, Trugman AT, Badgley G, Anderson CM, Bartuska A, Ciais P, Cullenward D, Field CB, Freeman J, Goetz SJ, Hicke JA, Huntzinger D, Jackson RB, Nickerson J, Pacala S, Randerson JT (2020) Climate-driven risks to the climate mitigation potential of forests. Science (80-) 368

Aspinwall MJ, Jacob VK, Blackman CJ, Smith RA, Tjoelker MG, Tissue DT (2017) The temperature response of leaf dark respiration in 15 provenances of *Eucalyptus grandis* grown in ambient and elevated CO_2. Funct Plant Biol 44:1075–1086.

Asshoff R, Zotz G, Körner C (2006) Growth and phenology of mature temperate forest trees in elevated CO_2. Glob Chang Biol 12:848–861.

Atkin OK, Bloomfield KJ, Reich PB, Tjoelker MG, Asner GP, Bonal D, Bönisch G, Bradford MG, Cernusak LA, Cosio EG, Creek D, Crous KY, Domingues TF, Dukes JS, Egerton JJG, Evans JR, Farquhar GD, Fyllas NM, Gauthier PPG, Gloor E, Gimeno TE, Griffin KL, Guerrieri R, Heskel MA, Huntingford C, Ishida FY, Kattge J, Lambers H, Liddell MJ, Lloyd J, Lusk CH, Martin RE, Maksimov AP, Maximov TC, Malhi Y, Medlyn BE, Meir P, Mercado LM, Mirotchnick N, Ng D, Niinemets Ü, O'Sullivan OS, Phillips OL, Poorter L, Poot P, Prentice IC, Salinas N, Rowland LM, Ryan MG, Sitch S, Slot M, Smith NG, Turnbull MH, VanderWel MC, Valladares F, Veneklaas EJ, Weerasinghe LK, Wirth C, Wright IJ, Wythers KR, Xiang J, Xiang S, Zaragoza-Castells J (2015) Biochemical models of leaf photosynthesis. http://doi.wiley.com/10.1111/nph.13253

Atwell BJ, Henery ML, Whitehead D (2003) Sapwood development in *Pinus radiata* trees grown for three years at ambient and elevated carbon dioxide partial pressures. Tree Physiol 23:13–21.

Avila RT, de Almeida WL, Costa LC, Machado KLG, Barbosa ML, de Souza RPB, Martino PB, Juárez MAT, Marçal DMS, Martins SCV, Ramalho JDC, DaMatta FM (2020) Elevated air [CO_2] improves photosynthetic performance and alters biomass accumulation and partitioning in drought-stressed coffee plants. Environ Exp Bot 177

Azcón-Bieto J, Osmond CB (1983) Relationship between photosynthesis and respiration. Plant Physiol 71:574–581.

De Baerdemaeker NJF, Arachchige KNR, Zinkernagel J, Van Den Bulcke J, Van Acker J, Schenk HJ, Steppe K, Tognetti R (2019a) The stability enigma of hydraulic vulnerability curves: Addressing the link between hydraulic conductivity and drought-induced embolism. Tree Physiol 39:1646–1664.

De Baerdemaeker NJF, Salomón RL, De Roo L, Steppe K (2017) Sugars from woody tissue

photosynthesis reduce xylem vulnerability to cavitation. New Phytol 216:720–727.

De Baerdemaeker NJF, Stock M, Van Den Bulcke J, De Baets B, Van Hoorebeke L, Steppe K (2019b) X-ray microtomography and linear discriminant analysis enable detection of embolism-related acoustic emissions. Plant Methods 15:1–18.

Bartlett MK, Detto M, Pacala SW (2019) Predicting shifts in the functional composition of tropical forests under increased drought and CO_2 from trade-offs among plant hydraulic traits. Ecol Lett 22:67–77.

Bartlett MK, Klein T, Jansen S, Choat B, Sack L (2016) The correlations and sequence of plant stomatal, hydraulic, and wilting responses to drought. Proc Natl Acad Sci 113:13098–13103. http://www.pnas.org/lookup/doi/10.1073/pnas.1604088113

Bassham JA, Shibata K, Steenberg K, Bourdon J, Calvin M (1956) The Photosynthetic cycle and respiration: Light-dark transients1. J Am Chem Soc 78:4120–4124. https://doi.org/10.1021/ja01597a071

Bastos A, Ciais P, Friedlingstein P, Sitch S, Pongratz J, Fan L, Wigneron JP, Weber U, Reichstein M, Fu Z, Anthoni P, Arneth A, Haverd V, Jain AK, Joetzjer E, Knauer J, Lienert S, Loughran T, McGuire PC, Tian H, Viovy N, Zaehle S (2020) Direct and seasonal legacy effects of the 2018 heat wave and drought on European ecosystem productivity. Sci Adv 6:1–14.

Batke SP, Yiotis C, Elliott-Kingston C, Holohan A, McElwain J (2020) Plant responses to decadal scale increments in atmospheric CO_2 concentration: comparing two stomatal conductance sampling methods. Planta 251:1–12. https://doi.org/10.1007/s00425-020-03343-z

Bauweraerts I, Wertin TM, Ameye M, Mcguire MA, Teskey RO, Steppe K (2013) The effect of heat waves, elevated [CO_2] and low soil water availability on northern red oak (*Quercus rubra* L.) seedlings. Glob Chang Biol 19:517–528.

Beall FC (2002) Overview of the use of ultrasonic technologies in research on wood properties. Wood Sci Technol 36:197–212.

Becklin KM, Walker SM, Way DA, Ward JK (2017) CO_2 studies remain key to understanding a future world. New Phytol 214:34–40.

Begg JE, Turner NC (1970) Water potential gradients in field tobacco. Plant Physiol 46:343–346.

Bellasio C, Quirk J, Beerling DJ (2018) Stomatal and non-stomatal limitations in savanna trees and C4 grasses grown at low, ambient and high atmospheric CO_2. Plant Sci 274:181–192.

Bernacchi CJ, Calfapietra C, Davey PA, Wittig VE, Scarascia-Mugnozza GE, Raines CA, Long SP (2003) Photosynthesis and stomatal conductance responses of poplars to free-air CO_2 enrichment (PopFACE) during the first growth cycle and immediately following

coppice. New Phytol 159:609–621.

Bernacchi CJ, Vanloocke A (2015) Terrestrial ecosystems in a changing environment: A dominant role for water. Annu Rev Plant Biol 66:599–622.

Bigras FJ, Bertrand A (2006) Responses of Picea mariana to elevated CO_2 concentration during growth, cold hardening and dehardening: Phenology, cold tolerance, photosynthesis and growth. Tree Physiol 26:875–888.

Birami B, Nägele T, Gattmann M, Preisler Y, Gast A, Arneth A, Ruehr NK (2020) Hot drought reduces the effects of elevated CO_2 on tree water-use efficiency and carbon metabolism. New Phytol:1607–1621.

Blackman CJ, Brodribb TJ, Jordan GJ (2010) Leaf hydraulic vulnerability is related to conduit dimensions and drought resistance across a diverse range of woody angiosperms. New Phytol 188:1113–1123.

Blackman CJ, Creek D, Maier C, Aspinwall MJ, Drake JE, Pfautsch S, O'Grady A, Delzon S, Medlyn BE, Tissue DT, Choat B, Meinzer F (2019) Drought response strategies and hydraulic traits contribute to mechanistic understanding of plant dry-down to hydraulic failure. Tree Physiol 39:910–924.

Block RMA, Van Rees KCJ, Knight JD (2006) A review of fine root dynamics in Populus plantations. Agrofor Syst 67:73–84.

Bobich EG, Barron-Gafford GA, Rascher KG, Murthy R (2010) Effects of drought and changes in vapour pressure deficit on water relations of Populus deltoides growing in ambient and elevated CO_2. Tree Physiol 30:866–875.

Bogeat-Triboulot MB, Brosché M, Renaut J, Jouve L, Le Thiec D, Fayyaz P, Vinocur B, Witters E, Laukens K, Teichmann T, Altman A, Hausman JF, Polle A, Kangasjärvi J, Dreyer E (2007) Gradual soil water depletion results in reversible changes of gene expression, protein profiles, ecophysiology, and growth performance in Populus euphratica, a poplar growing in arid regions. Plant Physiol 143:876–892.

Bonan GB (2008) Forests and climate change: Forcings, feedbacks, and the climate benefits of forests. Science (80-) 320:1444–1449.

Brodribb TJ, McAdam SAM, Carins Murphy MR (2017) Xylem and stomata, coordinated through time and space. Plant Cell Environ 40:872–880.

Brodribb TJ, McAdam SAM, Jordan GJ, Martins SCV (2014) Conifer species adapt to low-rainfall climates by following one of two divergent pathways. Proc Natl Acad Sci U S A 111:14489–14493.

Brodribb TJ, Powers J, Cochard H, Choat B (2020) Hanging by a thread? Forests and drought. Science (80-) 368:261–266.

Broeckx LS, Verlinden MS, Berhongaray G, Zona D, Fichot R, Ceulemans R (2014) The effect of a dry spring on seasonal carbon allocation and vegetation dynamics in a poplar

bioenergy plantation. GCB Bioenergy 6:473–487.

Von Caemmerer S (2000) Biochemical models of leaf photosynthesis. CSIRO Publishing, Collingwood, Australia.

Cai J, Tyree MT (2010) The impact of vessel size on vulnerability curves : data and models for within-species variability in saplings of aspen, *Populus tremuloides* Michx. :1059–1069.

Calfapietra C, Gielen B, Galema ANJ, Lukac M, De Angelis P, Moscatelli MC, Ceulemans R, Scarascia-Mugnozza G (2003) Free-air CO_2 enrichment (FACE) enhances biomass production in a short-rotation poplar plantation. Tree Physiol 23:805–814.

Camarero JJ, Franquesa M, Sangüesa-Barreda G (2015) Timing of drought triggers distinct growth responses in holm oak: Implications to predict warming-induced forest defoliation and growth decline. Forests 6:1576–1597.

Van Camp J, Hubeau M, Van Den Bulcke J, Van Acker J, Steppe K (2018) Cambial pinning relates wood anatomy to ecophysiology in the African tropical tree *Maesopsis eminii*. Tree Physiol 38:232–242.

Campany CE, Medlyn BE, Duursma RA (2017) Reduced growth due to belowground sink limitation is not fully explained by reduced photosynthesis. Tree Physiol 37:1042–1054. http://academic.oup.com/treephys/article/37/8/1042/3100231/Reduced-growth-due-to-belowground-sink-limitation

Carey E V., DeLucia EH, Ball JT (1996) Stem maintenance and construction respiration in *Pinus ponderosa* grown in different concentrations of atmospheric CO_2. Tree Physiol 16:125–130.

Caudullo G, Commission E, Rigo D De (2016) Populus tremula in Europe: distribution, habitat, usage and threats San-Miguel-Ayanz J, Rigo D de, Caudullo G, Durrant TH, Mauri A (eds). Publication Office of the European Union, Luxembourg.

Cavender-Bares J, Potts M, Zacharias E, Bazzaz FA (2000) Consequences of CO_2 and light interactions for leaf phenology, growth, and senescence in *Quercus rubra*. Glob Chang Biol 6:877–887.

Cech PG, Pepin S, Körner C (2003) Elevated CO_2 reduces sap flux in mature deciduous forest trees. Oecologia 137:258–268.

Cernusak LA, Haverd V, Brendel O, Le Thiec D, Guehl JM, Cuntz M (2019) Robust response of terrestrial plants to rising CO_2. Trends Plant Sci 24:578–586.

Ceulemans R, Jach ME, Van De Velde R, Lin JX, Stevens M (2002) Elevated atmospheric CO_2 alters wood production, wood quality and wood strength of Scots pine (*Pinus sylvestris* L) after three years of enrichment. Glob Chang Biol 8:153–162.

Challis A, Blackman CJ, Ahrens CW, Medlyn BE, Rymer PD, Tissue DT (2020) Adaptive plasticity in plant traits increases time to hydraulic failure under drought in a foundation

tree.   bioRxiv:2020.08.19.258186.
http://biorxiv.org/content/early/2020/08/20/2020.08.19.258186.abstract

Chen SG, Impens I, Ceulemans R (1997) Modelling the effects of elevated atmospheric CO_2 on crown development, light interception and photosynthesis of poplar in open top chambers. Glob Chang Biol 3:97–106.

Choat B, Brodribb TJ, Brodersen CR, Duursma RA, López R, Medlyn BE (2018) Triggers of tree mortality under drought. Nature 558:531–539.

Choat B, Jansen S, Brodribb TJ, Cochard H, Delzon S, Bhaskar R, Bucci SJ, Feild TS, Gleason SM, Hacke UG, Jacobsen AL, Lens F, Maherali H, Martínez-Vilalta J, Mayr S, Mencuccini M, Mitchell PJ, Nardini A, Pittermann J, Pratt RB, Sperry JS, Westoby M, Wright IJ, Zanne AE (2012) Global convergence in the vulnerability of forests to drought. Nature 491:752–755.

Choat B, Lahr EC, Melcher PJ, Zwieniecki MA, Holbrook NM (2005) The spatial pattern of air seeding thresholds in mature sugar maple trees. Plant, Cell Environ 28:1082–1089.

Christman MA, Sperry JS, Smith DD (2012) Rare pits, large vessels and extreme vulnerability to cavitation in a ring-porous tree species. New Phytol 193:713–720.

Cleland EE, Chuine I, Menzel A, Mooney HA, Schwartz MD (2007) Shifting plant phenology in response to global change. Trends Ecol Evol 22:357–365.

Cochard H, Badel E, Herbette S, Delzon S, Choat B, Jansen S (2013) Methods for measuring plant vulnerability to cavitation: A critical review. J Exp Bot 64:4779–4791.

Cochard H, Cruiziat P, Tyree MT (1992) Use of positive pressures to establish vulnerability curves. Plant Physiol 100:205–209.

Collalti A, Prentice IC (2019) Is NPP proportional to GPP? Waring's hypothesis 20 years on. Tree Physiol 39:1473–1483.

Colli F (2020) The end of ' business as usual '? COVID -19 and the European Green Deal. Eur policy Br:1–5.

Crous KY, Campany C, López R, Cano FJ, Ellsworth DS (2021) Canopy position affects photosynthesis and anatomy in mature *Eucalyptus* trees in elevated CO_2 Whitehead D (ed). Tree Physiol 41:206–222. https://academic.oup.com/treephys/article/41/2/206/5904881

Cuny HE, Rathgeber CBK, Frank D, Fonti P, Makinen H, Prislan P, Rossi S, Del Castillo EM, Campelo F, Vavrčík H, Camarero JJ, Bryukhanova M V., Jyske T, Gricar J, Gryc V, De Luis M, Vieira J, Cufar K, Kirdyanov A V., Oberhuber W, Treml V, Huang JG, Li X, Swidrak I, Deslauriers A, Liang E, Nojd P, Gruber A, Nabais C, Morin H, Krause C, King G, Fournier M (2015) Woody biomass production lags stem-girth increase by over one month in coniferous forests. Nat Plants 1:1–6.

Curtis PS, Teeri JA (1992) Seasonal responses of leaf gas exchange to elevated carbon

dioxide in *Populus grandidentata*. Can J For Res 22:1320–1325.

Curtis PS, Vogel CS, Pregitzer KS, Zak DR, Teeri JA (1995) Interacting effects of soil fertility and atmospheric CO_2 on leaf area growth and carbon gain physiology in *Populus×euramericana* (Dode) Guinier. New Phytol 129:253–263.

D'Orangeville L, Maxwell J, Kneeshaw D, Pederson N, Duchesne L, Logan T, Houle D, Arseneault D, Beier CM, Bishop DA, Druckenbrod D, Fraver S, Girard F, Halman J, Hansen C, Hart JL, Hartmann H, Kaye M, Leblanc D, Manzoni S, Ouimet R, Rayback S, Rollinson CR, Phillips RP (2018) Drought timing and local climate determine the sensitivity of eastern temperate forests to drought. Glob Chang Biol 24:2339–2351.

Darbah JNT, Kubiske ME, Nelson N, Kets K, Riikonen J, Sober A, Rouse L, Karnosky DF (2010) Will photosynthetic capacity of aspen trees acclimate after long-term exposure to elevated CO_2 and O_3? Environ Pollut 158:983–991.

Dawes MA, Zweifel R, Dawes N, Rixen C, Hagedorn F (2014) CO_2 enrichment alters diurnal stem radius fluctuations of 36-yr-old *Larix decidua* growing at the alpine tree line. New Phytol 202:1237–1248.

Delzon S, Cochard H (2014) Recent advances in tree hydraulics highlight the ecological significance of the hydraulic safety margin. New Phytol 203:355–358.

Deng Q, Zhou G, Liu J, Liu S, Duan H, Zhang D (2010) Responses of soil respiration to elevated carbon dioxide and nitrogen addition in young subtropical forest ecosystems in China. Biogeosciences 7:315–328.

Deslauriers A, Fonti P, Rossi S, Rathgeber CBK, Gričar J (2017) Ecophysiology and Plasticity of Wood and Phloem Formation. In: Amoroso MM, Daniels LD, Baker PJ, Camarero JJ (eds) Dendroecology: Tree-ring analyses applied to ecological studies. Springer International Publishing, Cham, pp 13–33. https://doi.org/10.1007/978-3-319-61669-8_2

Diaconu D, Stangler DF, Kahle HP, Spiecker H (2016) Vessel plasticity of European beech in response to thinning and aspect. Tree Physiol 36:1260–1271.

Dietrich L, Zweifel R, Kahmen A (2018) Daily stem diameter variations can predict the canopy water status of mature temperate trees. Tree Physiol 38:941–952.

Dijkstra P, Hymus GJ, Colavito D, Vieglais DA, Cundari CM, Johnson DP (2002) Elevated atmospheric CO_2 stimulates aboveground biomass in a fire regenerated scrub-oak ecosystem. :90–103.

Dixon HH, Joly J (1895) On the ascent of sap. Philos Trans R Soc London 186:563–576.

Doelman JC, Stehfest E, van Vuuren DP, Tabeau A, Hof AF, Braakhekke MC, Gernaat DEHJ, van den Berg M, van Zeist WJ, Daioglou V, van Meijl H, Lucas PL (2020) Afforestation for climate change mitigation: Potentials, risks and trade-offs. Glob Chang Biol 26:1576–1591.

Domec JC, Palmroth S, Oren R (2016) Effects of *Pinus taeda* leaf anatomy on vascular and

extravascular leaf hydraulic conductance as influenced by N-fertilization and elevated CO_2. J Plant Hydraul 3:e007.

Domec JC, Schäfer K, Oren R, Kim HS, McCarthy HR (2010) Variable conductivity and embolism in roots and branches of four contrasting tree species and their impacts on whole-plant hydraulic performance under future atmospheric CO_2 concentration. Tree Physiol 30:1001–1015.

Domec JC, Smith DD, McCulloh KA (2017) A synthesis of the effects of atmospheric carbon dioxide enrichment on plant hydraulics: implications for whole-plant water use efficiency and resistance to drought. Plant Cell Environ 40:921–937.

Drake BG, Azcon-Bieto J, Berry J, Bunce J, Dijkstra P, Farrar J, Gifford RM, Gonzalez-Meler MA, Koch G, Lambers H, Siedow J, Wullschleger SD (1999) Does elevated atmospheric CO_2 concentration inhibit mitochondrial respiration in green plants? Plant, Cell Environ 22:649–657.

Drake JE, Furze ME, Tjoelker MG, Carrillo Y, Barton CVM, Pendall E (2019) Climate warming and tree carbon use efficiency in a whole-tree 13 CO_2 tracer study. New Phytol 222:1313–1324.

Drake JE, Gallet-Budynek A, Hofmockel KS, Bernhardt ES, Billings SA, Jackson RB, Johnsen KS, Lichter J, Mccarthy HR, Mccormack ML, Moore DJP, Oren R, Palmroth S, Phillips RP, Pippen JS, Pritchard SG, Treseder KK, Schlesinger WH, Delucia EH, Finzi AC (2011) Increases in the flux of carbon belowground stimulate nitrogen uptake and sustain the long-term enhancement of forest productivity under elevated CO_2. Ecol Lett 14:349–357.

Drake BL, Hanson DT, Lowrey TK, Sharp ZD (2017) The carbon fertilization effect over a century of anthropogenic CO_2 emissions: higher intracellular CO_2 and more drought resistance among invasive and native grass species contrasts with increased water use efficiency for woody plants in the US Southwest. Glob Chang Biol 23:782–792.

Drake JE, Power SA, Duursma RA, Medlyn BE, Aspinwall MJ, Choat B, Creek D, Eamus D, Maier C, Pfautsch S, Smith RA, Tjoelker MG, Tissue DT (2017) Stomatal and non-stomatal limitations of photosynthesis for four tree species under drought: A comparison of model formulations. Agric For Meteorol 247:454–466.

Drake JE, Tjoelker MG, Aspinwall MJ, Reich PB, Barton CVM, Medlyn BE, Duursma RA (2016) Does physiological acclimation to climate warming stabilize the ratio of canopy respiration to photosynthesis? New Phytol 211:850–863.

Duan H, O'Grady AP, Duursma RA, Choat B, Huang G, Smith RA, Jiang Y, Tissue DT (2015) Drought responses of two gymnosperm species with contrasting stomatal regulation strategies under elevated [CO_2] and temperature. Tree Physiol 35:756–770.

Duan H, Ontedhu J, Milham P, Lewis JD, Tissue DT (2019) Effects of elevated carbon dioxide

and elevated temperature on morphological, physiological and anatomical responses of *Eucalyptus tereticornis* along a soil phosphorus gradient. Tree Physiol 39:1821–1837.

Dusenge ME, Duarte AG, Way DA (2019) Plant carbon metabolism and climate change: elevated CO_2 and temperature impacts on photosynthesis, photorespiration and respiration. New Phytol 221:32–49.

Duursma RA, Gimeno TE, Boer MM, Crous KY, Tjoelker MG, Ellsworth DS (2016) Canopy leaf area of a mature evergreen *Eucalyptus* woodland does not respond to elevated atmospheric [CO_2] but tracks water availability. Glob Chang Biol 22:1666–1676.

Duursma RA, Mäkelä A (2007) Summary models for light interception and light-use efficiency of non-homogeneous canopies. Tree Physiol 27:859–870.

Edwards NT, Tschaplinski TJ, Norby RJ (2002) Stem respiration increases in CO_2 -enriched sweetgum trees. New Phytol 155:239–248.

Egli P, Maurer S, Günthardt-Goerg MS, Körner C (1998) Effects of elevated CO_2 and soil quality on leaf gas exchange and above-ground growth in beech-spruce model ecosystems. New Phytol 140:185–196.

Ellison D, Morris CE, Locatelli B, Sheil D, Cohen J, Murdiyarso D, Gutierrez V, Noordwijk M van, Creed IF, Pokorny J, Gaveau D, Spracklen D V., Tobella AB, Ilstedt U, Teuling AJ, Gebrehiwot SG, Sands DC, Muys B, Verbist B, Springgay E, Sugandi Y, Sullivan CA (2017) Trees, forests and water: Cool insights for a hot world. Glob Environ Chang 43:51–61.

Ellsworth DS, Anderson IC, Crous KY, Cooke J, Drake JE, Gherlenda AN, Gimeno TE, Macdonald CA, Medlyn BE, Powell JR, Tjoelker MG, Reich PB (2017) Elevated CO_2 does not increase eucalypt forest productivity on a low-phosphorus soil. Nat Clim Chang 7:279–282.

Ellsworth DS, Thomas R, Crous KY, Palmroth S, Ward EJ, Maier C, Delucia E, Oren R (2012) Elevated CO_2 affects photosynthetic responses in canopy pine and subcanopy deciduous trees over 10 years: A synthesis from Duke FACE. Glob Chang Biol 18:223–242.

Engineer CB, Hashimoto-Sugimoto M, Negi J, Israelsson-Nordström M, Azoulay-Shemer T, Rappel W-J, Iba K, Schroeder JI (2016) CO_2 sensing and CO_2 regulation of stomatal conductance: Advances and open questions. Trends Plant Sci 21:16–30. https://linkinghub.elsevier.com/retrieve/pii/S1360138515002290

Van Der Ent RJ, Savenije HHG, Schaefli B, Steele-Dunne SC (2010) Origin and fate of atmospheric moisture over continents. Water Resour Res 46:1–12.

Epila J, De Baerdemaeker NJF, Vergeynst LL, Maes WH, Beeckman H, Steppe K (2017) Capacitive water release and internal leaf water relocation delay drought-induced cavitation in African *Maesopsis eminii*. Tree Physiol 37:481–490.

Epron D, Liozon R, Mousseau M (1996) Effects of elevated CO_2 concentration on leaf

characteristics and photosynthetic capacity of beech (*Fagus sylvatica*) during the growing season. Tree Physiol 16:425–432.

Esperon-Rodriguez M, Rymer PD, Power SA, Challis A, Marchin RM, Tjoelker MG (2020) Functional adaptations and trait plasticity of urban trees along a climatic gradient. Urban For Urban Green 54

European Commission (2019) The European Green Deal. Brussel.

Evans JR, Clarke VC (2019) The nitrogen cost of photosynthesis. J Exp Bot 70:7–15.

Evert RF, Eichhorn SE (2013) Biology of plants Anderson S, Rolfes M, Weiss V (eds), Eighth. W.H. Freeman and Company Publishers, New York.

Ewert F (2004) Modelling plant responses to elevated CO_2: How important is leaf area index? Ann Bot 93:619–627.

Fan H, McGuire MA, Teskey RO (2017) Effects of stem size on stem respiration and its flux components in yellow-poplar (*Liriodendron tulipifera* L.) trees. Tree Physiol 37:1536–1545.

Fatichi S, Leuzinger S, Körner C (2014) Moving beyond photosynthesis: From carbon source to sink-driven vegetation modeling. New Phytol 201:1086–1095.

Fatichi S, Leuzinger S, Paschalis A, Adam Langley J, Barraclough AD, Hovenden MJ (2016) Partitioning direct and indirect effects reveals the response of water-limited ecosystems to elevated CO_2. Proc Natl Acad Sci U S A 113:12757–12762.

Fatichi S, Pappas C, Zscheischler J, Leuzinger S (2019) Modelling carbon sources and sinks in terrestrial vegetation. New Phytol 221:652–668.

Ferris R, Sabatti M, Miglietta F, Mills RF, Taylor G (2001) Leaf area is stimulated in *Populus* by free air CO_2 enrichment (POPFACE), through increased cell expansion and production. Plant, Cell Environ 24:305–315.

Fichot R, Brignolas F, Cochard H, Ceulemans R (2015) Vulnerability to drought-induced cavitation in poplars: Synthesis and future opportunities. Plant, Cell Environ 38:1233–1251.

Flexas J, Medrano H (2002) Drought-inhibition of photosynthesis in C3 plants: Stomatal and non-stomatal limitations revisited. Ann Bot 89:183–189.

Forner A, Valladares F, Bonal D, Granier A, Grossiord C, Aranda I (2018) Extreme droughts affecting Mediterranean tree species' growth and water-use efficiency: The importance of timing. Tree Physiol 38:1127–1137.

Franks SJ, Weber JJ, Aitken SN (2014) Evolutionary and plastic responses to climate change in terrestrial plant populations. Evol Appl 7:123–139.

Frédéric S (2020a) Green Deal facing delays due to coronavirus, EU admits. Euractive

Frédéric S (2020b) LEAKED: Full list of delayed European Green Deal initiatives. Euractive. https://www.euractiv.com/section/energy-environment/news/leaked-full-list-of-delayed-

european-green-deal-initiatives/

Friedlingstein P, Jones MW, Sullivan MO, Andrew RM, Hauck J, Peters GP, Peters W, Pongratz J, Sitch S, Quéré C Le (2019) Global Carbon Budget 2019. :1783–1838.

Fu X, Meinzer FC, Woodruff DR, Liu YY, Smith DD, McCulloh KA, Howard AR (2019) Coordination and trade-offs between leaf and stem hydraulic traits and stomatal regulation along a spectrum of isohydry to anisohydry. Plant Cell Environ 42:2245–2258.

Fujii JA, Kennedy RA (1985) Seasonal changes in the photosynthetic rate in apple trees: A comparison between fruiting and nonfruiting trees. Plant Physiol 78:519–524.

Le Gall H, Philippe F, Domon JM, Gillet F, Pelloux J, Rayon C (2015) Cell wall metabolism in response to abiotic stress. Plants 4:112–166.

Galmés J, Aranjuelo I, Medrano H, Flexas J (2013) Variation in Rubisco content and activity under variable climatic factors. Photosynth Res 117:73–90.

Gamage D, Thompson M, Sutherland M, Hirotsu N, Makino A, Seneweera S (2018) New insights into the cellular mechanisms of plant growth at elevated atmospheric carbon dioxide concentrations. Plant Cell Environ 41:1233–1246.

Gartner BL, Roy J, Huc R (2003) Effects of tension wood on specific conductivity and vulnerability to embolism of *Quercus ilex* seedlings grown at two atmospheric CO_2 concentrations. Tree Physiol 23:387–395.

Gattmann M, Birami B, Sala DN, Ruehr N (2020) Dying by drying: timing of physiological stress thresholds related to tree death is not significantly altered by highly elevated CO_2. Plant Cell Environ:pce.13937. https://onlinelibrary.wiley.com/doi/10.1111/pce.13937

Ge Q, Wang H, Rutishauser T, Dai J (2015) Phenological response to climate change in China: A meta-analysis. Glob Chang Biol 21:265–274.

Gielen B, Scarascia-Mugnozza G, Ceulemans R (2003) Stem respiration of *Populus* species in the third year of free-air CO_2 enrichment. Physiol Plant 117:500–507.

Gifford RM (2003) Plant respiration in productivity models: Conceptualisation, representation and issues for global terrestrial carbon-cycle research. Funct Plant Biol 30:171–186.

Gill AL, Gallinat AS, Sanders-DeMott R, Rigden AJ, Short Gianotti DJ, Mantooth JA, Templer PH (2015) Changes in autumn senescence in northern hemisphere deciduous trees: A meta-analysis of autumn phenology studies. Ann Bot 116:875–888.

Gimeno TE, Crous KY, Cooke J, O'Grady AP, Ósvaldsson A, Medlyn BE, Ellsworth DS (2016) Conserved stomatal behaviour under elevated CO_2 and varying water availability in a mature woodland. Funct Ecol 30:700–709.

Gimeno TE, McVicar TR, O'Grady AP, Tissue DT, Ellsworth DS (2018) Elevated CO_2 did not affect the hydrological balance of a mature native *Eucalyptus* woodland. Glob Chang Biol 24:3010–3024.

Gleason SM, Westoby M, Jansen S, Choat B, Hacke UG, Pratt RB, Bhaskar R, Brodribb TJ,

Bucci SJ, Cao KF, Cochard H, Delzon S, Domec JC, Fan ZX, Feild TS, Jacobsen AL, Johnson DM, Lens F, Maherali H, Martínez-Vilalta J, Mayr S, Mcculloh KA, Mencuccini M, Mitchell PJ, Morris H, Nardini A, Pittermann J, Plavcová L, Schreiber SG, Sperry JS, Wright IJ, Zanne AE (2016) Weak tradeoff between xylem safety and xylem-specific hydraulic efficiency across the world's woody plant species. New Phytol 209:123–136.

Goodfellow J, Eamus D, Duff G (1997) Diurnal and seasonal changes in the impact of CO_2 enrichment on assimilation, stomatal conductance and growth in a long-term study of Mangifera indica in the wet-dry tropics of Australia. Tree Physiol 17:291–299.

Gornall J (2020) Climate change will still be a threat after COVID-19 is gone. March. https://www.euractiv.com/section/climate-environment/opinion/climate-change-will-still-be-a-threat-after-covid-19-is-gone/

Granda E, Camarero JJ, Gimeno TE, Martínez-Fernández J, Valladares F (2013) Intensity and timing of warming and drought differentially affect growth patterns of co-occurring Mediterranean tree species. Eur J For Res 132:469–480.

Greer DH (2015) Seasonal changes in the photosynthetic response to CO_2 and temperature in apple (*Malus domestica* cv. 'Red Gala') leaves during a growing season with a high temperature event. Funct Plant Biol 42:309–324.

Grossiord C, Buckley TN, Cernusak LA, Novick KA, Poulter B, Siegwolf RTW, Sperry JS, McDowell NG (2020) Plant responses to rising vapor pressure deficit. New Phytol

Guet J, Fichot R, Lédée C, Laurans F, Cochard H, Delzon S, Bastien C, Brignolas F (2015) Stem xylem resistance to cavitation is related to xylem structure but not to growth and water-use efficiency at the within-population level in *Populus nigra* L. J Exp Bot 66:4643–4652.

Gunderson CA, Norby RJ, Wullschleger SD (1993) Foliar gas exchange responses of two deciduous hardwoods during 3 years of growth in elevated CO_2: no loss of photosynthetic enhancement. Plant Cell Environ 16:797–807.

Hacke UG, Sperry JS, Wheeler JK, Castro L (2006) Scaling of angiosperm xylem structure with safety and efficiency. Tree Physiol 26:689–701.

Hamilton JG, Thomas RB, Delucia EH (2001) Direct and indirect effects of elevated CO_2 on leaf respiration in a forest ecosystem. Plant, Cell Environ 24:975–982.

Hammond WM, Johnson DM, Meinzer FC (2021) A thin line between life and death: Radial sap flux failure signals trajectory to tree mortality. Plant Cell Environ:pce.14033. https://onlinelibrary.wiley.com/doi/10.1111/pce.14033

Hammond WM, Yu K, Wilson LA, Will RE, Anderegg WRL, Adams HD (2019) Dead or dying? Quantifying the point of no return from hydraulic failure in drought-induced tree mortality. New Phytol 223:1834–1843.

Hao Z, Hao F, Singh VP, Zhang X (2018a) Changes in the severity of compound drought and

hot extremes over global land areas. Environ Res Lett 13:124022. http://dx.doi.org/10.1088/1748-9326/aaee96

Hao GY, Holbrook NM, Zwieniecki MA, Gutschick VP, BassiriRad H (2018b) Coordinated responses of plant hydraulic architecture with the reduction of stomatal conductance under elevated CO_2 concentration. Tree Physiol 38:1041–1052.

Harrison EL, Arce Cubas L, Gray JE, Hepworth C (2020) The influence of stomatal morphology and distribution on photosynthetic gas exchange. Plant J 101:768–779.

Hartmann H, Moura CF, Anderegg WRL, Ruehr NK, Salmon Y, Allen CD, Arndt SK, Breshears DD, Davi H, Galbraith D, Ruthrof KX, Wunder J, Adams HD, Bloemen J, Cailleret M, Cobb R, Gessler A, Grams TEE, Jansen S, Kautz M, Lloret F, O'Brien M (2018) Research frontiers for improving our understanding of drought-induced tree and forest mortality. New Phytol 218:15–28. http://doi.wiley.com/10.1111/nph.15048

Hartmann H, Trumbore S (2016) Understanding the roles of nonstructural carbohydrates in forest trees - from what we can measure to what we want to know. New Phytol 211:386–403.

Hasper TB, Wallin G, Lamba S, Hall M, Jaramillo F, Laudon H, Linder S, Medhurst JL, Räntfors M, Sigurdsson BD, Uddling J (2016) Water use by Swedish boreal forests in a changing climate. Funct Ecol 30:690–699.

Hatch MD, Slack CR (1966) Photosynthesis by sugar-cane leaves. A new carboxylation reaction and the pathway of sugar formation. Biochem J 101:103–111. https://doi.org/10.1042/bj1010103

Hausfather Z, Peters GP (2020) Emissions - the 'business as usual' story is misleading. Nature 577:618–620.

Haworth M, Killi D, Materassi A, Raschi A, Centritto M (2016) Impaired stomatal control is associated with reduced photosynthetic physiology in crop species grown at elevated [CO_2]. Front Plant Sci 7:1–13.

Heath J (1998) Stomata of trees growing in CO_2-enriched air show reduced sensitivity to vapour pressure deficit and drought. Plant, Cell Environ 21:1077–1088.

Herrick JD, Maherali H, Thomas RB (2004) Reduced stomatal conductance in sweetgum (*Liquidambar styraciflua*) sustained over long-term CO_2 enrichment. New Phytol 162:387–396.

Herrick JD, Thomas RB (1999) Effects of CO_2 enrichment on the photosynthetic light response of sun and shade leaves of canopy sweetgum trees (*Liquidambar styraciflua*) in a forest ecosystem. Tree Physiol 19:779–786.

Herrick JD, Thomas RB (2003) Leaf senescence and late-season net photosynthesis of sun and shade leaves of overstory sweetgum (*Liquidambar styraciflua*) grown in elevated and ambient carbon dioxide concentrations. Tree Physiol 23:109–118.

Hochberg U, Windt CW, Ponomarenko A, Zhang YJ, Gersony J, Rockwell FE, Holbrook NM (2017) Stomatal closure, basal leaf embolism, and shedding protect the hydraulic integrity of grape stems. Plant Physiol 174:764–775.

Hogan KP, Whitehead D, Kallaracka J, Buwalda JG, Meekings J, Rogers GND (1996) Photosynthetic activity of leaves of *Pinus radiata* and *Nothofagus fusca* after 1 year of growth at elevated CO_2. Aust J Plant Physiol 23:623–630.

Hölttä T, Cochard H, Nikinmaa E, Mencuccini M (2009) Capacitive effect of cavitation in xylem conduits: Results from a dynamic model. Plant, Cell Environ 32:10–21.

Hovenden MJ (2003) Photosynthesis of coppicing poplar clones in a free-air CO_2 enrichment (FACE) experiment in a short-rotation forest. Funct Plant Biol 30:391–400.

Hymus GJ, Johnson DP, Dore S, Anderson HP, Hinkle CR, Drake BG (2003) Effects of elevated atmospheric CO_2 on net ecosystem CO_2 exchange of a scrub–oak ecosystem. Glob Chang Biol 9:1802–1812.

Hymus GJ, Pontailler JY, Li J, Stiling P, Hinkle CR, Drake BG (2002) Seasonal variability in the effect of elevated CO_2 on ecosystem leaf area index in a scrub-oak ecosystem. Glob Chang Biol 8:931–940.

IPCC, 2019: Summary for Policymakers. In: *Climate Change and Land: an IPCC special report on climate change, desertification, land degradation, sustainable land management, food security, and greenhouse gas fluxes in terrestrial ecosystems* [P.R. Shukla, J. Skea, E. Calvo Buendia, V. Masson-Delmotte, H.- O. Pörtner, D. C. Roberts, P. Zhai, R. Slade, S. Connors, R. van Diemen, M. Ferrat, E. Haughey, S. Luz, S. Neogi, M. Pathak, J. Petzold, J. Portugal Pereira, P. Vyas, E. Huntley, K. Kissick, M. Belkacemi, J. Malley, (eds.)]. In press*.

IRENA (2020) Renewable Energy statistics 2020.

Jach ME, Ceulemans R (1999) Effects of elevated atmospheric CO_2 on phenology, growth and crown structure of Scots pine (*Pinus sylvestris*) seedlings after two years of exposure in the field. Tree Physiol 19:289–300.

Jach ME, Ceulemans R (2000) Effects of season, needle age and elevated atmospheric CO_2 on photosynthesis in Scots pine (*Pinus sylvestris*). Tree Physiol 20:145–157.

Jahnke S (2001) Atmospheric CO_2 concentration does not directly affect leaf respiration in bean or poplar. Plant, Cell Environ 24:1139–1151.

Jansen S, Choat B, Pletsers A (2009) Morphological variation of intervessel pit membranes and implications to xylem function in angiosperms. Am J Bot 96:409–419. http://doi.wiley.com/10.3732/ajb.0800248

Janssen TAJ, Hölttä T, Fleischer K, Naudts K, Dolman H (2020) Wood allocation trade-offs between fiber wall, fiber lumen, and axial parenchyma drive drought resistance in neotropical trees. Plant Cell Environ 43:965–980.

Jiang M, Medlyn BE, Drake JE, Duursma RA, Anderson IC, Barton CVM, Boer MM, Carrillo Y, Castañeda-Gómez L, Collins L, Crous KY, De Kauwe MG, dos Santos BM, Emmerson KM, Facey SL, Gherlenda AN, Gimeno TE, Hasegawa S, Johnson SN, Kännaste A, Macdonald CA, Mahmud K, Moore BD, Nazaries L, Neilson EHJ, Nielsen UN, Niinemets Ü, Noh NJ, Ochoa-Hueso R, Pathare VS, Pendall E, Pihlblad J, Piñeiro J, Powell JR, Power SA, Reich PB, Renchon AA, Riegler M, Rinnan R, Rymer PD, Salomón RL, Singh BK, Smith B, Tjoelker MG, Walker JKM, Wujeska-Klause A, Yang J, Zaehle S, Ellsworth DS (2020) The fate of carbon in a mature forest under carbon dioxide enrichment. Nature 580:227–231.

Johnson DM, Berry ZC, Baker K V., Smith DD, McCulloh KA, Domec JC (2018) Leaf hydraulic parameters are more plastic in species that experience a wider range of leaf water potentials. Funct Ecol 32:894–903.

Johnson D, Eckart P, Alsamadisi N, Noble H, Martin C, Spicer R (2018) Polar auxin transport is implicated in vessel differentiation and spatial patterning during secondary growth in Populus. 105:186–196.

Johnson DW, Thomas RB, Griffin KL, Tissue DT, Ball JT, Strain BR, Walker RF (1998) Effects of carbon dioxide and nitrogen on growth and nitrogen uptake in ponderosa and loblolly pine. J Environ Qual 27:414–425.

Jolliffe PA, Ehret DL (1985) Growth of bean plants at elevated carbon dioxide concentrations. Can J Bot 63:2021–2025.

Jones HG (2004) Irrigation scheduling: Advantages and pitfalls of plant-based methods. J Exp Bot 55:2427–2436.

Jump AS, Ruiz-Benito P, Greenwood S, Allen CD, Kitzberger T, Fensham R, Martínez-Vilalta J, Lloret F (2017) Structural overshoot of tree growth with climate variability and the global spectrum of drought-induced forest dieback. Glob Chang Biol 23:3742–3757.

Kaack L, Weber M, Isasa E, Karimi Z, Li S, Pereira L, Trabi CL, Zhang Y, Schenk HJ, Schuldt B, Schmidt V, Jansen S (2021) Pore constrictions in intervessel pit membranes provide a mechanistic explanation for xylem embolism resistance in angiosperms. New Phytol:nph.17282. https://onlinelibrary.wiley.com/doi/10.1111/nph.17282

Kangur O, Steppe K, Schreel JDM, Von Der Crone JS, Sellin A (2021) Variation in nocturnal stomatal conductance and development of predawn disequilibrium between soil and leaf water potentials in nine temperate deciduous tree species. Funct Plant Biol

De Kauwe MG, Medlyn BE, Zaehle S, Walker AP, Dietze MC, Hickler T, Jain AK, Luo Y, Parton WJ, Prentice IC, Smith B, Thornton PE, Wang S, Wang YP, Wårlind D, Weng E, Crous KY, Ellsworth DS, Hanson PJ, Seok Kim H, Warren JM, Oren R, Norby RJ (2013) Forest water use and water use efficiency at elevated CO_2: A model-data intercomparison at two contrasting temperate forest FACE sites. Glob Chang Biol 19:1759–1779.

De Kauwe MG, Medlyn BE, Zaehle S, Walker AP, Dietze MC, Wang YP, Luo Y, Jain AK, El-Masri B, Hickler T, Wårlind D, Weng E, Parton WJ, Thornton PE, Wang S, Prentice IC, Asao S, Smith B, Mccarthy HR, Iversen CM, Hanson PJ, Warren JM, Oren R, Norby RJ (2014) Where does the carbon go? A model-data intercomparison of vegetation carbon allocation and turnover processes at two temperate forest free-air CO_2 enrichment sites. New Phytol 203:883–899.

Keel SG, Pepin S, Leuzinger S, Körner C (2007) Stomatal conductance in mature deciduous forest trees exposed to elevated CO_2. Trees - Struct Funct 21:151–159.

Kerstiens G (1996) Cuticular water permeability and its physiological significance. J Exp Bot 47:1813–1832.

Kim K, Labbé N, Warren JM, Elder T, Rials TG (2015) Chemical and anatomical changes in *Liquidambar styraciflua* L. xylem after long term exposure to elevated CO_2. Environ Pollut 198:179–185.

Kimball BA, Idso SB, Johnson S, Rillig MC (2007) Seventeen years of carbon dioxide enrichment of sour orange trees: Final results. Glob Chang Biol 13:2171–2183.

Klein T, Bader MKF, Leuzinger S, Mildner M, Schleppi P, Siegwolf RTW, Körner C (2016) Growth and carbon relations of mature *Picea abies* trees under 5 years of free-air CO_2 enrichment. J Ecol 104:1720–1733.

Knipfer T, Reyes C, Earles JM, Berry ZC, Johnson DM, Brodersen CR, McElrone AJ (2019) Spatiotemporal coupling of vessel cavitation and discharge of stored xylem water in a tree sapling. Plant Physiol 179:1658–1668.

El Kohen A, Mousseau M (1994) Interactive effects of elevated CO_2 and mineral nutrition on growth and CO_2 exchange of sweet chestnut seedlings (*Castanea sativa*). Tree Physiol 14:679–690.

Körner C (2003) Carbon limitation in trees. J Ecol 91:4–17.

Körner C (2006) Plant CO_2 responses: An issue of definition, time and resource supply. New Phytol 172:393–411.

Körner C (2015) Paradigm shift in plant growth control. Curr Opin Plant Biol 25:107–114.

Körner C (2019) No need for pipes when the well is dry—a comment on hydraulic failure in trees. Tree Physiol 39:695–700.

Kostiainen K, Saranpää P, Lundqvist SO, Kubiske ME, Vapaavuori E (2014) Wood properties of *Populus* and *Betula* in long-term exposure to elevated CO_2 and O_3. Plant, Cell Environ 37:1452–1463.

Krause A, Haverd V, Poulter B, Anthoni P, Quesada B, Rammig A, Arneth A (2019) Multimodel analysis of future land use and climate change impacts on ecosystem functioning. Earth's Futur 7:833–851. https://doi.org/10.1029/2018EF001123

Krejza J, Cienciala E, Světlík J, Bellan M, Noyer E, Horáček P, Štěpánek P, Marek M V. (2020)

Evidence of climate-induced stress of Norway spruce along elevation gradient preceding the current dieback in Central Europe. Trees - Struct Funct. https://doi.org/10.1007/s00468-020-02022-6

Kubiske ME, Pregitzer KS, Zak DR, Mikan CJ (1998) Growth and C allocation of *Populus tremuloides* genotypes in response to atmospheric CO_2 and soil N availability. New Phytol 140:251–260.

Kumar S, Chaitanya BSK, Ghatty S, Reddy AR (2014) Growth, reproductive phenology and yield responses of a potential biofuel plant, *Jatropha curcas* grown under projected 2050 levels of elevated CO_2. Physiol Plant 152:501–519.

Laurentin A, Edwards CA (2003) A microtiter modification of the anthrone-sulfuric acid colorimetric assay for glucose-based carbohydrates. Anal Biochem 315:143–145.

Leuzinger S, Körner C (2007) Water savings in mature deciduous forest trees under elevated CO_2. Glob Chang Biol 13:2498–2508.

Lévesque M, Saurer M, Siegwolf R, Eilmann B, Brang P, Bugmann H, Rigling A (2013) Drought response of five conifer species under contrasting water availability suggests high vulnerability of Norway spruce and European larch. Glob Chang Biol 19:3184–3199.

Lewis JD, Tissue DT, Strain BR (1996) Seasonal response of photosynthesis to elevated CO_2 in loblolly pine (*Pinus taeda* L.) over two growing seasons. Glob Chang Biol 2:103–114.

Li X, Blackman CJ, Choat B, Duursma RA, Rymer PD, Medlyn BE, Tissue DT (2018) Tree hydraulic traits are coordinated and strongly linked to climate-of-origin across a rainfall gradient. Plant Cell Environ 41:646–660.

Li X, Blackman CJ, Peters JMR, Choat B, Rymer PD, Medlyn BE, Tissue DT (2019a) More than iso/anisohydry: Hydroscapes integrate plant water use and drought tolerance traits in 10 eucalypt species from contrasting climates. Funct Ecol 33:1035–1049.

Li JH, Dijkstra P, Hinkle CR, Wheeler RM, Drake BG (1999) Photosynthetic acclimation to elevated atmospheric CO_2 concentration in the Florida scrub-oak species *Quercus geminata* and *Quercus myrtifolia* growing in their native environment. Tree Physiol 19:229–234.

Li JH, Dugas WA, Hymus GJ, Johnson DP, Hinkle CR, Drake BG, Hungate BA (2003) Direct and indirect effects of elevated CO_2 on transpiration from *Quercus myrtifolia* in a scrub-oak ecosystem. Glob Chang Biol 9:96–105.

Li W, Hartmann H, Adams HD, Zhang H, Jin C, Zhao C, Guan D, Wang A, Yuan F, Wu J (2018) The sweet side of global change-dynamic responses of non-structural carbohydrates to drought, elevated CO_2 and nitrogen fertilization in tree species. Tree Physiol 38:1706–1723.

Li S, Lens F, Espino S, Karimi Z, Klepsch M, Schenk HJ, Schmitt M, Schuldt B, Jansen S (2016) Intervessel pit membrane thickness as a key determinant of embolism resistance

in angiosperm xylem. IAWA J 37:152–171.

Li S, Li X, Wei Z, Liu F (2020) ABA-mediated modulation of elevated CO_2 on stomatal response to drought. Curr Opin Plant Biol 56:174–180. https://doi.org/10.1016/j.pbi.2019.12.002

Li Y, Liu J, Chen G, Zhou G, Huang W, Yin G, Zhang D, Li Y (2013) Water-use efficiency of four native trees under CO_2 enrichment and N addition in subtropical model forest ecosystems. J Plant Ecol 8:411–419.

Li Q, Lu X, Wang Y, Huang X, Cox PM, Luo Y (2018) Leaf area index identified as a major source of variability in modeled CO_2 fertilization. Biogeosciences 15:6909–6925.

Li L, Wang X, Manning WJ (2019b) Effects of elevated CO_2 on leaf senescence, leaf nitrogen resorption, and late-season photosynthesis in *Tilia americana* L. Front Plant Sci 10:1–9.

Liberloo M, De Angelis P, Ceulemans R (2008) Stem CO_2 efflux of a *Populus nigra* stand: Effects of elevated CO_2, fertilization, and shoot size. Biol Plant 52:299–306.

Liberloo M, Calfapietra C, Lukac M, Godbold D, Luo Z Bin, Polle A, Hoosbeck MR, Kull O, Marek M, Raines C, Rubino M, Taylor G, Scarascia-Mugnozza G, Ceulemans R (2006) Woody biomass production during the second rotation of a bio-energy *Populus* plantation increases in a future high CO_2 world. Glob Chang Biol 12:1094–1106.

Liberloo M, Dillen SY, Calfapietra C, Marinari S, Zhi BL, De Angelis P, Ceulemans R (2005) Elevated CO_2 concentration, fertilization and their interaction: Growth stimulation in a short-rotation poplar coppice (EUROFACE). Tree Physiol 25:179–189.

Liberloo M, Lukac M, Calfapietra C, Hoosbeek MR, Gielen B, Miglietta F, Scarascia-Mugnozza GE, Ceulemans R (2009) Coppicing shifts CO_2 stimulation of poplar productivity to above-ground pools: A synthesis of leaf to stand level results from the POP/EUROFACE experiment. New Phytol 182:331–346.

Liberloo M, Tulva I, Raïm O, Kull O, Ceulemans R (2007) Photosynthetic stimulation under long-term CO_2 enrichment and fertilization is sustained across a closed *Populus* canopy profile (EUROFACE). New Phytol 173:537–549.

Lin YS, Medlyn BE, Duursma RA, Prentice IC, Wang H, Baig S, Eamus D, De Dios VR, Mitchell P, Ellsworth DS, De Beeck MO, Wallin G, Uddling J, Tarvainen L, Linderson ML, Cernusak LA, Nippert JB, Ocheltree TW, Tissue DT, Martin-StPaul NK, Rogers A, Warren JM, De Angelis P, Hikosaka K, Han Q, Onoda Y, Gimeno TE, Barton CVM, Bennie J, Bonal D, Bosc A, Löw M, Macinins-Ng C, Rey A, Rowland L, Setterfield SA, Tausz-Posch S, Zaragoza-Castells J, Broadmeadow MSJ, Drake JE, Freeman M, Ghannoum O, Hutley LB, Kelly JW, Kikuzawa K, Kolari P, Koyama K, Limousin JM, Meir P, Da Costa ACL, Mikkelsen TN, Salinas N, Sun W, Wingate L (2015) Optimal stomatal behaviour around the world. Nat Clim Chang 5:459–464.

Lin T, Zheng H, Huang Z, Wang J, Zhu J (2018) Non-structural carbohydrate dynamics in leaves and branches of *Pinus massoniana* (Lamb.) following 3-year rainfall exclusion.

Forests 9:1–15.

Liu J, Hu T, Fang L, Peng X, Liu F (2019) CO_2 elevation modulates the response of leaf gas exchange to progressive soil drying in tomato plants. Agric For Meteorol 268:181–188.

Liu J, Kang S, Davies WJ, Ding R (2020) Elevated [CO_2] alleviates the impacts of water deficit on xylem anatomy and hydraulic properties of maize stems. Plant Cell Environ 43:563–578.

Liu J, Zhou G, Xu Z, Duan H, Li Y, Zhang D (2011) Photosynthesis acclimation, leaf nitrogen concentration, and growth of four tree species over 3 years in response to elevated carbon dioxide and nitrogen treatment in subtropical China. J Soils Sediments 11:1155–1164.

Lockhart JA (1965) An analysis of irreversible plant cell elongation. J Theor Biol 8:264–275.

Long SP (1991) Modification of the response of photosynthetic productivity to rising temperature by atmospheric CO_2 concentrations: Has its importance been underestimated? Plant Cell Environ 14:729–739.

Long SP, Ainsworth EA, Rogers A, Ort DR (2004) Rising atmospheric carbon dioxide: Plants FACE the future. Annu Rev Plant Biol 55:591–628.

Long SP, Hällgren J-E (1993) Measurement of CO_2 assimilation by plants in the field and the laboratory. In: Hall DO, Scurlock JMO, Bolhàr-Nordenkampf HR, Leegood RC, Long SP (eds) Photosynthesis and Production in a Changing Environment: A field and laboratory manual. Springer Netherlands, Dordrecht, pp 129–167. https://doi.org/10.1007/978-94-011-1566-7_9

Lotfiomran N, Fromm J, Luinstra GA (2015) Effects of elevated CO_2 and different nutrient supplies on wood structure of European beech (*Fagus sylvatica*) and gray poplar (*Populus × canescens*). IAWA J 36:84–97.

De Lucia EH, Drake JE, Thomas RB, Gonzàlez-Meler MA (2007) Forest carbon use efficiency: Is respiration a constant fraction of gross primary production? Glob Chang Biol 13:1157–1167.

Lupi C, Morin H, Deslauriers A, Rossi S (2010) Xylem phenology and wood production: Resolving the chicken-or-egg dilemma. Plant, Cell Environ 33:1721–1730.

Lüthi D, Le Floch M, Bereiter B, Blunier T, Barnola JM, Siegenthaler U, Raynaud D, Jouzel J, Fischer H, Kawamura K, Stocker TF (2008) High-resolution carbon dioxide concentration record 650,000-800,000 years before present. Nature 453:379–382.

Machado R, Loram-Lourenço L, Farnese FS, Alves RDFB, Sousa LF, Silva FG, Filho SCV, Torres-Ruiz JM, Cochard H, Menezes-Silva PE (2020) Where do leaf water leaks come from? Trade-offs underlying the variability in minimum conductance across tropical savanna species with contrasting growth strategies. New Phytol

Maherali H, Delucia EH (2000) Interactive effects of elevated CO_2 and temperature on water

transport in ponderosa pine. Am J Bot 87:243–249.

Maness N (2010) Extraction and analysis of soluble carbohydrates. In: Sunkar R (ed) Plant Stress Tolerance: Methods and Protocols. Humana Press, Totowa, NJ, pp 341–370. https://doi.org/10.1007/978-1-60761-702-0_22

Martínez-Cabrera HI, Jochen Schenk H, Cevallos-Ferriz SRS, Jones CS (2011) Integration of vessel traits, wood density, and height in angiosperm shrubs and trees. Am J Bot 98:915–922.

Martinez-Vilalta J, Anderegg WRL, Sapes G, Sala A (2019) Greater focus on water pools may improve our ability to understand and anticipate drought-induced mortality in plants. New Phytol 223:22–32.

Martínez-Vilalta J, Garcia-Forner N (2017) Water potential regulation, stomatal behaviour and hydraulic transport under drought: deconstructing the iso/anisohydric concept. Plant Cell Environ 40:962–976.

Mcadam SAM, Brodribb TJ (2015) Hormonal dynamics contributes to divergence in seasonal stomatal behaviour in a monsoonal plant community. Plant, Cell Environ 38:423–432.

McCarroll D, Loader NJ (2004) Stable isotopes in tree rings. Quat Sci Rev 23:771–801.

McCarthy HR, Oren R, Finzi AC, Ellsworth DS, Kim HS, Johnsen KH, Millar B (2007) Temporal dynamics and spatial variability in the enhancement of canopy leaf area under elevated atmospheric CO_2. Glob Chang Biol 13:2479–2497.

McCarthy HR, Oren R, Finzi AC, Johnsen KH (2006) Canopy leaf area constrains [CO_2]-induced enhancement of productivity and partitioning among aboveground carbon pools. Proc Natl Acad Sci U S A 103:19356–19361.

McCulloh KA, Domec JC, Johnson DM, Smith DD, Meinzer FC (2019) A dynamic yet vulnerable pipeline: Integration and coordination of hydraulic traits across whole plants. Plant Cell Environ 42:2789–2807. https://doi.org/10.1111/pce.13607

McDowell NG (2011) Mechanisms linking drought, hydraulics, carbon metabolism, and vegetation mortality. Plant Physiol 155:1051–1059.

McDowell NG, Allen CD, Anderson-Teixeira K, Aukema BH, Bond-Lamberty B, Chini L, Clark JS, Dietze M, Grossiord C, Hanbury-Brown A, Hurtt GC, Jackson RB, Johnson DJ, Kueppers L, Lichstein JW, Ogle K, Poulter B, Pugh TAM, Seidl R, Turner MG, Uriarte M, Walker AP, Xu C (2020) Pervasive shifts in forest dynamics in a changing world. Science (80-) 368

McDowell N, Pockman WT, Allen CD, Breshears DD, Cobb N, Kolb T, Plaut J, Sperry JS, West A, Williams DG, Yepez EA (2008) Mechanisms of plant survival and mortality during drought: Why do some plants survive while others succumb to drought? New Phytol 178:719–739.

McElrone AJ, Choat B, Gambetta GA, Brodersen CR (2013) Water uptake and transport in

vascular plants. Nat Educ Knowl 4:1–13.

McGuire MA, Teskey RO (2004) Estimating stem respiration in trees by a mass balance approach that accounts for internal and external fluxes of CO_2. Tree Physiol 24:571–578.

Medlyn BE, Barton CVM, Broadmeadow MSJ, Ceulemans R, De Angelis P, Forstreuter M, Freeman M, Jackson SB, Kellomäki S, Laitat E, Rey A, Roberntz P, Sigurdsson BD, Strassemeyer J, Wang KY, Curtis PS, Jarvis PG (2001) Stomatal conductance of forest species after long-term exposure to elevated CO_2 concentration: A synthesis. New Phytol 149:247–264.

Meeussen C, Govaert S, Vanneste T, Haesen S, Meerbeek K Van, Bollmann K, Brunet J, Calders K, Cousins SAO, Diekmann M, Graae BJ, Iacopetti G, Lenoir J, Orczewska A, Ponette Q, Plue J, Selvi F, Spicher F, Vedel M, Verbeeck H, Vermeir P, Verheyen K, Vangansbeke P, Frenne P De (2021) Science of the Total Environment Drivers of carbon stocks in forest edges across Europe. 759

Meinshausen M, Nicholls ZRJ, Lewis J, Gidden MJ, Vogel E, Freund M, Beyerle U, Gessner C, Nauels A, Bauer N, Canadell JG, Daniel JS, John A, Krummel PB, Luderer G, Meinshausen N, Montzka SA, Rayner PJ, Reimann S, Smith SJ, Van Den Berg M, Velders GJM, Vollmer MK, Wang RHJ (2020) The shared socio-economic pathway (SSP) greenhouse gas concentrations and their extensions to 2500. Geosci Model Dev 13:3571–3605.

Meinzer FC, James SA, Goldstein G (2004) Dynamics of transpiration, sap flow and use of stored water in tropical forest canopy trees. Tree Physiol 24:901–909.

Meinzer FC, Johnson DM, Lachenbruch B, McCulloh KA, Woodruff DR (2009) Xylem hydraulic safety margins in woody plants: Coordination of stomatal control of xylem tension with hydraulic capacitance. Funct Ecol 23:922–930.

Meinzer FC, Woodruff DR, Marias DE, Smith DD, McCulloh KA, Howard AR, Magedman AL (2016) Mapping 'hydroscapes' along the iso- to anisohydric continuum of stomatal regulation of plant water status. Ecol Lett 19:1343–1352.

Menezes-Silva PE, Loram-Lourenço L, Alves RDFB, Sousa LF, Almeida SE da S, Farnese FS (2019) Different ways to die in a changing world: Consequences of climate change for tree species performance and survival through an ecophysiological perspective. Ecol Evol 9:11979–11999.

Mildner M, Bader MKF, Baumann C, Körner C (2015) Respiratory fluxes and fine root responses in mature *Picea abies* trees exposed to elevated atmospheric CO_2 concentrations. Biogeochemistry 124:95–111.

Mitchell PJ, O'Grady AP, Tissue DT, Worledge D, Pinkard EA (2014) Co-ordination of growth, gas exchange and hydraulics define the carbon safety margin in tree species with contrasting drought strategies. Tree Physiol 34:443–458.

Moore DJP, Aref S, Ho RM, Pippen JS, Hamilton JG, De Lucia EH (2006) Annual basal area increment and growth duration of *Pinus taeda* in response to eight years of free-air carbon dioxide enrichment. Glob Chang Biol 12:1367–1377.

Morey RD (2008) Confidence intervals from normalized data: A correction to cousineau (2005). Tutor Quant Methods Psychol 4:61–64.

Morris J, Mann L, Collopy J (1998) Transpiration and canopy conductance in a eucalypt plantation using shallow saline groundwater. Tree Physiol 18:547–555.

Morse SR, Wayne P, Miao SL, Bazzaz FA (1993) Elevated CO_2 and drought alter tissue water relations of birch (*Betula populifolia* Marsh.) seedlings. Oecologia 95:599–602.

Moss JL, Doick KJ, Smith S, Shahrestani M (2019) Influence of evaporative cooling by urban forests on cooling demand in cities. Urban For Urban Green 37:65–73.

Mrad A, Domec JC, Huang CW, Lens F, Katul G (2018) A network model links wood anatomy to xylem tissue hydraulic behaviour and vulnerability to cavitation. Plant Cell Environ 41:2718–2730. https://doi.org/10.1111/pce.13415

Muller B, Pantin F, Génard M, Turc O, Freixes S, Piques M, Gibon Y (2011) Water deficits uncouple growth from photosynthesis, increase C content, and modify the relationships between C and growth in sink organs. J Exp Bot 62:1715–1729.

Mund M, Herbst M, Knohl A, Matthäus B, Schumacher J, Schall P, Siebicke L, Tamrakar R, Ammer C (2020) It is not just a 'trade-off': indications for sink- and source-limitation to vegetative and regenerative growth in an old-growth beech forest. New Phytol 226:111–125.

Murthy R, Zarnoch SJ, Dougherty PM (1997) Seasonal trends of light-saturated net photosynthesis and stomatal conductance of loblolly pine trees grown in contrasting environments of nutrition, water and carbon dioxide. Plant, Cell Environ 20:558–568.

Myking T, Bøhler F, Austrheim G, Solberg EJ (2011) Life history strategies of aspen (*Populus tremula* L.) and browsing effects: A literature review. Forestry 84:61–71.

Nardini A, Savi T, Losso A, Petit G, Pacilè S, Tromba G, Mayr S, Trifilò P, Lo Gullo MA, Salleo S (2017) X-ray microtomography observations of xylem embolism in stems of *Laurus nobilis* are consistent with hydraulic measurements of percentage loss of conductance. New Phytol 213:1068–1075.

Newaz MS, Dang QL, Man R (2018) Jack pine becomes more vulnerable to cavitation with increasing latitudes under doubled CO_2 concentration. Botany 96:111–119.

NOAA (2020) Global Monitoring Laboratory - Global Greenhouse Gas Reference Network. https://www.esrl.noaa.gov/gmd/ccgg/trends/mlo.html (6 December 2020, date last accessed).

Nolf M, Beikircher B, Rosner S, Nolf A, Mayr S (2015) Xylem cavitation resistance can be estimated based on time-dependent rate of acoustic emissions. New Phytol 208:625–

632.

Nolf M, Lopez R, Peters JMR, Flavel RJ, Koloadin LS, Young IM, Choat B (2017) Visualization of xylem embolism by X-ray microtomography: a direct test against hydraulic measurements. New Phytol 214:890–898.

Noormets A, Sôber A, Pell EJ, Dickson RE, Podila GK, Sôber J, Isebrands JG, Karnosky DF (2001) Stomatal and non-stomatal limitation to photosynthesis in two trembling aspen (*Populus tremuloides* Michx.) clones exposed to elevated CO_2 and/or O_3. Plant, Cell Environ 24:327–336.

Norby RJ, DeLucia EH, Gielen B, Calfapietra C, Giardina CP, Kings JS, Ledford J, McCarthy HR, Moore DJP, Ceulemans R, De Angelis P, Finzi AC, Karnosky DF, Kubiske ME, Lukac M, Pregitzer KS, Scarascia-Mugnozza GE, Schlesinger WH, Oren R (2005) Forest response to elevated CO_2 is conserved across a broad range of productivity. Proc Natl Acad Sci U S A 102:18052–18056.

Norby RJ, De Kauwe MG, Domingues TF, Duursma RA, Ellsworth DS, Goll DS, Lapola DM, Luus KA, MacKenzie AR, Medlyn BE, Pavlick R, Rammig A, Smith B, Thomas R, Thonicke K, Walker AP, Yang X, Zaehle S (2016) Model-data synthesis for the next generation of forest free-air CO_2 enrichment (FACE) experiments. New Phytol 209:17–28.

Norby RJ, Sholtis JD, Gunderson CA, Jawdy SS (2003) Leaf dynamics of a deciduous forest canopy: No response to elevated CO_2. Oecologia 136:574–584.

Norby RJ, Warren JM, Iversen CM, Medlyn BE, McMurtrie RE (2010) CO_2 enhancement of forest productivity constrained by limited nitrogen availability. Proc Natl Acad Sci U S A 107:19368–19373.

Norby RJ, Zak DR (2011) Ecological lessons from Free-Air CO_2 Enrichment (FACE) experiments . Annu Rev Ecol Evol Syst 42:181–203.

O'Neill BC, Kriegler E, Ebi KL, Kemp-Benedict E, Riahi K, Rothman DS, van Ruijven BJ, van Vuuren DP, Birkmann J, Kok K, Levy M, Solecki W (2017) The roads ahead: Narratives for shared socioeconomic pathways describing world futures in the 21st century. Glob Environ Chang 42:169–180.

Oksanen E, Sober J, Karnosky DF (2001) Impacts of elevated CO_2 and/or O_3 on leaf ultrastructure of aspen (*Populus tremuloides*) and birch (*Betula papyrifera*) in the Aspen FACE experiment. Environ Pollut 115:437–446.

Olson ME (2020) From Carlquist's ecological wood anatomy to Carlquist's Law: why comparative anatomy is crucial for functional xylem biology. Am J Bot 107:1328–1341.

Oren R, Pataki DE (2001) Transpiration in response to variation in microclimate and soil moisture in southeastern deciduous forests. Oecologia 127:549–559.

Ortuño MF, Brito JJ, García-Orellana Y, Conejero W, Torrecillas A (2009) Maximum daily trunk

shrinkage and stem water potential reference equations for irrigation scheduling of lemon trees. Irrig Sci 27:121–127.

Palacio S, Hoch G, Sala A, Körner C, Millard P (2014) Letters Does carbon storage limit tree growth? New Phytol 201:1096–1100.

Pandey R, Zinta G, AbdElgawad H, Ahmad A, Jain V, Janssens IA (2015) Physiological and molecular alterations in plants exposed to high [CO_2] under phosphorus stress. Biotechnol Adv 33:303–316.

Pantin F, Simonneau T, Muller B (2012) Coming of leaf age: Control of growth by hydraulics and metabolics during leaf ontogeny. New Phytol 196:349–366.

Paschalis A, Katul GG, Fatichi S, Palmroth S, Way DA (2017) On the variability of the ecosystem response to elevated atmospheric CO_2 across spatial and temporal scales at the Duke Forest FACE experiment. Agric For Meteorol 232:367–383.

Pathare VS, Crous KY, Cooke J, Creek D, Ghannoum O, Ellsworth DS (2017) Water availability affects seasonal CO_2-induced photosynthetic enhancement in herbaceous species in a periodically dry woodland. Glob Chang Biol 23:5164–5178.

Peltola H, Kilpeläinen A, Kellomäki S (2002) Diameter growth of Scots pine (*Pinus sylvestris*) trees grown at elevated temperature and carbon dioxide concentration under boreal conditions. Tree Physiol 22:963–972.

Peters GP, Andrew RM, Canadell JG, Friedlingstein P, Jackson RB, Korsbakken JI, Le Quéré A, Peregon A (2020a) Carbon dioxide emissions continue to grow amidst slowly emerging climate policies. Nat Clim Chang 10:3–6.

Peters RL, Steppe K, Cuny HE, De Pauw DJW, Frank DC, Schaub M, Rathgeber CBK, Cabon A, Fonti P (2020b) Turgor – a limiting factor for radial growth in mature conifers along an elevational gradient. New Phytol:213–229.

Phillips NG, Ryan MG, Bond BJ, McDowell NG, Hinckley TM, Čermák J (2003) Reliance on stored water increases with tree size in three species in the Pacific Northwest. Tree Physiol 23:237–245.

Piao S, Liu Q, Chen A, Janssens IA, Fu Y, Dai J, Liu L, Lian X, Shen M, Zhu X (2019) Plant phenology and global climate change: Current progresses and challenges. Glob Chang Biol 25:1922–1940.

Piao S, Luyssaert S, Ciais P, Janssens IA, Chen A, Chao CAO, Fang J, Friedlingstein P, Yiqi LUO, Wang S (2010) Forest annual carbon cost: A global-scale analysis of autotrophic respiration. Ecology 91:652–661.

Pittermann J (2010) The evolution of water transport in plants: An integrated approach. Geobiology 8:112–139.

Pivovaroff AL, Burlett R, Lavigne B, Cochard H, Santiago LS, Delzon S (2016) Testing the 'microbubble effect' using the Cavitron technique to measure xylem water extraction

curves. AoB Plants 8:1–10.

Poorter H, Bühler J, Van Dusschoten D, Climent J, Postma JA (2012a) Pot size matters: A meta-analysis of the effects of rooting volume on plant growth. Funct Plant Biol 39:839–850.

Poorter L, McDonald I, Alarcón A, Fichtler E, Licona JC, Peña-Claros M, Sterck F, Villegas Z, Sass-Klaassen U (2010) The importance of wood traits and hydraulic conductance for the performance and life history strategies of 42 rainforest tree species. New Phytol 185:481–492.

Poorter H, Niinemets Ü, Ntagkas N, Siebenkäs A, Mäenpää M, Matsubara S, Pons T (2019) A meta-analysis of plant responses to light intensity for 70 traits ranging from molecules to whole plant performance. New Phytol 223:1073–1105. https://onlinelibrary.wiley.com/doi/abs/10.1111/nph.15754

Poorter H, Niklas KJ, Reich PB, Oleksyn J, Poot P, Mommer L (2012b) Biomass allocation to leaves, stems and roots: Meta-analyses of interspecific variation and environmental control. New Phytol 193:30–50.

Pratt RB, Jacobsen AL (2017) Conflicting demands on angiosperm xylem: Tradeoffs among storage, transport and biomechanics. Plant Cell Environ 40:897–913.

Pritchard SG, Rogers HH, Prior SA, Peterson CM (1999) Elevated CO_2 and plant structure: a review. Glob Chang Biol 5:807–837.

Pritzkow C, Williamson V, Szota C, Trouvé R, Arndt SK (2020) Phenotypic plasticity and genetic adaptation of functional traits influences intra-specific variation in hydraulic efficiency and safety. Tree Physiol 40:215–229.

Puerto P, Domingo R, Torres R, Pérez-Pastor A, García-Riquelme M (2013) Remote management of deficit irrigation in almond trees based on maximum daily trunk shrinkage: Water relations and yield. Agric Water Manag 126:33–45. http://dx.doi.org/10.1016/j.agwat.2013.04.013

Pugh TAM, Lindeskog M, Smith B, Poulter B, Arneth A, Haverd V, Calle L (2019) Role of forest regrowth in global carbon sink dynamics. Proc Natl Acad Sci U S A 116:4382–4387.

Purcell C, Batke SP, Yiotis C, Caballero R, Soh WK, Murray M, McElwain JC (2018) Increasing stomatal conductance in response to rising atmospheric CO_2. Ann Bot 121:1137–1149.

Qaderi MM, Martel AB, Dixon SL (2019) Environmental factors influence plant vascular system and water regulation. Plants 8:1–23.

Quentin AG, Crous KY, Barton CVM, Ellsworth DS (2015) Photosynthetic enhancement by elevated CO_2 depends on seasonal temperatures for warmed and non-warmed *Eucalyptus globulus* trees. Tree Physiol 35:1249–1263.

Le Quéré C, Jackson RB, Jones MW, Smith AJP, Abernethy S, Andrew RM, De-Gol AJ, Willis DR, Shan Y, Canadell JG, Friedlingstein P, Creutzig F, Peters GP (2020) Temporary

reduction in daily global CO_2 emissions during the COVID-19 forced confinement. Nat Clim Chang 10:647–653. http://dx.doi.org/10.1038/s41558-020-0797-x

Radoglou KM, Jarvis PG (1990) Effects of CO_2 enrichment on four poplar clones. II. Leaf Surface Properties. Ann Bot 65:627–632.

Rakocevic M, Braga KSM, Batista ER, Maia AHN, Scholz MBS, Filizola HF (2020) The vegetative growth assists to reproductive responses of Arabic coffee trees in a long-term FACE experiment. Plant Growth Regul 91:305–316. https://doi.org/10.1007/s10725-020-00607-2

Ranson SL, Thomas M (1960) Crassulacean Acid Metabolism. Annu Rev Plant Physiol 11:81–110. https://doi.org/10.1146/annurev.pp.11.060160.000501

Reddy AR, Rasineni GK, Raghavendra AS (2010) The impact of global elevated CO_2 concentration on photosynthesis and plant productivity. Curr Sci 99:46–57.

Reich PB, Oleksyn J, Wright IJ (2009) Leaf phosphorus influences the photosynthesis-nitrogen relation: A cross-biome analysis of 314 species. Oecologia 160:207–212.

Reich PB, Sendall KM, Stefanski A, Rich RL, Hobbie SE, Montgomery RA (2018) Effects of climate warming on photosynthesis in boreal tree species depend on soil moisture. Nature 562:263–267. http://www.nature.com/articles/s41586-018-0582-4

Rey A, Jarvis PG (1998) Long-term photosynthetic acclimation to increased atmospheric CO_2 concentration in young birch (*Betula pendula*) trees. Tree Physiol 18:441–450.

Reyes-Fox M, Steltzer H, Trlica MJ, McMaster GS, Andales AA, Lecain DR, Morgan JA (2014) Elevated CO_2 further lengthens growing season under warming conditions. Nature 510:259–262. http://dx.doi.org/10.1038/nature13207

Riahi K, van Vuuren DP, Kriegler E, Edmonds J, O'Neill BC, Fujimori S, Bauer N, Calvin K, Dellink R, Fricko O, Lutz W, Popp A, Cuaresma JC, KC S, Leimbach M, Jiang L, Kram T, Rao S, Emmerling J, Ebi K, Hasegawa T, Havlik P, Humpenöder F, Da Silva LA, Smith S, Stehfest E, Bosetti V, Eom J, Gernaat D, Masui T, Rogelj J, Strefler J, Drouet L, Krey V, Luderer G, Harmsen M, Takahashi K, Baumstark L, Doelman JC, Kainuma M, Klimont Z, Marangoni G, Lotze-Campen H, Obersteiner M, Tabeau A, Tavoni M (2017) The Shared Socioeconomic Pathways and their energy, land use, and greenhouse gas emissions implications: An overview. Glob Environ Chang 42:153–168.

Ribeiro R V., Machado EC, Habermann G, Santos MG, Oliveira RF (2012) Seasonal effects on the relationship between photosynthesis and leaf carbohydrates in orange trees. Funct Plant Biol 39:471–480.

Richet N, Afif D, Tozo K, Pollet B, Maillard P, Huber F, Priault P, Banvoy J, Gross P, Dizengremel P, Lapierre C, Perré P, Cabané M (2012) Elevated CO_2 and/or ozone modify lignification in the wood methylation and chromatin patterning. J Exp Bot 63:4291–4301.

Riikonen J, Holopainen T, Oksanen E, Vapaavuori E (2005) Leaf photosynthetic

characteristics of silver birch during three years of exposure to elevated concentrations of CO_2 and O_3 in the field. Tree Physiol 25:621–632.

Riikonen J, Lindsberg MM, Holopainen T, Oksanen E, Lappi J, Peltonen P, Vapaavuori E (2004) Silver birch and climate change: Variable growth and carbon allocation responses to elevated concentrations of carbon dioxide and ozone. Tree Physiol 24:1227–1237.

Riikonen J, Oksanen E, Peltonen P, Holopainen T, Vapaavuori E (2003) Seasonal variation in physiological characteristics of two silver birch clones in the field. Can J For Res 33:2164–2176.

Riikonen J, Syrjälä L, Tulva I, Mänd P, Oksanen E, Poteri M, Vapaavuori E (2008) Stomatal characteristics and infection biology of *Pyrenopeziza betulicola* in *Betula pendula* trees grown under elevated CO_2 and O_3. Environ Pollut 156:536–543.

Ripple W, Wolf C, Newsome T, Barnard P, Moomaw W, Grandcolas P, Ripple W, Wolf C, Newsome T, Barnard P, Moomaw W, Ripple WJ, Wolf C, Newsome TM, Barnard P, Moomaw WR (2020) World Scientists ' Warning of a Climate Emergency To cite this version : World Scientists ' Warning of a Climate Emergency.

Ritchie H, Roser M (2020) Access to Energy. Publ online OurWorldInData.org. https://ourworldindata.org/energy-access

Robredo A, Pérez-López U, de la Maza HS, González-Moro B, Lacuesta M, Mena-Petite A, Muñoz-Rueda A (2007) Elevated CO_2 alleviates the impact of drought on barley improving water status by lowering stomatal conductance and delaying its effects on photosynthesis. Environ Exp Bot 59:252–263.

Rogelj J, Popp A, Calvin K V., Luderer G, Emmerling J, Gernaat D, Fujimori S, Strefler J, Hasegawa T, Marangoni G, Krey V, Kriegler E, Riahi K, Van Vuuren DP, Doelman J, Drouet L, Edmonds J, Fricko O, Harmsen M, Havlík P, Humpenöder F, Stehfest E, Tavoni M (2018) Scenarios towards limiting global mean temperature increase below 1.5 °c. Nat Clim Chang 8:325–332. http://dx.doi.org/10.1038/s41558-018-0091-3

Rogers PC, Pinno BD, Šebesta J, Albrectsen BR, Li G, Ivanova N, Kusbach A, Kuuluvainen T, Landhäusser SM, Liu H, Myking T, Pulkkinen P, Wen Z, Kulakowski D (2020) A global view of aspen: Conservation science for widespread keystone systems. Glob Ecol Conserv 21

De Roo L, Lauriks F, Salomón RL, Oleksyn J, Steppe K (2020a) Woody tissue photosynthesis increases radial stem growth of young poplar trees under ambient atmospheric CO_2 but its contribution ceases under elevated CO_2. Tree Physiol:1–11.

De Roo L, Salomón RL, Steppe K (2020b) Woody tissue photosynthesis reduces stem CO_2 efflux by half and remains unaffected by drought stress in young *Populus tremula* trees. Plant Cell Environ 43:981–991.

De Roo L, Vergeynst LL, De Baerdemaeker NJF, Steppe K (2016) Acoustic emissions to

measure drought-induced cavitation in plants. Appl Sci 6

Rosner S (2017) Wood density as a proxy for vulnerability to cavitation: Size matters. J Plant Hydraul 4:e001.

Sala A, Woodruff DR, Meinzer FC (2012) Carbon dynamics in trees: Feast or famine? Tree Physiol 32:764–775.

Salleo S, Hinckley TM, Kikuta SB, Lo Gullo MA, Richter H, Weilgony P, Yoon T. (1992) A method for inducing xylem emboli in situ : experiments with a field-grown tree. Plant Cell Environ 15:491–497.

Salomón RL, Limousin JM, Ourcival JM, Rodríguez-Calcerrada J, Steppe K (2017a) Stem hydraulic capacitance decreases with drought stress: implications for modelling tree hydraulics in the Mediterranean oak Quercus ilex. Plant Cell Environ 40:1379–1391.

Salomón RL, Rodríguez-Calcerrada J, Staudt M (2017b) Carbon losses from respiration and emission of volatile organic compounds---The overlooked side of tree carbon budgets. In: Gil-Pelegrín E, Peguero-Pina JJ, Sancho-Knapik D (eds) Oaks Physiological Ecology. Exploring the Functional Diversity of Genus Quercus L. Springer International Publishing, Cham, pp 327–359. https://doi.org/10.1007/978-3-319-69099-5_10

Salomón RL, De Schepper V, Valbuena-Carabaña M, Gil L, Steppe K (2018a) Daytime depression in temperature-normalised stem CO_2 efflux in young poplar trees is dominated by low turgor pressure rather than by internal transport of respired CO_2. New Phytol 217:586–598.

Salomón RL, De Schepper V, Valbuena-Carabaña M, Gil L, Steppe K (2018b) Daytime depression in temperature-normalised stem CO_2 efflux in young poplar trees is dominated by low turgor pressure rather than by internal transport of respired CO2. New Phytol 217:586–598.

Salomón RL, Steppe K, Crous KY, Noh NJ, Ellsworth DS (2019) Elevated CO_2 does not affect stem CO_2 efflux nor stem respiration in a dry Eucalyptus woodland, but it shifts the vertical gradient in xylem $[CO_2]$. Plant Cell Environ 42:2151–2164. https://doi.org/10.1111/pce.13550

Samuelson LJ, Seiler JR (1994) Red spruce gas exchange in response to elevated CO_2, water stress, and soil fertility treatments. Can J For Res 24:954–959.

Sanches RFE, Centeno da CD, Braga MR, da Silva EA (2020) Impact of high atmospheric CO_2 concentrations on the seasonality of water-related processes, gas exchange, and carbohydrate metabolism in coffee trees under field conditions. Clim Change 162:1231–1248.

Sause MGR (2011) Investigation of pencil-lead breaks as acoustic emission sources. J Acoust Emiss 29:184–196. https://www3.epa.gov/climatechange/ghgemissions/sources.html

Saveyn A, Steppe K, Lemeur R (2007) Daytime depression in tree stem CO_2 efflux rates: Is it

caused by low stem turgor pressure? Ann Bot 99:477–485.

Saxe H, Ellsworth DS, Heath J (1998) Tree and forest functioning in an enriched CO_2 atmosphere. New Phytol 139:395–436.

Scholz A, Klepsch M, Karimi Z, Jansen S (2013) How to quantify conduits in wood? Front Plant Sci 4:1–11.

Scholz FG, Phillips NG, Bucci SJ, Meinzer FC, Goldstein G (2011) Hydraulic capacitance: Biophysics and functional significance of internal water sources in relation to tree size. :341–361.

Schurgers G, Ahlström A, Arneth A, Pugh TAM, Smith B (2018) Climate sensitivity controls Uncertainty in future terrestrial carbon sink. Geophys Res Lett 45:4329–4336. https://doi.org/10.1029/2018GL077528

Seiler TJ, Rasse DP, Li J, Dijkstra P, Anderson HP, Johnson DP, Powell TL, Hungate BA, Hinkle CR, Drake BG (2009) Disturbance, rainfall and contrasting species responses mediated aboveground biomass response to 11 years of CO_2 enrichment in a Florida scrub-oak ecosystem. Glob Chang Biol 15:356–367.

Sergent AS, Varela SA, Barigah TS, Badel E, Cochard H, Dalla-Salda G, Delzon S, Fernández ME, Guillemot J, Gyenge J, Lamarque LJ, Martinez-Meier A, Rozenberg P, Torres-Ruiz JM, Martin-StPaul NK (2020) A comparison of five methods to assess embolism resistance in trees. For Ecol Manage 468

Sholtis JD, Gunderson CA, Norby RJ, Tissue DT (2004) Persistent stimulation of photosynthesis by elevated CO_2 in a sweetgum (*Liquidambar styraciflua*) forest stand. New Phytol 162:343–354.

Sigurdsson BD (2001a) Elevated [CO_2] and nutrient status modified leaf phenology and growth rhythm of young *Populus trichocarpa* trees in a 3-year field study. Trees - Struct Funct 15:403–413.

Sigurdsson BD (2001b) Environmental control of carbon uptake and growth in a *Populus trichocarpa* plantation in Iceland. Swedish University of Agricultural Sciences

Sigurdsson BD, Medhurst JL, Wallin G, Eggertsson O, Linder S (2013) Growth of mature boreal Norway spruce was not affected by elevated [CO_2] and/or air temperature unless nutrient availability was improved. Tree Physiol 33:1192–1205.

Sigurdsson BD, Roberntz P, Freeman M, Næss M, Saxe H, Thorgeirsson H, Linder S (2002) Impact studies on Nordic forests: Effects of elevated CO_2 and fertilization on gas exchange. Can J For Res 32:779–788.

Sigurdsson BD, Thorgeirsson H, Linder S (2001) Growth and dry-matter partitioning of young *Populus trichocarpa* in response to carbon dioxide concentration and mineral nutrient availability. Tree Physiol 21:941–950.

da Silva JR, Patterson AE, Rodrigues WP, Campostrini E, Griffin KL (2017) Photosynthetic

acclimation to elevated CO_2 combined with partial rootzone drying results in improved water use efficiency, drought tolerance and leaf carbon balance of grapevines (*Vitis labrusca*). Environ Exp Bot 134:82–95.

Skelton RP, West AG, Dawson TE (2015) Predicting plant vulnerability to drought in biodiverse regions using functional traits. Proc Natl Acad Sci U S A 112:5744–5749.

Smith NG (2017) Plant Respiration Responses to Elevated CO_2: An overview from cellular processes to global impacts. In: Tcherkez G, Ghashghaie J (eds) Plant Respiration: Metabolic Fluxes and Carbon Balance. Springer International Publishing, Cham, pp 69–87. https://doi.org/10.1007/978-3-319-68703-2_4

Smith DM, Allen SJ (1996) Measurement of sap flow in plant stems. J Exp Bot 47:1833–1844.

Sonnleitner MA, Günthardt-Goerg MS, Bucher-Wallin IK, Attinger W, Reis S, Schulin R (2001) Influence of soil type on the effects of elevated atmospheric CO_2 and N deposition on the water balance and growth of a young spruce and beech forest. Water Air Soil Pollut 126:271–290.

Sorek Y, Greenstein S, Netzer Y, Shtein I, Jansen S, Hochberg U (2020) An increase in xylem embolism resistance of grapevine leaves during the growing season is coordinated with stomatal regulation, turgor loss point and intervessel pit membranes. New Phytol

Sperry JS (2000) Hydraulic constraints on plant gas exchange. Agric For Meteorol 104:13–23.

Sperry JS, Hacke UG, Pittermann J (2006) Size and function in conifer tracheids and angiosperm vessels. Am J Bot 93:1490–1500.

Sperry JS, Saliendra NZ (1994) Intra- and inter-plant variation in xylem cavitation in *Betula occidentalis*. Plant Cell Environ 17:1233–1241.

Sperry J, Tyree MT (1988) A method for measuring hydraulic conductivity and embolism in xylem.

Spinnler D, Egli P, Körner C (2003) Provenance effects and allometry in beech and spruce under elevated CO_2 and nitrogen on two different forest soils. Basic Appl Ecol 4:467–478.

Spinoni J, Naumann G, Vogt J V. (2017) Pan-European seasonal trends and recent changes of drought frequency and severity. Glob Planet Change 148:113–130.

Springer CJ, Thomas RB (2007) Photosynthetic responses of forest understory tree species to long-term exposure to elevated carbon dioxide concentration at the Duke Forest FACE experiment. Tree Physiol 27:25–32.

Steppe K (2018) The potential of the tree water potential. Tree Physiol 38:937–940.

Steppe K, Cochard H, Lacointe A, Améglio T (2012) Could rapid diameter changes be facilitated by a variable hydraulic conductance? Plant, Cell Environ 35:150–157.

Steppe K, Lemeur R (2007) Effects of ring-porous and diffuse-porous stem wood anatomy on

the hydraulic parameters used in a water flow and storage model. Tree Physiol 27:43–52.

Steppe K, De Pauw DJW, Lemeur R, Vanrolleghem PA (2006) A mathematical model linking tree sap flow dynamics to daily stem diameter fluctuations and radial stem growth. Tree Physiol 26:257–273.

Steppe K, Sterck F, Deslauriers A (2015) Diel growth dynamics in tree stems: Linking anatomy and ecophysiology. Trends Plant Sci 20:335–343. http://dx.doi.org/10.1016/j.tplants.2015.03.015

Steppe K, Zeugin F, Zweifel R (2009) Low-decibel ultrasonic acoustic emissions are temperature-induced and probably have no biotic origin. New Phytol 183:928–931. https://nph.onlinelibrary.wiley.com/doi/abs/10.1111/j.1469-8137.2009.02976.x

De Swaef T, De Schepper V, Vandegehuchte MW, Steppe K (2015) Stem diameter variations as a versatile research tool in ecophysiology. Tree Physiol 35:1047–1061.

De Swaef T, Steppe K, Lemeur R (2009) Determining reference values for stem water potential and maximum daily trunk shrinkage in young apple trees based on plant responses to water deficit. Agric Water Manag 96:541–550.

Taylor G, Tallis MJ, Giardina CP, Percy KE, Miglietta F, Gupta PS, Gioli B, Calfapietra C, Gielen B, Kubiske ME, Scarascia-Mugnozza GE, Ket K, Long SP, Karnosky DF (2008) Future atmospheric CO_2 leads to delayed autumnal senescence. Glob Chang Biol 14:264–275.

Taylor G, Tricker PJ, Zhang FZ, Alston VJ, Miglietta F, Kuzminsky E (2003) Spatial and temporal effects of free-air CO_2 enrichment (POPFACE) on leaf growth, cell expansion, and cell production in a closed canopy of poplar. Plant Physiol 131:177–185.

Temperton VM, Grayston SJ, Jackson G, Barton CVM, Millard P, Jarvis PG (2003) Effects of elevated carbon dioxide concentration on growth and nitrogen fixation in *Alnus glutinosa* in a long-term field experiment. Tree Physiol 23:1051–1059.

Terrer C, Jackson RB, Prentice IC, Keenan TF, Kaiser C, Vicca S, Fisher JB, Reich PB, Stocker BD, Hungate BA, Peñuelas J, McCallum I, Soudzilovskaia NA, Cernusak LA, Talhelm AF, Van Sundert K, Piao S, Newton PCD, Hovenden MJ, Blumenthal DM, Liu YY, Müller C, Winter K, Field CB, Viechtbauer W, Van Lissa CJ, Hoosbeek MR, Watanabe M, Koike T, Leshyk VO, Polley HW, Franklin O (2019) Nitrogen and phosphorus constrain the CO_2 fertilization of global plant biomass. Nat Clim Chang 9:684–689.

Terrer C, Vicca S, Hungate BA, Phillips RP, Prentice IC (2016) Mycorrhizal association as a primary control of the CO_2 fertilization effect. Science (80-) 353:72–74.

Teskey RO, Saveyn A, Steppe K, McGuire MA (2008) Origin, fate and significance of CO_2 in tree stems. New Phytol 177:17–32.

Teskey R, Wertin T, Bauweraerts I, Ameye M, McGuire MA, Steppe K (2015) Responses of tree species to heat waves and extreme heat events. Plant Cell Environ 38:1699–1712.

Tingey DT, Johnson MG, Phillips DL, Johnson DW, Ball JT (1996) Effects of elevated CO_2 and nitrogen on the synchrony of shoot and root growth in ponderosa pine. Tree Physiol 16:905–914.

Tissue DT, Griffin KL, Ball JT (1999) Photosynthetic adjustment in field-grown ponderosa pine trees after six years of exposure to elevated CO_2. Tree Physiol 19:221–228.

Tissue DT, Thomas RB, Strain BR (1997) Atmospheric CO_2 enrichment increases growth and photosynthesis of *Pinus taeda*: A 4 year experiment in the field. Plant, Cell Environ 20:1123–1134.

Tixier A, Guzmán-Delgado P, Sperling O, Amico Roxas A, Laca E, Zwieniecki MA (2020) Comparison of phenological traits, growth patterns, and seasonal dynamics of non-structural carbohydrate in Mediterranean tree crop species. Sci Rep 10:1–11.

Tjoelker MG, Oleksyn J, Reich PB (2001) Modelling respiration of vegetation: Evidence for a general temperature-dependent Q_{10}. Glob Chang Biol 7:223–230.

Tognetti R, Longobucco A, Raschi A (1999) Seasonal embolism and xylem vulnerability in deciduous and evergreen mediterranean trees influenced by proximity to a carbon dioxide spring. Tree Physiol 19:271–277.

Tomasella M, Petrussa E, Petruzzellis F, Nardini A, Casolo V (2020) The possible role of non-structural carbohydrates in the regulation of tree hydraulics. Int J Mol Sci 21

Tor-ngern P, Oren R, Ward EJ, Palmroth S, Mccarthy HR, Domec JC (2015) Increases in atmospheric CO_2 have little influence on transpiration of a temperate forest canopy. New Phytol 205:518–525.

Tricker PJ, Pecchiari M, Bunn SM, Vaccari FP, Peressotti A, Miglietta F, Taylor G (2009) Water use of a bioenergy plantation increases in a future high CO_2 world. Biomass and Bioenergy 33:200–208.

Tricker PJ, Trewin H, Kull O, Clarkson GJJ, Eensalu E, Tallis MJ, Colella A, Doncaster CP, Sabatti M, Taylor G (2005) Stomatal conductance and not stomatal density determines the long-term reduction in leaf transpiration of poplar in elevated CO_2. Oecologia 143:652–660.

Turnbull MH, Tissue DT, Griffin KL, Rogers GND, Whitehead D (1998) Photosynthetic acclimation to long-term exposure to elevated CO_2 concentration in *Pinus radiata* D. Don. is related to age of needles. Plant, Cell Environ 21:1019–1028.

Tyree MT, Alexander JD (1993) Plant water relations and the effects of elevated CO_2: a review and suggestions for future research. Vegetatio 104–105:47–62.

Tyree MT, Ewers FW (1991) The hydraulic architecture of trees and other woody plants. New Phytol 119:345–360.

Tyree MT, Sperry JS (1989) Characterization and propagation of acoustic emission signals in woody plants: towards an improved acoustic emission counter. Plant Cell Environ 12:371–382.

Tyree MT, Yang S (1990) Water-storage capacity of Thuja, Tsuga and Acer stems measured by dehydration isotherms - The contribution of capillary water and cavitation. Planta 182:420–426.

Uddling J, Teclaw RM, Kubiske ME, Pregitzer KS, Ellsworth DS (2008) Sap flux in pure aspen and mixed aspen-birch forests exposed to elevated concentrations of carbon dioxide and ozone. Tree Physiol 28:1231–1243.

Uddling J, Wallin G (2012) Interacting effects of elevated CO_2 and weather variability on photosynthesis of mature boreal Norway spruce agree with biochemical model predictions. Tree Physiol 32:1509–1521.

UN (2015) Paris agreement.

Urban O, Hrstka M, Holub P, Veselá B, Večeřová K, Novotná K, Grace J, Klem K (2019) Interactive effects of ultraviolet radiation and elevated CO_2 concentration on photosynthetic characteristics of European beech saplings during the vegetation season. Plant Physiol Biochem 134:20–30.

Urban L, Six S, Barthélémy L, Bearez P (2002) Effect of elevated CO_2 on leaf water relations, water balance and senescence of cut roses. J Plant Physiol 159:717–723.

Valentini R, Matteucci G, Dolman AJ, Schulze ED, Rebmann C, Moors EJ, Granier A, Gross P, Jensen NO, Pilegaard K, Lindroth A, Grelle A, Bernhofer C, Grünwald T, Aubinet M, Ceulemans R, Kowalski AS, Vesala T, Rannik Ü, Berbigier P, Loustau D, Guomundsson J, Thorgeirsson H, Ibrom A, Morgenstern K, Clement R, Moncrieff J, Montagnani L, Minerbi S, Jarvis PG (2000) Respiration as the main determinant of carbon balance in European forests. Nature 404:861–865.

Vaz M, Cochard H, Gazarini L, Graça J, Chaves MM, Pereira JS (2012) Cork oak (*Quercus suber* L.) seedlings acclimate to elevated CO_2 and water stress: Photosynthesis, growth, wood anatomy and hydraulic conductivity. Trees - Struct Funct 26:1145–1157.

Venturas MD, Pratt RB, Jacobsen AL, Castro V, Fickle JC, Hacke UG (2019) Direct comparison of four methods to construct xylem vulnerability curves: Differences among techniques are linked to vessel network characteristics. Plant Cell Environ 42:2422–2436. https://doi.org/10.1111/pce.13565

Venturas MD, Sperry JS, Hacke UG (2017) Plant xylem hydraulics: What we understand, current research, and future challenges. J Integr Plant Biol 59:356–389.

Vergeynst LL, Bogaerts J, Baert A, Kips L, Steppe K (2013) New type of vulnerability curve gives insight in the hydraulic capacitance and conductivity of the xylem. Acta Hortic 991:341–348.

Vergeynst LL, Dierick M, Bogaerts JAN, Cnudde V, Steppe K (2015a) Cavitation: A blessing in disguise? New method to establish vulnerability curves and assess hydraulic capacitance of woody tissues. Tree Physiol 35:400–409.

Vergeynst LL, Sause MGR, De Baerdemaeker NJF, De Roo L, Steppe K (2016) Clustering reveals cavitation-related acoustic emission signals from dehydrating branches. Tree Physiol 36:786–796.

Vergeynst LL, Sause MGR, Hamstad MA, Steppe K (2015b) Deciphering acoustic emission signals in drought stressed branches: The missing link between source and sensor. Front Plant Sci 6:1–11.

Vestager M, Timmermans F, Dombrovskis V, Breton T, Vălean A (2020) Letter to U. con der Leyen.

Viger M, Smith HK, Cohen D, Dewoody J, Trewin H, Steenackers M, Bastien C, Taylor G (2016) Adaptive mechanisms and genomic plasticity for drought tolerance identifed in European black poplar (*Populus nigra* L.). Tree Physiol 36:909–928.

Walker AP, De Kauwe MG, Bastos A, Belmecheri S, Georgiou K, Keeling RF, McMahon SM, Medlyn BE, Moore DJP, Norby RJ, Zaehle S, Anderson-Teixeira KJ, Battipaglia G, Brienen RJW, Cabugao KG, Cailleret M, Campbell E, Canadell JG, Ciais P, Craig ME, Ellsworth DS, Farquhar GD, Fatichi S, Fisher JB, Frank DC, Graven H, Gu L, Haverd V, Heilman K, Heimann M, Hungate BA, Iversen CM, Joos F, Jiang M, Keenan TF, Knauer J, Körner C, Leshyk VO, Leuzinger S, Liu Y, MacBean N, Malhi Y, McVicar TR, Penuelas J, Pongratz J, Powell AS, Riutta T, Sabot MEB, Schleucher J, Sitch S, Smith WK, Sulman B, Taylor B, Terrer C, Torn MS, Treseder KK, Trugman AT, Trumbore SE, van Mantgem PJ, Voelker SL, Whelan ME, Zuidema PA (2020) Integrating the evidence for a terrestrial carbon sink caused by increasing atmospheric CO_2. New Phytol

Walter A, Christ MM, Barron-Gafford GA, Grieve KA, Murthy R, Rascher U (2005) The effect of elevated CO_2 on diel leaf growth cycle, leaf carbohydrate content and canopy growth performance of *Populus deltoides.* Glob Chang Biol 11:1207–1219.

Wang KY, Kellomaki S (1997) Stomatal conductance and transpiration in shoots of Scots pine after 4-year exposure to elevated CO_2 and temperature. Can J Bot 75:552–561.

Wang KY, Kellomaki S, Laitinen K (1995) Effects of needle age, long-term temperature and CO_2 treatments on the photosynthesis of Scots pine. Tree Physiol 15:211–218.

Wang KY, Kellomäki S, Zha T, Peltola H (2005) Annual and seasonal variation of sap flow and conductance of pine trees grown in elevated carbon dioxide and temperature. J Exp Bot 56:155–165.

Wang X, Lewis JD, Tissue DT, Seemann JR, Griffin KL (2001) Effects of elevated atmospheric CO_2 concentration on leaf dark respiration of *Xanthium strumarium* in light and in darkness. Proc Natl Acad Sci U S A 98:2479–2484.

Ward EJ, Oren R, Bell DM, Clark JS, McCarthy HR, Kim HS, Domec JC (2013) The effects of elevated CO_2 and nitrogen fertilization on stomatal conductance estimated from 11 years of scaled sap flux measurements at Duke FACE. Tree Physiol 33:135–151.

Warren JM, Jensen AM, Medlyn BE, Norby RJ, Tissue DT (2015) Carbon dioxide stimulation of photosynthesis in *Liquidambar styraciflua* is not sustained during a 12-year field experiment. AoB Plants 7:1–13.

Warren JM, Norby RJ, Wullschleger SD, Oren R (2011) Elevated CO_2 enhances leaf senescence during extreme drought in a temperate forest. Tree Physiol 31:117–130.

Watanabe Y, Satomura T, Sasa K, Funada R, Koike T (2010) Differential anatomical responses to elevated CO_2 in saplings of four hardwood species. Plant, Cell Environ 33:1101–1111.

Way DA, Stinziano JR, Berghoff H, Oren R (2017) How well do growing season dynamics of photosynthetic capacity correlate with leaf biochemistry and climate fluctuations? Tree Physiol 37:879–888.

Wertin TM, McGuire MA, Teskey RO (2010) The influence of elevated temperature, elevated atmospheric CO_2 concentration and water stress on net photosynthesis of loblolly pine (*Pinus taeda* L.) at northern, central and southern sites in its native range. Glob Chang Biol 16:2089–2103.

Wertin TM, Teskey RO (2008) Close coupling of whole-plant respiration to net photosynthesis and carbohydrates. Tree Physiol 28:1831–1840.

Wheeler JK, Huggett BA, Tofte AN, Rockwell FE, Holbrook NM (2013) Cutting xylem under tension or supersaturated with gas can generate PLC and the appearance of rapid recovery from embolism. Plant, Cell Environ 36:1938–1949.

Wheeler JK, Sperry JS, Hacke UG, Hoang N (2005) Inter-vessel pitting and cavitation in woody Rosaceae and other vessel led plants: A basis for a safety versus efficiency trade-off in xylem transport. Plant, Cell Environ 28:800–812.

Wu J, Albert LP, Lopes AP, Restrepo-Coupe N, Hayek M, Wiedemann KT, Guan K, Stark SC, Christoffersen B, Prohaska N, Tavares J V., Marostica S, Kobayashi H, Ferreira ML, Campos KS, Dda Silva R, Brando PM, Dye DG, Huxman TE, Huete AR, Nelson BW, Saleska SR (2016) Leaf development and demography explain photosynthetic seasonality in Amazon evergreen forests. Science (80-) 351:972–976.

von Wühlisch G (2009) Technical Guidelines for genetic conservation and use of Eurasian aspen (*Populus tremula*). Bioversity International, Rome.

Wujeska-Klause A, Crous KY, Ghannoum O, Ellsworth DS (2019) Leaf age and eCO_2 both influence photosynthesis by increasing light harvesting in mature *Eucalyptus tereticornis* at EucFACE. Environ Exp Bot 167

Wullschleger SD, Gunderson CA, Hanson PJ, Wilson KB, Norby RJ (2002a) Sensitivity of

stomatal and canopy conductance to elevated CO_2 concentration - Interacting variables and perspectives of scale. New Phytol 153:485–496.

Wullschleger SD, Norby RJ (2001) Sap velocity and canopy transpiration in a sweetgum stand exposed to free-air CO_2 enrichment (FACE). New Phytol 150:489–498.

Wullschleger SD, Tschaplinski TJ, Norby RJ (2002b) Plant water relations at elevated CO_2 - Implications for water-limited environments. Plant, Cell Environ 25:319–331.

Xu L, Baldocchi DD (2003) Seasonal trends in photosynthetic parameters and stomatal conductance of blue oak (*Quercus douglasii*) under prolonged summer drought and high temperature. Tree Physiol 23:865–877.

Xu Z, Jiang Y, Jia B, Zhou G (2016) Elevated-CO_2 response of stomata and its dependence on environmental factors. Front Plant Sci 7:1–15.

Xu J, Lv Y, Liu X, Wei Q, Qi Z, Yang S, Liao L (2019) A general non-rectangular hyperbola equation for photosynthetic light response curve of rice at various leaf ages. Sci Rep 9:1–8. http://dx.doi.org/10.1038/s41598-019-46248-y

Yamori W (2015) Photosynthesis and respiration. Elsevier Inc. http://dx.doi.org/10.1016/B978-0-12-801775-3.00009-3

Yamori W, Hikosaka K, Way DA (2014) Temperature response of photosynthesis in C3, C4, and CAM plants: Temperature acclimation and temperature adaptation. Photosynth Res 119:101–117.

Yazaki K, Ishida S, Kawagishi T, Fukatsu E, Maruyama Y, Kitao M, Tobita H, Koike T, Funada R (2004) Effects of elevated CO_2 concentration on growth, annual ring structure and photosynthesis in *Larix kaempferi* seedlings. Tree Physiol 24:941–949.

Zas R, Sampedro L, Solla A, Vivas M, Lombardero MJ, Alía R, Rozas V (2020) Dendroecology in common gardens: Population differentiation and plasticity in resistance, recovery and resilience to extreme drought events in *Pinus pinaster*. Agric For Meteorol 291

Zhang L, Liu L, Zhao H, Jiang Z, Cai J (2020) Differences in near isohydric and anisohydric behavior of contrasting poplar hybrids (I-101 (*Populus alba* L.) x 84K (*Populus alba* L. x Populus glandulosa Uyeki) under drought-rehydration treatments. Forests 11

Zotz G, Pepin S, Körner C (2005) No down-regulation of leaf photosynthesis in mature forest trees after three years of exposure to elevated CO_2. Plant Biol 7:369–374.

Zweifel R (2016) Radial stem variations - a source of tree physiological information not fully exploited yet. Plant, Cell Environ 39:231–232.

Zweifel R, Haeni M, Buchmann N, Eugster W (2016) Are trees able to grow in periods of stem shrinkage? New Phytol 211:839–849.

Zweifel R, Item H, Häsler R (2000) Stem radius changes and their relation to stored water in stems of young Norway spruce trees. Trees - Struct Funct 15:50–57.

Zweifel R, Item H, Häsler R (2001) Link between diurnal stem radius changes and tree water

relations. Tree Physiol 21:869–877.

S
Summary

Trees are exposed to unprecedented climate changes and resulting drought-driven forest mortality has been reported worldwide. Effects of elevated $[CO_2]$ (eCO_2) on tree functioning has been an important research topic over the last decades. Nonetheless, crucial questions remain largely unexplored: Is the tree response to eCO_2 variable over time? Do leaf scale responses to eCO_2 upscale to the whole-tree scale? Is eCO_2 capable to alleviate detrimental effects of drought stress? Along this PhD dissertation, we aim at unravelling the interactions between seasonal tree carbon demand and eCO_2 at the leaf and the whole-tree scale and under well-watered and drought conditions. To this end, a literature review was performed, and two sets of one-year-old European aspen (*Populus tremula* L.) trees were grown under ambient (approximately 445 ppm, aCO_2) or elevated (approximately 701 ppm, eCO_2) $[CO_2]$ during two consecutive growing seasons to study early (2019) and late (2018) season responses. Leaf scale net carbon assimilation, stomatal conductance and respiration, together with whole-tree scale stem growth, sap flow as a proxy for transpiration and stem CO_2 efflux were monitored. In addition, dry biomass and non-structural carbohydrate concentration (NSC) were measured across tree organs and tissues. Finally, vulnerability (VCs) and desorption (DCs) curves were established via the bench dehydration method.

Literature review yielded two important insights. First, tree responses to eCO_2 are highly variable within a single growing season. Seasonal differences in carbon requirements

largely determine the magnitude of tree responses to eCO₂, with largest photosynthetic stimulation commonly occurring during the early season, when stem volumetric growth rates are higher. Second, across free soil eCO₂ experiments of more than one year in duration, responses of tree carbon and water processes to eCO₂ can substantially differ between leaf and whole-tree scales. Nutrient or water limitation can constrain tree growth despite eCO₂-induced carbon surplus. Likewise, stimulation of total canopy leaf area under eCO₂ can nullify potential reductions of water use at the leaf scale. Accordingly, in the young European aspen trees, stimulation of photosynthesis was larger during the early season, and additional carbon led to enhanced stem volumetric growth and dry biomass in the early and late season, respectively. In contrast to our expectations, water loss at both the leaf and the whole-tree scale was not affected by eCO₂. Leaf and stem respiration did not differ between [CO₂] treatments either. The widespread occurrence of dynamic eCO₂ responses over time and space highlights likely misjudgement of complex eCO₂ effects on tree functioning when assessment is based on single-point measurements at the leaf scale.

Benefits of eCO₂ under drought were limited to the late season and leaf scale, and none of the eCO₂-induced shifts in leaf responses to drought upscaled to the whole-tree. Independently of the [CO₂] treatment, stem volumetric growth ceased before photosynthesis when facing drought. Leaf respiration rates and stem CO₂ efflux remained significant, at 30 % of pre-drought conditions, leading to the progressive depletion of NSC pools throughout tissues, hence offsetting any potential benefit of CO₂ fertilization prior to drought. Overall vessel size increased and wood density seemingly decreased under eCO₂ during the early season, likely determining increases in xylem vulnerability to drought-induced embolism formation and hydraulic capacitance under severe drought stress. Contrastingly, differences between [CO₂] treatments in xylem vulnerability to embolism formation and capacitance were not observed during the late season. Furthermore, stomata were almost completely closed before the onset of vessel embolism denoting a conservative hydraulic behaviour. With increasing levels of drought stress and after halfway of complete stomatal closure, depletion of elastic and inelastic water pools occurred simultaneously, thereby challenging the classic view of sequential capacitive water release.

S

Samenvatting

Wereldwijd worden bomen blootgesteld aan een ongeëvenaarde klimaatverandering, met grootschalige bossterfte door droogte als gevolg. Tijdens de afgelopen jaren is het effect van verhoogde $[CO_2]$ (eCO_2) op het functioneren van bomen een belangrijk onderzoeksonderwerp geworden. Toch blijven enkele cruciale vragen onbeantwoord: Is het effect van eCO_2 op bomen variabel in de tijd? Kunnen de effecten van eCO_2 eenvoudig worden vertaald van blad- naar boomniveau? Is een verhoging van $[CO_2]$ in staat om de negatieve gevolgen van droogte tegen te gaan? In dit doctoraatsproefschrift worden de interacties tussen seizoensgebonden groei en de effecten van eCO_2 onderzocht, en dit zowel op blad- als boomniveau en onder goed bewaterde en droogtestress condities. Hiervoor werd een literatuurstudie uitgevoerd en werden twee sets van eenjarige ratelpopulieren (*Populus tremula* L.) opgegroeid onder actuele $(aCO_2$, 445 ppm) en verhoogde $(eCO_2$, 701 ppm) atmosferische $[CO_2]$ gedurende twee opeenvolgende groeiseizoenen om zo de gevolgen van eCO_2 in het begin (2019) en op het einde (2018) van het groeiseizoen te kunnen bestuderen. Koolstofassimilatie, stomatale geleidbaarheid en respiratie op bladniveau, en stamdiametervariaties, sapstroom (als schatting voor transpiratie) en stam CO_2 efflux op boomniveau werden gemeten. Daarnaast werd de droge biomassa en de concentratie aan niet structurele koolhydraten (NSC) bepaald in verschillende plantorganen. Tenslotte werden ook vatbaarheids- en desorptiecurves opgesteld.

De uitgevoerde literatuurstudie toonde twee belangrijke zaken aan. Op de eerste plaats werd vastgesteld dat de effecten van eCO_2 erg variabel zijn over de tijd, ook binnen eenzelfde groeiseizoen. De wisselende vraag naar koolstof doorheen het seizoen, toe te schrijven aan de boomfenologie, bepaalt de intensiteit van de effecten van eCO_2. De grootste stimulatie van fotosynthese wordt daarom vooral gemeten in het begin van het seizoen, wanneer de stam het snelst toeneemt in volume en koolstofvraag hoog is. Ten tweede werd een duidelijk verschil opgemerkt in de gevolgen van eCO_2 op blad- en boomniveau. Nutriëntentekort of gebrek aan water kunnen leiden tot limitatie van boomgroei, en dit ondanks de verhoogde koolstoffixatie op bladniveau. Voor de waterprocessen kan zich eveneens een tegenstrijdigheid in de gevolgen van eCO_2 voordoen, aangezien stimulatie van totale bladoppervlakte bij blootstelling aan eCO_2, eventuele dalingen in waterverbruik op bladniveau ongedaan kan maken. In overeenstemming met de literatuur was ook in de jonge ratelpopulieren de verhoging van fotosynthese onder eCO_2 het hoogst vroeg in het seizoen, met een verhoging van volumetrische stamgroei en productie van droge biomassa tot gevolg. In tegenstelling, werd het waterverbruik op blad- en boomniveau niet beïnvloedt onder eCO_2. Ook op de respiratie in het blad en CO_2 efflux door de stam had de [CO_2] behandeling geen effect. Het voorkomen van deze dynamische responsen van bomen op eCO_2, in zowel tijd als ruimte, duidt op het gevaar van misinterpretatie van de complexe gevolgen van eCO_2 indien deze worden gebaseerd op een beperkt aantal metingen op bladniveau.

De voordelen van eCO_2 onder droogte bleven beperkt tot bladniveau en werden enkel vastgesteld op het einde van het groeiseizoen. Geen van de veranderingen ten gevolge van eCO_2 vertaalde zich tot op boomniveau. Onafhankelijk van de [CO_2] behandeling en de timing van droogte in het seizoen, stopte stamgroei bij lagere niveaus aan droogtestress dan koolstoffixatie op bladniveau. Bij sterke droogtestress bleef blad respiratie en stam CO_2 efflux hoog, tot 30 % van de waarden onder goed bewaterde omstandigheden. Dit zorgde voor een geleidelijke daling van de NSC-concentratie en een eliminatie van de eventuele voordelen van eCO_2. In het begin van het groeiseizoen was de gemiddelde vatdiameter groter en daalde de houtdichtheid ogenschijnlijk onder eCO_2. Dit had als gevolg dat de vatbaarheid voor embolisme en de hydraulische capaciteit toenam. In tegenstelling, werden geen verschillen in vatbaarheid of hydraulische capaciteit tussen [CO_2] behandelingen vastgesteld aan het einde van het seizoen. Onder beide [CO_2] behandeling sloten stomata bijna volledig voor de start van embolismevorming. Dit duidt op een voorzichtig en conservatief hydraulisch gedrag. Met toenemende droogte, en vanaf meer dan 50 % sluiting van de stomata, werden elastische en onelastische waterreserves

gelijktijdig uitgeput, waarmee het klassieke en sequentiële uitdrogingspatroon in vraag werd gesteld.

CV
Curriculum Vitae

Personal information

Name	Fran Lauriks
Date of birth	13 December 1992
Place of birth	Edegem – Belgium
E-mail	lauriksfran@gmail.com

Education

2016 – 2020	PhD student at the Laboratory of Plant Ecology Faculty of Bioscience Engineering, Ghent University
PhD dissertation	Temporal variability in leaf and whole-tree responses of *Populus tremula* L. to elevated CO_2 and drought
Promoters	Prof. dr. ir. Kathy Steppe dr. ir. Roberto Luis Salomón
2015 – 2016	Researcher (Sense-IT) at the Laboratory of Plant Ecology Faculty of Bioscience Engineering, Ghent University
2013 – 2015	Master of Science in Bioscience Engineering: Environmental technology, Ghent University
Thesis	Bast als waterreservoir: dynamisch radiaal watertransport tussen bast en xyleem in *Quercus agrifolia*
Promoter	Prof. dr. ir. Kathy Steppe

| 2010 – 2013 | Bachelor of Science in Bioscience Engineering: Environmental technology, Antwerp University |

Grant

| 2016 – 2020 | PhD grant for Strategic Basic Research (1S19317N) provided by the Research Foundation Flanders (FWO) for the project "Tree hydraulic functioning under changing climate regimes" |

| 2015 – 2016 | Funding for the Sense-IT, LA-project (IWT140961) was provided by the Agency for Innovation by Science and Technology in Flanders (IWT) and granted to Kathy Steppe |

Teaching and tutoring activities

| 2019 – 2020 | Tutor of master thesis Merel Degroote "Stedelijke CO_2-concentraties: leven we in een +400 ppm CO_2 atmosfeer?" |

Tutor of master thesis Simon Dequeker
"Intra-site variabiliteit van de hydraulische eigenschappen van lianen: een case study in Horizontes, Costa Rica"

| 2018 – 2019 | Tutor of master thesis Klara Bouwen "How resilient are *Polylepis reticulata* and *Escallonia myrtilloides* to drought?" |

Tutor of master thesis Justine Monville
"Biomimicry of water transport in trees: the use of surfactants to reduce embolism risk"

Tutor of master thesis Liselot Tack
"Hydraulic traits of tropical trees and lianas in the High Andean forest in the Azuay province, Ecuador"

| 2015 – 2019 | Teaching of special topics "Stomatal characteristics" and "Porometry" and excursion (use of Ecophysiological instruments) for the course Ecofysiologie |

International publications with peer review

Lauriks, F., Salomón, R.L., De Roo, L., Steppe, K. (under review) Leaf and tree responses of young European aspen trees to elevated atmospheric CO_2 concentration vary over the season

Lauriks, F., Salomón, R.L., Steppe, K. (In press) Temporal variability in tree responses to elevated atmospheric CO_2, Plant, Cell & Environment, https://doi.org/10.1111/pce.13986

De Roo, L., **Lauriks, F.**, Salomón, R.L., Oleksyn, J., Steppe, K. (2020) Woody tissue photosynthesis increases radial stem growth of young poplar trees under ambient atmospheric CO_2 but its contribution ceases under elevated CO_2, Tree Physiology, tpaa085, https://doi.org/10.1093/treephys/tpaa085

Padilla-Diaz, C.M., **Lauriks, F.S**., Cuevas, M.V., Fernández, J.E., Diaz-Espejo, A., Steppe, K. (2020) Scheduling regulated deficit irrigation in olive using leaf turgor measurements: another twist for the method. Acta Horticulturae. Accepted

Lauriks, F., Van de Put, H., De Pauw, D., Steppe, K. (2017). Use of leaf thickness sensors in horticultural crops. In V International symposium on Models for Plant Growth, Environment Control and Farming Management in Protected Cultivation, Acta Horticulturae, Vol. 1182 (pp. 79–85).

Van de Put, H., **Lauriks, F**., De Pauw, D., & Steppe, K. (2017). Simulation of long-term stem diameter variation of *Ficus benjamina* based on simulated transpiration. Use of leaf thickness sensors in horticultural crops. In V International symposium on Models for Plant Growth, Environment Control and Farming Management in Protected Cultivation, Acta Horticulturae, Vol. 1182 (pp. 219–226).

Oral presentations

Padilla-Diaz, C.M., **Lauriks, F.S**., Cuevas, M.V., Fernández, J.E., Diaz-Espejo, A., Steppe, K. Scheduling regulated deficit irrigation in olive using leaf turgor measurements: another twist for the method. IX International Symposium on Irrigation of Horticultural Crops. Matera, 17-20 June 2019. Book of abstracts, p. 31. Oral communication.

Padilla-Diaz, C.M., De Baerdemaeker N.J.F., De Roo L., **Lauriks F**., Diaz-Espejo A., Fernández J.E., Steppe K. Is the coordination between leaf and stem hydraulic capacitance the "power bank" to delay embolism in olive? Fourth Xylem International Meeting. Padua, 25-27 September 2019. Book of abstracts, p. 33. Oral communication.

Lauriks, F., Van de Put, H., De Pauw, D., Steppe, K. (2016). Use of leaf thickness sensors in horticultural crops. Hortimodel 2016, 19-22 September 2016, Avignon, France

Lauriks, F., Van de Put, H., Steppe K. (2016) Towards drought detection and irrigation scheduling in ornamentals with continuous plant-based measurements. First European Conference of Post Graduate Horticulture Scientists, 12 – 13 May 2016, Palermo, Italy.

Posters

Lauriks, F., De Roo, L., Salomón, R.L; Steppe, K. Effects of elevated CO_2 on *Populus tremula* during severe drought stress: aggravation or mitigation?, Presented at the EGU General Assembly 2019, Vienna, Austria, 7-12 April

Padilla-Díaz, C.M., **Lauriks, F.S**., Fernández, J.E., Cuevas, M.V., Diaz-Espejo. A., Steppe, K. Leaf turgor related measurements and leaf thickness under drought stress in olive. Presented at the XIV International Plant Water Relations Symposium. Madrid, 3rd-5th October 2018, p. 73.